



MONASH University

Mechanisms Regulating the Increase in Pulmonary Blood Flow at Birth

Justin Anthony Ross Lang

Bachelor of Biomedical Sciences (Hons)

A thesis submitted in fulfilment of the requirements for the degree of
Doctor of Philosophy

2016

The Ritchie Centre

The Hudson Institute of Medical Research

Faculty of Medicine, Nursing and Health Sciences

Monash University

Notice 1

© Justin Lang (2016). Except as provided in the Copyright Act 1968, this thesis may not be reproduced in any form without the written permission of the author.

Notice 2

I certify that I have made all reasonable efforts to secure copyright permissions for third-party content included in this thesis and have not knowingly added copyright content to my work without the owner's permission.

*"I love deadlines.
I love the whooshing noise they make as they go by."*

DOUGLAS ADAMS

Abstract	i
Declaration	iii
Acknowledgements	v
Publications and Abstracts	vii
Abbreviations and Symbols	xi

Chapter One

General Introduction	1
1.1 Cardiopulmonary Growth and Development	4
1.1.1 Early structural development of the lungs and heart.....	5
1.1.2 Establishment of the fetal cardiovascular system	8
1.1.3 Late maturation of pulmonary tissue and vasculature.....	14
1.2 Fetal Pulmonary Haemodynamics	16
1.2.1 Maintenance of a high pulmonary vascular resistance	18
1.2.2 Fetal breathing movements	19
1.3 Transitional Mechanisms: Adapting to Air Breathing at Birth	20
1.3.1 Lung aeration at birth: the first breath.....	20
1.3.2 Fetal airway liquid clearance	21
1.3.3 Neonatal vascular remodelling.....	23
1.3.4 Hypoxic pulmonary vasoconstriction	25
1.4 Regulation of the Pulmonary Vasomotor Tone in the Perinatal Period	27
1.4.1 Mechanical factors	28
1.4.2 The endothelium.....	29
1.4.4 Circulating vasoactive substances.....	34
1.4.5 Pulmonary innervation	35
1.5 Evaluating Current Problems	36
1.5.1 Consequences of a compromised fetal-to-neonatal transition	37
1.5.2 Imaging the lung at birth.....	38
1.6 Summary and Aims	40

Chapter Two

General Methodology	42
2.1 Animal Experiments	43
2.1.1 Pre-operative preparation.....	43
2.1.2 Surgical procedure	44
2.2 General Experimental Procedure	46
2.2.1 Details of beamline and PC X-ray imaging protocol.....	47
2.2.2 Ventilation and angiography protocol.....	50

2.3 X-ray Image Analysis	55
2.3.1 Normalisation of X-ray images	55
2.3.2 Blood vessel visibility	56
2.3.3 Blood vessel diameter estimation.....	56
2.3.4 Pulmonary arterial transit time.....	60
2.3.5 Relative measures of flow rate.....	60
2.4 Statistical Analysis	61

Chapter Three

Ventilation/Perfusion Mismatch During Lung Aeration at Birth.....63

Declaration for Chapter 3	65
3.1 Abstract	66
3.2 Introduction	67
3.3 Methods	69
3.3.1 Experimental procedure	69
3.3.2 X-ray and angiography imaging.....	70
3.3.3 Image analysis.....	70
3.3.4 Statistical analysis	73
3.4 Results	74
3.4.1 Animal data	74
3.4.2 Observations from PC X-ray videos	74
3.4.3 Numbers of visible vessels.....	76
3.4.4 Internal vessel diameter.....	76
3.4.5 Heart rate and beat-to-beat changes in iodine ejection	79
3.4.6 Temporal changes in iodine levels within the IVC and aorta	79
3.4.7 Change in mean pixel grey level over time within the pulmonary artery	82
3.5 Discussion	84

Chapter Four

Increase in Pulmonary Blood Flow at Birth: Role of Oxygen and Lung Aeration.....91

Declaration for Chapter 4	93
4.1 Abstract	94
4.2 Introduction	95
4.3 Methods	97
4.3.1 Experimental procedure	97
4.3.2 X-ray and angiography imaging.....	98
4.3.3 Image analysis.....	99
4.3.4 Statistical analysis	101
4.4 Results	101
4.4.1 Animal data	101
4.4.2 Observations from PC X-ray videos	101
4.4.3 Indices of vessel recruitment.....	103

4.4.4 Heart rate and opacity changes in the MPA and aorta over time	105
4.4.5 Arterial vessel internal diameter	108
4.4.6 Iodine bolus transit time	108
4.4.7 Changes in relative PBF indices	111
4.5 Discussion	112

Chapter Five

Vagal Denervation Inhibits the Increase in Pulmonary Blood Flow During Partial Lung Aeration at Birth	118
--	------------

Declaration for Chapter 5	120
5.1 Abstract	121
5.2 Introduction	122
5.3 Methods	124
5.3.1 Experimental procedure	124
5.3.2 X-ray and angiography imaging	127
5.3.3 Image analysis	127
5.3.4 Statistical analysis	129
5.4 Results	130
5.4.1 Animal data	130
5.4.2 Observations from PC X-ray videos	130
5.4.3 Pulmonary blood vessel recruitment	130
5.4.4 Heart rate	135
5.4.5 Arterial vessel internal diameter	137
5.4.6 Iodine bolus transit time	140
5.4.7 Relative PBF index	140
5.5 Discussion	146

Chapter Six

General Discussion	153
6.1 Mechanisms Regulating the Increase in Blood Flow at Birth	155
6.2 Implications of Ventilation/Perfusion Mismatch at Birth	158
6.3 Limitations	159
6.4 Future Directions	160
6.4 Overall Summary	162

Chapter Seven

References	165
-------------------------	------------

Appendices	187
-------------------------	------------

Abstract

At birth, pulmonary blood flow (PBF) significantly increases from the relatively low levels during fetal life and underpins the transition to newborn life. Air entry into the lungs triggers significant reorganisation of the cardiovascular system and allows pulmonary gas-exchange to commence, but the underlying mechanisms remain not well understood. Despite much research into this process, failure to transition from fetal to neonatal life remains the greatest cause of morbidity and mortality in newborn infants. Difficulties in investigating lung aeration and PBF at birth are exacerbated by the difficulty in imaging the aerated lung, which the development of phase contrast (PC) X-ray imaging is able to address. This thesis aimed to combine PC X-ray imaging and angiography to provide a unique perspective on the complex relationship between aeration and the increase in PBF at birth.

There remains no well-established, direct spatial correlation between local aeration and lung perfusion during the transition to newborn life. The first aim of my thesis used synchrotron X-ray imaging to address this gap in the literature by imaging near-term newborn rabbits with partial lung aeration immediately following birth (Chapter 3). Unilateral ventilation dilated pulmonary vessels and increased PBF in both aerated and unaerated regions of the lungs, indicating that the initial ventilation-induced increase in PBF is not spatially related to aerated lung regions. The primary mechanisms thought to mediate the ventilation-induced increase in PBF (e.g. increased oxygenation, mechanical expansion of the lungs) should act locally to dilate adjacent blood vessels, yet significant non-local effects of aeration were observed. The second aim of this thesis was to isolate the effect of oxygenation on this process, using

variable oxygen content in the inspired gas (Chapter 4). Entry of gas without oxygen into the lungs was sufficient to induce a similar increase in global PBF and ventilation/perfusion mismatch in unaerated regions. Oxygen was found to have an additive effect on this observation, suggesting underlying mechanisms are able to act independently of oxygenation but are enhanced by high oxygen levels. This led to the possibility of a neural reflex acting via the vagus nerve and was the focus of my third aim (Chapter 5). Ligation of the vagus nerve via vagotomy inhibited the increase in PBF with partial aeration, which was partially mitigated by high inspired oxygen concentrations. This suggests that a vagally-mediated reflex is a much higher contributing factor to pulmonary vasodilation with lung aeration at birth than previously considered.

Overall, the studies contained in this thesis increase our understanding of the changes in the lung during the transition to newborn life. The underlying mechanisms that can induce a global PBF increase with only partial aeration appear largely independent of oxygenation and involve neural signalling via the vagus nerve. This may be part of an adaptive advantage to maintain left ventricle preload and cardiac output that is lost following umbilical cord occlusion. Further knowledge of this complex process will benefit caregivers seeking to minimise harm in ventilation strategies, with these studies demonstrating potential outcomes of regionalised aeration and providing valuable insight into the mechanisms regulating the increase in PBF at birth.

Declaration

In accordance with Monash University Doctor of Philosophy (PhD) regulations, the following declarations are made:

- I hereby declare that this thesis contains no material which has been accepted for the award of any other degree or diploma at any university of equivalent institution and that, to the best of my knowledge and belief, this thesis contains no material previously published or written by another person, except where due reference is made in the text of the thesis.

- This thesis includes three original manuscripts published in peer-reviewed journals (Chapters 3, 4 and 5); the core theme of the thesis is neonatal physiology. The ideas, development and writing of all the papers in this thesis were the principal responsibility of myself, the candidate, working within the Ritchie Centre under the supervision of Professor Stuart B. Hooper, Doctor James T. Pearson and Doctor Graeme R. Polglase.

- The inclusion of co-authors reflects the fact that the work came from active collaboration between researchers and acknowledges input into team-based research.

My contributions to the manuscripts in this thesis are as follows:

Thesis Chapter	Publication Title	Publication Status	Nature and Extent of Candidate's Contribution *
3	Ventilation/Perfusion Mismatch in the Lungs at Birth	Published	Performed all of the experimental and laboratory work, data analysis and wrote the manuscript
4	Increase in Pulmonary Blood Flow at Birth: Role of Oxygen and Lung Aeration	Published	Performed all of the experimental and laboratory work, data analysis and wrote the manuscript
5	Vagal Denervation Inhibits the Increase in Pulmonary Blood Flow During Partial Lung Aeration at Birth	Published	Performed all of the experimental and laboratory work, data analysis and wrote the manuscript

* Note: Co-author contributions are listed with each chapter

I have renumbered sections of published papers in order to generate a consistent presentation within the thesis.

Student signature:



Date: 15/12/16

The undersigned hereby certify that the above declaration correctly reflects the nature and extent of the student's contributions to this work.

Main Supervisor signature:



Date: 15/12/16

Acknowledgements

To my supervisors during this PhD, Prof. Stuart Hooper, Dr. James Pearson and Dr. Graeme Polglase, thank you for providing me with much scientific insight over the last few years. I appreciate being a part of this fascinating project, with the unique opportunity to travel to Japan and work with such interesting and varied studies, technology and people. Thank you for all that you have provided me towards the end goal of this thesis, and I hope to use the guidance you have given me well into the future.

To the SPring-8 team: Megan, Mel, Marcus, Rob, Andreas and Arjan, while it could partly be the Stockholm syndrome of being cooped up in the beamline for long periods of time, you were always a great group of people to work with. Beamtime could be physically and mentally draining, but the effort, passion and expertise of everyone that was involved with these projects could not be topped. Thank you to Yagi and Uesugi for looking after all of our needs at SPring-8. Also thanks to Katie and Genevieve for helping with the terabytes of X-ray images that needed to be transferred and sifted through, if I never have to touch a harddrive again it would be too soon.

I would like to give a special shout-out to Dr Sammy Barton aka Pablo aka Dr Bogan. Hola! We got through the best of times and the blurst of times, somehow. You have always been good friend and a great scientist, ¿porqué no los dos? I have no doubt you will do incredible things in science and should probably be minted on a coin someday. Also, congratulations to Bauer for putting a ring on it.

To the rest of the PhD trials/tribulation team: Tracey Ong, you're the bomb and should never let anyone change you, James Aridas, you always impressed me with the effort you put into your work and have contributed to some great times we've had together. I have always loved our Game of Thrones watching parties, and between you two and Sam, I couldn't imagine better people to go through this PhD with (plus Leigh, even if he did nap during GoT).

Thank you to everyone else in the Hooper Lab: Ali, Val, Annie, Kelly, Ilias, Karyn and Dal, all of you are an integral part of the great science that this lab puts out and your helpful and welcoming nature keeps everything together. To everyone else at the Ritchie Centre (past and present): Amy, Tamara, Melinda, Madison, Dom, Anzari, Azu, Karinna, and all of the supporting staff and anyone I've forgotten to mention, thank you for providing the much needed laughs, support and great times. Everyone in the Ritchie Centre makes it much more than simply a sum of its parts.

To Nick: I choo-choo choose you to continue on this journey through life with me, while I don't expect you to read the whole of this book, you can definitely see that there's nothing more exciting than science. You get all the fun of sitting still, being quiet, writing down numbers, paying attention. Science has it all. Thank you to my family: Mum and Dad and everyone else, I couldn't have done it without your love and support.

I would also like to acknowledge all of the animals that have lost their lives in the pursuit of medical research. Without this oft overlooked contribution, these studies would not be possible and I will always remember the monument to the research animals near the SPring-8 synchrotron in Japan.

Lastly, to everyone who asked if my thesis has been read and I can submit yet: Yes, the answer is finally yes.

Publications and Abstracts

Original Article Publications Arising From This Thesis

Lang, JAR, Pearson JT, Binder-Heschl C, Wallace MJ, Siew ML, Kitchen MJ, te Pas AB, Fouras A, Lewis RA, Polglase GR, Shirai M & Hooper SB (2017) Vagal denervation inhibits the increase in pulmonary blood flow during partial lung aeration at birth. *The Journal of Physiology* **595**(5): 1593-1606

Lang JA, Pearson JT, Binder-Heschl C, Wallace MJ, Siew ML, Kitchen MJ, te Pas AB, Fouras A, Lewis RA, Polglase GR, Shirai M & Hooper SB (2016) Increase in pulmonary blood flow at birth: role of oxygen and lung aeration. *The Journal of Physiology* **594**(5): 1389-1398 (First published online 10 September 2015)

Lang JA, Pearson JT, te Pas AB, Wallace MJ, Siew ML, Kitchen MJ, Fouras A, Lewis RA, Wheeler K, Polglase GR, Shirai M, Sonobe T & Hooper SB (2014) Ventilation/perfusion mismatch during lung aeration at birth. *Journal of Applied Physiology* **117**(5): 535-543.

Review Article Publications Arising From Collaboration

Hooper SB, te Pas AB, **Lang J**, van Vonderen JJ, Roehr CC, Kluckow M, Gill AW, Wallace EM & Polglase GR (2015) Cardiovascular transition at birth: a physiological sequence. *Pediatric Research*. Advance online publication. doi: 0.1038/pr.2015.21

Abstracts/Conference Proceedings – Invited Presentations

Lang JA, Pearson JT, Binder-Heschl C, Wallace MJ, Siew ML, Kitchen MJ, te Pas AB, Fouras A, Lewis RA, Polglase GR, Shirai M & Hooper SB (2015) The cardiopulmonary transition at birth. *The Ritchie Centre Colloquium*, Melbourne, Australia

Lang JAR, Pearson JT, Polglase GR, Hooper SB (2014) Changes in pulmonary blood flow at birth. *Special Seminar Invited Speaker*: University of Alberta, Edmonton, Canada

Abstracts/Conference Proceedings – Published Conference Abstracts

Lang JA, Pearson JT, te Pas AB, Wallace MJ, Siew ML, Kitchen MJ, Fouras A, Polglase GR, & Hooper SB (2015) Pulmonary blood flow increases at birth regardless of local aeration or pO₂. *Journal of Paediatrics and Child Health* 51(Suppl. S1): 18

Lang JA, Pearson JT, Wallace MJ, Siew ML, Kitchen MJ, Fouras A, Polglase GR, te Pas AB & Hooper SB (2014) The initial increase in pulmonary blood flow at birth in aerated and unaerated lung regions at birth is not related to oxygen. *Journal of Paediatrics and Child Health* 50(Suppl. S1): 18

Lang JA, Pearson JT, Wallace MJ, Siew ML, Kitchen MJ, Fouras A, Wheeler K, Polglase GR, te Pas AB & Hooper SB (2013) Limited aeration of the lung at birth leads to a significant ventilation/perfusion mismatch. *Journal of Paediatrics and Child Health* 49(Suppl. S2): 107

Lang JA, Pearson JT, Wallace MJ, Siew ML, Kitchen MJ, Fouras A, Wheeler K, Polglase GR, te Pas AB & Hooper SB (2012) Partial lung aeration leads to ventilation/perfusion mismatch in the lungs immediately following birth. *Journal of Paediatrics and Child Health* 48(Suppl. S1): 77

Abstracts/Conference Proceedings – Other Conference Abstracts

Lang JA, Pearson JT, Wallace MJ, Siew ML, Kitchen MJ, Fouras A, Polglase GR, te Pas AB & Hooper SB (2014) Ventilation of the lungs at birth without oxygen increases pulmonary blood flow in aerated and unaerated regions. *Pediatric Academic Society, Vancouver, Canada*

Lang JA, Pearson JT, Wallace MJ, Siew ML, Kitchen MJ, Fouras A, Wheeler K, Polglase GR, te Pas AB & Hooper SB (2014) Partial aeration with 100% oxygen at birth increases pulmonary blood flow in aerated and non-aerated regions. *Fetal and Neonatal Workshop of Australia and New Zealand, Yanchep, Australia*

Lang JA, Pearson JT, Wallace MJ, Siew ML, Kitchen MJ, Fouras A, Polglase GR, te Pas AB & Hooper SB (2013) Partial aeration without oxygen induces a ventilation/perfusion mismatch in the lungs immediately following birth. *Australian Society for Medical Research (ASMR), Melbourne, Australia*

Lang JA, Pearson JT, Wallace MJ, Siew ML, Kitchen MJ, Fouras A, Polglase GR, te Pas AB & Hooper SB (2013) Limited pulmonary aeration leads to a significant ventilation/perfusion mismatch in the lungs immediately following birth. *Australian Society for Medical Research (ASMR), Melbourne, Australia*

Hooper SB, **Lang JA**, Pearson JT, Wallace MJ, Siew ML, Kitchen MJ, Fouras A, Polglase GR & te Pas AB (2013) Ventilation of the lungs at birth without oxygen increases pulmonary blood flow in aerated and unaerated regions. *Pediatric Academic Society, Washington, USA*

Lang JA, Pearson JT, Wallace MJ, Siew ML, Kitchen MJ, Fouras A, Wheeler K, Polglase GR, te Pas AB & Hooper SB (2014) Partial aeration with 100% nitrogen at birth induces a global increase in pulmonary blood flow. *Fetal and Neonatal Workshop of Australia and New Zealand, Barossa Valley, Australia*

Lang JA, Pearson JT, Wallace MJ, Siew ML, Kitchen MJ, Fouras A, Lewis RA, te Pas AB, Wheeler K, Polglase GR & Hooper SB (2012) The role of regional lung aeration in the increase in pulmonary blood flow at birth. *Australian Synchrotron User's Meeting, Melbourne, Australia*

Abbreviations and Symbols

~	Approximately
°C	Degrees Celsius
μg	Micrograms
μL	Microlitres
μm	Micrometres
%	Per Cent
±	Plus or Minus
A	Aerated
ACh	Acetylcholine
ANOVA	Analysis of Variance
ATPase	Adenosine Triphosphatase
BLV	Bilateral Ventilation
bpm	Beats Per Minute
C	Control
Ca ²⁺	Calcium Ion
cAMP	Cyclic Adenosine Monophosphate
cGMP	Cyclic Guanosine Monophosphate
Cl ⁻	Chloride Ion
cm	Centimetres
cmH ₂ O	Centimetres of Water
CO	Cardiac Output

CO ₂	Carbon Dioxide
DA	Ductus Arteriosus
ECG	Electrocardiogram
e.g.	<i>Exempli Gratia</i> ; “For Example”
ET	Endotracheal
ET-1	Endothelin-1
<i>et. al</i>	<i>Et Alia</i> ; “and others”
eNOS	Endothelial Nitric Oxide Synthase
FBM	Fetal breathing movement
Fig.	Figure
FRC	Functional Residual Capacity
G	Gauge
g	Grams
GA	Gestational Age
HPV	Hypoxic Pulmonary Vasoconstriction
HR	Heart Rate
Hz	Hertz
ID	Internal Diameter
i.e.	<i>Id Est</i> ; “it is”
IVC	Inferior Vena Cava
I.P.	Intraperitoneal
I.V.	Intravenous
J	Juxtacapillary
keV	Kiloelectron Volt
kg	Kilograms

kPa	Kilopascals
LV	Left Ventricle
N ₂	Nitrogen
Na ⁺	Sodium Ion
NO	Nitric Oxide
NOS	Nitric Oxide Synthase
NV	Not Ventilated
mg	Milligrams
min	Minutes
mL	Millilitres
mm	Millimetres
mmHg	Millimetres of Mercury
MPA	Main Pulmonary Artery
mRNA	Messenger Ribonucleic Acid
n	Number
nm	Nanometres
NOS	Nitric Oxide Synthase
NV	Not Ventilated
O ₂	Oxygen
p	P Value; Level of Significance
PA	Pulmonary Artery
PAF	Platelet Activating Factor
PAF-R	Platelet Activating Factor Receptor
PaCO ₂	Partial Pressure of Carbon Dioxide
PaO ₂	Partial Pressure of Oxygen

PBF	Pulmonary Blood Flow
PC	Phase Contrast
PDE5	Phosphodiesterase 5
PEEP	Positive End-Expiratory Pressure
PG	Prostaglandin
PKG	Protein Kinase G (cGMP-Dependent Protein Kinase)
PPHN	Persistent Pulmonary Hypertension of the Newborn
PVR	Pulmonary Vascular Resistance
RV	Right Ventricle
s	Seconds
SD	Standard Deviation
SEM	Standard Error of the Mean
sGC	Soluble Guanylyl Cyclase
SP	Surfactant Protein
UA	Unaerated
ULV	Unilateral Ventilation
V	Vagotomy
vs.	Versus

Chapter One

General Introduction

Review of the Literature

The transition from intra- to extra- uterine life at birth is a complex yet coordinated series of physiological events that facilitates the rapid adaptation to newborn life (Rudolph, 1985). Birth events include: aeration of the lungs, the start of pulmonary gas-exchange and reorganisation of the cardiovascular system, which mostly results from a large increase in pulmonary blood flow (PBF) (Dawes, 1961). These events are fundamentally linked, as it is the entry of air into the lungs that initiates a rapid and sustained increase in PBF, which leads to a significant reorganisation of the cardiovascular system (Rudolph, 1979; Hooper & Harding, 2005). During fetal life the future airways are filled with liquid, contributing to the high pulmonary vascular resistance (PVR) and consequential very low pulmonary perfusion (Rudolph, 1985; Hooper & Harding, 1995). In order for a healthy transition of the newborn to extra-uterine life, multiple mechanical and vasoactive stimuli must quickly and efficiently aerate the lungs and decrease PVR (Teitel *et al.*, 1990); failure of this process represents a significant source of morbidity and mortality in vulnerable newborns (Sinha & Donn, 2006).

Problems related to an unfavourable transition are often exacerbated in infants born premature, prior to 37 weeks gestation (term ~40 weeks), as organs such as lungs can still be very immature and unprepared for the challenges of birth (Alcorn *et al.*, 1981; Moss, 2006). Despite the critical nature of the transitional period, much remains unknown about the underlying physiological processes involved (Gao & Raj, 2010). While the temporal link between initial aeration of the lungs at birth and the rapid rise in global PBF are well established (Figure 1.1) (Dawes *et al.*, 1953; Iwamoto *et al.*, 1987; Polglase & Hooper, 2006), there is no simple, direct correlation with local aeration and perfusion during the perinatal period in which these changes occur. A lack of understanding of this area at the most basic level has prompted much research to improve health outcomes in infants with a compromised

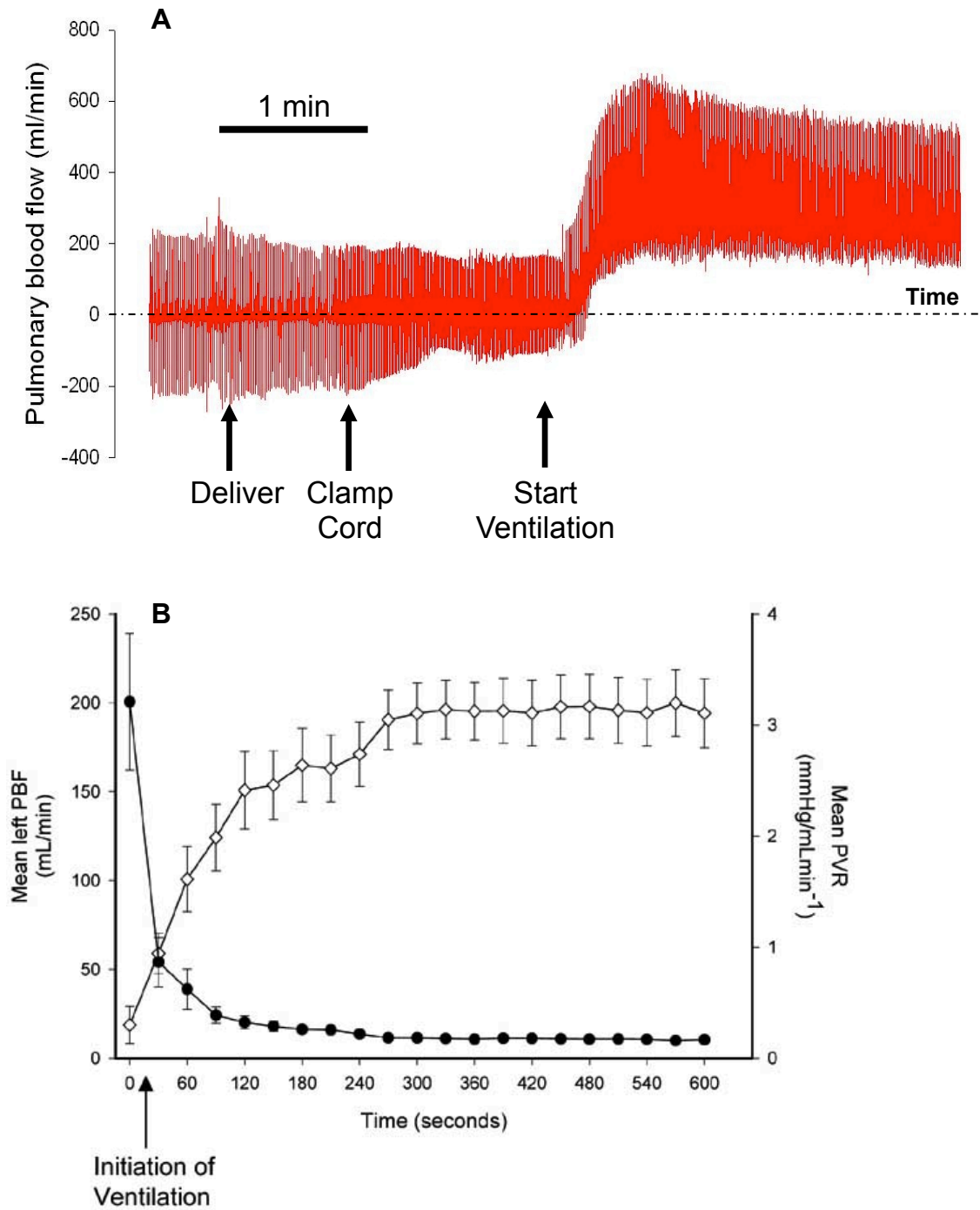


Figure 1.1: Pulmonary blood flow at birth

A: Representative blood flow recording obtained from the left pulmonary artery immediately before, during and immediately after the premature delivery and then ventilation of a lamb at 125 days gestational age. **B:** The increase in mean PBF (open diamonds; mL/min) compared to the decrease in PVR (closed circles; mmHg/mLmin⁻¹) associated with birth and the onset of ventilation (time 0).

Adapted from Polglase and Hooper (2006)

birth transition.

The focus of this thesis is to examine the spatial relationship between local aeration and pulmonary perfusion immediately after birth in order to identify mechanisms regulating the increase in PBF at birth. The studies herein provide unique insights into the pulmonary haemodynamics in the perinatal period and the relative role of the various mechanical and vasoactive stimuli that influence this process. What follows is a description of pulmonary development leading up to and following the birth transition and the known aspects of how this sequence of events is influenced. The clinical relevance of these changes is also discussed, and how pulmonary haemodynamics can be examined using a unique combination of microangiography and phase contrast X-ray imaging.

1.1 Cardiopulmonary Growth and Development

The lungs represent a unique organ in fetal life, being inactive in regards to their primary postnatal role of gas-exchange, yet having to be at a sufficient level of maturity to quickly assume this role at the time of birth. It is critical, therefore, that multiple aspects of the lungs have developed by the time of birth in order for it to take over the role of respiratory gas-exchange at birth. These include the mechanisms involved in lung liquid clearance, altering PVR and the production of surfactant, which is essential to oppose lung collapse at end-expiration (Rudolph & Heyman, 1974; Siew *et al.*, 2009b). Understanding the appropriate development of these cardiopulmonary structures is critical to understanding the relevant pathophysiology and possible treatments, and this understanding has been informed by studies in humans as well as animal models such as rabbits and sheep.

1.1.1 Early structural development of the lungs and heart

While the heart and blood vessels of the lung are mesoderm derived, the airways and alveoli originate from the endoderm germ layer, both becoming intimately linked as the pulmonary vascular bed and alveolar walls eventually mature into the blood-gas barrier (Spooner & Wessells, 1970). The third germ layer, the ectoderm, provides pulmonary innervation when neurogenesis is later completed. Development of the lungs progresses through five major stages approximately segregated based on histological appearance of the pulmonary tissue: termed embryonic, pseudoglandular, canalicular, sacular and alveolar stages (Figure 1.2) (Burri, 1984; Hislop, 2005). Early periods of lung growth are primarily controlled by a predetermined developmental program; this leads to a highly coordinated process of cell proliferation, differentiation and cell-cell interaction that gives rise to the branched structure of the airways (Hislop, 2002). An endodermal outgrowth of the foregut, the respiratory diverticulum, elongates to form a rudimentary trachea during the embryonic stage (Jeffery, 1998). From this point, the growing lung buds divide and begin a dichotomous branching process that forms the basic structure of the airways, regulated by the surrounding mesenchymal cells (Alcorn *et al.*, 1981; Shannon *et al.*, 1998).

Throughout these early periods of pulmonary development, there is an associated blood vessel network to supply the developing lungs (Hislop & Reid, 1972); dividing airway tubules are matched by axial artery divisions, with terminal airways surrounded by a capillary plexus (Hall *et al.*, 2000). The cardiopulmonary circulation is connected from around the fifth week of gestation, when the heart divides into respective atria and ventricles; the pulmonary arteries form as branches from the sixth aortic arch while the pulmonary veins form as an outgrowth from the fetal heart (Anderson *et al.*, 2003). By the end of the pseudoglandular stage, around

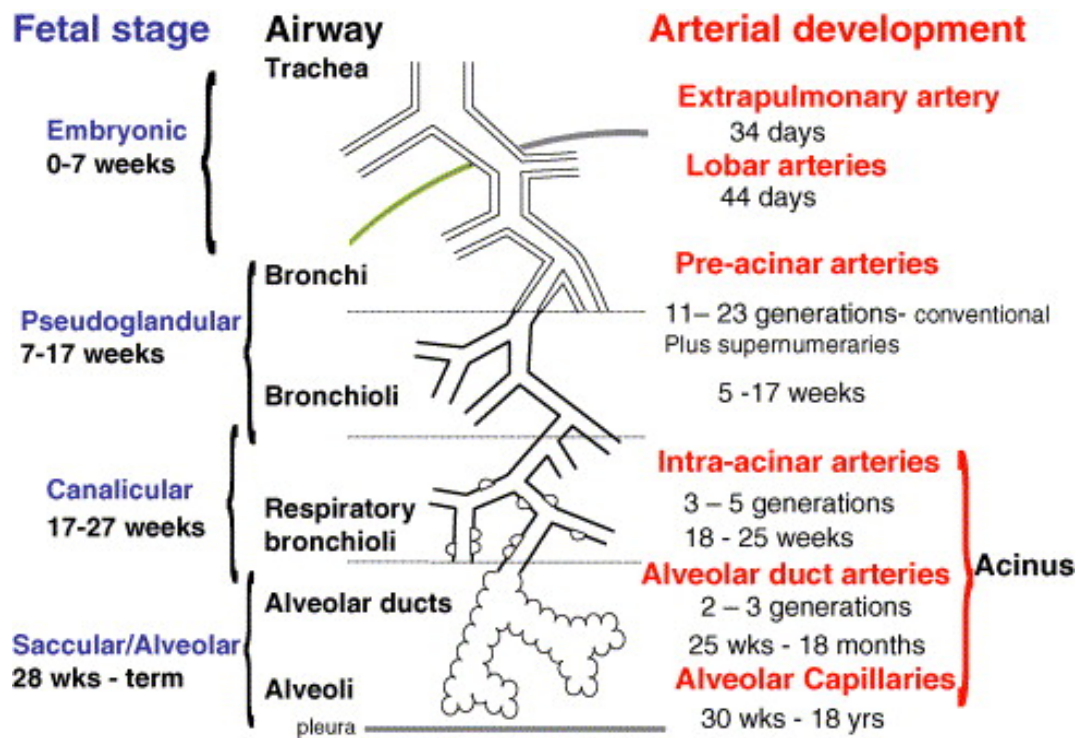


Figure 1.2: Schematic of lung developmental stages (embryonic, pseudoglandular, canalicular, saccular and alveolar)

Comparisons of stage (left), airway branching (middle) with vasculature branching (right)

From Hislop (2005)

17 weeks of gestation in humans, all pre-alveolar airways and their supplementary arteries have been established (Hislop, 2002). The complementary lymphatic vessels have also developed by this stage, having started development several weeks later than the cardiovascular system (Butler *et al.*, 2009). The lymphatic system is essential for the drainage of liquid and proteins from the interstitium, as well as having roles in immune system responses (Bland *et al.*, 1980; Butler *et al.*, 2009). Recent studies have shown that prenatal lymphatics are functional through the demonstration that the absence of lymphatics dramatically reduces lung compliance in late gestation mouse embryos (Jakus *et al.*, 2014). The developing airways form a template for the growth of blood vessels which develop in parallel, with the volume of airway liquid retained within the future airways providing a critical stimulus for lung growth (Hislop & Reid, 1972; Hooper & Harding, 1995).

1.1.1.1 Lung liquid secretion

Throughout lung development, from at least six weeks of GA or earlier, the lung lumen is filled with liquid derived from the airway epithelium (McCray *et al.*, 1992; Olver *et al.*, 2004). An electrochemical gradient, established by $\text{Na}^+ - \text{K}^+ - \text{ATPase}$ on the basolateral surface of the respiratory epithelium, drives chloride ion secretion into the lumen of the developing lung (Olver & Strang, 1974). The resultant transmembrane osmotic gradient then promotes water movement into the lung lumen. The secreted liquid then leaves the lungs by flowing out of the trachea, principally during fetal breathing movements, and its rate of efflux is determined by activity of the larynx. By resisting the efflux of liquid from the trachea, laryngeal activity contributes to the hyperexpanded state of the fetal lungs at rest in comparison to their resting volume postnatally (Hooper & Harding, 1995; Harding & Hooper, 1996).

The distension of the pulmonary bronchi and bronchioles with liquid during fetal life provides an essential stimulus for lung growth and maturation (Moessinger *et al.*, 1990; Hooper & Harding, 1995). Prolonged periods of lung over-expansion, via tracheal occlusion, has been shown to be a potent stimulator for fetal lung growth and tissue remodelling (Alcorn *et al.*, 1977; Nardo *et al.*, 1998). Conversely, sustained reduction of fetal lung expansion can slow the structural development of the vascular bed, as well as alveolar cell phenotypes (Alcorn *et al.*, 1977; Moessinger *et al.*, 1990). Experiments involving drainage of lung liquid has been found to cause severe lung hypoplasia, with thick alveolar walls and fewer total alveoli (Alcorn *et al.*, 1977; Moessinger *et al.*, 1990). Following on from these observations, DiFiore *et al.* (1994) showed that the effects of experimental diaphragmatic hernia, and associated lung hypoplasia, can be reversed by lung liquid accumulation via tracheal ligation. This was able to increase lung compliance in lungs that would otherwise not be able to perform gas-exchange, while preserving the normal maturation process (DiFiore *et al.*, 1994). Indeed, the intra-luminal pressure of lung liquid has an integral impact on both pulmonary structure and function.

1.1.2 Establishment of the fetal cardiovascular system

Following initial formation of the cardiovascular system, several characteristics of the fetus' physiology enable it to maintain oxygen delivery to vital organs despite low partial pressures of oxygen in fetal blood. Blood vessels in the fetal lung initially form through a combination of vasculogenesis, new vessel growth via endothelial progenitor cells, and angiogenesis, the sprouting of blood vessels from pre-existing vessels (Hislop & Reid, 1972; de Mello *et al.*, 1997; Hall *et al.*, 2000). These new vessels mature into the distinct layers of intima, media and adventitia (Jain, 2003); the innermost layer, the intima, is composed of endothelial cells,

which line the entire circulatory system, from the heart and the large vessels through to the single-cell thick capillaries (Hall *et al.*, 2000). Oxygen delivery is essential for growth and development, yet the oxygen partial pressure of the fetal pulmonary circuit is only around 17-20 mmHg (Lakshminrusimha & Steinhorn, 1999). Compensation for this low oxygen includes a different haemoglobin structure to the adult, allowing for higher oxygen saturation at any given partial pressure of oxygen (Lister *et al.*, 1979), and alterations in cardiac output. There are fewer myofibrils present during development, which are poorly organised compared to the parallel structure of the mature adult heart (Smolich *et al.*, 1989; Li *et al.*, 1996). This smaller contractile mass contributes to modulation of cardiac output being dependent on heart rate rather than stroke volume (Shaddy *et al.*, 1988), although still in a very limited capacity compared to the adult (Teitel & Rudolph, 1985). Therefore, although capacity for absolute cardiac output is low due to cardiac immaturity, relative cardiac output is high to maintain oxygen delivery to tissues.

Once the primitive fetal circulation is formed it acts, as in the adult, to deliver nutrients such as oxygen to tissues as well as remove waste metabolites such as carbon dioxide. Unlike the adult, the fetus relies on the mother for this exchange, with the placenta existing as the interface at which this occurs (Kiserud & Acharya, 2004). The placenta is a highly vascular organ present from implantation onwards, developing into an intricate network of both maternal and fetal vessels in close proximity to facilitate metabolic exchange (Rudolph, 1985). This extensive vascular bed contributes to the placenta having the lowest vascular resistance in the mother, thereby taking a large percentage of cardiac output (Rudolph & Heymann, 1970; Stuart *et al.*, 1980). The fetal circulatory system is thus uniquely arranged to facilitate this configuration, with umbilical vessels forming a connection to the placenta, and several fetal-specific vascular shunts existing to redistribute blood flow (Rudolph, 1979).

1.1.2.1 *Fetal vascular shunts*

The fetus has several specialised and unique vascular shunts, which include the foramen ovale and ductus venosus on the venous side and the ductus arteriosus on the arterial side (Figure 1.3) (Rudolph, 1985). The ductus venosus connects the umbilical vein directly to the inferior vena cava immediately prior to the right atrium, bypassing the liver (Bellotti *et al.*, 2000; Kiserud *et al.*, 2000). A higher proportion of blood is shunted through the ductus venosus in sheep (Edelstone *et al.*, 1978) when compared with humans (Kiserud *et al.*, 2000), possibly suggesting a higher developmental priority for the liver in humans.

The foramen ovale is an intra-atrial shunt, that preferentially streams blood returning from the umbilical vein, via the ductus venosus, directly into the left atrium and left ventricle (Rudolph 1985); this valve-like shunt remains open during fetal life because right atrial pressure exceeds left atrial pressure (Rudolph, 1985). When blood is pumped out of the right ventricle into the main pulmonary trunk, a third shunt, the ductus arteriosus, preferentially directs most (~90%) of this output into the descending aorta instead of the lungs. This is because pulmonary vascular resistance is high and the low-resistance placenta contributes to a relatively low systemic vascular resistance (Kiserud & Acharya, 2004). As a result, a pressure gradient exists (of ~5mmHg) during fetal life between the main pulmonary artery and the dorsal aorta (Reid & Thornburg, 1990; Hooper, 1998), which directs right ventricular output through the ductus arteriosus into the descending aorta; this is referred to as right-to-left shunting (Rudolph, 1985; Hooper, 1998). Patency of the ductus arteriosus is maintained by multiple factors during fetal life, which include low oxygen tension levels present in the fetus and elevated prostaglandins PGE₂ and PGI₂ from the placenta (Clyman *et al.*, 1978).

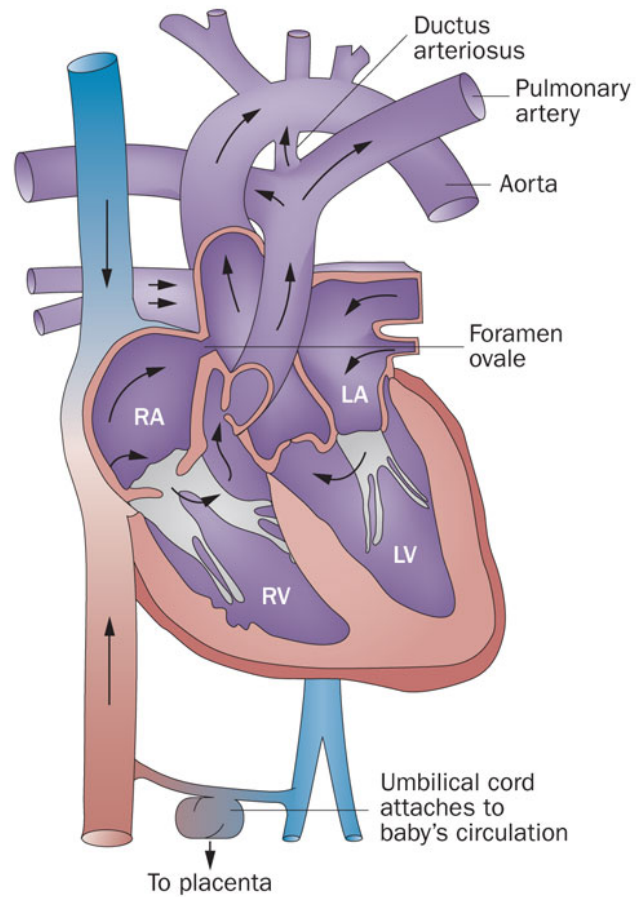


Figure 1.3: The fetal circulation

Blood returning from the placenta, umbilical arteries and ductus venosus passes through the foramen ovale (between the left and right atria) and the ductus arteriosus (between the main pulmonary artery and descending aorta) to bypass the lungs.

Adapted from Hunter and Simpson (2014)

The overall consequence of these fetal vascular shunts is the direction of blood with relatively higher oxygen saturation levels into arteries perfusing the upper body (preductal) compared to the descending aorta. This is mostly due to the foramen ovale, which allows highly oxygenated umbilical venous blood to bypass the right heart and the lungs (Rudolph, 1985). The presence of these shunts results in the fetal circulation operating in parallel, unlike the adult where the circulations are in series. As such, the fetal systemic circulation is supplied from both the left and right ventricles, with only a small portion of right ventricular output supplying the lungs (Rudolph, 1985). In fetal sheep at around 60-80 days of GA, the pulmonary circulation receives only ~4% of the cardiac output which increases to about ~7% of cardiac output near-term (Rudolph & Heymann, 1970), although this very much depends on whether the fetus is making breathing movements (Polglase *et al.*, 2004). In a Doppler study of human fetuses by Mielke and Benda (2001), this distribution was found to be higher, at around 11% of combined cardiac output, but the overall blood flow patterns were found to be similar between humans and lambs. This study also showed the right heart dominance in the human fetus, with the RV providing about 60% of the fetal cardiac output and the LV ejecting the remaining 40% (Mielke & Benda, 2001). Fetal blood flow distribution is thus considerably different to the neonate and adult, and changes throughout gestation as development of the circulation progresses (Rudolph & Heymann, 1970).

1.1.2.2 Acceleration of pulmonary vascularisation in late gestation

Vascular resistance in the pulmonary blood vessels gradually reduces with advancing gestation (Cassin *et al.*, 1964a), mainly because the cross-sectional surface area of the vascular bed gradually increasing as it grows. Capillary growth and development in the lungs accelerates in the canalicular stage, between 16 and 26 weeks of GA in humans, and interruption of this process severely restricts the gas-exchange potential of the lungs (Alcorn *et al.*, 1981; Smith *et al.*, 2010). Work by Alcorn *et al.* (1981) showed that during the canalicular stage, a compact connective tissue framework develops, which is essential for lung function. Studies such as these showed that the morphological appearance of the lungs dramatically changes as the lumen expands and the interstitial tissue surrounding the distal airways thins (Alcorn *et al.*, 1981; Smith *et al.*, 2010). The epithelium of the airways begins to differentiate into the different alveolar epithelial cell types: type I cells are essential for the thin air-blood barrier, and type II cells are the source of surfactant production (Flecknoe *et al.*, 2003).

The canalicular stage is a critical period of capillary network organisation around the air spaces. Multiple different models have been proposed about how this blood vessel maturation takes place. A combination of vasculogenesis and angiogenesis has been suggested by de Mello *et al.* (1997), whereby distal vessels arise *de novo* while proximal vessels differentiate via proliferation and migration from existing vessels; these individual segments then connect around the end of the pseudoglandular stage. Hall *et al.* (2000) suggest that vasculogenesis is the primary method of intrapulmonary vascular development, via continuous expansion of the capillary plexus in the pulmonary mesenchyme. Further, work by Parera *et al.* (2005) has

proposed distal angiogenesis is the critical mechanism for vascularisation through the continuous expansion of capillaries from the terminal lung buds starting in very early development. Thus, the exact mechanisms regarding pulmonary vascularisation remain controversial. More recent studies suggest the pulmonary vasculature is generated through a multi-lineage process (Peng *et al.*, 2013) but much remains to be clarified.

1.1.3 Late maturation of pulmonary tissue and vasculature

Following the formation of the conducting airways and major vessels, the later stages of lung development are primarily in the functional gas-exchange regions of the airways (Hislop, 2005). Rapid structural maturation of the lungs occurs after 24 weeks of gestation in humans, as lung growth enters the saccular stage. The lung lumen rapidly expands in relation to the surrounding tissue, which leads to further thinning of the peri-saccular tissue and a marked increase in lung volume (Alcorn *et al.*, 1981). Crests begin to project into airspaces from primary saccule walls, and then begin to form secondary septal crests. These develop further during the alveolar stage of lung development, from 36 weeks onwards, as the primitive air sacs subdivide into many alveoli, greatly increasing the surface area of the lungs (Kotecha, 2000). Alveolarisation persists for at least several years post-natally in several species, including humans, sheep and rabbits (Hislop, 2002). Although intra-acinar arteries and veins start to form via angiogenesis around the canalicular stage, pulmonary microvasculature completes development during the later saccular and alveolar stages (Hislop & Reid, 1972; Hall *et al.*, 2000). The development of the blood-gas barrier is critical for efficient postnatal function of the lungs, and is only established late in gestation as the final subdivisions of both the airways and blood vessels occur (Di Maio *et al.*, 1989).

1.1.3.1 *The (future) air-blood barrier*

The primitive air-blood barrier ultrastructure has been identified as early as 19 weeks of GA in humans (Di Maio *et al.*, 1989) and involves the thinning of septa to allow airways and capillaries to come into close apposition as well as the gradual differentiation of cuboidal epithelium into type I and type II alveolar epithelial cells. The thin cytoplasmic extensions of the type I cells cover much of the total alveolar surface, with studies reporting this to be around 93% in humans (Crapo *et al.*, 1983) and over 97% in mice (Haies *et al.*, 1981). Increasing proximity of blood vessels and alveoli occurs during the alveolar stage, the two layers of capillaries that exists in immature septa merge into a single layer as the septa thin (Caduff *et al.*, 1986). The basement membranes underlying the alveolar epithelial cells and adjacent capillary endothelial cells merge and then fuse, resulting in an extremely thin (~200nm) air/blood gas barrier (Alcorn *et al.*, 1981). This membrane becomes extremely important for the efficient passive diffusion of gases, with premature birth occurring well before this essential stage of maturation. Along with inadequate surfactant production, an immature and thick diffusion barrier is the primary mechanism for respiratory failure in premature infants (Ballard *et al.*, 2003; Smith *et al.*, 2010)

1.1.3.2 *Surfactant production*

At rest, the air-filled lung has a tendency to collapse largely due to the presence of surface tension at the air/liquid interface, particularly within the gas-exchange regions which have a large surface area (Avery & Cook, 1961). Surfactant is a mixture of phospholipids, neutral lipids and proteins, that is produced by type II pneumocytes to counter this surface tension at the air-liquid interface (Kikkawa *et al.*, 1975). The surfactant proteins (SP) assist the surface active function of the phospholipids (SP-B and SP-C) and are also associated with innate host

defence (SP-A and SP-D), with the ability to bind to microorganism surfaces and modulate leukocyte activity (Crouch & Wright, 2001). Exocytosis of surfactant into the lung lumen does not begin until ~32 weeks of GA, although lamellar bodies, where storage of surfactant takes place, appear much earlier in gestation (King *et al.*, 1975). As surfactant stabilises distal airsacs and reduces the likelihood of collapse at end-expiration, surfactant deficiency, as can occur following premature birth, can cause severe respiratory distress (Jobe & Ikegami, 1987). The production of surfactant is a key stage of late lung development, with exogenous surfactant treatment significantly decreasing morbidity and mortality in preterm infants (Soll, 2000).

1.2 Fetal Pulmonary Haemodynamics

Fetal pulmonary haemodynamics are very different to the newborn and adult, with the majority (~90%) of right ventricular output bypassing the fetal lungs and flowing directly from the main pulmonary artery into the descending aorta, due to the presence of the ductus arteriosus (DA) (Figure 1.3) (Rudolph, 1985). Blood flow towards the lungs, through the left and right pulmonary arteries, occurs only briefly during systole with retrograde flow occurring during late systole and most of diastole (Figure 1.4) (Crossley *et al.*, 2009). This backward flow is due to the reflected pressure waves from the highly constricted pulmonary vascular bed and the presence of the DA offering an alternative low-pressure shunt (Rudolph, 1979; Grant *et al.*, 1999). Fetal PBF thus fluctuates around 0 ml/min over the cardiac cycle, being directed through the DA throughout both systole and diastole into the systemic circulation (Polglase & Hooper, 2006). This state of the pulmonary circuit is maintained by multiple mechanisms, and influenced by a number of factors, that are also involved in the fall in PVR immediately after birth (Gao & Raj, 2010).

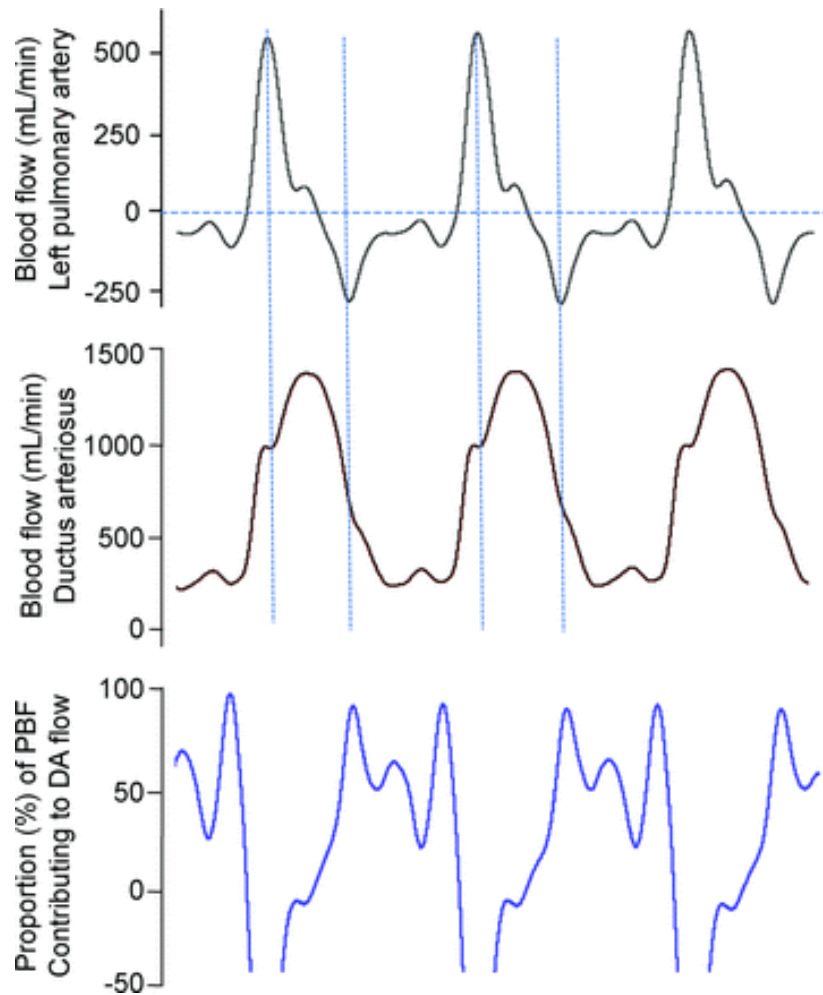


Figure 1.4: Blood flow waveforms recorded in the left pulmonary artery (top panel) and ductus arteriosus (middle panel) acquired over 3 consecutive cardiac cycles from a fetal sheep

The bottom panel shows the percentage of total pulmonary blood flow (PBF) contributing to right-to-left (from pulmonary into systemic circulation) flow of blood through the ductus arteriosus. Negative PBF values (top panel) indicate retrograde flow of blood away from the lungs.

From Crossley et al. (2009)

1.2.1 Maintenance of a high pulmonary vascular resistance

The vascular resistance of the fetal pulmonary circuit is much higher than the newborn and adult, and rapidly decreases to 10% of the fetal value of 0.26 kPa.min.kg/mL in lambs following ventilation and oxygenation at birth (Teitel *et al.*, 1990). Maintenance of this elevated PVR in the fetus is due to a combination of factors, that include low rates of vasodilator production, increased production of vasoconstrictors and the developing state of the microvasculature (Ghanayem & Gordon, 2001). In addition, although lung expansion is critical for fetal lung development, the expanding influence of lung liquid compresses the small pulmonary vessels, which contributes to a higher PVR (Walker *et al.*, 1988; Hooper, 1998). The low density of pulmonary vessels as the fetus develops translates to a lower cross-sectional area of the vascular bed (Levin *et al.*, 1976). These pulmonary vessels also have relatively thick, muscular walls, which contributes to a higher PVR (Hislop & Reid, 1972; Levin *et al.*, 1976). Moreover, throughout fetal development pulmonary fetal blood has a relatively low PO₂ and is relatively hypercapnic and acidotic, all of which contribute to vessel constriction (Rudolph & Yuan, 1966).

The heightened vasomotor tone of fetal pulmonary vessels contributes to an elevated PVR and is sensitive to a number of physiological stimuli, with increasing reactivity amid advancing gestation. Studies such as those performed by Lewis *et al.* (1976) showed that PVR becomes sensitive to small changes in PO₂ from about mid-gestation onwards, with alterations in PO₂ having a greater effect as gestation progresses. This observation is reinforced by elevated blood oxygenation in human pregnancies, which increases PBF in near term fetuses (31-36 weeks) but not in midterm fetuses (Rasanen *et al.*, 1998). In addition, reductions in fetal PaO₂, induced by ventilating ewes with low oxygen gas mixtures, cause pulmonary vasoconstriction (Cohn *et al.*, 1974; Lewis *et al.*, 1976). Blood oxygenation acts

directly to cause vasodilation via mitochondria (e.g. via altering sarcoplasmic reticulum Ca^{2+} release), as well as through vasodilator mediators such as nitric oxide (NO) (Weissmann *et al.*, 2006). Endothelin-1 (ET-1), a vasoconstrictor produced mainly in endothelial cells as well as pulmonary arterial smooth muscle cells and lung fibroblasts, is an important contributor to fetal PVR (Ivy *et al.*, 2000). ET-1 and ET-1 receptor expression increases during gestation and decreases after birth (Levy *et al.*, 2005), with impaired clearance of ET-1 associated with the development of persistent pulmonary hypertension of the newborn (PPHN) (Abman, 2007). Despite this, experiments in fetal sheep have shown that a reduction in ET-1 prior to birth is not necessarily associated with a fall in PVR, suggesting that other factors have a more significant role (Ivy *et al.*, 2000).

1.2.2 Fetal breathing movements

Fetal breathing movements (FBMs), caused by rhythmical contractions of the fetal diaphragm, occur around 30-40% of the time in late gestation and have been described in many mammals (Dawes *et al.*, 1972). These movements are important for normal pulmonary maturation, although it is unclear whether the absence of phasic stretch or a prolonged reduction in lung expansion are responsible for lung hypoplasia associated with the abolition of fetal breathing movements (Adzick *et al.*, 1984). FBMs strongly influence fetal pulmonary hemodynamics, with episodes of vigorous FBMs leading to significant changes in PBF and PVR (Polglase *et al.*, 2004). These transient increases in PBF associated with FBMs are unlikely to be mediated by vasodilators but were thought to result from transmural pressure changes across the capillary-alveolar wall (Polglase *et al.*, 2004).

Hypoxia has been shown to suppress FBMs, by altering the neural output of the respiratory centre in unanaesthetised fetal sheep (Maloney *et al.*, 1975) The inhibitory input into the

respiratory centre has been localised to the upper lateral pons region in fetal sheep (Gluckman & Johnston, 1987). Overall, the series of rhythmic contractions during FBMs appear to assist the lung in preparing to replace lung liquid with air at birth, contributing to normal lung differentiation and growth (Davis & Mychaliska, 2013).

1.3 Transitional Mechanisms: Adapting to Air Breathing at Birth

The cardiopulmonary system undergoes a significant transition at birth, to prepare for an immediate and significant shift in hemodynamics required to adapt to newborn life. The rapid switch of gas-exchange organ from the placenta to the lungs poses a major challenge for newborns, with the vascular activity of the pulmonary vascular bed directly influencing this process (Teitel *et al.*, 1990). Following lung aeration the pulmonary vessels markedly vasodilate, allowing the lungs to transition into the postnatal phenotype of high perfusion and low vascular resistance (Dawes *et al.*, 1953; Fineman *et al.*, 1995). The adaptation of the lungs at birth is part of a series of interrelated events, involving the removal of the placental circulation, the clearance of airways of liquid and the adjustment of the heart and blood vessels to an altered load distribution (Rudolph, 1985).

1.3.1 Lung aeration at birth: the first breath

The entry of air into the lungs induces a dramatic transformation of the lung phenotype, the first postnatal breaths establishing an air-liquid interface across the entire luminal surface (Hooper & Harding, 2005). During fetal life the airways are liquid-filled and replacing this fluid with air, which is compressible, at birth increases the tendency of the lung to collapse (Hooper & Harding, 2005). Despite the presence of surfactant, the development of surface

tension also increases the lungs' recoil properties (Kikkawa *et al.*, 1975). While the mature adult chest wall counters lung collapse, the newborn chest wall is very compliant, taking upwards of two weeks to stiffen (Avery & Cook, 1961; Papastamelos *et al.*, 1995). This limitation increases the difficulty for newborn infants to establish and maintain a functional residual capacity (FRC), requiring it to adopt mechanisms to assist this process. Siew *et al.* (2009b) demonstrated that the majority (~95%) of lung aeration was the result of inspiratory effort, which generates large transepithelial pressures during air-breathing which clears the airways of liquid. FRC is also maintained by expiratory braking manoeuvres, where expiratory airflow is restricted or stopped, which extends expiratory flow time and increases passive expiratory airway pressures (Kosch & Stark, 1984). These manoeuvres increase in frequency as FRC increases after birth, with air movement into the lungs critical for the proper removal of lung liquid (Siew *et al.*, 2009b).

1.3.2 Fetal airway liquid clearance

Clearance of lung liquid at birth is thought to occur through three main mechanisms. These include: (i) the reversal of the Cl^- ion gradient across the pulmonary epithelium, which is responsible for airway liquid secretion during fetal development (Olver *et al.*, 1986), (ii) postural changes which increase transpulmonary pressures and force liquid out through the nose and mouth during labour and delivery (te Pas *et al.*, 2008); and (iii) the generation of transpulmonary pressure with inspiratory efforts at birth (Hooper *et al.*, 2007; Siew *et al.*, 2009b). Vaginal birth causes a large increase in circulating adrenaline, which stimulates active sodium (Na^+) transport through Na^+ channels on the pulmonary epithelial surface (Brown *et al.*, 1983). With a net increase in Na^+ and Na^+ linked Cl^- movement across the epithelium from the lumen into lung interstitial tissue, the osmotic gradient reverses and this promotes airway liquid reabsorption (Olver *et al.*, 1986). Uterine contractions during labour

also impose major postural changes in the infant leading to increased dorsoventral flexion at the level of the fetal trunk. This generates significant abdominal pressure, leading to upward displacement of the diaphragm which reduces thoracic volume and forces liquid out of the lungs (Harding *et al.*, 1990). However, after birth considerable evidence demonstrates that lung inflation clears any remaining liquid through generation of a hydrostatic pressure gradient across the airway wall during inspiration (Siew *et al.*, 2009b).

Lung aeration has been observed using phase contrast (PC) X-ray imaging in newborn rabbits, which is able to image the movement of air and liquid with very high resolution. Significant liquid clearance can be observed by imaging over the first 5 inflations when very large tidal volumes are applied during mechanical ventilation (Siew *et al.*, 2009b). This clearance is enhanced with the use of a positive end-expiratory pressure (PEEP), without which liquid re-enters small airways during expiration, particularly in the immature lung (Siew *et al.*, 2009a). This rate of liquid clearance is orders of magnitude higher than what can be achieved by stimulation with adrenaline in late gestation fetuses (Jain & Eaton, 2006; Hooper *et al.*, 2007). This mechanism also allows infants born by Caesarean section without labour, or very prematurely when Na^+ reabsorption is ineffective, to clear their airways of liquid (Hooper *et al.*, 2015). Since the rate of liquid clearance from the airways exceeds the rate of removal from lung tissue, lung liquid accumulation in the interstitial tissue causes the temporary formation of perivascular fluid cuffs around large blood vessels and airways (Bland *et al.*, 1980). This leads to an increase in interstitial pressure, as observed in rabbit kittens after birth, that is similar to pulmonary edema in adults and reaches maximal values 30 minutes after birth (Miserocchi *et al.*, 1994). This liquid is gradually removed from lung tissue primarily via the blood vessels and lymphatics, with the cuffs disappearing and interstitial tissue

pressures decreasing by ~6 hours post-birth (Adams *et al.*, 1971; Bland *et al.*, 1980; Bland *et al.*, 1982).

1.3.3 Neonatal vascular remodelling

While the right ventricle is more dominant in the fetus and the right and left ventricular wall thicknesses are similar before birth, after birth and with separation of the circulations left ventricular afterload increases whereas right ventricular afterload decreases. As a result, the left ventricular wall becomes progressively thicker during childhood, whereas the right ventricular wall becomes thinner (Hew & Keller, 2003). The newborn cardiovascular system rapidly adjusts to independence from the mother, with the removal of the vascular features that were required for surviving intra-uterine life but become detrimental after birth.

1.3.3.1 Clamping of the umbilical cord

A significant proportion of fetal cardiac output flows through the placenta, with the placenta containing approximately 110 mL/kg of fetal weight (Wardrop & Holland, 1995). The placenta receives 30-50% of fetal cardiac output, but this varies and decreases with increasing gestational age as the relative weight differences between the fetus and the placenta change (Crossley *et al.*, 2009). Immediate clamping of the umbilical cord at birth separates the blood volume remaining in the placenta from the newborn, and venous blood returning to the heart is lost. As umbilical blood flow represents a substantial component of cardiac output (30-50%), this loss of umbilical venous return causes a substantial reduction in cardiac output (Crossley *et al.*, 2009; Bhatt *et al.*, 2013). Loss of the low-resistance placental circuit also results in an increase in systemic vascular resistance, with associated increases in arterial pressure in the carotid and pulmonary arteries if cord clamping occurs before ventilation onset

(Bhatt *et al.*, 2013). This reduction in venous return and cardiac output is only restored following the redistribution of blood flow towards the lungs with lung aeration at birth (Bhatt *et al.*, 2013; Polglase *et al.*, 2015). The timing of this sequence of events is therefore imperative, with much recent focus placed on the optimal sequence of birth events (Kluckow & Hooper, 2015).

Randomised control trials, such as those conducted by Andersson *et al.* (2011), have demonstrated that delayed umbilical cord clamping results in improvements in iron status and lower incidence of iron deficiency at 4 months of age when compared with early clamping. Delayed cord clamping allows for the lungs to aerate fully and the pulmonary transition to complete, which helps mitigate the detrimental but inevitable impacts of placental removal (Bhatt *et al.*, 2013). The pulmonary transition is central to these benefits, as circulatory stability afforded by delayed cord clamping facilitates systemic and cerebral oxygenation during the transition (Polglase *et al.*, 2015).

1.3.3.2 Closure of the ductus arteriosus

With clamping of the umbilical cord, the loss of venous return to the heart reduces right atrium pressure, which together with the increase in pulmonary perfusion associated with lung aeration, increases left atrial pressure above right atrial pressure which promotes closure of the foramen ovale (Dawes *et al.*, 1955). While the closures of these shunts follow straightforward mechanics, the haemodynamics of the DA closure are more complex (Crossley *et al.*, 2009). The reduction in PVR due to lung aeration and the increase in systemic vascular resistance caused by cord clamping leads the pressure gradient across the DA to reverse. As a result, the continuous right-to-left flow of blood across the DA reverses and becomes predominantly left-to-right, with blood flowing from the descending aorta into

the pulmonary circulation (Figure 1.5); this flow contributes significantly to neonatal PBF immediately after birth (Crossley *et al.*, 2009). This blood flow across the DA is very dynamic and bidirectional over the cardiac cycle, passing right-to-left briefly during the beginning of systole and then mostly flowing left-to-right at the end of systole and throughout most of diastole. The flow wave steadily reduces as the duct closes via smooth muscle constriction (Crossley *et al.*, 2009). This turbulent flow and consequent shear stress likely contributes to the closure of the DA via release of vasoconstrictive factors from the endothelium (Abman & Accurso, 1989). Similarly, increased oxygen levels from ventilation and a decrease in circulating prostaglandin E2, due to cord clamping and the loss of placental production also likely contribute (Heymann *et al.*, 1976). Functional closure of the three fetal shunts usually occurs within 48 hours of birth, with anatomical closure as a result of tissue proliferation occurring later (Moss *et al.*, 1963; Coceani & Olley, 1988).

1.3.4 Hypoxic pulmonary vasoconstriction

Aeration of the lungs at birth produces the need to proportionally adjust local blood flow with local ventilation for efficient gas-exchange. Indeed, the adult lung has a robust mechanism for adjusting shunt fraction and matching perfusion to differing local tissue aeration. Hypoxic pulmonary vasoconstriction (HPV) is a multifactorial response of muscular resistance arteries to alveolar hypoxia, a complex phenomenon that remains not fully understood (Sylvester 2012). This mechanism involves multiple oxygen sensory signalling components, including mitochondria within smooth muscle cells (Waypa *et al.*, 2001; Sylvester *et al.*, 2012), that increase potassium channel activity in pulmonary vessels (Post *et al.*, 1992). Unlike in the systemic circulation, the response to local hypoxia in pulmonary blood vessels is vasoconstriction, occurring mostly in small pulmonary arteries but also throughout the

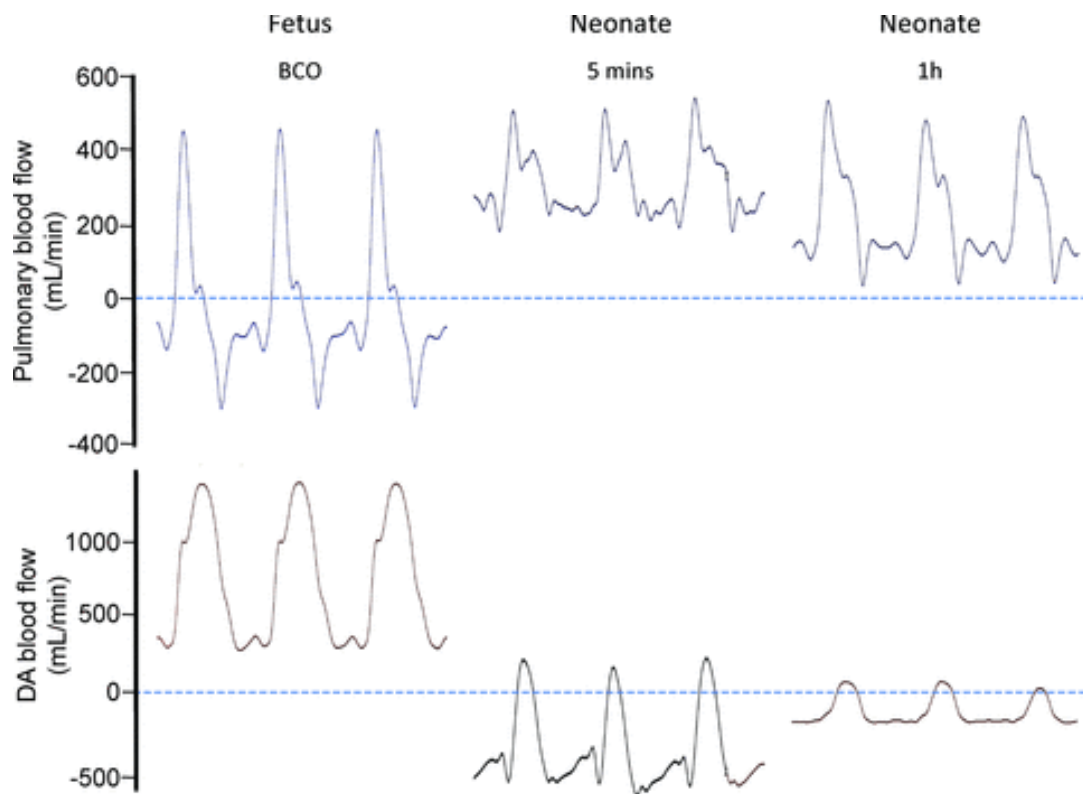


Figure 1.5: Examples of the blood flow wave forms recorded in the left pulmonary artery (top panel) and in the ductus arteriosus (DA) in the fetus (before umbilical cord occlusion; BCO) and in the neonate at 5 min and 1 h after the onset of ventilation

Negative values of pulmonary blood flow indicate retrograde flow away from the lungs, whereas negative blood flow values through the DA indicate flow that is directed from the systemic (aorta) into the pulmonary circulation.

From Crossley et al. (2009)

pulmonary vascular bed (Stroud & Rahn, 1953; Schwenke *et al.*, 2008). The full extent of O₂ sensory mechanisms is still under much debate, with multiple mechanisms likely acting in concert. Nevertheless, it is likely located within smooth muscle cells as HPV persists in isolated smooth muscle cells, endothelium-denuded arteries as well as in intact, denervated lungs (Robin *et al.*, 1987; Murray *et al.*, 1990; Post *et al.*, 1992). Although seemingly not essential for initial HPV, the endothelium and pulmonary innervation appear to provide a strong modulatory influence (Brimioulle *et al.*, 1997; Liu *et al.*, 2001; Robertson *et al.*, 2003).

The precise time during development that the lung becomes capable of HPV is unclear, but is likely to be related to the gestational sensitivity to PO₂. On this basis, it has been suggested to develop within the middle of the third trimester of gestation in humans (Morin & Egan, 1992). During late gestation, the total number of resistance vessels increases 10-fold, as the cross-sectional area of the vascular bed dramatically increases. This would be expected to cause a major drop in PVR but it only results in a small increase in PBF, from 3.5% to 7% of fetal cardiac output. This indicates that HPV or some other mechanism is active in maintaining a relatively high PVR in the fetus (Rudolph, 1979; Morin & Egan, 1992). Thus, active modulation of HPV is thought to be critical to the distribution of perfusion to the newly inflated lung regions as the successful fetal-to-neonatal transition is highly dependent on the capability of the lungs to receive the full cardiac output at birth.

1.4 Regulation of the Pulmonary Vasomotor Tone in the Perinatal Period

Management of the cardiovascular system, in both the adult and in the transitional period at birth, is a complex coordination between the central and peripheral components of the

autonomic system, endocrine and paracrine regulatory mechanisms, the cardiovascular system itself, and renal function (Gao & Raj, 2010). The physical forces of lung movement are also influential, including the pressure across tissue walls and generation of shear stress within vessels consequent to the abrupt increase in PBF at birth (Storme *et al.*, 1999; Polglase & Hooper, 2006). As vasomotor tone can be detected in the human fetal pulmonary circulation by the last trimester of pregnancy (Rasanen *et al.*, 1998), the pulmonary circulation is well prepared to rapidly alter blood flow distribution at birth.

1.4.1 Mechanical factors

Lung movement itself influences PVR both before, as demonstrated by fetal breathing movements, and after birth, alongside the additional forces caused by the entry of air into the lungs (Polglase & Hooper, 2006). The replacement of airway liquid with air reduces PVR, through the development of surface tension in the alveoli and a consequent increase in transmural pressure across airway/capillary walls, which dilates capillaries (Leffler *et al.*, 1984; Hooper, 1998). The increase in lung recoil caused by surface tension within the distal airways not only decreases interstitial tissue pressures, but also increases capillary wall transmural pressures and in effect pulls the capillaries open ((Reynolds, 1956; Hooper & Harding, 2005). Similarly, alterations in alveolar/capillary wall transmural pressures are a major influence on PVR within the mature lung, with vessel recruitment following an increase in cardiac output leading to a reduction in PVR (Fuhrman *et al.*, 1986). Furthermore, large inspiratory efforts in the fetus transiently increase PBF, again due to increase in capillary/airway wall transmural pressure. In contrast, increases in airway pressure reduce the capillary/airway wall transmural pressure causing capillary collapse and an increase in PVR (Fuhrman *et al.* 1986). Additionally, increased shear stress within blood vessels resulting from increases in PBF also stimulate vasodilation, via activation of potassium channels, which lead

to membrane hyperpolarization and Ca^{2+} channel closure (Storme *et al.*, 1999); shear forces also stimulate an increase in NO synthesis via the vascular endothelium (Wedgwood *et al.*, 2001).

1.4.2 The endothelium

The endothelium is a single layer of cells that forms the interface between the blood and vascular smooth muscle and has a substantial role in regulation of vasomotor tone in the fetus and newborn (Luscher, 1990). It performs this role by generating a variety of vasoactive mediators that act in a paracrine fashion on the surrounding vascular smooth muscle cells. These include NO and prostacyclin as vasodilators and ET, which can act as both a vasoconstrictor via binding to ET_A receptors and a vasodilator by binding to ET_B receptors to cause NO release (Leffler *et al.*, 1984; Heymann, 1999). The endothelium also regulates smooth muscle growth and proliferation, which can alter the vascular structure present in the lungs (Hirschi *et al.*, 1999). With this delicate monolayer acting as both sensor and effector to vascular resistance modulation, it is highly active in the perinatal period (Luscher, 1990).

1.4.2.1 Nitric oxide

NO is well known to be a potent vasodilator, via acting on smooth muscle which lines blood vessels, and has a key role in the control of pulmonary transition at birth (Abman *et al.*, 1990). Synthesised on demand by the conversion of L-arginine to L-citrulline, via nitric oxide synthase (NOS), NO is released from endothelial cells in response to stimuli such as bradykinin, an inflammatory mediator released at birth in response to lung expansion and oxygenation, as well as acetylcholine (ACh) and shear stress (Heymann *et al.*, 1969; Lu & Kassab, 2011). NO then acts on vascular smooth muscle cells to cause muscle relaxation and

vessel dilatation, through activation of soluble guanylyl cyclase (sGC) which catalyses a cascade of molecules to decrease calcium ion concentration (Moro *et al.*, 1996). Oxygen has various intermediates to NO synthesis, including bradykinin and ET-1 (via the ET_B receptor), which bind to endothelial cells. Oxygenation can also inhibit the activity of phosphodiesterase 5 (PDE5), which breaks down cyclic guanosine monophosphate (cGMP), thereby enhancing vasodilation (Hanson *et al.*, 1998a; Hanson *et al.*, 1998b). Increased oxygenation also upregulates the expression and activity of sGC and cGMP-dependent protein kinase (PKG), which mediates the effects of cGMP and opposes muscle contraction (Moro *et al.*, 1996).

The activity of NOS increases during the last trimester of gestation and its expression is up-regulated further at birth (Arrigoni *et al.*, 2002); ventilation of lambs with 100% oxygen gas has been found to increase endothelial NOS (eNOS) mRNA expression within the endothelium of both small and large pulmonary blood vessels (Black *et al.*, 1997). Conversely, inhibition of NOS attenuates the fall in PVR at birth and can be demonstrated using derivatives of L-arginine with modified methyl or nitrogen groups, which impede the production and subsequent effects of NO (Abman & Accurso, 1989; Tikitsky & Morin, 1993; Rairigh *et al.*, 2001). Experiments in term lambs treated with NG-monomethyl-L-arginine reversed the increase in PBF at birth, while those treated with NG-nitro-L-arginine experienced a diminished PBF increase, which then reduced to negligible levels by the end of the experiment (Tikitsky & Morin, 1993). Despite extensive research on this area, the active role of oxygen and molecules such as NO are not fully understood. Work by Sobotka *et al.* (2011) demonstrated that lambs experiencing a decrease in PaO₂ after birth, due to poor lung aeration, displayed a large increase in PBF that was identical to lambs experiencing a normal increase in PaO₂ after birth. Although much of the literature suggests oxygenation is a crucial

component of the pulmonary transition at birth, the full extent of the contributing factors has yet to be established.

1.4.2.2 Prostaglandins

Prostaglandins (PGs), which are important mediators of biological function, are mostly synthesised by the endothelium on demand and have a very diverse range of actions, including potent effects on vascular tone (Challis *et al.*, 1976). Vasodilator PGs bind to smooth muscle cell membrane receptors to activate adenylyl cyclase, which increases cytosolic cyclic adenosine monophosphate (cAMP) concentrations, leading to reduced calcium levels and therefore lowering vasomotor tone (Armstead, 1995). PGs play critical roles during development, changing in synthesis and type of PG synthesised over the course of gestation (Challis *et al.*, 1976). Early in gestation, the major PG released is PGF_{2α}, which is a vasoconstrictor, while closer to term vasodilatory prostaglandins are released such as prostacyclin (PGI₂) as well as PGE₂ (Challis *et al.*, 1976; Lévy *et al.*, 2005). Leffler *et al.* (1984) have shown that the onset of ventilation is associated with the intrapulmonary synthesis of PGI₂. Another study by Velvis *et al.* (1991) demonstrated that rhythmic distension of the lungs stimulates the release of vasodilatory prostaglandins and decreases PVR, and that inhibition of synthesis opposed the fall in PVR in response to ventilation with a hypoxic gas mixture. This study also showed the independent effects of ventilation with oxygen on PVR, as inhibition of PGs still led to a 12-fold decrease in PVR in lambs ventilated with either air or 100% oxygen (Velvis *et al.*, 1991).

While PGs are not as significant in birth-related changes in PVR as oxygenation (Velvis *et al.*, 1991), they may contribute via multiple pathways; for instance PGI₂ may also act to stimulate NO release (Zenge *et al.*, 2001). Other stimuli that evoke PGI₂ release during birth

include shear forces, bradykinin, both in intact lungs and endothelial cells in culture, and angiotensin II, which increases in concentration at birth (Dusting *et al.*, 1981; van Grondelle *et al.*, 1984; McIntyre *et al.*, 1985; Frantz *et al.*, 1989). The actions of prostaglandins are complex, with prostaglandin D₂ (PGD₂) acting as a vasodilator only in fetal goats and a vasoconstrictor in older animals (Soifer *et al.*, 1983). PGD₂ is released from mast cells, which have been shown to increase at the end of gestation and decrease following birth. Combined with its action as a vasodilator only in this period suggests a role for PGD₂ in the perinatal PVR changes. As the fall in PVR at birth is likely to be a combination of both an increase in vasodilators as well as a decrease in vasoconstrictors, of interest are the vasoconstrictory leukotrienes and thromboxanes, which are related to the PG synthesis pathway from arachidonic acid (Shimizu & Wolfe, 1990). Treatment of fetal lambs with a leukotriene receptor blocker and newborn lambs with a thromboxane A₂ inhibitor both reduced PVR markedly, implicating these molecules in this complex process (Soifer *et al.*, 1985; Tod & Cassin, 1985).

1.4.2.3 *Endothelin-1*

Endothelins are a family of endothelium-derived peptides, with the predominant vasoactive isoform, ET-1, modulating perinatal pulmonary vasomotor tone and contributing to DA closure after birth (Coceani *et al.*, 1992; Ziegler *et al.*, 1995). ET-1 is synthesised and released in response to stimuli such as hypoxia, an increase in pressure and shear forces (Ziegler *et al.*, 1995; Lu & Kassab, 2011). Released ET-1 then binds to either the receptors ET_A on smooth muscle cells, causing vasoconstriction by elevating intracellular calcium, or ET_B on endothelial cells, causing vasodilation via NO and PGI₂ pathways (Ivy *et al.*, 1994; Heymann, 1999). While *in vivo* data establishing ET-1 as an important factor in the transitional changes in the pulmonary circulation is mixed (Winters *et al.*, 1996; Ivy *et al.*, 2000), some studies

suggest a notable contribution (Ivy et al., 2000; Ivy et al., 2004; Levy et al., 2005). In ovine fetuses, the mRNA concentrations of ET-1 and ET_A peak at around 125-130 days of gestation and then decline at the end of term prior to birth along with the related PVR fall (Ivy et al., 2000); as PVR remains high during this period, this implies only a modest role for ET-1 in modulating perinatal PVR. While ET receptor blockade appears to have little effect on fetal pulmonary vasomotor tone (Ivy et al., 2004) or the *in utero* ventilation of term lambs with oxygen (Winters et al., 1996), specific blockade of ET_B has been found to dampen the reduction in PVR with ventilation and oxygenation at birth (Ivy et al., 2004). Indeed, in human fetuses, the expression of ET_B is most abundant at term and becomes greater than ET_A (Levy et al., 2005). As ET-1 infusion has been shown to either cause arterial dilation or constriction depending on the dose and gestational age in animal studies (Tod & Cassin, 1992; Ivy et al., 1997; Ivy et al., 2000). However, the net effect in humans at birth is likely to be a balance between the opposing effects of ET_A and ET_B receptor activation.

1.4.2.4 *Platelet activating factor*

Platelet activating factor (PAF) is an endogenous phospholipid active in a multitude of roles as an inflammatory mediator and vasoconstrictor, thought to contribute to the high fetal PVR (Ibe *et al.*, 1998). Released from a number of cells, including endothelial cells and smooth muscle cells, PAF is particularly active in the pulmonary circulation. Stimulated by hypoxia, PAF activates PAF receptor (PAF-R) to increase intracellular inositol triphosphate levels, which increases sarcoplasmic reticulum calcium release and thus, muscle contraction (Uhlig *et al.*, 2005). Studies by Ibe *et al.* (1998) have shown that circulating levels of PAF are high during fetal life, with levels decreasing by fivefold at birth. Experiments that infused PAF in guinea pig lungs induced pulmonary hypertension, while treatment of term lambs with PAF-R antagonist led to a 68% reduction in PVR when lungs were pre-treated by PAF (Hamasaki *et*

al., 1984; Ibe *et al.*, 1998). Additionally, expression and levels of acetylhydrolase, which inactivates PAF, is upregulated in the newborn period (Ibe *et al.*, 2000). These series of experiments suggest the downregulation of PAF expression and activity contribute to the modulation of PVR at birth.

1.4.4 Circulating vasoactive substances

While many locally generated vasoactive substances influence PVR, the lung is also involved in the interaction, production and degradation of circulating substances. As such, the switch from the placenta to the lungs as the organ of gas-exchange also likely changes the bioactivity of some circulating hormones. The lungs are a major site of noradrenaline release and clearance in the perinatal period (Smolich *et al.*, 1997) and are also a major site of prostaglandin metabolism.

Noradrenaline can act as a vasodilator, likely through NO pathways as its effect is abolished with inhibition of NOS in lambs (Jaillard *et al.*, 2001). These experiments also showed that infusion of dopamine has little effect at low doses, but increases PVR when the dose was doubled to 10 µg/kg/min. Antenatal glucocorticoids mainly augment pulmonary vascular reactivity in response to vasodilatory stimuli such as prostaglandins and NO, acting via enhancement of sGC and adenylyl cyclase activity (Zhou *et al.*, 1996; Gao *et al.*, 1998). Similarly, hormones such as adrenomedullin (Takahashi *et al.*, 1999), as well as estrogens and natriuretic peptides provide an indirect vasodilatory influence on PVR (Cargill & Lipworth, 1996; Parker *et al.*, 2001; Lahm *et al.*, 2008). The primary role of these substances appears to be minor modulation and facilitation of the PVR changes in the birth transition, with substances such as adenosine acting as mediators of oxygen-induced pulmonary vasodilatation (Konduri *et al.*, 1993).

1.4.5 Pulmonary innervation

The pulmonary circulation is well innervated with the autonomic branches of the sympathetic and parasympathetic fibres as well as sensory nerve fibres (Downing & Lee, 1980; El-Bermani *et al.*, 1982). In the fetal lung, the elevated vasomotor tone of the pulmonary vasculature is highly sensitive to autonomic agonists (Colebatch *et al.*, 1965). Acetylcholine (ACh) released from parasympathetic nerve terminals causes pulmonary vasodilation via the production of NO from L-arginine (Colebatch *et al.*, 1965; Rairigh *et al.*, 2001), with work by Rairigh *et al.* (2001) demonstrating ACh-induced vasodilation was abolished with non-selective NOS blockade. The sensitivity to ACh develops from around mid-gestation onwards, during the same period as the sensitivity to oxygen (Lewis *et al.*, 1976). Although parasympathetic signalling via the vagus nerve does not appear to modify basal pulmonary vascular tone under normal circumstances, which was demonstrated via little effect elicited from vagotomy in lambs, stimulating the cut ends of the vagus nerve induces pulmonary vasodilation (Colebatch *et al.*, 1965). The study by Colebatch *et al.* (1965) also showed that sympathetic nervous activity contributes to the highly constricted pulmonary vascular bed, as bilateral thoracic sympathectomy in lambs initiated pulmonary vasodilation and direct stimulation of these nerves initiated vasoconstriction. Hence, pulmonary innervation can be considered as being functional in the perinatal period and can be activated by a number of stimuli and receptor pathways.

Multiple sensory reflexes are present at birth, including the Hering-Breuer, carotid body and pulmonary respiratory chemoreceptor reflexes (Dawes & Mott, 1959). The sensory pathways from the lungs are principally mediated by the vagus nerve and associated afferent endings, the bronchopulmonary C-fibres. Mechanoreceptors involved in these nerve endings and autonomic reflexes include stretch receptors, activated by lung inflation, and juxtacapillary (J)

receptors, which are activated by pulmonary congestion and a rise in interstitial tissue pressure (Paintal, 1969). Whether the development of pulmonary congestion with lung liquid clearance relates to the PVR changes at birth is unclear, but some studies suggest impaired vagal signaling has a detrimental effect on newborn PBF (Wong *et al.*, 1998). Experiments on newborn lambs with intrathoracic vagal denervation show that selectively denervating the lungs caused respiratory failure and a failure to increase arterial oxygenation at birth (Wong *et al.*, 1998; Lalani *et al.*, 2002). This is thought to result from a reduced breathing rate and lower functional residual capacity (Wong *et al.*, 1998; Lalani *et al.*, 2002), although possibly relating to a failure to increase PBF (Wong *et al.*, 1998). Subsequent studies failed to confirm a role for vagal denervation in the increase in PBF at birth (Hasan *et al.*, 2000) but separating out all of the contributing factors that may regulate PBF in that experimental model was problematic. While the active role of the autonomic system in the perinatal period is well represented in the literature, the full extent to which birth-related stimuli might activate these pathways has yet to be established.

1.5 Evaluating Current Problems

Gaps in our current knowledge about the newborn transition hinder efforts to target strategies to help vulnerable newborns. Over one-fifth of Australian births in 2013 required some form of active resuscitation, with about a third of those babies receiving ventilatory assistance (Eldridge *et al.*, 2015). Recent studies in very preterm lambs, similar to humans born prior to 28 weeks of gestation, suggest the ability to raise PBF when mechanical ventilation is applied may be much lower than previously thought (Allison *et al.*, 2010). This study by Allison *et al.* (2010) indicates that mechanisms underlying the pulmonary transition at birth are still not fully understood, especially in the very immature lung. If the pulmonary vasculature fails to

dilate at birth, and PBF does not increase, the newborn can encounter multiple cardiorespiratory consequences. These include hypoxic/ischemic events, PPHN and patent ductus arteriosus, all of which carry serious risks of morbidity and mortality. The ability to improve health outcomes therefore relies on increasing understanding of the physiological processes involved on a basic level.

1.5.1 Consequences of a compromised fetal-to-neonatal transition

As the transition at birth comprises a series of complex pathways, a disruption of a number of events can result in serious consequences. Failure of the lungs to clear airway liquid and properly aerate is a major cause of neonatal dyspnea and respiratory-related morbidity (Jain & Eaton, 2006). The closure of the ductus arteriosus is an important stage in neonatal adaptation, distributing the entire load of the right ventricle towards the lungs. If a patent shunt persists beyond the first few days of life, this can cause major changes in the microcirculation of premature infants and lead to development of pulmonary hypertension, pulmonary haemorrhage and pulmonary edema as the pulmonary lymphatic vasculature becomes overloaded (Hiedl *et al.*, 2010).

Failure of PVR to fall at birth can relate to the serious disorder PPHN, involving a perpetuating cycle of increased PVR, reversal of blood flow across fetal shunts and lowered PBF, which exacerbates the resulting hypoxia (Ostrea *et al.*, 2006). PPHN can arise from a number of mechanisms such as maladaptation of the neonatal circulation, increased muscularisation of pulmonary arterioles and pulmonary hypoplasia, resulting in under-development of the pulmonary vascular bed (Walther *et al.*, 1993; Ostrea *et al.*, 2006). Even after intervention with treatments such as NO inhalation, mortality can still be 10-20% and survivors of PPHN can suffer from complications such as chronic lung disease, seizures and

neurodevelopmental problems (Berhrsin & Gibson, 2011). Although improvements in techniques in recent times have reduced the severity of health problems associated with premature birth, such as PPHN, respiratory distress syndrome and bronchopulmonary dysplasia, they remain serious health concerns (Moss, 2006; Ostrea *et al.*, 2006; Schellenberg, 2006; Bartle *et al.*, 2010).

1.5.2 Imaging the lung at birth

To properly appreciate the structural and functional changes in the perinatal pulmonary microcirculation, the ability to image the circulation within a closed-chest model is ideal. Difficulties in examining pulmonary dynamics during this period are exacerbated by the problems in real-time imaging of the lungs. As a low-density, soft tissue and air-filled organ, the lungs only weakly absorb X-rays, which leads to poor radiographic contrast using conventional techniques (Kitchen 2005). The development of phase contrast (PC) X-ray imaging, which uses synchrotron radiation as an X-ray source, has allowed imaging of the lungs with high temporal and spatial resolution down to the smallest air sacs. This technique avoids multiple problems associated with X-rays from conventional sources such as the requirement for inhalation of a contrast gas or long exposure times to obtain high contrast images. By using the phase change of coherent monochromatic X-rays as they propagate through objects with non-uniform refractive indices (e.g. air and water), image contrast can be greatly enhanced. Refraction of spatially coherent X-rays creates interference patterns over a sufficient propagation distance, generating a “speckle” pattern by refraction through millions of air-filled alveoli (Kitchen *et al.*, 2004). As the change from liquid- to air-filled lungs involves a significant change in relative refractive indices, this process is an ideal target for PC X-ray imaging.

X-ray generation by a synchrotron light source involves bending the path of electrons travelling close to the speed of light. The change in direction of the electron, results in acceleration of the electrons, which increases their energy state. The electrons release this energy in the form of light, with the photons generated at a tangent to the electron beam. The extremely intense beams of light produced by these facilities can be used to image from the atomic and molecular scale up to cells, tissues and whole organs in outstanding detail far superior to conventional X-rays (Kitchen *et al.*, 2005). The high coherence and brightness of these X-rays facilitates not only allows PC X-ray imaging, but also techniques such as angiography, allowing for high resolution imaging of the microvasculature in an intact animal with the use of a contrast agent (usually iodine). Studies by Schwenke *et al.* (2007) have demonstrated the effectiveness of synchrotron X-rays in visualising the distribution and dynamic changes in pulmonary microvasculature. Other studies by Hooper *et al.* (2007) have provided unique insights into lung liquid clearance at birth, which was only possible by using PC X-ray imaging with synchrotron radiation. These studies have been expanded to demonstrate image processing algorithms that can obtain quantitative information of lung gas volumes from single projection phase contrast X-ray image sequences (Siew *et al.*, 2009b). The ability to image intricate processes during the perinatal period, such as lung liquid clearance studies, allows for the potential to examine other aspects of the neonatal transition and expand current knowledge of this area.

1.6 Summary and Aims

The neonatal transition is a complex process, with many interconnected mechanisms still remaining to be fully understood. The efficient transferral from placenta to lungs as the organ of gas-exchange is reliant on the rapid relaxation of the pulmonary vasculature to decrease PVR from the high levels during fetal life, representing a delicate balance between the opposing factors causing vasodilation (e.g. NO, PGI₂) or vasoconstriction (e.g. ET-1, PAF). Despite much research in this area, our limited understanding about the relationships between aeration and perfusion in the lungs at birth makes it difficult to target improvements in outcomes to vulnerable newborns.

The studies in this thesis used simultaneous synchrotron microangiography and PC X-ray imaging to assess the spatial and temporal relationships between aeration and perfusion in the newborn lung immediately after birth; the factors that promote the increase in pulmonary perfusion relative to local aeration were examined. Specifically, the aims of this thesis were:

- ❖ **Aim 1:** To determine the spatial relationship between local aeration and perfusion in the newborn lungs immediately after birth
- ❖ **Aim 2:** To investigate the specific role of PO₂ on the increase and regional distribution of PBF immediately after birth
- ❖ **Aim 3:** To investigate the relative roles of vagal innervation and local PO₂ on the increase and regional distribution of PBF immediately after birth

Chapter Two

General Methodology

All animal procedures were approved by the Spring-8/ Japan Synchrotron Radiation Research Institute (JASRI), Japan, Animal Experiment Committee and Monash University's School of Biomedical Sciences' Animal Ethics Committee. All studies were conducted in experimental hutch 3 of beamline 20B2, in the Biomedical Imaging Center at the Spring-8 synchrotron, Japan.

2.1 Animal Experiments

Pregnant New Zealand white rabbits were housed at the Spring-8/JASRI animal holding facility at least five days before the experiment. Rabbits had constant access to food and clean water and were maintained in a 12 hour light (7am to 7pm) and dark cycle at an ambient temperature of 18-20 °C.

2.1.1 Pre-operative preparation

Experiments were performed on pregnant does at near-term 30 days of gestational age (term ~32 days). Following restraint within a box and transportation to the surgery room, fur overlying the doe's inner ear vein was shaved and applied with topical analgesia (2% lidocaine hydrochloride; Xylocaine jelly, AstraZeneca, Sweden). An ear vein catheter (24G Intracath, Becton Dickinson, USA) was then inserted into the vein, directed towards the heart. A saline-filled three-way stopcock was attached to the catheter and secured to the ear (Leukoplast Sleek tape, Smith & Nephew Healthcare Ltd., Australia). Anaesthesia was induced with a bolus of propofol (i.v.; 12 mg/kg bolus; Rapinivet, Schering-Plough Animal Health, Japan) via ear vein catheter. The doe was then removed from the box, placed on her side on a heat pad and anaesthesia was maintained by a continuous infusion of propofol (i.v.; 40 mL/hour of 10 mg/mL) using a syringe pump (CFV-3200; Nihon Kohden Co., Japan).

Intubation of the doe took place using an endotracheal (ET) tube (Portal Cole Neonatal Tube 2.5 mm I.D., 4 mm O.D.; Smiths Medical Australia, Australia) with the aid of a laryngoscope (Parker Healthcare Pty. Ltd., Australia). The intubated doe was then connected to a mechanical ventilator (Model 683 Rodent Ventilator; Harvard Apparatus Inc., USA) and ventilated at a rate of ~40-45 inflations/minute, tidal volume of 25 mL and a flow rate of 1.2 L/min of 60-100% oxygen. The propofol infusion was stopped and anaesthesia was then maintained by isoflurane inhalation (1.5–4%; Isoflu, Dainippon Sumitomo Pharma Co., Japan) for the remainder of the experimental period. Doe wellbeing was monitored via absence of withdrawal reflexes (corneal reflex and toe pinch reflex), measuring oxygenation and heart rate (using a pulse oximeter) and pupil diameter, with the isoflurane concentration adjusted accordingly.

2.1.2 Surgical procedure

2.1.2.1 Caesarean section

The doe was arranged supine on a heat mat, and fur located on the mid-ventral region of the abdomen was closely shorn (Oster® Golden A5, Sunbeam Products Inc., USA) from the umbilicus to the groin, taking care to avoid lacerating the nipples. Topical analgesic gel (lidocaine hydrochloride 2%) was applied liberally to the abdominal area as the intended incision site. A midline incision (~9 cm) was made through the abdominal skin, underlying fat and linea alba to expose the pregnant uterus. A small portion of one uterine horn was located and gently exteriorised, supported on a raised platform against the abdomen of the doe, shifted to the right lateral position. The location and orientation of kittens was determined by gentle palpation, with an additional application of lidocaine hydrochloride made on the surface of the uterus before an incision was made through the uterus and fetal membranes overlying each kitten's hind-limbs. Kittens were delivered sequentially and positioned supine

alongside its placenta, with an application of diclofenac sodium topical gel 1% (Voltaren Emulgel; Novartis Pharmaceuticals Australia Pty. Ltd., Australia) on the umbilical cord to prevent vasoconstriction of the placental blood supply. Fetal membranes were left intact over the nose and mouth of each kitten during surgery to prevent air from entering the lungs.

2.1.2.2 Kitten tracheotomy and jugular catheterisation

Following exteriorisation of a kitten from the uterus, it was immediately sedated with diluted sodium pentobarbitone (13 mg/kg *i.p.*; Somnopentyl, Kyoritsu Seiyaku Co., Ltd., Japan). Kitten wellbeing was monitored via absence of withdrawal reflex (toe pinch), with additional sodium pentobarbitone given accordingly. Topical analgesic gel (lidocaine hydrochloride) was applied to the skin overlying the trachea before a midline incision (~10 mm) was made in the anterior fetal neck. Underlying subcutaneous tissue was dissected away to expose the trachea, and a small horizontal incision (~1 mm) was made through the cricoid cartilage. Kittens in the vagotomy group of Chapter 5 underwent bilateral sectioning of the mid-cervical branches of the vagus nerve, with all other groups left with the vagus nerve intact. An ET tube (outer plastic shield of an 18G Intracath; Nippon Becton-Dickinson Co. Ltd., Japan) was inserted into the trachea, carefully directed into the right bronchus through arrangement of the kitten (described further in Section 2.2.2), and securely tied into place. ET tubes were plugged (at the hub end) to prevent air entry and bent at an angle of ~30° 15 mm from the tip of the catheter, assisting insertion into the trachea and right bronchus. An internal jugular vein (typically on the right side) was located and catheterised (24G Intracath; Nippon Becton-Dickinson Co. Ltd., Japan) for iodine administration, remaining plugged (at the hub end) to prevent bleeding out. The kitten's umbilical cord was occluded and ligated distal to the kitten and site of occlusion, then weighed and transferred to an upright Perspex frame and positioned inside the experimental hutch.

2.2 General Experimental Procedure

Kittens were arranged with their chest wall in the path of the X-ray beam, positioned for a posteroanterior projection, and the remaining fetal membranes over the nose and mouth were removed; a motorised control stage allowed fine control of kitten position. The ET tube was unplugged and joined to a three-way tap leading to an inspiration / expiration circuit connected to a purpose-built, time-cycled, pressure-controlled ventilator (Kitchen *et al.*, 2010). Electrocardiogram (ECG) leads were attached to the skin of the upper limb and upper abdomen, arranged diagonally at opposite points across the heart, and a heat lamp was adjusted to maintain a warm kitten body temperature. Ventilation parameters (airway pressure, tidal volume), heart rate and times when the shutter and detector were open or functional were recorded continuously using the program LabChart (ADInstruments, Australia). Immediately after preparations were completed, all personnel evacuated the hutch and the hutch door closing sequence commenced. Once the hutch was secured, the downstream X-ray shutter was opened and imaging recordings began (average of 2 min after umbilical cord ligation). At the conclusion of the ~13 minute experimental period (~10 minutes after ventilation onset for each kitten), animals were humanely killed with an overdose of sodium pentobarbitone (Pentobarbital; >100 mg/kg) administered *I.V.* (doe) or *I.P.* (kittens).

2.2.1 Details of beamline and PC X-ray imaging protocol

PC X-ray imaging (described previously in Section 1.5.2) at Hutch 3 was located ~210 m downstream of the bending magnet source, which greatly increases the coherence of illuminating X-rays. X-rays passed through the Si(111) monochromator to remove broad spectrum radiation, thus allowing the user to select a single X-ray energy (wavelength) for imaging. The downstream shutter, normally closed, prevented irradiation of the hutch when experimenters were inside, but was opened once the hutch was securely shut. The pre-object (fast) shutter was opened only when an image was acquired, thereby greatly reducing the radiation dosage received by the kitten. The cables from the detector and mechanical ventilator were passed outside of the hutch through the radiation-protective labyrinth to individual computers that controlled and recorded imaging and ventilation. A schematic of the PC X-ray imaging setup is depicted in Figure 2.1.

Imaging was achieved using monochromatic X-rays at 33.2 keV, just above the iodine K-edge, with a 1.0 m object-to-detector distance. Imaging at this energy utilises the sudden increase in attenuation of photons by iodine when they have more energy than the binding energy of the K shell electrons (K-edge), greatly increasing angiography contrast. Due to the posteroanterior projection, images were taken dorsally therefore all images and videos described in this thesis are such that the right lung is on the right side and left lung on the left side. The specific detector used and its pixel size differed between experiments and will be described in each chapter. Images were obtained with contrast agent injection according to each ventilation stage (detailed in Section 2.2.2), with the imaging briefly stopped when adjustments to the kitten ET tube were required. At the end of each experiment, the motorised stage moved the Perspex frame out of the field of view and ~20 flat-field images were obtained. The fast shutter was closed and ~20 dark-field images were recorded. PC X-ray

movies referred to in this thesis are PC X-ray images replayed in sequence with the same framerate (Hz) that they were obtained. These can be viewed via links in the appendix and in the supplementary data material found in the back cover of this thesis.

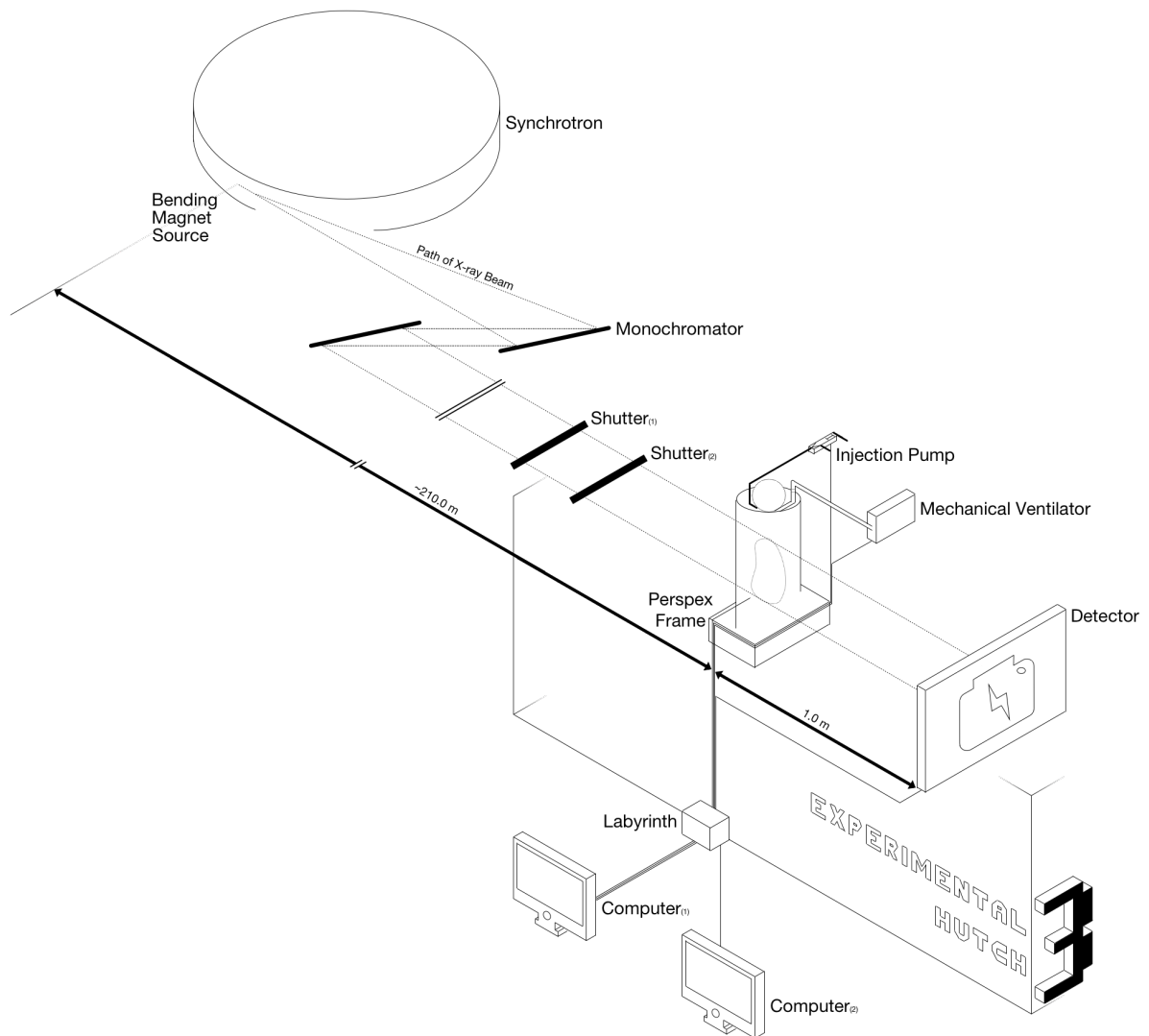


Figure 2.1: Schematic diagram of the PC-imaging process

X-ray beams from a bending magnet source at the SPring-8 synchrotron facility are directed through a monochromator, a downstream shutter (Shutter₍₁₎) and pre-object (fast) shutter (Shutter₍₂₎) before passing through a kitten in a Perspex frame ~210 m from the source. The detector recorded transmitted X-rays 1 m from the kitten. The shutters, ventilator, injection pump and detector were all controlled by and/or recorded from computers located outside the hutch by passing cables through a shielded labyrinth. Diagram is not drawn to scale.

2.2.2 Ventilation and angiography protocol

Once the kitten was in the experimental hutch and imaging had commenced, image sequences were obtained: before ventilation onset (not ventilated, NV), during initial mechanical ventilation of a single lung (at 30 sec after ventilation start), again during ventilation of a single lung (for an additional 2 minutes, both time points are referred to as unilateral ventilation; ULV) and finally following ventilation of both lungs in air for 2 minutes (bilateral ventilation: BLV). The second ULV imaging point was only added after Chapter 3 to observe the time-related effects of single lung ventilation and improve analysis. The initial inspired gas was either air (21% O₂; Chapter 3) or randomly divided into ventilation with 100% N₂, air or 100% O₂ (Chapters 4 and 5). These protocols are detailed in Table 2.1 and Figures 2.2-2.4. As the kitten was prepared with the ET tube directed down the right bronchus (detailed in Section 2.1.2.2), this formed an airtight seal due to the ET tube and kitten bronchus being approximately the same diameter and made unilateral ventilation possible. Ventilation of a single lung was confirmed visually on the real-time X-ray imaging output, by presence or absence of the speckle pattern generated by air in the alveoli (Kitchen *et al.*, 2004). Once imaging of unilateral ventilation was completed for several minutes, the ET tube was retracted into the trachea and imaging of bilateral ventilation commenced. Kittens were ventilated using a peak inflation pressure of 25 cmH₂O and a positive end-expiratory pressure of 5 cmH₂O.

During each of the ventilation stages, angiography images were obtained by injecting single boluses of iodine (Iomeron 350 mg/ml iodine; Bracco-Eisai Pty. Ltd., Japan; 1.5 µL per g of kitten body weight at 11 ml/s), administered via the jugular vein using a remote-controlled syringe pump (PHD2000, Harvard Apparatus Inc., USA). Successive iodine infusions allowed comparative analysis of pulmonary vasculature at each stage of ventilation.

Table 2.1

Animal numbers (n) for each research chapter. A total of 54 newborn rabbit kittens were analysed for X-ray quantitative data.

CHAPTER		INITIAL VENTILATION WITH:		
		100% N ₂	Air	100% O ₂
3			n = 6	
4		n = 6	n = 6	n = 6
5	Control	n = 5	n = 5	n = 5
	Vagotomy	n = 5	n = 5	n = 5

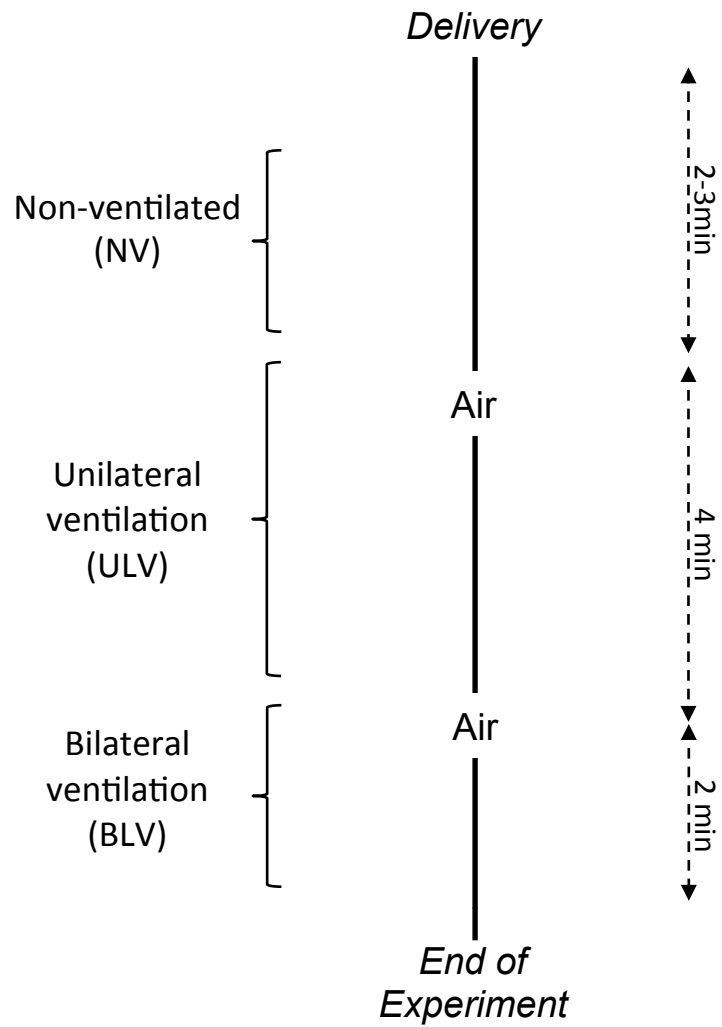


Figure 2.2: Flowchart of experimental procedure for Chapter 3

Timecourse of imaging/ventilation between delivery and the end of the experiment, indicating the ventilation of all kittens with atmospheric air (21% O₂).

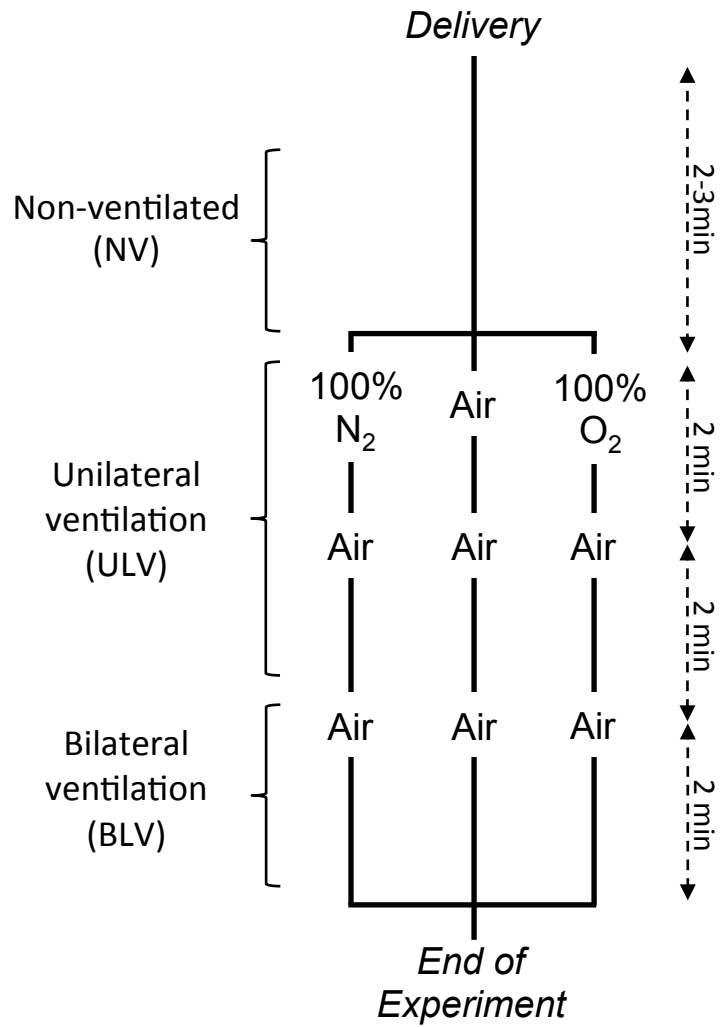


Figure 2.3: Flowchart of experimental procedure for Chapter 4

Shown are: experimental groups (initial gas ventilation of 100% N₂, air or 100% O₂) and timecourse of imaging/ventilation.

2.3 X-ray Image Analysis

Images were analysed using ImageJ (v1.47-1.50b; NIH, USA), to derive quantitative data from the X-ray images. As direct flow measurements were not viable, a number of PBF indicators were used instead. These included comparisons of the number of visible pulmonary vessels, vessel diameters, iodine ejection per beat, pulmonary transit time and change in mean grey level profiles over time within the left and right main axial arteries (to give relative PBF), the aorta and inferior vena cava (IVC). Heart rate was also calculated using the image sequences to supplement ECG recordings.

2.3.1 Normalisation of X-ray images

PC X-ray images were processed using the software High Performance Imaging Control Programs (HiPic; Hamamatsu Photonics, Japan) and ImageJ. Dark current and non-uniform X-ray beam effects were removed using dark and flat field images collected at the end of each imaging sequence. Regions of the field of view that did not contain the Perspex frame or kitten were used to normalise the intensity of each image to the first image of the sequence; this was to correct for fluctuations in X-ray beam intensity that resulted from heat load-related monochromator movement during the experiment.

2.3.2 Blood vessel visibility

Visible blood vessels were counted using a composite image constructed from all X-ray images beginning from the first heartbeat immediately after iodine administration until after the iodine had left the pulmonary arteries (image summation). This was also correlated with a background-subtracted image in which the average background (images of kitten with no contrast agent present) was digitally subtracted from the composite image with all vessels visible using ImageJ (Figure 2.5). Images acquired during lung inflation were excluded due to motion blur and to ensure maximum possible overlap of vessels. Branches of each axial artery were classified according to branching generation; vessels distal to branching points were counted as individual vessels and were visible up to the 3rd order of branching.

2.3.3 Blood vessel diameter estimation

Changes in pixel grey level (intensity) along virtual lines transecting vessels perpendicular to a vessel wall were used to measure vessel internal diameter. Line profiles were drawn over the left and right main axial arteries (taken mid-lung at the 7th intercostal space), to measure changes in internal diameter from the baseline pre-ventilation period. The mid-lung point was chosen as it provided a centrally-located, clear and unobstructed view of the large conduit arteries during both the pre-ventilation and ventilation imaging time periods. To correct for background intensity variations during iodine perfusion, line profiles were divided by the average background intensity averaged over the 1 s of frames (5-20 frames depending on framerate) immediately prior to the first appearance of iodine within the vessel. Internal vessel edges were determined as the first pixel to drop below 1 standard deviation of the mean intensity of the background at either end of the line profile (~5 pixels past the vessel edge) (Figure 2.6). Vessel diameters measured in pixels from each frame were averaged over 5 frames then multiplied by the known pixel size to estimate a mean vessel internal diameter.

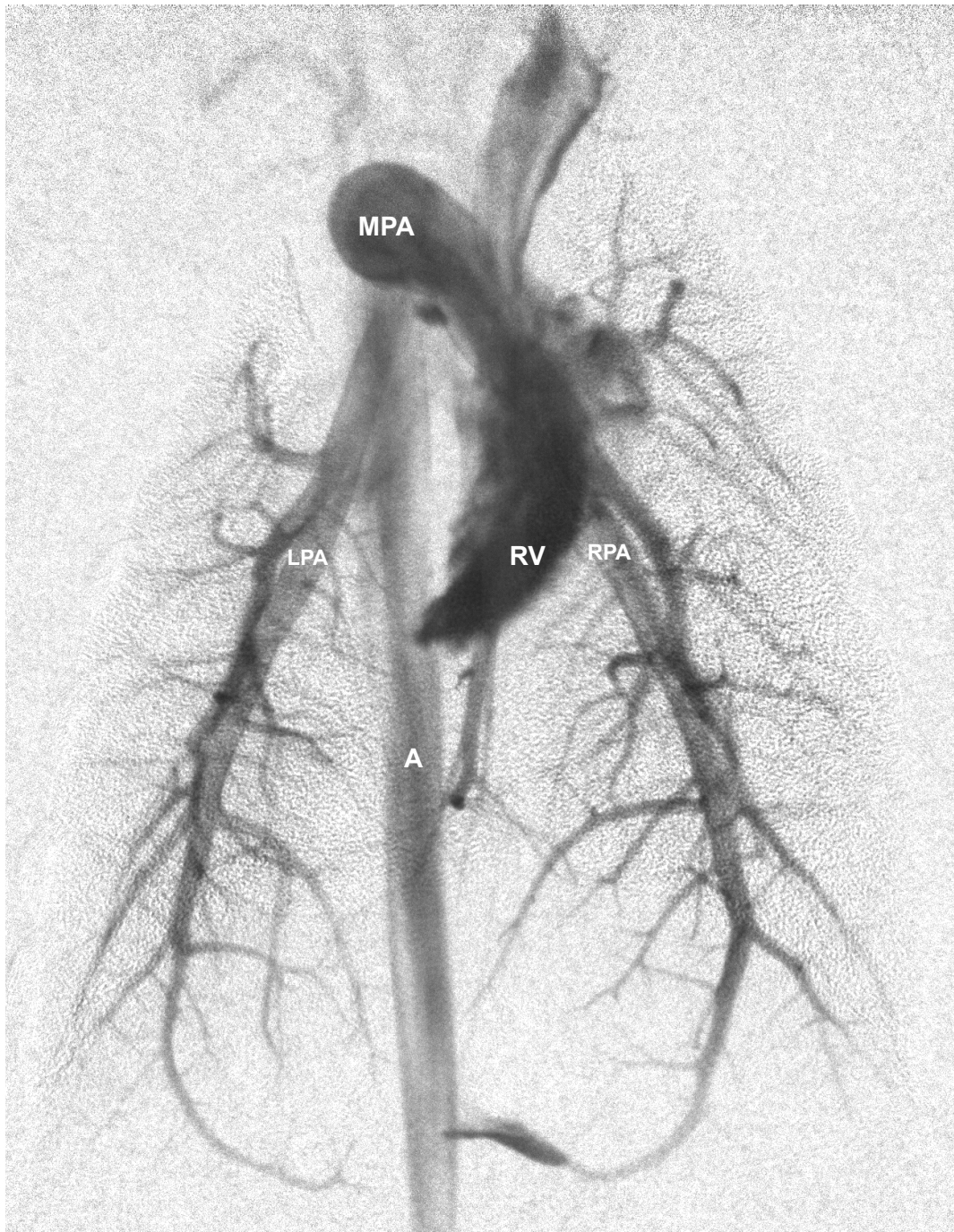


Figure 2.5: Background-subtracted image of peak iodine visibility

Composite image constructed by performing image summation of X-ray images with iodine perfused pulmonary vessels, then using an average background (images of kitten with no contrast agent present) to perform digital subtraction and enhance vessel visibility. Labelled are the right ventricle (RV), main pulmonary artery (MPA), aorta (A), left pulmonary artery (LPA) and right pulmonary artery (RPA).

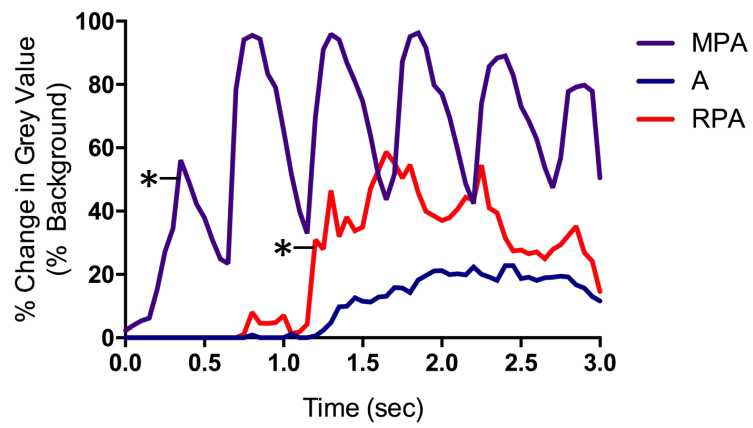
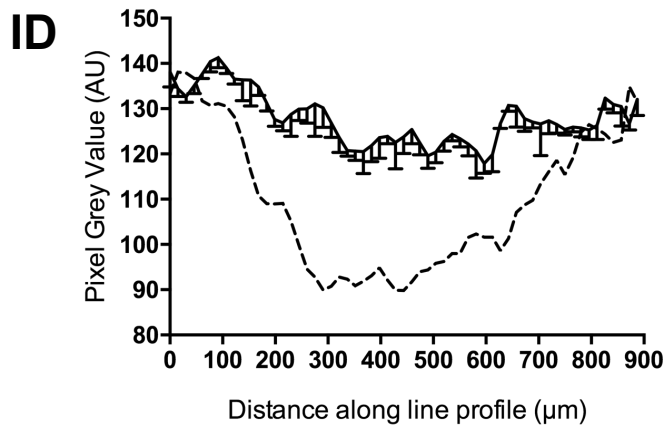
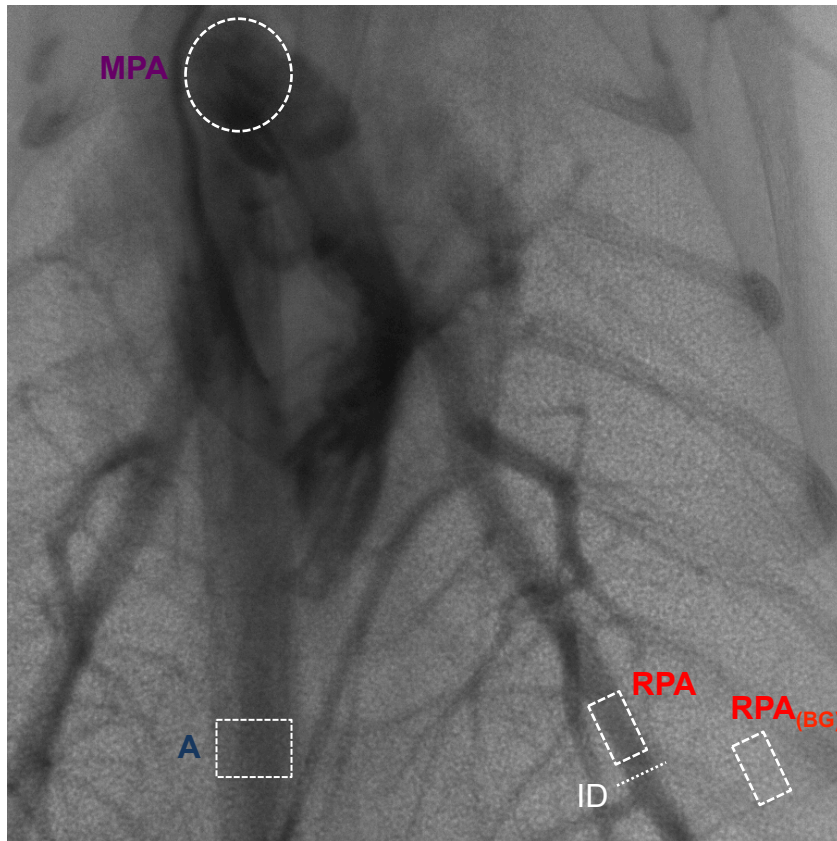


Figure 2.6: Analysis methods of a PC X-ray angiogram

ID: The pixel grey level along a virtual line (white dotted line) placed perpendicular to the vessel wall and transecting the vessel was measured to provide a profile of the pixel grey level change across the vessel. The change in pixel grey level was plotted against distance along the line both before (background; unbroken line; mean \pm SD) and after (broken line; mean) iodine injection to define the vessel edges and determine vessel internal diameter (ID).

MPA, A, RPA: Virtual boxes were placed over various vessels in order to plot mean intensity within each box against time as a percentage change from background levels (mean background intensity averaged over 10 frames before iodine injection) throughout each iodine injection sequence. The box over each PA (RPA shown here) was first divided by a nearby clear region of lung tissue ($RPA_{(BG)}$) to remove speckle background interference. Marked with asterisks (*) are the half-peak opacity for the MPA and RPA, which were used to calculate pulmonary arterial transit time (elapsed time between the two points).

Non-uniform line profile plots, typically caused by iodine streaming towards the end of a heartbeat, were excluded from analysis.

2.3.4 Pulmonary arterial transit time

Virtual boxes were placed over the distal end of the left and right main axial arteries before 1st order branching (Figure 2.6). The mean intensity of this region was calculated for each frame. Bolus arrival time was designated as the frame in which half of the peak opacity (maximum % change from background) is reached for the first time (half-peak opacity), this corrects for problems due to steady state peak opacity values in cases of poor wash-out (Shpilfoygel *et al.*, 2000). The elapsed time between the half-peak opacity value in the main pulmonary artery (MPA) compared to the left and right axial arteries was calculated to give an approximation of bolus transit time through the pulmonary artery.

2.3.5 Relative measures of flow rate

Virtual boxes were placed over the aorta, IVC, MPA, left and right main axial arteries at the level of the 7th intercostal space (providing a consistent measurement point as above) (Figure 2.6). The changes in mean intensity within each box were plotted against time as a percentage change from background levels (mean background intensity averaged over 10 frames before iodine injection) throughout each iodine injection sequence. Initially, area integration of this curve was calculated to provide relative PBF indicators (Chapter 3). This was later modified to divide the maximum of the time-opacity curve by the pulmonary arterial transit time to provide a more robust indicator of changes in pulmonary arterial flow in both lungs; this value was termed the relative PBF index (Chapters 4 and 5).

2.4 Statistical Analysis

All values presented in this thesis are presented as mean \pm standard error of the mean (SEM).

All data were tested for normality and equal variance. A p value of <0.05 was considered statistically significant. Statistical tests are described in each chapter and pertain to the experiments of that chapter.

Chapter Three

Ventilation/Perfusion Mismatch During Lung Aeration at Birth

Lang JA, Pearson JT, te Pas AB, Wallace MJ, Siew ML, Kitchen MJ, Fouras A, Lewis RA, Wheeler K, Polglase GR, Shirai M, Sonobe T & Hooper SB (2014) Ventilation/perfusion mismatch during lung aeration at birth. *Journal of Applied Physiology* **117**(5): 535-543

I have renumbered and reformatted sections of this published paper in order to generate a consistent presentation within this thesis.

See Appendix A for published PDF.

Although lung aeration increases PBF at birth, the regional relationships between lung aeration and the increase in PBF are not well known. Examining this process non-invasively can only be achieved by imaging. However, real-time imaging of regional pulmonary ventilation has been difficult due to the low density of lung tissue. Development of PC X-ray imaging not only allows imaging of the lungs with high temporal and spatial resolution, down to the smallest air sacs, but can be combined with simultaneous microangiography. This allows investigation of the regional distribution of pulmonary dynamics during the transition period, and is able to address this gap in the literature.

The aim of this chapter was to determine the spatial relationship between local aeration and perfusion in the newborn lungs immediately after birth. While the temporal relationship between initial aeration of the lungs and the PBF increase at birth is well established, the mechanisms by which aeration of the lungs exerts this effect is less certain. This was examined by aerating only part of the lungs, with the expectation that lung aeration would only increase PBF in aerated lung regions.

Declaration for Chapter 3

Ventilation/Perfusion Mismatch During Lung Aeration at Birth

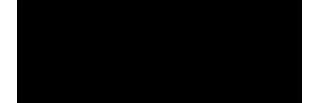
In the case of Chapter 3, the nature and extent of my contribution to the work was the following:

Nature of Contribution	Extent of Contribution
Experimental design, performed all experimental work, data collection and analysis and wrote and edited the manuscript	70%

The following co-authors contributed to the work. No co-authors were students at Monash University.

Name	Nature of Contribution
James T. Pearson	Experimental design and work and manuscript editing
Arjan B. te Pas	Experimental work and manuscript editing
Megan J. Wallace	Experimental work and manuscript editing
Melissa L. Siew	Experimental work and manuscript editing
Marcus J. Kitchen	Experimental work and manuscript editing
Andreas Fouras	Experimental work and manuscript editing
Robert A. Lewis	Experimental design and work and manuscript editing
Kevin Wheeler	Experimental work and manuscript editing
Graeme R. Polglase	Experimental work and manuscript editing
Mikiyasu Shirai	Experimental work and manuscript editing
Takashi Sonobe	Experimental work and manuscript editing
Stuart B. Hooper	Experimental design and work and manuscript editing

The undersigned hereby certify that the above declaration correctly reflects the nature and extent of the candidate and co-authors' contributions to this work.

Candidate's Signature		Date: 15/12/16
Main Supervisor's Signature		Date: 15/12/16

3.1 Abstract

At birth, the transition to newborn life is triggered by lung aeration, which stimulates a large increase in pulmonary blood flow (PBF). Current theories predict that the increase in PBF is spatially related to ventilated lung regions as they aerate after birth. Using simultaneous phase-contrast X-ray imaging and angiography we investigated the spatial relationships between lung aeration and the increase in PBF after birth. Six near-term (30-day gestation) rabbits were delivered by caesarean section, intubated and an intravenous catheter inserted, before they were positioned for X-ray imaging. During imaging, iodine was injected before ventilation onset, after ventilation of the right lung only, and after ventilation of both lungs. Unilateral ventilation increased iodine levels entering both left and right pulmonary arteries (PAs) and significantly increased heart rate, iodine ejection per beat, diameters of both left and right PAs, and number of visible vessels in both lungs. Within the 6th intercostal space, the mean grey level (relative measure of iodine level) increased from 68.3 ± 11.6 and $70.3 \pm 7.5\%$ to 136.3 ± 22.6 and $136.3 \pm 23.7\%$ in the left and right PAs, respectively. No differences were observed between vessels in the left and right lungs, despite the left lung not initially being ventilated. The increase in PBF at birth is not spatially related to lung aeration allowing a large ventilation/perfusion mismatch, or pulmonary shunting, to occur in the partially aerated lung at birth.

3.2 Introduction

During fetal life, pulmonary vascular resistance (PVR) is high and ~90% of right ventricular output bypasses the lungs and enters the systemic circulation via the ductus arteriosus. As pulmonary blood flow (PBF) is low, preload for the left ventricle depends on umbilical venous return, which flows via the ductus venosus, inferior vena cava and foramen ovale before entering the left ventricle (Rudolph, 1979). Thus, clamping the umbilical cord at birth causes umbilical venous return to cease and preload for the left and right ventricles to suddenly decrease (Rudolph, 1979; Teitel *et al.*, 1990; Bhatt *et al.*, 2013). As a result, the increase in PBF after birth is not only critical for facilitating pulmonary gas-exchange, but also provides preload for the left ventricle (Crossley *et al.*, 2009; Bhatt *et al.*, 2013). As such, the decrease in PVR and increase in PBF at birth are central to the transition to newborn life and although lung aeration is known to be the primary trigger, the major underlying mechanisms remain unclear (Gao & Raj, 2010; Berhrsin & Gibson, 2011).

The decrease in PVR at birth is thought to be an integrated response to a number of vasoactive stimuli (Heymann, 1999; Ghanayem & Gordon, 2001; Gao & Raj, 2010). Increased oxygenation and mechanical shear stress, caused by ventilation onset, are thought to increase nitric oxide (NO) and prostaglandin synthesis causing vasodilation of pulmonary vessels (Velvis *et al.*, 1991; Heymann, 1999; Coggins & Bloch, 2007). In addition, the development of surface tension at the air-liquid interface following lung aeration, increases transmural pressures across the fused capillary/alveolar wall, causing an increase in capillary recruitment and reduction in capillary resistance (Dawes *et al.*, 1968; Hooper, 1998; Polglase & Hooper, 2006). However, the underlying assumption with these mechanisms is that vasodilation is spatially related to aerated or ventilated regions of the lung. Although the temporal association is well established (Cassin *et al.*, 1964b; Teitel *et al.*, 1990; Polglase &

Hooper, 2006), the spatial relationship between lung aeration and the increase in PBF at birth is unknown.

Ventilation/perfusion ratios normally vary in a spatially dependent manner across the adult lung and are thought to be largely oxygen and gravity dependent. The effect of oxygen is driven by increased NO synthesis, whereas the effect of gravity is mediated by altering capillary/alveolar wall transmural pressures. Higher transmural pressures (capillary > alveolar) cause capillary distension and recruitment leading to a decrease in PVR. Ideally, regional perfusion should spatially match regional ventilation for efficient gas-exchange as a large mismatch reduces gas-exchange efficiency (Gale *et al.*, 1985). Despite the existence of this relationship in adult lung, the possibility that partial lung aeration may cause global vasodilation of the lung at birth has previously been raised, albeit in an animal model that involved major surgical alterations to the pulmonary arterial supply (Cassin *et al.*, 1964b).

Phase contrast (PC) X-ray imaging studies have provided new insights into the process of lung aeration after birth in both spontaneously breathing and ventilated neonates (Hooper *et al.*, 2007; Kitchen *et al.*, 2008; Fouras *et al.*, 2009; Siew *et al.*, 2009a; te Pas *et al.*, 2009; Leong *et al.*, 2013). PC X-ray imaging exploits the refractive index differences between air and water to provide contrast of the air/liquid interfaces within the lung (Snigirev *et al.*, 1995; Kitchen *et al.*, 2005). This technique is ideal for studying and measuring the temporal and spatial pattern of lung aeration (Lewis *et al.*, 2005) and can be combined with the use of contrast agents to simultaneously highlight pulmonary blood vessels (Schwenke *et al.*, 2007; Schwenke *et al.*, 2008; Shirai *et al.*, 2009). Our aim was to combine PC X-ray imaging with angiography to examine regional ventilation/perfusion relationships during lung aeration at birth. We hypothesised that the increase in PBF would be spatially related to regional lung

aeration, with the greatest increase in PBF occurring in aerated regions. The relationship between PBF and lung aeration was examined by imaging pulmonary vessels using an iodine-based contrast agent before lung aeration, during aeration of the right lung and following aeration of both lungs in ventilated newborn rabbits.

3.3 Methods

3.3.1 Experimental procedure

All animal procedures were approved by the SPring-8 Animal Care and Monash University's School of Biomedical Science's Animal Ethics Committees. All studies were conducted in experimental hutch 3 of beamline 20B2, in the Biomedical Imaging Centre at the SPring-8 synchrotron, Japan.

Pregnant New Zealand White rabbits at 30 days gestation (term \approx 32 days) were anaesthetised using Rapinovet (12 mg/kg bolus _{I.V.}; propofol, Schering-Plough Animal Health), and intubated, and anaesthesia was maintained by isoflurane inhalation (1.5– 4%; Isoflurane, Delvet, Australia). Fetal rabbits (n = 6) were partially delivered by caesarean section, sedated with sodium pentobarbitone (pentobarbital; 0.1 mg _{I.P.}) and a jugular vein catheter (24G intracath, Becton-Dickson) and an endotracheal (ET) tube (18G; via tracheostomy) were inserted; the tip of the ET tube was directed into the right bronchus so that with ventilation onset only the right lung was ventilated (unilateral ventilation). During the surgical procedure, the kitten's head remained covered with fetal membranes to prevent lung aeration and the umbilical cord remained intact. The kittens were then delivered, the umbilical cord ligated and placed upright in a Perspex frame before the ET tube was connected to a purpose-built, time-cycled, pressure-controlled ventilator (Kitchen *et al.*, 2010); image acquisition began as soon as possible after the kittens were positioned. Kittens were ventilated in air using a peak

inflation pressure of 25 cmH₂O and a positive end-expiratory pressure of 5 cmH₂O. At the conclusion of the experiment (~10 minutes after ventilation onset for kittens), all animals were humanely killed with an overdose of sodium pentobarbitone (pentobarbital; 100 mg/kg) administered _{I.V.} (doe) or _{I.P.} (kittens).

3.3.2 X-ray and angiography imaging

The energy was 33.2 keV, just above the iodine k-edge, and kittens were positioned 1.0 m upstream of the detector. The detectors used (either: EM-CCD C9100-02 or C9300-124F, Hamamatsu Photonics Hamamatsu, Japan or pco.edge, PCO AG, Germany) had a maximum effective pixel size of 31.8 μm (range 15.3-31.8 μm) and an active field of view of 21-29 (W) x 21-30 (H) mm²; images were acquired at frame rates of 5-10Hz. During imaging, iodine boluses (Iopromide 370mg/ml iodine; Schering, Germany; 1.5 $\mu\text{L/g}$ of kitten weight) were infused into the kitten via the jugular vein using a remote-controlled syringe pump (PHD2000, Harvard Apparatus). Iodine boluses were injected and images acquired for ~2 min before ventilation onset, during ventilation of the right lung (for ~3 min) and then during ventilation of both lungs (for ~2 min); the latter was achieved by retracting the tip of the ET tube. Subsequent iodine infusions allowed comparative analysis of pulmonary vasculature at each stage of ventilation.

3.3.3 Image analysis

Images were analysed using ImageJ (v1.47; NIH) to compare the heart rate, iodine ejection per beat, number of visible pulmonary vessels, vessel diameters and change in mean grey level profiles within the left and right pulmonary arteries (PAs), the aorta and IVC following iodine injection.

3.3.3.1 *Vessel quantification*

Visible blood vessels were counted using a composite image constructed from all X-ray images beginning from the first heartbeat immediately after iodine administration until after the iodine had left the pulmonary arteries. Images acquired during lung inflation were excluded due to motion blur and to ensure maximum possible overlap of vessels. Branches of each PA were classified according to branching generation; vessels distal to branching points were counted as individual vessels and were visible up to the 3rd order of branching.

3.3.3.2 *Pulmonary artery vessel diameter*

Changes in pixel grey level (intensity) along virtual lines transecting vessels perpendicular to the vessel wall were used to measure vessel diameter. For each line profile, the average background pixel grey level was calculated by measuring the average grey level along the line over 2-10 frames immediately prior to the first appearance of contrast within the vessel. This background grey level was subtracted from the pixel grey level along the transecting line following contrast injection and the resulting grey level plotted as a function of distance (pixels) along each line (Figure 3.1). Vessel edges were identified when the pixel grey level decreased below 1 standard deviation (SD) of the background average on each side (Figure 3.1 bottom panel). Non-uniform line profile plots, typically caused by iodine streaming towards the end of a heartbeat, were excluded from analysis. Vessel diameters from each frame were averaged over 10 frames to calculate a mean vessel diameter.

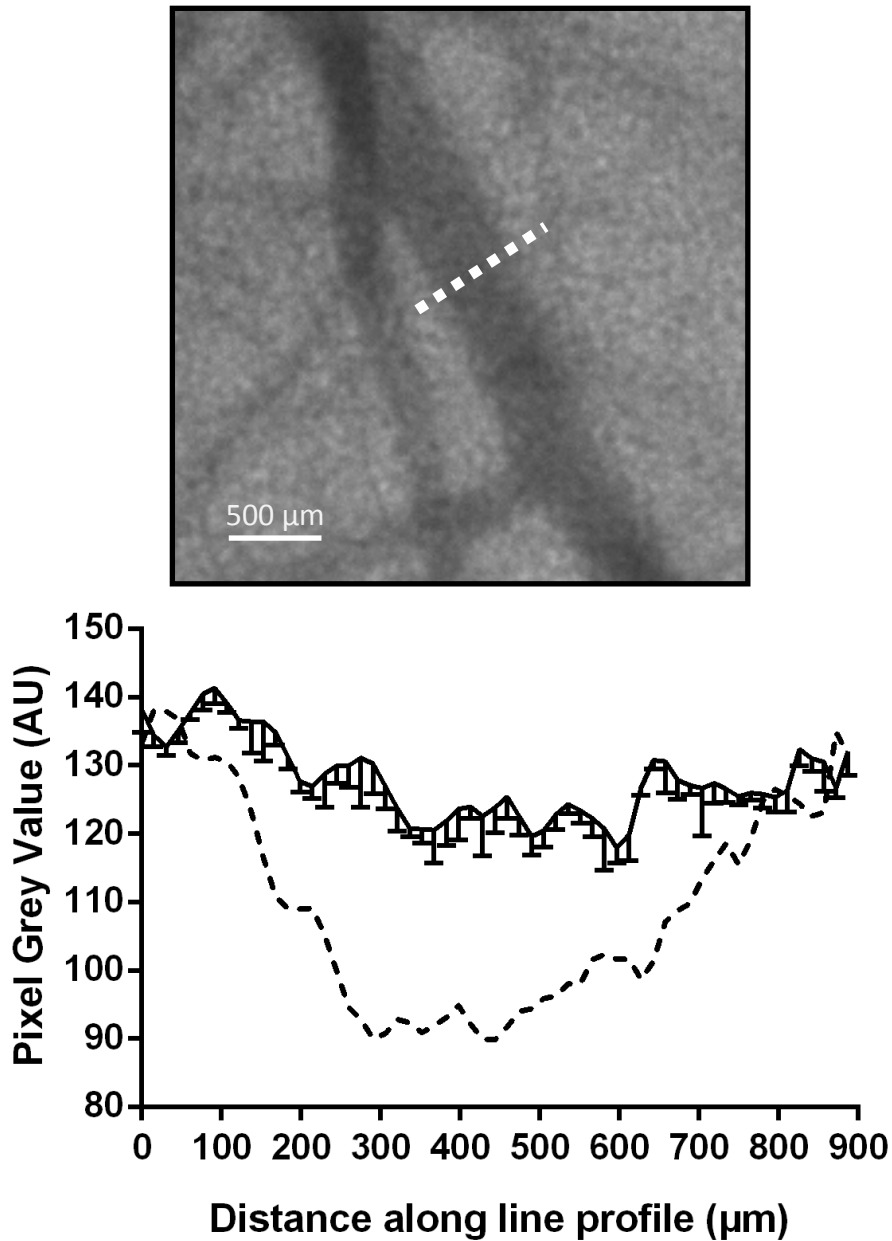


Figure 3.1

Simultaneous phase contrast X-ray image and angiogram (top panel), using iodine as a contrast agent, of a small segment of the right pulmonary artery acquired following lung aeration. The background speckle pattern surrounding the vessel is caused by the small airways, particularly alveoli, acting as aberrant focusing lenses causing X-ray diffraction at each air/liquid interface. The pixel grey level along a virtual line (white dotted line) placed perpendicular to the vessel wall and transecting the vessel was measured to provide a profile of the pixel grey level change across the vessel. The bottom panel shows the change in pixel grey level plotted against distance along the line both before (background; unbroken line; mean SD) and after (broken line; mean) iodine injection to define the vessel edges and determine vessel diameter.

3.3.3.3 Changes in relative iodine levels within vessels

A virtual box was placed over the aorta, the IVC, the main PA immediately distal to the right ventricular outlet as well as over the left and right PAs at specific points along the main axial arteries. The latter were located within clear sections of the 6th, 7th and 8th intercostal spaces, which provided the clearest, unobstructed view of the vessel during both the pre-ventilation and ventilation imaging stages. The changes in mean pixel grey level within each box were measured throughout an iodine injection sequence and expressed as a percentage of the background mean pixel grey level averaged over 2-10 frames before iodine injection. The temporal changes in relative iodine levels within the 3 virtual boxes along the left and right pulmonary arteries following iodine injection were integrated to provide a relative measure of iodine flow over time within these vessels. Heart rates were determined from the mean pixel grey level changes within the main pulmonary artery collected over several heart beats during an iodine injection sequence.

3.3.4 Statistical analysis

Data are presented as mean \pm SEM. Changes in vessel quantity, vessel diameter and integrated relative iodine levels within vessels were analysed using a two-way repeated measures ANOVA. Post-hoc analysis used the Holm-Sidak method. A $p < 0.05$ was considered statistically significant.

3.4 Results

3.4.1 Animal data

Six near-term rabbit kittens (from 5 does) underwent imaging before ventilation, during ventilation of the right lung (unilateral ventilation) and then during ventilation of both lungs (bilateral ventilation). Non-aerated regions of the lung are clearly evident by the absence of speckle pattern in the X-ray images. The gestational age of kittens at delivery was 30 days.

3.4.2 Observations from PC X-ray videos

Compared with pre-ventilation, the flow of iodine (contrast agent) into both main PAs markedly increased ($p < 0.05$) in response to unilateral ventilation (Figure 3.2; Supplemental Video 3.1). As such, the number and amount of iodine flowing into the pulmonary vessels were markedly increased (Figure 3.2; Supplemental Video 3.1). The increase in iodine flow through vessels of the non-aerated left lung was very similar to the aerated right lung, displaying a uniform global increase in iodine visibility and, therefore, in PBF. This effect was consistently observed in all animals ($n = 6$) and was sustained following bilateral ventilation (Figure 3.2).

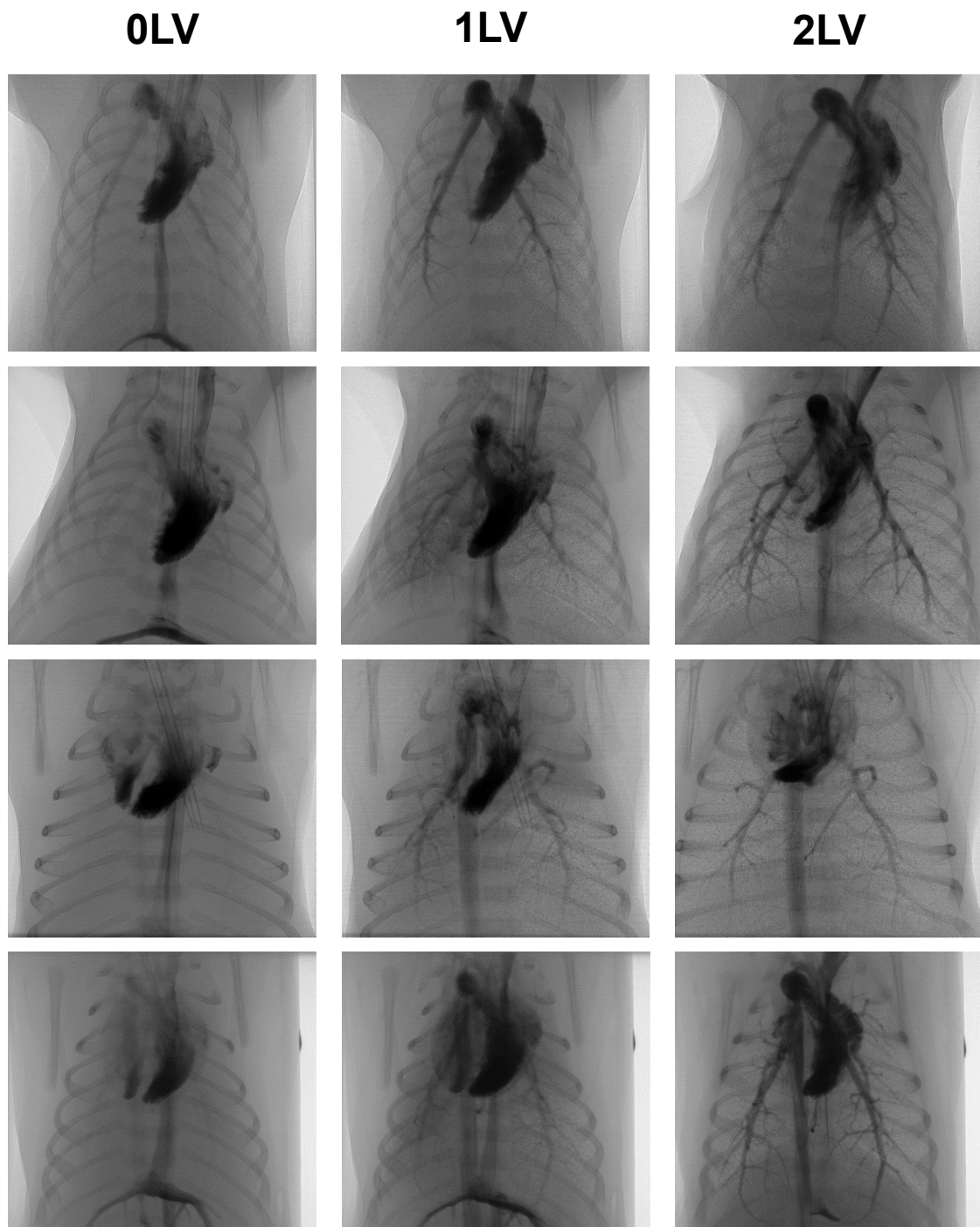


Figure 3.2

Simultaneous PC X-ray images and angiograms of 4 newborn rabbits prior to ventilation (0LV), following unilateral ventilation of the right lung (1LV) and following ventilation of both lungs (2LV). Images were acquired 2–6 s after iodine injection.

3.4.3 Numbers of visible vessels

Compared to pre-ventilation, unilateral ventilation of the right lung markedly increased the number of vessels visible in both lungs using angiography (Figure 3.3). The number of vessels increased significantly from 21 ± 4 and 19 ± 5 vessels to 44 ± 4 and 42 ± 4 vessels in the left and right lungs, respectively, in response to unilateral ventilation of the right lung. Bilateral ventilation further increased the number of visible vessels (compared to unilateral ventilation) to 49 ± 8 and 59 ± 11 in the left and right lungs, respectively ($p < 0.05$); at this time the number of vessels in the right lung was significantly greater than the left lung. This difference in vessel visibility between left and right lungs during bilateral ventilation was due to the number of third order branching generation vessels (10 ± 4 in left vs. 14 ± 4 in right).

3.4.4 Internal vessel diameter

The axial PAs (both left and right) gradually narrow as they branch and penetrate into the more caudal lung lobes, penetrating at least into the 8th intercostal space (see Figures 3.2 & 3.3). Internal vessel diameters of both the left and right axial PAs were measured in each intercostal space between ribs 6 to 8. Prior to ventilation, mean vessel diameters were $\sim 550 \mu\text{m}$ (intercostal space 6), $\sim 430 \mu\text{m}$ (intercostal space 7) and $\sim 315 \mu\text{m}$ (intercostal space 8), which reflects the decreasing vessel diameter as it branches and penetrates into the distal lung regions (Figure 3.4). Compared to pre-ventilation values, the PA diameters in both lungs were significantly increased by unilateral ventilation in all intercostal spaces measured. In the 7th intercostal space, unilateral ventilation increased the vessel diameter from 432 ± 46 and $428 \pm 31 \mu\text{m}$ to 490 ± 45 and $498 \pm 31 \mu\text{m}$ in the left and right lungs, respectively; in the 8th intercostal spaces, vessel diameters increased from 299 ± 21 and $332 \pm 13 \mu\text{m}$ to 352 ± 18 and $379 \pm 18 \mu\text{m}$ in the left and right lungs, respectively. Compared to unilateral ventilation,

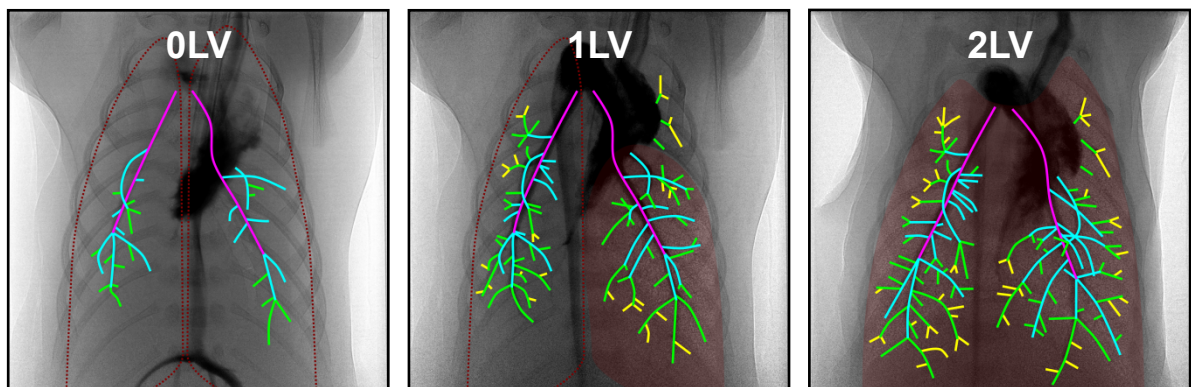
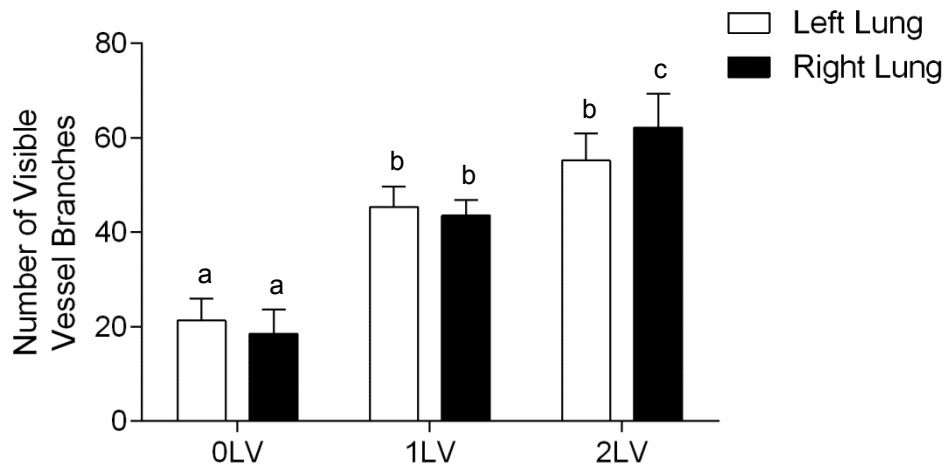


Figure 3.3

Top: no. of visible vessels measured in the right and left lungs before ventilation (0LV), during unilateral ventilation of the right lung (1LV), and during ventilation of both lungs (2LV).

Bottom: traced overlay of all visible blood vessels (filled with iodine) superimposed over the X-ray images of the lung acquired before ventilation onset (0LV), during unilateral ventilation of the right lung (1LV), and during ventilation of both lungs (2LV) in the same kitten. Outlined are the approximate boundaries of non-aerated regions of the lungs (red dotted line) and aerated regions of the lungs (solid red background). Shown are the left and right pulmonary arteries (purple), 1st generation branches (blue), 2nd generation branches (green), and 3rd generation branches (yellow). Within each graph, bars that do not share a letter are significantly different from each other ($P < 0.05$).

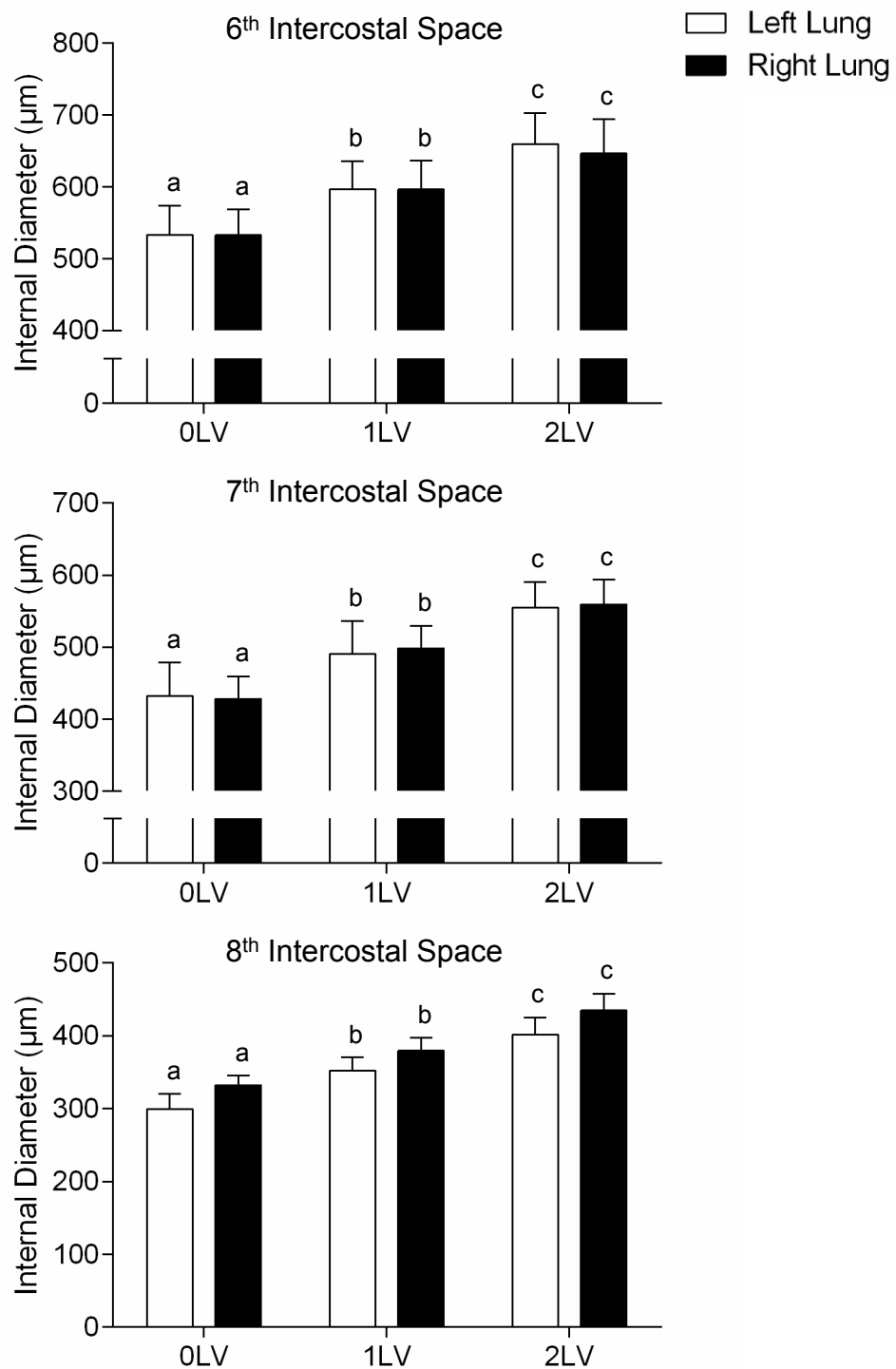


Figure 3.4

Changes in internal vessel diameter along the main axial branches of the left and right pulmonary arteries at the level of the 6th (top panel), 7th (middle panel), and 8th (bottom panel) intercostal spaces, measured before ventilation onset (0LV), during unilateral ventilation of the right lung (1LV), and during ventilation of both lungs (2LV). Within each graph, bars that do not share a letter are significantly different from each other ($P < 0.05$).

bilateral ventilation significantly increased vessel diameter further to $555 \pm 36 \mu\text{m}$ (left lung) and $559 \pm 34 \mu\text{m}$ (right lung) in the 7th intercostal space and to $401 \pm 23 \mu\text{m}$ (left lung) and $434 \pm 23 \mu\text{m}$ (right lung) in the 8th intercostal space (Figure 3.4).

3.4.5 Heart rate and beat-to-beat changes in iodine ejection

Compared to the pre-ventilation period, unilateral ventilation increased the heart rate from 69 ± 7 to 98 ± 17 beats/min, which was increased further to 140 ± 14 beats/min following bilateral ventilation ($p < 0.05$; Figure 3.5). The relative amount of iodine ejected per heart beat, as determined by the % change in grey level (below background) measured within the main pulmonary trunk, was increased by unilateral ventilation ($p < 0.05$; Figure 3.5). The amount of iodine ejected during the first and second heart beats was significantly increased from $23.2 \pm 6.3\%$ and $31.0 \pm 5.1\%$ to $54.8 \pm 7.1\%$ and $64.4 \pm 5.0\%$, respectively, following ventilation onset (Figure 3.5).

3.4.6 Temporal changes in iodine levels within the IVC and aorta

The temporal increase in relative iodine levels (% change in pixel grey level below background) within the IVC following iodine injection was significantly reduced in response to both unilateral and bilateral ventilation (Figure 3.6). At 0.8 s after iodine injection, the relative iodine level was $29.6 \pm 6.2\%$ (% change in pixel grey level below background) before ventilation onset and was reduced to $17.4 \pm 7.1\%$ in response to unilateral ventilation and to $5.7 \pm 2.2\%$ following bilateral ventilation of the lung (Figure 3.6); this indicates less iodine flowing into the IVC following injection in response to ventilation. The dissipation of the iodine bolus appears at 1.6 s at 0LV and 0.2 s at 2LV. Within the descending thoracic aorta, the temporal increase in relative iodine levels was significantly increased in response to unilateral ventilation and was increased further following bilateral ventilation (Figure 3.6).

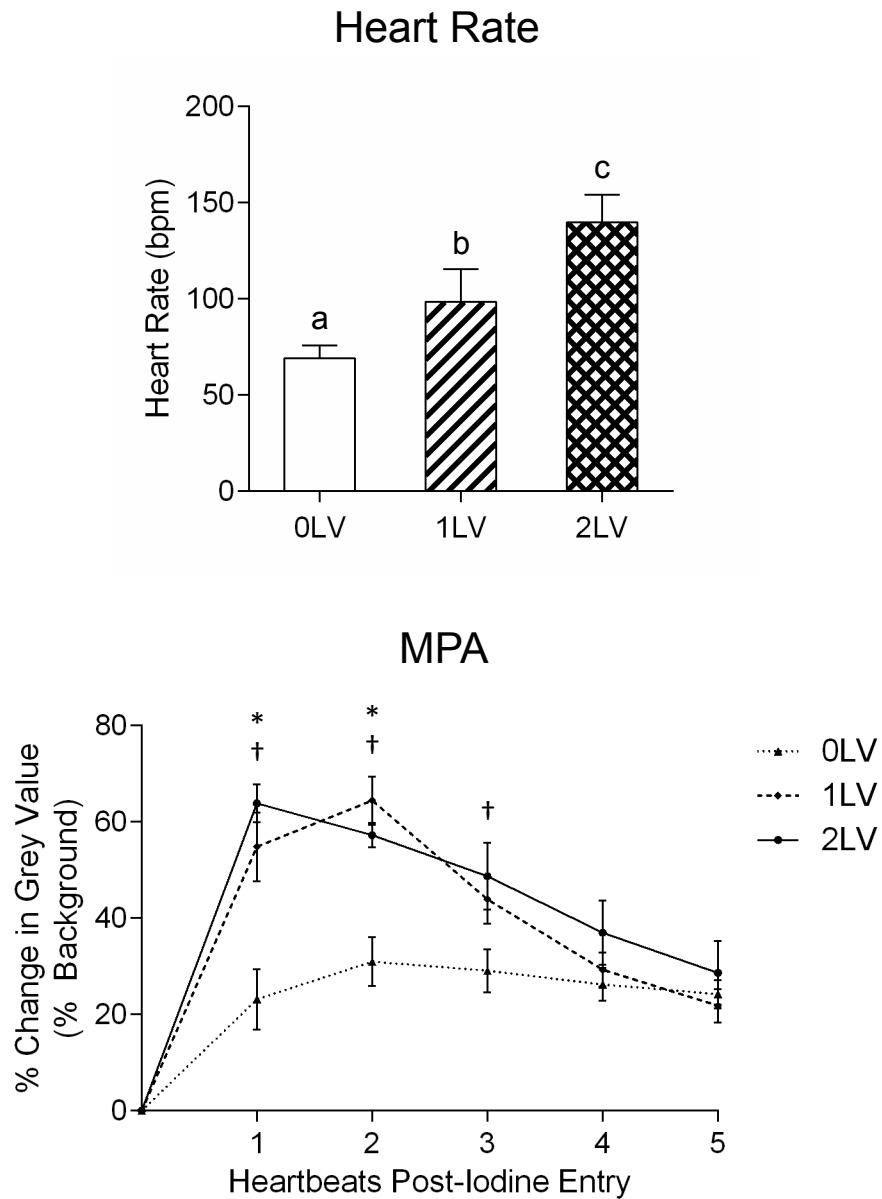


Figure 3.5

Changes in heart rate (top panel) and the change in relative iodine levels (% change in pixel grey level below background) measured within the main pulmonary artery (MPA) immediately distal to the right ventricular outlet during peak systole over consecutive heartbeats following iodine injection (bottom panel). The latter provides a relative measure of the amount of iodine ejected per ventricular contraction. Measurements were made before ventilation onset (0LV), during unilateral ventilation of the right lung (1LV), and during ventilation of both lungs (2LV). * $P < 0.05$, 0LV vs. 1LV; † $P < 0.05$, 0LV vs. 2LV. Within each graph, bars that do not share a letter are significantly different from each other ($P < 0.05$).

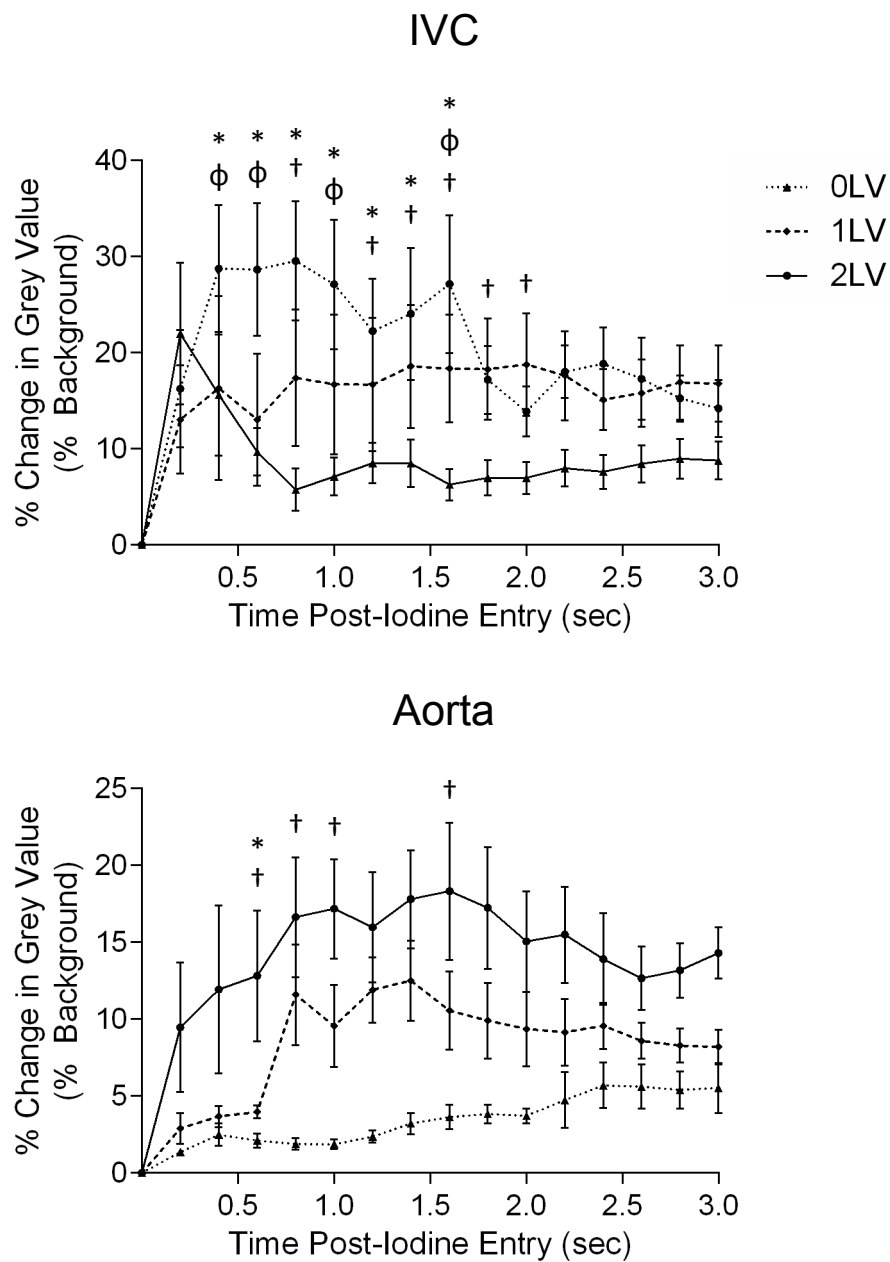


Figure 3.6

Changes in relative iodine levels (% change in pixel grey level below background) measured in the mid-thoracic inferior vena cava (top panel) and aorta (bottom panel) at fixed time intervals after iodine injection. Measurements were made before ventilation onset (0LV), during unilateral ventilation of the right lung (1LV), and during ventilation of both lungs (2LV). *P < 0.05, 0LV vs. 1LV; †P < 0.05, 0LV vs. 2LV; φ P < 0.05, 1LV vs. 2LV.

3.4.7 Change in mean pixel grey level over time within the pulmonary artery

In response to unilateral ventilation, the integrated (over time) changes in relative iodine levels (% change in pixel grey level below background) within the left and right PAs following iodine injection were significantly and equally increased (Figure 3.7). At the level of the 6th intercostal space, the integrated relative iodine level (%.s) increased from 68.3 ± 11.6 and 70.3 ± 7.5 %.s to 136.3 ± 22.6 and 136.3 ± 23.7 %.s in the left and right PAs, respectively. In the 7th intercostal space, the integrated relative iodine level increased from 59.2 ± 10.0 and 64.7 ± 8.6 %.s to 138.6 ± 34.8 and 139.1 ± 22.5 %.s in the left and right PAs respectively. Bilateral ventilation tended to increase the integrated relative iodine level further, but these changes were not significant except for the region of PA within the 6th intercostal space (Figure 3.7).

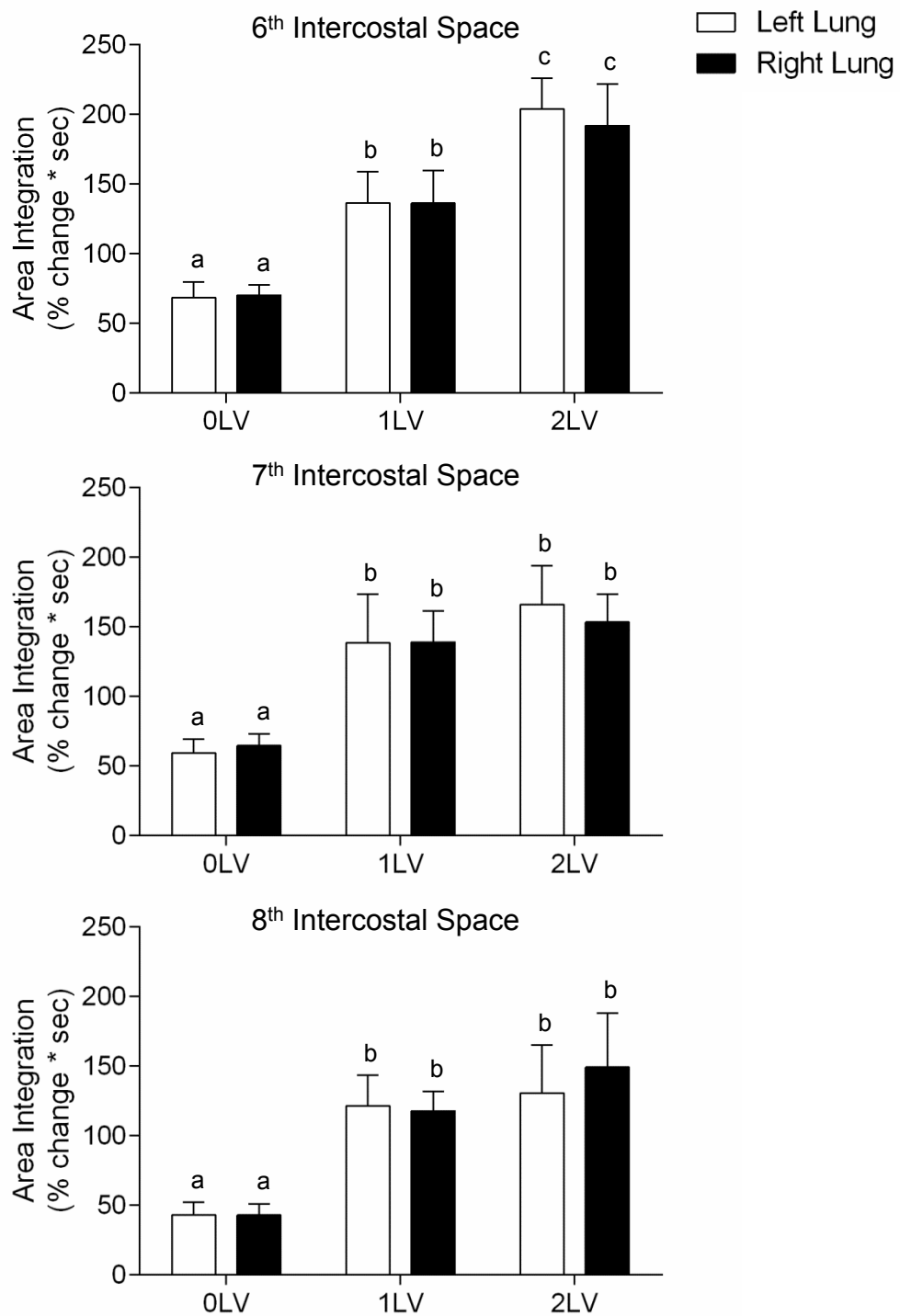


Figure 3.7

Integrated (over time) change in relative iodine levels (% change in pixel grey level below background) measured in the left and right axial pulmonary arteries within the 6th (top panel), 7th (middle panel), and 8th (bottom panel) intercostal spaces. Within each graph, bars that do not share a letter are significantly different from each other ($P < 0.05$).

3.5 Discussion

Our results confirm previous studies demonstrating that lung aeration at birth triggers a major haemodynamic response in the newborn, particularly an increase in PBF. However, contrary to what was hypothesised, we found that the relationship between lung aeration and the increase in PBF at birth was not spatially related. Specifically, we found that partial lung aeration triggered a marked increase in PBF in both aerated and unaerated lung regions, resulting in a major ventilation/perfusion mismatch in unaerated regions (Figures 3.2 & 3.7; Supplemental Video 3.1). These findings were unexpected as, based on the mechanisms thought to be responsible for the increase in PBF at birth (e.g. increased oxygen and NO release), we hypothesised that the stimulus would be greatest in aerated compared to unaerated lung regions. However, in every parameter examined, we found that the response to unilateral ventilation was similar in pulmonary vessels supplying aerated and non-aerated lung regions. Although some differences were observed between unilateral and bilateral ventilation periods, as the observed changes were mostly similar between lungs, irrespective of whether they were previously aerated (right) or unaerated (left), these changes more likely reflect an “increasing time after birth” related response. For example, due to a gradual increase in oxygenation.

The images clearly show major differences in iodine flow into the PAs before and after lung aeration, which greatly alters their visibility, with only the primary branches (Figures 3.2 & 3.3) being visible before lung aeration. As it is well established that PVR is high and PBF is low before lung aeration (Abman, 2007), the primary reason for this reduced flow of iodine is due to the low PBF, although other factors may have contributed. For instance, a reduced venous return likely contributed via a substantial reduction in IVC flow caused by umbilical cord clamping, which causes umbilical venous return to cease. As umbilical venous return is

an important contributor to IVC flow and preload for the fetal heart, these factors are dramatically reduced upon cord clamping and are only restored following the increase in PBF. This explanation is consistent with the finding that retrograde iodine flow along the IVC was substantially reduced following lung aeration, indicating that venous return and forward flow in the IVC was rapidly restored following ventilation onset and the associated increase in cardiac output (CO) (Bhatt *et al.*, 2013). This is also consistent with previous studies showing that RV output is reduced by ~50% following umbilical cord clamping and the loss of umbilical venous return (Crossley *et al.*, 2009; Bhatt *et al.*, 2013). Our finding that the amount of iodine ejected per beat from the RV and the heart rate were significantly lower prior to lung aeration and markedly increased with ventilation onset are entirely consistent with these previous observations.

The integrated changes (over time) in relative iodine levels measured at different positions along the main left and right axial PAs were used to assess the relative amounts of iodine passing through the PAs following iodine injection (Figure 3.7). Although this analysis does not provide a quantitative measure of PBF, the changes measured must reflect increases in PBF resulting from decreases in PVR, which are known to occur following ventilation onset (Crossley *et al.*, 2009; Bhatt *et al.*, 2013). These findings are consistent with the increases in vessel diameters measured at specific points along these vessels. Although the vessel diameter changes are relatively modest (~10% and 20%), as the resistance to blood flow is inversely proportional to the vessel radius to the 4th power, these increases in diameter reflect substantial decreases in resistance; a 10% increase in diameter equates to a 40% reduction, whereas a 20% increase equates to a 60% reduction in resistance. These reductions in resistance are similar in magnitude to the reductions in PVR that have been reported previously with ventilation onset at birth (Rudolph, 1979, 1985; Teitel *et al.*, 1990).

Our finding that unilateral ventilation dilated pulmonary vessels and increased PBF in both aerated and unaerated regions of the lung indicates that the initial ventilation-induced increase in PBF is not spatially related to aerated lung regions. This was a surprising finding as the primary mechanisms thought to mediate the ventilation-induced increase in PBF should act locally to dilate adjacent blood vessels (Abman, 2007). For instance, the increase in tissue PO_2 associated with aerating distal gas-exchange regions was thought to stimulate endothelial NO release, which acts on vascular smooth muscle to dilate resistance vessels within the lung (Iwamoto *et al.*, 1987). Similarly, the entry of air and the formation of surface tension within the lungs is thought to decrease PVR by increasing alveolar wall recoil, which increases pulmonary capillary recruitment and expansion. Based on this mechanism, one would also assume that the decrease in PVR would be limited to aerated lung regions (Hooper, 1998). Thus, it is possible that an additional, currently unknown, mechanism is responsible for initiating the increase in PBF at birth, which is largely independent of oxygen and the localised effects of surface tension and increased lung recoil. One possible explanation is the activation of “J” receptors (Paintal, 1969) in response to liquid accumulation within the tissue, which triggers a parasympathetic mediated decrease in PVR via vagal reflex. Whatever the mechanism, its activation only requires aeration of a small region of the lung and includes global vasodilation of the pulmonary vascular bed. Theoretically, this should benefit the infant, because lung aeration is often not uniform at birth and if the increase in PBF was dependent on complete lung aeration, then both CO and gas-exchange will be compromised until this is achieved. As increasing PBF and restoring CO is arguably more important than simply achieving complete lung aeration immediately after birth, it is of greater benefit to the transitioning infant if the increase in PBF is not quantitatively linked to the degree of lung aeration.

The contention that the initial ventilation-induced increase in PBF is not oxygen dependent is also supported by previous studies (Iwamoto *et al.*, 1987; Sobotka *et al.*, 2011). For example, in fetal sheep ventilated *in utero*, the majority (~70%) of the increase in PBF was achieved by ventilating fetuses with a hypoxic gas mixture (Teitel *et al.*, 1990). Switching ventilation to 100% O₂ increased PBF further, indicating that increasing oxygen can contribute, but they concluded that oxygen is not the dominant factor and an unknown “effect of ventilation” was primarily responsible. Similarly, in lambs delivered and ventilated at birth using strategies that either increased or decreased oxygenation levels, both methods resulted in a similar increase in PBF (Sobotka *et al.*, 2011). In our study, we found that some of the factors measured increased, or tended to increase, between the periods of unilateral and bilateral ventilation, which may reflect increased oxygenation of the kitten. Indeed, it is well established that the pulmonary vasculature is sensitive to changes in oxygen tension from early in gestation, with both fetal hypoxia and hyperoxia causing vasoconstriction and vasodilation of the pulmonary vasculature bed, respectively (Lewis *et al.*, 1976). However, the fact that the increase was similar in both lungs, irrespective of whether the lung had previously been aerated (right) or unaerated (left), indicates that this mechanism is time-related and may be independent of the mechanism that was initially triggered by lung aeration.

Increased cardiac function, resulting from both an increase in HR and contractility, may have also contributed to the time-related increases of our indirect measures of PBF. With the onset of lung aeration, the infused iodine primarily entered the right ventricle and was immediately ejected, within one or two heartbeats, into either the pulmonary vasculature or the descending aorta via the ductus arteriosus. As a result, both the proportion of iodine entering the RV and

the amount of iodine that was ejected per beat increased (Figure 3.5), indicating that RV output had increased. This finding is consistent with the finding of an increase in HR (Figure 3.5) and is also consistent with numerous previous studies (Momma *et al.*, 1992; Crossley *et al.*, 2009; Berhrsin & Gibson, 2011). However, recent studies have also indicated that the increase in PBF is a critical determinant of the increase in cardiac function (HR and contractility) after birth, which increases before an increase in oxygenation can be detected (Bhatt *et al.*, 2013). As preload for both ventricles is greatly diminished following umbilical cord clamping, causing large reductions in both stroke volumes and HR, it is not until PBF increases that preload for the LV is restored (Crossley *et al.*, 2009; Bhatt *et al.*, 2013). The important role of PBF in CO at birth was recently demonstrated by a study that delayed umbilical cord clamping until after ventilation had commenced and PBF had increased. This procedure completely abolished the reduction in CO associated with umbilical cord clamping, indicating that the source of preload can immediately switch from the umbilical circulation to PBF, without disrupting CO (Bhatt *et al.*, 2013). As such, the increase in RV output and increase in HR we observed in response to unilateral ventilation, is more likely to be a consequence of the increase in PBF than a cause.

We have used simultaneous angiography and PC X-ray imaging, to investigate the spatial relationship between lung aeration and the increase in PBF at birth. Although we hypothesised that lung aeration and the increase in PBF would be spatially related, our finding that they are unrelated demonstrates that our current understanding of the mechanisms driving the initial increase in PBF require re-evaluation. Indeed, we found that partial lung aeration can lead to large ventilation/perfusion mismatches in non-aerated lung regions. This suggests that factors such as PO_2 and mechanical expansion, which are well-established factors thought to reduce PVR at birth, may have non-local effects in the lungs. However, it is not known

how these factors could lead to reductions in resistance simultaneously across the entire lung, particularly in unaerated regions, when perfusion is initially so low. It is possible that other physiological factors, such as vasodilators, simultaneously reduce resistance across the aerated and non-aerated regions, but these are generally thought not to be dominant factors (Gao & Raj, 2010; Berhrsin & Gibson, 2011). Again, while these factors may potentiate any response, it is hard to envisage how they could initiate such an effect when pulmonary perfusion is initially so low.

Our observations of a global increase in PBF within the lungs were observed to occur within ~ 40 s of ventilation onset, which indicates the presence of a rapidly acting highly potent vasoactive process. This may be the result of a previously unsuspected mechanism that provides the initial stimulus for the increase in PBF at birth. In any event, it highlights our lack of understanding of the mechanisms that regulate this crucial process, despite the fact that it underpins the transition to newborn life.

Chapter Four

Increase in Pulmonary Blood Flow at Birth: Role of Oxygen and Lung Aeration

Lang JA, Pearson JT, Binder-Heschl C, Wallace MJ, Siew ML, Kitchen MJ, te Pas AB, Fouras A, Lewis RA, Polglase GR, Shirai M & Hooper SB (2016) Increase in pulmonary blood flow at birth: role of oxygen and lung aeration. *The Journal of Physiology* **594**(5): 1389-1398 (First published online 10 September 2015)

I have renumbered and reformatted sections of this published paper in order to generate a consistent presentation within this thesis.

See Appendix B for published PDF.

Given that a major ventilation/perfusion mismatch in unaerated regions appears to occur with partial lung aeration at birth, this is not fully explainable with our current knowledge of this process. Synchrotron X-ray images were able to demonstrate that air entry into a single lung rapidly increases perfusion throughout the lung; an unexpected and intriguing finding that warrants further investigation. Although unlikely, it was possible that regional lung aeration increased levels of circulating partial pressure of oxygen, causing vasodilatation in non-aerated lung regions. This possibility was addressed by using the same technique of simultaneous X-ray imaging and angiography on partially ventilated newborn rabbit kittens, comparing inspired gas with varying levels of oxygen (0% O₂, air with 21% O₂ and 100% O₂). Ventilation with 100% N₂ (0% O₂) was expected to trigger a global increase in PBF, with increasing inspired O₂ concentrations corresponding to an enhanced increase in PBF at birth.

Declaration for Chapter 4

Increase in pulmonary blood flow at birth: role of oxygen and lung aeration

In the case of Chapter 4, the nature and extent of my contribution to the work was the following:

Nature of Contribution	Extent of Contribution
Experimental design, performed all experimental work, data collection and analysis and wrote and edited the manuscript	70%

The following co-authors contributed to the work. No co-authors were students at Monash University.

Name	Nature of Contribution
James T. Pearson	Experimental design and work and manuscript editing
Corinna Binder-Heschl	Experimental work and manuscript editing
Megan J. Wallace	Experimental work and manuscript editing
Melissa L. Siew	Experimental work and manuscript editing
Marcus J. Kitchen	Experimental work and manuscript editing
Arjan B. te Pas	Experimental work and manuscript editing
Andreas Fouras	Experimental work and manuscript editing
Robert A. Lewis	Experimental design and work and manuscript editing
Graeme R. Polglase	Experimental work and manuscript editing
Mikiyasu Shirai	Experimental work and manuscript editing
Stuart B. Hooper	Experimental design and work and manuscript editing

The undersigned hereby certify that the above declaration correctly reflects the nature and extent of the candidate and co-authors' contributions to this work.

Candidate's Signature		Date: 15/13/16
Main Supervisor's Signature		Date: 15/12/16

4.1 Abstract

Lung aeration stimulates the increase in pulmonary blood flow (PBF) at birth, but the spatial relationships between PBF and lung aeration and the role of increased oxygenation remain unclear. Using simultaneous phase-contrast X-ray imaging and angiography, we have investigated the separate roles of lung aeration and increased oxygenation in PBF changes at birth using near-term (30 days of gestation) rabbit kits (n = 18). Rabbits were imaged before ventilation, then the right lung was ventilated with 100% nitrogen (N₂), air or 100% O₂ (oxygen), before all kits were switched to ventilation in air, followed by ventilation of both lungs using air. Unilateral ventilation of the right lung with 100% N₂ significantly increased heart rate (from 69.4 ± 4.9 to 93.0 ± 15.0 bpm), the diameters of both left and right pulmonary axial arteries, number of visible vessels in both left and right lungs, relative PBF index in both PAs and reduced bolus transit time for both left and right axial arteries (from 1.34 ± 0.39 s and 1.81 ± 0.43 s to 0.52 ± 0.17 s and 0.89 ± 0.21 s in the left and right axial arteries, respectively). Similar changes were observed with 100% oxygen, but increases in visible vessel number and vessel diameter of the axial arteries were greater in the ventilated right lung during unilateral ventilation. These findings confirm that PBF increase at birth is not spatially related to lung aeration and that the increase in PBF to unventilated regions is unrelated to oxygenation, although oxygen can potentiate this increase.

4.2 Introduction

The increase in pulmonary blood flow (PBF) at birth underpins the circulatory transition that is critical for postnatal survival (Iwamoto *et al.*, 1987). Shifting the site of gas-exchange from the placenta to the lungs requires aeration of the lung and a reduction in pulmonary vascular resistance (PVR) to increase pulmonary perfusion (Rudolph, 1979; Berhrsin & Gibson, 2011). This is not only necessary for efficient pulmonary gas-exchange but also restores venous return to the heart, which is markedly reduced following umbilical cord clamping (Rudolph, 1979; Crossley *et al.*, 2009; Bhatt *et al.*, 2013). The increase in PBF at birth is thought to result from an integration of multiple mechanical and vasoactive factors acting in concert and, until recently, was assumed to occur in a spatially dependent manner as lung regions aerated (Morin & Egan, 1992; Gao & Raj, 2010). Although the temporal relationship between lung aeration and the rapid increase in PBF at birth is well established (Teitel *et al.*, 1990; Polglase & Hooper, 2006), recent findings suggest there is no simple, direct correlation between local aeration and perfusion (Lang *et al.*, 2014).

The factors contributing to the high PVR *in utero* are thought to include high intraluminal pressures induced by airway liquid accumulation and relatively low fetal oxygen tensions, resulting in sustained vasoconstriction of the pulmonary vasculature (Morin & Egan, 1992; Polglase & Hooper, 2006). As the developing pulmonary vasculature becomes sensitive to small changes in oxygen tension from about mid-gestation (Lewis *et al.*, 1976; Blanco *et al.*, 1988; Morin & Egan, 1992), increased oxygenation at birth is widely regarded as a major driver of pulmonary vasodilation at birth. Indeed, alteration in oxygen tension is a well known mediator of ventilation/perfusion relationships in the adult lung (Weissmann *et al.*, 2006; Sylvester *et al.*, 2012). Oxygen (O₂) stimulates vasodilation directly via mitochondria, as well as through vasodilator intermediates including nitric oxide (NO) (Tiktinsky & Morin, 1993),

the vasodilatory prostaglandins PGI₂ (prostacyclin) and PGE₂, bradykinin and purine nucleotides (Gao & Raj, 2010). However, despite the well-known role for O₂, ventilation with a hypoxic gas mixture is able to elicit the majority (60%) of the breathing-related increase in PBF at birth (Teitel *et al.*, 1990). Similarly, both increases and decreases in oxygenation status are associated with ventilation-induced increases in PBF that are identical in magnitude at birth (Sobotka *et al.*, 2011). While the precise mechanisms are unclear, it is clear that the initial entry of gas into the lungs is the most significant factor responsible for the increase in PBF at birth.

Our recent study has demonstrated that the increase in PBF at birth is not spatially related to lung aeration as partial lung aeration caused a global increase in PBF (Lang *et al.*, 2014). It was expected that regional lung aeration would cause localised reductions in PVR through (i) an increase in oxygenation and (ii) capillary expansion and recruitment due to an increase in alveolar/capillary wall transmural pressures resulting from a surface tension mediated increase in lung recoil (Hooper, 1998). As neither mechanism was expected to be active in non-ventilated lung regions the finding that the increase in PBF is not spatially related to lung aeration (Lang *et al.*, 2014) indicates that the mechanisms responsible for the increase in PBF at birth requires re-evaluation. It is possible that regional lung aeration increased circulating partial pressure of oxygen in arterial blood (PaO₂) levels, causing vasodilation in non-aerated lung regions. Our aim was to examine this hypothesis by partially aerating the lung in the absence of O₂, and determine the effect on PBF in unaerated lung regions. We hypothesised that partial lung aeration with 100% nitrogen (N₂) (0% oxygen) would trigger a global increase in PBF and increasing O₂ levels in the inspired gas would enhance the increase in PBF in aerated regions. To assess the regional changes in PBF and the spatial relationships between PBF and lung aeration, we used our previously established imaging technique that

combines phase-contrast (PC) X-ray imaging with angiography in near-term rabbit neonates (Lang *et al.*, 2014).

4.3 Methods

4.3.1 Experimental procedure

All animal procedures were approved by the SPring-8 Animal Care and Monash University's School of Biomedical Science's Animal Ethics Committees and the Japan Synchrotron Radiation Research Institute, SPring-8 Animal Experiment Committee (proposals 2012A0047, 2012A1314). All studies were conducted in experimental hutch 3 of beamline 20B2, in the Biomedical Imaging Centre at the SPring-8 synchrotron, Japan.

Pregnant New Zealand white rabbits at 30 days gestation (term \approx 32 days) were anaesthetised using propofol (i.v.; 12 mg/kg bolus; Rapinivet, Schering-Plough Animal Health, Tokyo, Japan) and intubated. Anaesthesia was maintained by isoflurane inhalation (1.5– 4%; Isoflu, Dainippon Sumitomo Pharma Co., Osaka, Japan). Fetal rabbits (n = 18) were partially delivered by cesarean section, sedated with sodium pentobarbitone (13 mg/kg i.p.; Somnopentyl, Kyoritsu Seiyaku Co., Ltd, Tokyo, Japan) and a jugular vein catheter (24 G Intracath, Becton Dickinson, Franklin Lakes, NJ, USA) and an endotracheal (ET) tube (18 G Intracath; via tracheostomy) were inserted. The tip of the ET tube was directed into the right bronchus so that with ventilation onset only the right lung was ventilated (unilateral ventilation). During the surgical procedure, the kit's head remained covered with fetal membranes to prevent lung aeration, the umbilical cord remained intact and the ET tube was obstructed to prevent breathing. The kits were then delivered and the umbilical cord ligated before they were placed upright in an acrylic frame. ECG leads were attached to the skin of the upper limb and both lower limbs. The ET tube was then connected to a purpose-built,

time-cycled, pressure-controlled ventilator (Kitchen *et al.*, 2010) and image acquisition began as soon as possible after the kits were positioned. Kits were initially ventilated in either 100% N₂, 21% O₂ (air) or 100% O₂ using a peak inflation pressure of 25 cmH₂O and a positive end-expiratory pressure of 5 cmH₂O. At the conclusion of the experiment (~10 minutes after ventilation onset for kits), all animals were humanely killed with an overdose of sodium pentobarbitone (Pentobarbital; >100 mg/kg) administered *I.V.* (doe) or *I.P.* (kits).

4.3.2 X-ray and angiography imaging

Monochromatic X-rays at 33.2 keV and a photon flux of $\sim 10^8$ photons/mm²/s was used for imaging with the kits positioned 1.0 m upstream of the detector. The scientific-CMOS (sCMOS) detector (pco.edge; PCO AG, Kehlheim, Germany) was coupled to a 25 μ m thick gadolinium oxysulfide (Gd₂O₂S:Tb⁺) powdered phosphor and a tandem lens system that provided an effective pixel size of 15.3 μ m and an active field of view of 29 (W) \times 30 (H) mm². Images were acquired at a frame rate of 10 Hz. During imaging, iodine boluses (Iomeron 350 mg/ml iodine; Bracco-Eisai Pty. Ltd, Tokyo, Japan; 1.5 μ L per g kit body weight at 11 ml/s) were administered via the jugular vein using a remote-controlled syringe pump (PHD2000, Harvard Apparatus Inc., Holliston, MA, USA). Iodine boluses were injected and images acquired for an average of 44 ± 9 s before ventilation onset and for a further 97 ± 14 s during unilateral ventilation of the right lung with either 100% N₂ (n = 6), 21% O₂ (n = 6) or 100% O₂ (n = 6). Following this period, unilateral ventilation continued in air in all groups for 184 ± 14 s, subsequently the ET tube was retracted to ventilate both lungs in air, which continued for 118 ± 12 s. The elapsed time between ventilation periods was consistent between groups.

4.3.3 Image analysis

Images were analysed using ImageJ (v1.49; NIH, Bethesda, MD, USA) as described previously (Lang *et al.*, 2014). Comparisons were made between the number of visible pulmonary vessels, vessel diameters, heart rate, iodine ejection per beat, pulmonary transit time and change in mean grey level profiles within the left and right main axial arteries and the aorta following iodine injection. When ECG recordings were unsuccessful, heart rate was calculated from the inter-beat interval derived from the imaging sequence.

4.3.3.1 Vessel quantification

Visible blood vessels were counted using a composite image constructed from 10 X-ray image frames (1 s) of peak opacification during an iodine bolus (Lang *et al.*, 2014). Images acquired during lung movement were excluded due to motion blur. Iodine-perfused arterial vessels distal to branching points were counted as individual vessels and were visible up to the 3rd order of branching.

4.3.3.2 Main axial artery vessel diameter

Changes in pixel grey level (intensity) along virtual lines transecting vessels perpendicular to a vessel wall were used to measure vessel internal diameter (ID). Line profiles were drawn over the left and right main axial arteries (taken mid-lung at the 7th intercostal space), tracking ID changes from the baseline pre-ventilation period (Lang *et al.*, 2014). To correct for background variation, during iodine perfusion line profiles were divided by the average background intensity, over the 10 frames (1 s) immediately prior to the first appearance of contrast within the vessel. Internal vessel edges were determined as the first pixel to drop below 1 standard deviation of the mean intensity of the background tissue at either end of the

line profile (~5 pixels past the vessel edge). Vessel diameters measured in pixels from each frame were averaged over 5 frames (0.5 s) then multiplied by the known pixel size (15.3 μm) to estimate a mean vessel ID.

4.3.3.3 *Pulmonary arterial transit time*

A virtual box was placed over the distal end of the left and right main axial arteries before first-order branching (taken at the level of the eighth intercostal space for consistency). The mean intensity of this region was calculated for each frame. Bolus arrival time was designated as the frame in which half of the peak opacity (maximum % change from background) is reached for the first time (half-peak opacity), this corrects for problems due to steady state peak opacity values in cases of poor wash-out (Shpilfoygel *et al.*, 2000). The elapsed time between the half-peak opacity value in the main pulmonary artery (MPA) compared to the left and right axial arteries (at the 8th intercostal space) was calculated to give an approximation of bolus pulmonary artery transit time.

4.3.3.4 *Changes in opacity over time within the MPA and aorta*

A virtual box was placed over the MPA immediately distal to the right ventricular outlet, the descending aorta, and the left and right main axial arteries at the level of the seventh intercostal space; the last providing a centrally-located, clear and unobstructed view of the large conduit arteries during both the pre-ventilation and ventilation imaging time periods. The changes in mean intensity within each box were plotted against time as a percentage change from background levels (mean background intensity averaged over 10 frames before iodine injection) throughout each iodine injection sequence. The maximum of this time-opacity curve was then divided by the pulmonary arterial transit time to provide an indicator

of changes in pulmonary arterial flow in both lungs, right ventricular output and the relative contribution of right ventricular output to flow in the aorta during all ventilation periods.

4.3.4 Statistical analysis

Changes in visible vessel number, blood vessel ID, heart rate, pulmonary arterial transit time and opacity of blood vessels were analysed using a two-way repeated measures ANOVA. Post-hoc analysis used the Holm-Sidak method. A $p < 0.05$ was considered statistically significant.

4.4 Results

4.4.1 Animal data

PC X-ray images were obtained from 18 kits (30 days gestational age) from eight pregnant rabbits. Mean kit weight was 42.3 ± 1.3 g, which was similar between groups.

4.4.2 Observations from PC X-ray videos

Consistent with our previous findings (Lang *et al.*, 2014), unilateral ventilation of the right lung (1LV₁) markedly increased iodine flow into both left (unaerated) and right (aerated) axial arteries compared to the pre-ventilation period (0LV). The increase in flow in the unaerated lung was similar irrespective of whether the initial gas used to ventilate the right lung was 100% N₂ (Figure 4.1; Supplementary Video 4.1), air (Lang *et al.*, 2014) or 100% O₂ (Figure 4.1; Supplementary Video 4.2). As such, iodine distribution increased to the non-aerated left lung despite ventilation with a gas mixture that had no oxygen. Continued unilateral ventilation in air (1LV₂) and subsequent ventilation of both lungs with air (2LV)

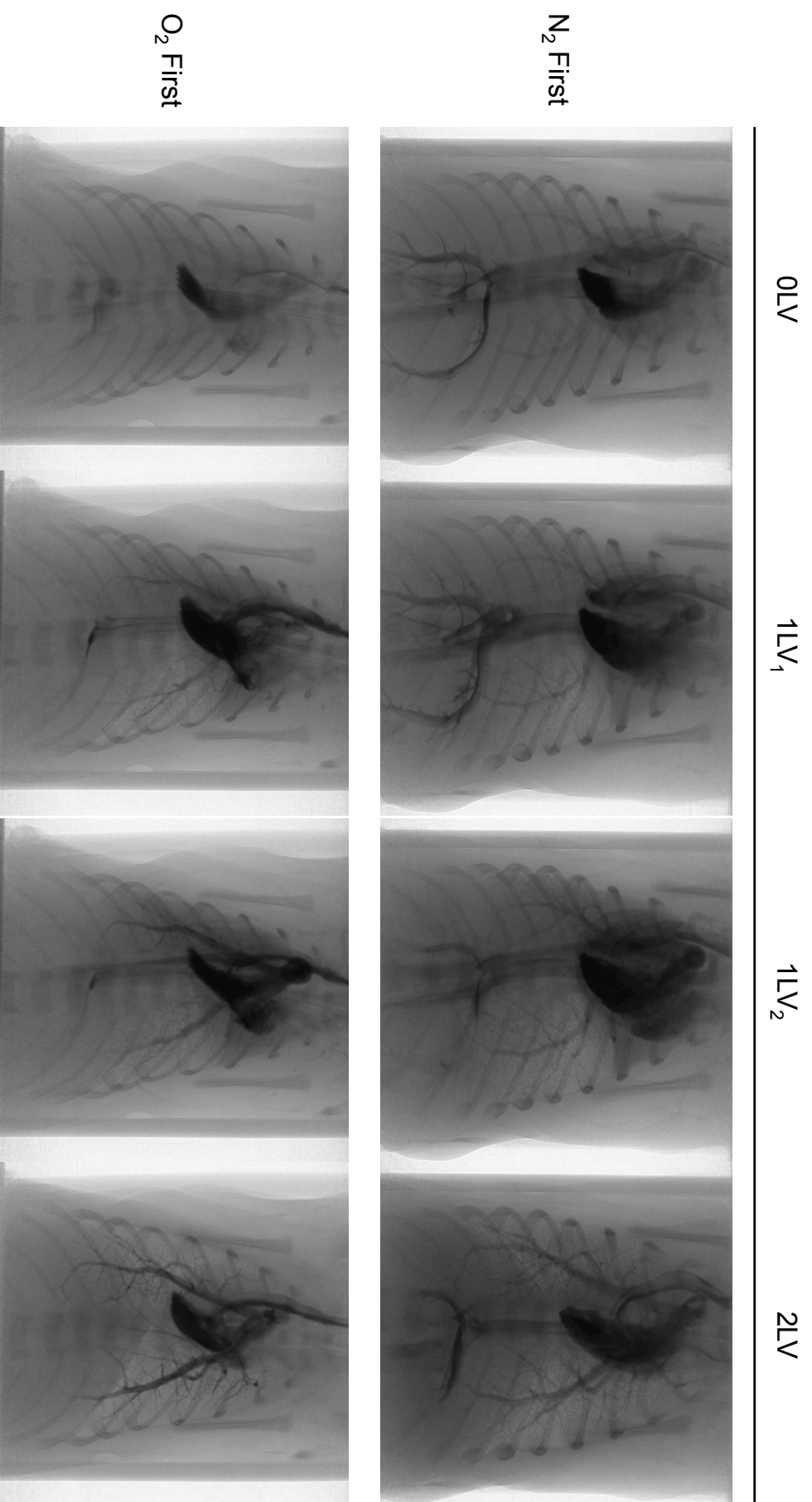


Figure 4.1: PC X-ray and angiography images

Representative X-ray image sequences of newborn rabbits imaged prior to ventilation (0LV), following unilateral ventilation of the right lung (1LV₁) with either 100% N₂ or 100% O₂, subsequent ventilation with air (21% O₂) in all kits (1LV₂), and later ventilation of both lungs in air (2LV). Images were obtained 1–3 s following iodine bolus injection.

sustained this increase in PBF and appeared to cause only modest (potentially time-related) increases compared to the initial increase in PBF in all groups (Figure 4.1).

4.4.3 Indices of vessel recruitment

Following unilateral ventilation of the right lung with 100% N₂ (1LV₁ in Figure 4.2), the total number of visible vessels increased in the left and right lungs respectively from 28 ± 5 and 28 ± 6 vessels to 48 ± 9 and 45 ± 8 vessels following ventilation onset. Similarly, unilateral ventilation of the right lung with air increased the number of visible vessels from 21 ± 5 and 19 ± 5 vessels to 45 ± 4 and 44 ± 4 vessels in the left and right lungs respectively; the percentage increase was similar to ventilation with 100% N₂. Unilateral ventilation with 100% O₂ (1LV₁) increased vessel numbers from 34 ± 6 and 33 ± 5 vessels to 65 ± 7 and 79 ± 8 vessels in left and right lungs, respectively. While unilateral ventilation of the right lung with 100% N₂ and air increased visible vessel numbers similarly in both left and right lungs, ventilation with 100% O₂ resulted in a greater increase in the ventilated right lung (79 ± 8 vessels in the right lung compared to 66 ± 7 vessels in the unventilated left lung). Following the period of unilateral ventilation with 100% N₂, unilateral ventilation of the right lung (1LV₂) and then bilateral ventilation (2LV) with air increased the number of visible vessels further to 59 ± 8 vessels and 55 ± 8 vessels at 1LV₂ then 70 ± 7 vessels and 71 ± 7 vessels at 2LV in the left and right lungs, respectively. Similarly, following the period of unilateral ventilation with air and 100% O₂, the subsequent ventilation periods of unilateral ventilation with air and bilateral ventilation with air tended to increase the number of visible vessels further, but this increase was not significant.

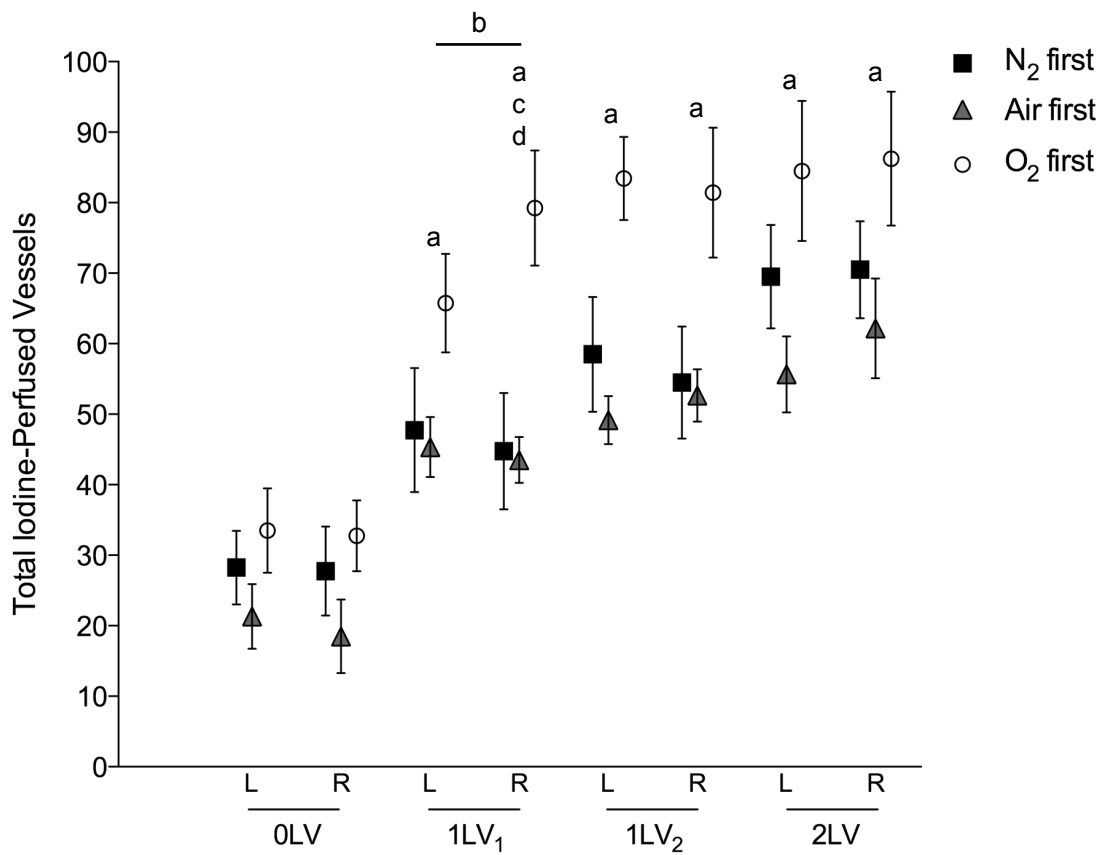


Figure 4.2: Changes in visualized blood vessel number

Mean iodine-perfused vessel number (\pm SEM) in the left and right lungs at each ventilation period (0LV, 1LV₁, 1LV₂ and 2LV) in the N₂ first (black solid squares), air first (grey solid triangles) and O₂ first (open circles) groups. ^aP < 0.05 compared to baseline (0LV) in the same lung in all groups; ^bP < 0.05 left lung vs. right lung in O₂ first; ^cP < 0.05 air first vs. O₂ first; ^dP < 0.05 N₂ first vs. O₂ first.

4.4.4 Heart rate and opacity changes in the MPA and aorta over time

Heart rate increased from 55.6 ± 5.4 bpm to 90.3 ± 13.4 bpm following unilateral ventilation of the right lung with 100% N₂. Similarly, unilateral ventilation of the right lung with air or 100% O₂ increased heart rates from 69.4 ± 4.9 bpm and 46.4 ± 3.3 bpm to 93.0 ± 15.0 bpm and 73.0 ± 10.0 bpm, respectively (Figure 4.3A). Heart rates were not significantly changed during the subsequent period of unilateral lung ventilation with air in all groups (1LV₂), but increased further to 129.9 ± 7.0 bpm, 136.0 ± 15.2 bpm and 115.6 ± 10 bpm during bilateral ventilation (2LV) in kits initially ventilated with 100% N₂, air and 100% O₂, respectively. No differences in heart rate were detected between groups.

Peak opacity within the MPA (Figure 4.3B), which provides an indicator of right ventricle output, significantly increased following unilateral ventilation of the right lung with either air or 100% O₂. Unilateral ventilation of the right lung with air increased peak opacity from 39.9 ± 7.3 % to 72.8 ± 4.4 % above background, whereas unilateral ventilation of the right lung with 100% O₂ increased peak opacity from 35.5 ± 6.1 % to 64.2 ± 5.6 % above background; these values did not increase further after continued ventilation (1LV₂ or 2LV). Unilateral ventilation of the right lung with 100% N₂ also tended to increase MPA peak opacity, from 31.3 ± 5.6 % to 45.8 ± 7.0 % above background, but this increase only became statistically significant after the switch to air and both lungs (2LV), when it increased to 66.0 ± 4.2 % above background. Peak opacification in the descending aorta (Figure 4.3C), representing the contrast agent diverted through the ductus arteriosus, significantly increased in response to unilateral ventilation when ventilated with either air or 100% O₂ but did not significantly increase further with continued ventilation.

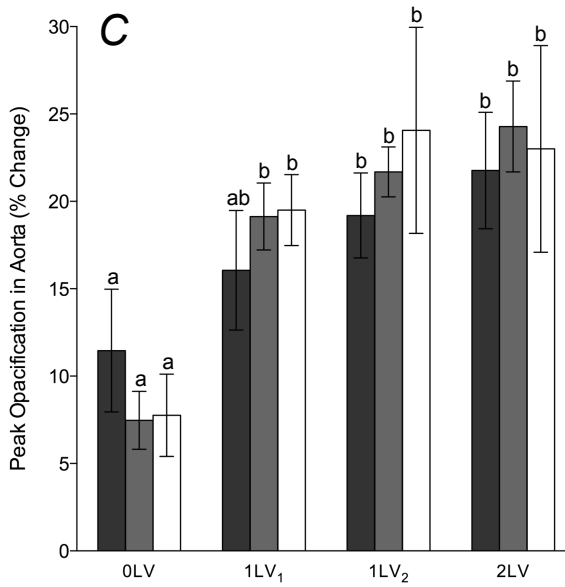
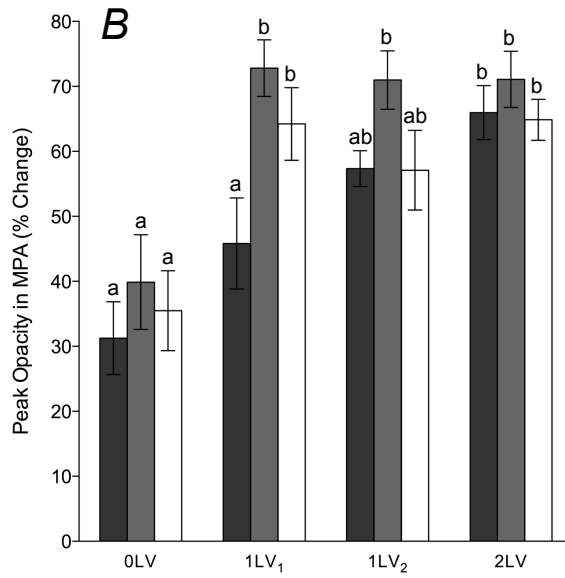
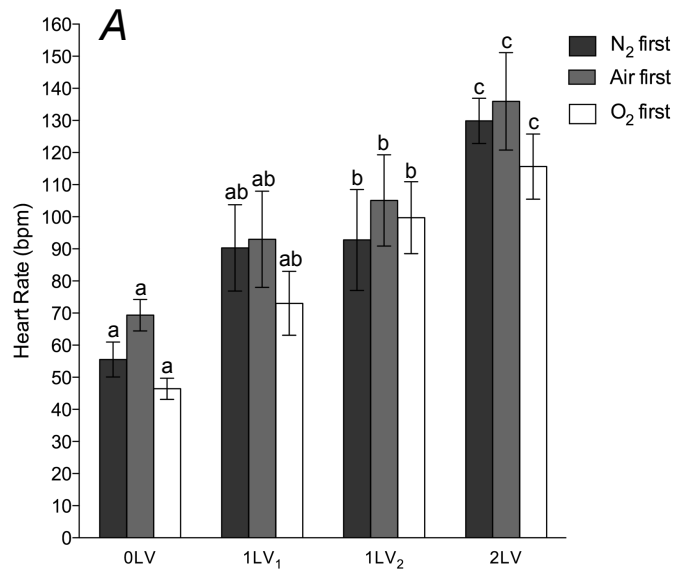


Figure 4.3: Heart rate and iodine distribution changes during ventilation

A: heart rate (bpm). **B:** an index of right ventricle output given by peak opacification (% intensity change from background) in the MPA (immediately distal to the right ventricle). **C:** peak opacification (% intensity change from background) in the descending aorta. In all panels, data shown are mean \pm SEM at each ventilation period (0LV, 1LV₁, 1LV₂ and 2LV) in the N₂ first (dark bars), air first (grey bars) and O₂ first (white bars) groups. Within each graph, bars that do not share a letter are significantly different from each other ($P < 0.05$).

4.4.5 Arterial vessel internal diameter

Compared to pre-ventilation values, unilateral ventilation (1LV₁) of the right lung significantly increased ID of the left and right main axial arteries at the level of the seventh intercostal space in both lungs in all three groups (Figure 4.4). The diameters increased from $505 \pm 49 \mu\text{m}$ and $505 \pm 39 \mu\text{m}$ in the left and right main axial arteries to $585 \pm 58 \mu\text{m}$ and $581 \pm 40 \mu\text{m}$, respectively, in response to unilateral ventilation of the right lung with 100% N₂. These increases were similar to those observed following unilateral ventilation with air (increased from $533 \pm 40 \mu\text{m}$ and $533 \pm 35 \mu\text{m}$ to $597 \pm 39 \mu\text{m}$ and $596 \pm 40 \mu\text{m}$, in left and right vessels respectively) and 100% O₂ (increased from $500 \pm 58 \mu\text{m}$ and $506 \pm 55 \mu\text{m}$ to $559 \pm 47 \mu\text{m}$ and $651 \pm 56 \mu\text{m}$ in left and right vessels respectively), except that the increase in the right axial artery ventilated with 100% O₂ tended to be greater. While ID tended to increase during the subsequent ventilation periods, this increase was not significant. IDs between the groups were not significantly different at any point although IDs in the right lung following initial ventilation with O₂ tended to be greater.

4.4.6 Iodine bolus transit time

Pulmonary arterial transit time, given by the elapsed time between iodine bolus passage from the MPA to arrival at the distal end of the left and right axial arteries, significantly decreased in response to unilateral ventilation (1LV₁) in all groups irrespective of the gas used (100% N₂, air or 100% O₂) (Figure 4.5A). Unilateral ventilation of the right lung with 100% N₂ decreased the transit time from $2.08 \pm 0.48 \text{ s}$ and $2.03 \pm 0.47 \text{ s}$ to $1.00 \pm 0.39 \text{ s}$ and $0.93 \pm 0.37 \text{ s}$ in the left and right pulmonary arteries, respectively. Similarly, unilateral ventilation with 100% O₂ decreased the transit times from $1.33 \pm 0.41 \text{ s}$ and $1.45 \pm 0.28 \text{ s}$ to $0.23 \pm 0.06 \text{ s}$ and $0.33 \pm 0.14 \text{ s}$ in the left and right axial arteries, respectively. Subsequent ventilation

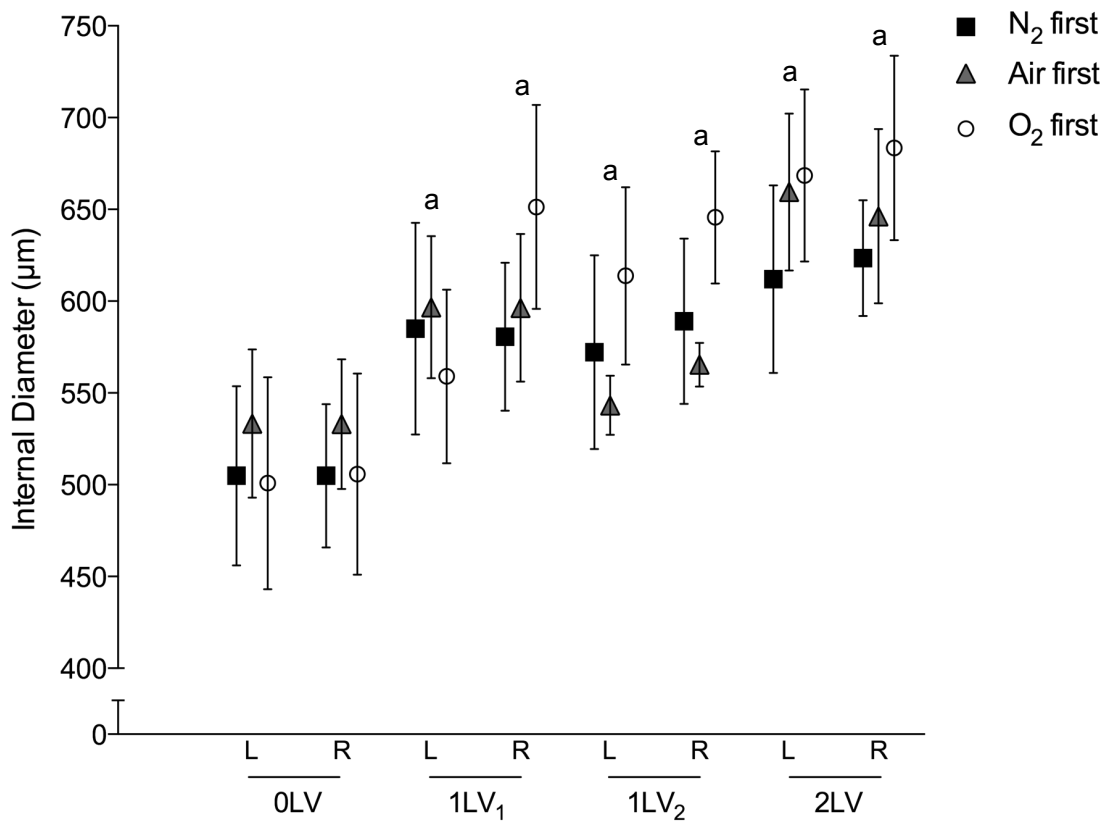
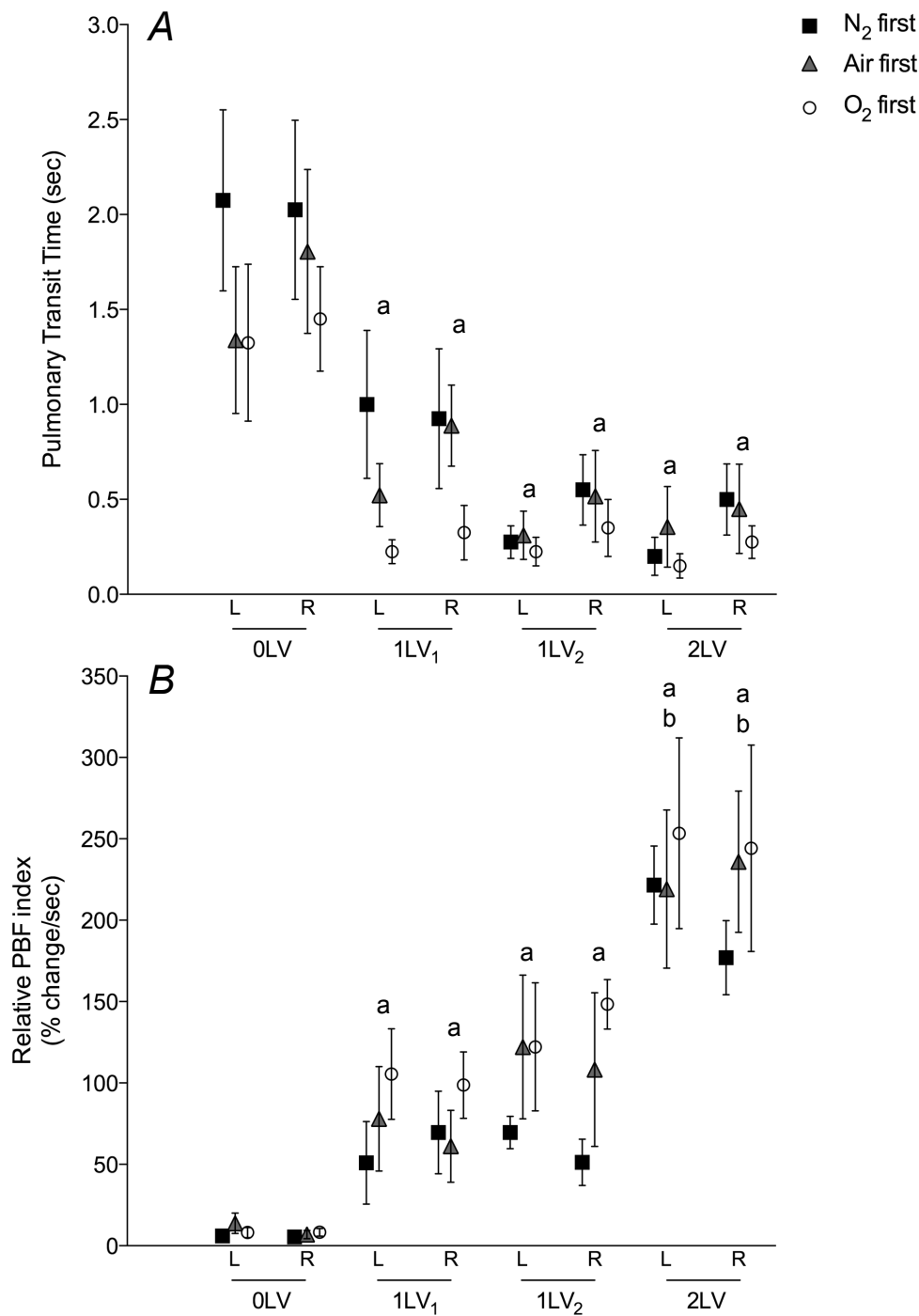


Figure 4.4: Blood vessel internal diameter changes during ventilation

Mean internal diameter (μm , \pm SEM) of the left and right axial arteries at the seventh intercostal space at each ventilation period (0LV, 1LV₁, 1LV₂ and 2LV) in the N₂ first (black solid squares), air first (grey solid triangles) and O₂ first (open circles) groups. ^aP < 0.05 compared to baseline (0LV) in the same lung in the same group.



periods (1LV₂, 2LV) did not significantly alter the transit time from the initial decrease and no difference was detected between lungs or between groups.

4.4.7 Changes in relative PBF indices

Relative PBF indices, given by the maximum change in relative iodine levels (% decrease in intensity below background) divided by the arterial transit time, significantly increased in response to unilateral ventilation in all groups irrespective of the gas used (100% N₂, air or 100% O₂) (Figure 4.5B). Unilateral ventilation of the right lung with 100% N₂ increased the relative PBF index from 6.0 ± 2.9 %/s and 5.5 ± 2.6 %/s to 51.0 ± 25.1 %/s and 69.7 ± 25.4 %/s in the left and right pulmonary arteries, respectively. Unilateral ventilation of the right lung with air increased relative PBF index from 13.8 ± 6.2 %/s and 6.9 ± 2.3 %/s to 78.0 ± 32.0 %/s and 61.1 ± 22.1 %/s in the left and right pulmonary arteries, respectively. Unilateral ventilation of the right lung with 100% O₂ increased relative PBF index from 8.1 ± 3.2 %/s and 8.3 ± 2.4 %/s to 105.5 ± 27.8 %/s and 98.7 ± 20.4 %/s in the left and right pulmonary arteries, respectively. The subsequent ventilation period (1LV₂) did not significantly alter the relative PBF values in any group but relative PBF increased significantly after changing to bilateral ventilation (2LV). No difference was detected between lungs or between groups.

4.5 Discussion

The recent finding that partial lung aeration causes a global increase in lung perfusion indicates that pulmonary vasodilation at birth is not spatially related to lung aeration and that an additional, previously unsuspected mechanism may be involved (Lang *et al.*, 2014). However, the possibility of re-circulation of oxygenated blood causing increased oxygenation and vasodilation in these unventilated lung regions could not be completely dismissed. The data presented in this study now confirm that the global increase in PBF that is initiated by partial lung aeration immediately following birth is independent of changes in oxygenation. However, inhalation of 100% oxygen was found to have an additive effect on pulmonary vasodilation and PBF, which was localised to aerated lung regions. This indicates that there are a number of factors that work independently to increase PBF at birth.

In this study, partial aeration of the right lung was confirmed by PC X-ray imaging, which gives rise to a distinctive speckle pattern caused by multiple phase shifts at the air/liquid boundaries in the distal airways (Kitchen *et al.*, 2004). As such, we are able to confirm from the images the lack of aeration in lung regions not being ventilated. Findings were consistent with previous studies, showing that a significant ventilation/perfusion mismatch occurs after birth when the lung is partially aerated (Figure 4.1; Supplementary Videos 4.1 & 4.2) (Lang *et al.*, 2014). This observation has been extended to show that unilateral ventilation of near-term newborn rabbit kits with an oxygen-free inspired gas also causes a global increase PBF. We consistently found that, in all parameters measured, the greatest change occurs between the pre-ventilation and the initial unilateral ventilation periods, with relatively minor changes occurring thereafter. This indicates that partial lung aeration induces a large global increase in PBF, which is mediated by a potent mechanism that is unrelated to oxygenation levels.

As pulmonary perfusion is low prior to lung aeration (Rudolph, 1979; Crossley *et al.*, 2009), the number of visible vessels and the penetration of contrast agent into distal vessels is low and the transit time for the flow of contrast through the pulmonary vessels is long. Following partial lung aeration, irrespective of the inspired gas content, the number of visible vessels, the diameter of the pulmonary vessels and the penetration of contrast agent into the distal pulmonary vasculature tree increased, and transit time for the flow of contrast agent markedly decreased (Figure 4.1; Supplementary Video 4.1 & 4.2). These changes are all indicative of downstream vasodilation, vessel recruitment and an associated fall in PVR. This confirms the role of initial lung aeration as the primary stimulus for the increase in PBF at birth, although the precise mechanism involved remains intriguing. Indeed, this mechanism is independent of oxygenation, but may be enhanced by oxygen, and while it can be activated by aeration of localised regions, it is translated into a global vasodilatory response. We speculate that, with gas entry into the lungs, the rapid lung liquid accumulation in the interstitial tissue (Bland *et al.*, 1980; Siew *et al.*, 2009b) may be the stimulus for these changes, possibly via activation of J-receptors. These receptors, located within the alveolar walls, are known to respond to fluid accumulation, particularly pulmonary edema, and signal via vagal C-fibres to cause global pulmonary vasodilation (Paintal, 1969).

Unilateral ventilation of the right lung with 100% O₂ caused a greater increase in the number of visible vessels and the vessel ID in the ventilated right lung compared to the unventilated left lung. As these differences between the left and right lungs were not evident in kits ventilated with 100% N₂ or air, this difference likely reflects an oxygen dependent effect. However, the vasodilatory effect of oxygen appeared to be localised to aerated lung regions and was additive to the effect of lung aeration with any gas. This provides further evidence to suggest that the initial effect of lung aeration on the global increase in PBF is mediated by

factors that are independent of oxygen. This suggestion is consistent with previous findings that ventilation with a hypoxic gas mixture can increase PBF in sheep without an increase in oxygenation (Teitel *et al.*, 1990). Similarly, the increase in PBF with ventilation onset was shown to be similar between two groups of neonatal lambs, despite the fact that oxygenation increased in one group, but decreased in the other compared with fetal levels (Sobotka *et al.*, 2011). In this study, an effect of local oxygen concentration is seen; however, the majority of the differences we observed derive from the initial entry of gas into the lungs after birth, irrespective of the gas content.

The increase in cardiac function in response to unilateral ventilation, as shown by the increase in heart rate and right ventricle output, likely also contributes to the increase in PBF observed (Figure 4.3). This is possible directly via the pulmonary arteries, or indirectly via an increase in aortic pressure from the increased left ventricle function, thereby supporting the increase in pulmonary blood flow via the patent ductus arteriosus. However, this increase in cardiac output is also dependent upon an increase in PBF. As the umbilical circulation provides a large component of the venous return and preload for both left and right ventricles, when the umbilical cord is clamped at birth, cardiac output can decrease by up to 50% (Crossley *et al.*, 2009; Bhatt *et al.*, 2013). Venous return is only restored after birth following lung aeration and the increase in PBF, which takes over the role of supplying preload for the left ventricle (Crossley *et al.*, 2009; Bhatt *et al.*, 2013). As such, the increase in PBF at birth is vital for sustaining cardiac output after birth. Interestingly, an increase in cardiac output was observed (Figure 4.3A) in response to unilateral ventilation of the right lung with 100% N₂ (Figure 4.3). As the increase in cardiac output could not be due to increased oxygenation, it can only have resulted from an increase in PBF leading to an increase in ventricular preload (Sylvester *et al.*, 2012). As such, we postulate that the increase in cardiac function at birth in humans is

mostly a consequence of the increase in PBF, which may or may not be a result of an increase in oxygenation. This underpins the importance of lung aeration as the defining event that initiates the cascade of changes that characterise the transition from fetal to newborn life at birth. It not only allows gas-exchange to commence and stimulates an increase in PBF, but it also increases cardiac output by restoring the venous return lost by cord clamping.

Although the increases in main axial artery IDs induced by lung aeration were modest (increase by ~10%; Figure 4.4), because the resistance decreases exponentially with increasing vessel radius (resistance $\approx 1/\text{radius}^4$), such increases in diameter reflect large decreases in resistance (Figure 4.5). This is consistent with the finding of markedly reduced pulmonary transit times, which is an index of flow velocity, resulting from the decrease in PVR, although an increase in cardiac output may also have contributed. Nevertheless, unilateral ventilation with 100% N₂ both increased vessel diameter and reduced pulmonary transit times. While the decrease in transit times were not different at any point between groups, kittens ventilated with 100% O₂ rapidly hit the maximum detection velocity as determined by the 10 Hz frame rate. As such, the reduction in transit times in this group may have been underestimated and may explain why a left/right difference was not observed in this parameter. Nonetheless, the rapid increase in flow velocity to both lungs and the large increase in relative PBF index (Figure 4.5 lower panel) provide a robust indication of the increase in PBF associated with lung aeration.

4: Increase in PBF at Birth: Role of O₂ and Aeration

In fetal life, the maintenance of a high PVR restricts perfusion of non-aerated lungs, whereas at birth, lung aeration rapidly decreases PVR resulting in a large increase in PBF so that gas-exchange can commence (Fineman *et al.*, 1995). This study confirms that lung aeration and the increase in PBF are not spatially related and that limited aeration of the lungs leads to global PBF changes (Lang *et al.*, 2014). Furthermore, we have now shown that partial aeration of the lung with a gas that has no oxygen can activate a global decrease in PVR. This indicates that a highly potent stimulus that is unrelated to oxygen can initiate the aeration-induced changes in PBF; however, the underlying mechanisms are currently unknown and require further investigation.

Chapter Five

*Vagal Denervation Inhibits the
Increase in Pulmonary Blood Flow
During Partial Lung Aeration at Birth*

Lang, JAR, Pearson JT, Binder-Heschl C, Wallace MJ, Siew ML, Kitchen MJ, te Pas AB, Fouras A, Lewis RA, Polglase GR, Shirai M & Hooper SB (2017) Vagal denervation inhibits the increase in pulmonary blood flow during partial lung aeration at birth. *The Journal of Physiology* **595**(5): 1593-1606

I have renumbered and reformatted sections of this published paper in order to generate a consistent presentation within this thesis.

See Appendix C for published PDF.

The aeration of a single lung at birth, even without inspired oxygen content, is able to rapidly increase PBF throughout both lungs in both aerated and non-aerated regions. As mechanisms unrelated to local oxygenation or the mechanical effects of lung aeration appear to induce these changes, other, not previously implicated stimuli must be considered. Various studies suggest that sensory nerves running within the vagal trunk may mediate some PBF changes at birth. Thus, a neural reflex triggered by air entry into the lungs may potentially be responsible for these observations. The aim of this chapter was to investigate the relative roles of vagal innervation and local PO₂ on the increase and regional distribution of PBF immediately after birth. We expected that vagal denervation would disrupt vasodilation in non-aerated lung regions following partial lung aeration, regardless of the O₂ content of the inspired gas.

Declaration for Chapter 5

Vagal denervation inhibits the increase in pulmonary blood flow during partial lung aeration at birth

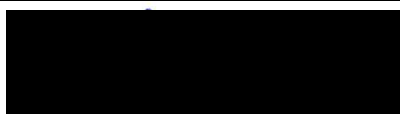
In the case of Chapter 5, the nature and extent of my contribution to the work was the following:

Nature of Contribution	Extent of Contribution
Experimental design, performed all experimental work, data collection and analysis and wrote and edited the manuscript	70%

The following co-authors contributed to the work. No co-authors were students at Monash University.

Name	Nature of Contribution
James T. Pearson	Experimental design and work and manuscript editing
Corinna Binder-Heschl	Experimental work and manuscript editing
Megan J. Wallace	Experimental work and manuscript editing
Melissa L. Siew	Experimental work and manuscript editing
Marcus J. Kitchen	Experimental work and manuscript editing
Arjan B. te Pas	Experimental work and manuscript editing
Andreas Fouras	Experimental work and manuscript editing
Robert A. Lewis	Experimental design and work and manuscript editing
Graeme R. Polglase	Experimental work and manuscript editing
Mikiyasu Shirai	Experimental work and manuscript editing
Stuart B. Hooper	Experimental design and work and manuscript editing

The undersigned hereby certify that the above declaration correctly reflects the nature and extent of the candidate and co-authors' contributions to this work.

Candidate's Signature		Date: 15/12/16
Main Supervisor's Signature		Date: 15/12/16

5.1 Abstract

Air entry into the lungs at birth triggers major cardiovascular changes, including a large increase in pulmonary blood flow (PBF) that is not spatially related to regional lung aeration. To investigate the possible underlying role of a vagally-mediated stimulus, we used simultaneous phase-contrast X-ray imaging and angiography in near-term (30 days of gestation) vagotomised (n = 15) or sham-operated (n = 15) rabbit kittens. Rabbits were imaged before ventilation, when one lung was ventilated (unilateral) with 100% nitrogen (N₂), air or 100% oxygen (O₂), before all kittens were switched to unilateral ventilation in air, then ventilation of both lungs using air. Compared to control kittens, vagotomised kittens had little or no increase in PBF in both lungs following unilateral ventilation when ventilation occurred with 100% N₂ or with air. However, relative PBF did increase in vagotomised animals ventilated with 100% O₂, indicating the independent stimulatory effects of local oxygen concentration and autonomic innervation on the changes in PBF at birth. These findings demonstrate that vagal denervation inhibits the previously observed increase in PBF with partial lung aeration, although high inspired oxygen concentrations can partially mitigate this effect.

5.2 Introduction

Lung aeration and the displacement of airway liquid into the pulmonary interstitium at birth not only allows pulmonary gas-exchange to commence, but also stimulates a large increase in pulmonary blood flow (PBF) (Rudolph, 1985; Hooper *et al.*, 2007; Hooper *et al.*, 2015). During fetal life, gas-exchange occurs across the placenta and PBF is low due to a high pulmonary vascular resistance (PVR). As such, in the fetus PBF contributes little to preload for the left ventricle, which is primarily derived from umbilical venous return, via the ductus venosus and foramen ovale (Rudolph, 1985; Crossley *et al.*, 2009; Bhatt *et al.*, 2013). Following birth, umbilical venous return is lost with clamping of the umbilical cord and so PBF must rapidly increase to facilitate pulmonary gas-exchange and supply preload for the left ventricle (Bhatt *et al.*, 2013). Although the increase in PBF underpins the transition to newborn life at birth, the precise mechanisms by which lung aeration triggers this process remain poorly understood.

Numerous factors, which include increased oxygenation, the release of vasodilators (e.g. nitric oxide (NO)) and mechanical factors are thought to contribute to the increase in PBF at birth (Gao & Raj, 2010). Increased oxygenation dilates pulmonary vessels through mediators such as NO, prostaglandin I₂ (PGI₂; prostacyclin), prostaglandin E₂ (PGE₂), bradykinin and purine nucleotides (Abman *et al.*, 1990). Similarly, an increase in lung recoil caused by air entry and the formation of surface tension at the air/liquid interface increases recruitment and expansion of peri-alveolar capillaries leading to a decrease in PVR (Hooper, 1998). Recent findings have identified an additional, previously unrecognised, factor that contributes to the increase in PBF at birth (Lang *et al.*, 2014; Lang *et al.*, 2016). Those studies showed that partial lung aeration without O₂ increased PBF equally in both aerated and non-aerated lung

regions (Lang *et al.*, 2016). While these findings are consistent with previous studies showing that ventilation can increase PBF in the absence of increased oxygenation (Teitel *et al.*, 1990; Sobotka *et al.*, 2011), the large increase in PBF in unventilated regions was surprising and could not be readily explained (Lang *et al.*, 2014).

The global increase in PBF following partial lung aeration indicates the possible role of a neural reflex at birth that is triggered by the entry of gas into the lungs. Intrathoracic vagal denervation, which selectively denervates the lungs, reduces respiratory function at birth and the increase in arterial oxygenation in newborn lambs (Wong *et al.*, 1998; Lalani *et al.*, 2002). While this was primarily thought to result from respiratory failure (Wong *et al.*, 1998; Lalani *et al.*, 2002), an impaired increase in PBF was raised as a possibility (Wong *et al.*, 1998), which is consistent with previous studies showing that vagal stimulation causes pulmonary vasodilation in fetal sheep (Colebatch *et al.*, 1965). Although a reduction in PBF was later discounted (Hasan *et al.*, 2000), the effects of vagotomy on regional changes in pulmonary blood flow or ventilation/perfusion relationships have not been examined previously.

In this study, we have investigated the role of the vagus nerve in mediating the increase in PBF at birth using our unique technique of simultaneous phase contrast X-ray imaging and angiography in newborn rabbits. We hypothesised that vagotomy would disrupt vasodilation in non-aerated lung regions following partial lung aeration, regardless of the O₂ content of the inspired gas.

5.3 Methods

5.3.1 Experimental procedure

All animal procedures were approved by: a Monash University Animal Ethics Committee and the Japan Synchrotron Radiation Research Institute, SPring-8 Animal Experiment Committee. All studies were conducted in experimental hutch 3 of beamline 20B2, in the Biomedical Imaging Center at the SPring-8 synchrotron, Japan.

Pregnant New Zealand white rabbits at 30 days gestation (term \approx 32 days) were initially anaesthetised using propofol (i.v.; 12 mg/kg bolus; Rapinivet, Schering-Plough Animal Health, Tokyo) and intubated. Anaesthesia was then maintained by isoflurane inhalation (1.5–4%; Isoflu, Dainippon Sumitomo Pharma Co., Osaka). Doe wellbeing was monitored via absence of withdrawal reflexes (corneal reflex and toe pinch reflex), measuring oxygenation and heart rate (using a pulse oximeter) and pupil diameter, with the isoflurane concentration adjusted accordingly. Fetal rabbits (n = 30) were partially delivered by caesarean section, and sedated with sodium pentobarbitone (13 mg/kg i.p.; Somnopentyl, Kyoritsu Seiyaku Co., Ltd, Tokyo). Kitten wellbeing was monitored via absence of withdrawal reflex (toe pinch), with additional sodium pentobarbitone given accordingly. Prior to delivery, kittens were randomly divided into either a sham operated, control group (C: n = 15; Figure 5.1) or into a group that underwent bilateral sectioning of the mid-cervical branches of the vagus nerve, above the cardiac and pulmonary vagus branches (V: n = 15; Figure 5.1). A jugular vein catheter (24G Intracath, Becton Dickinson, USA) and an endotracheal (ET) tube (18G Intracath; via tracheostomy) were also inserted. The tip of the ET tube was directed into one main bronchus under visual control, to ensure unilateral ventilation.

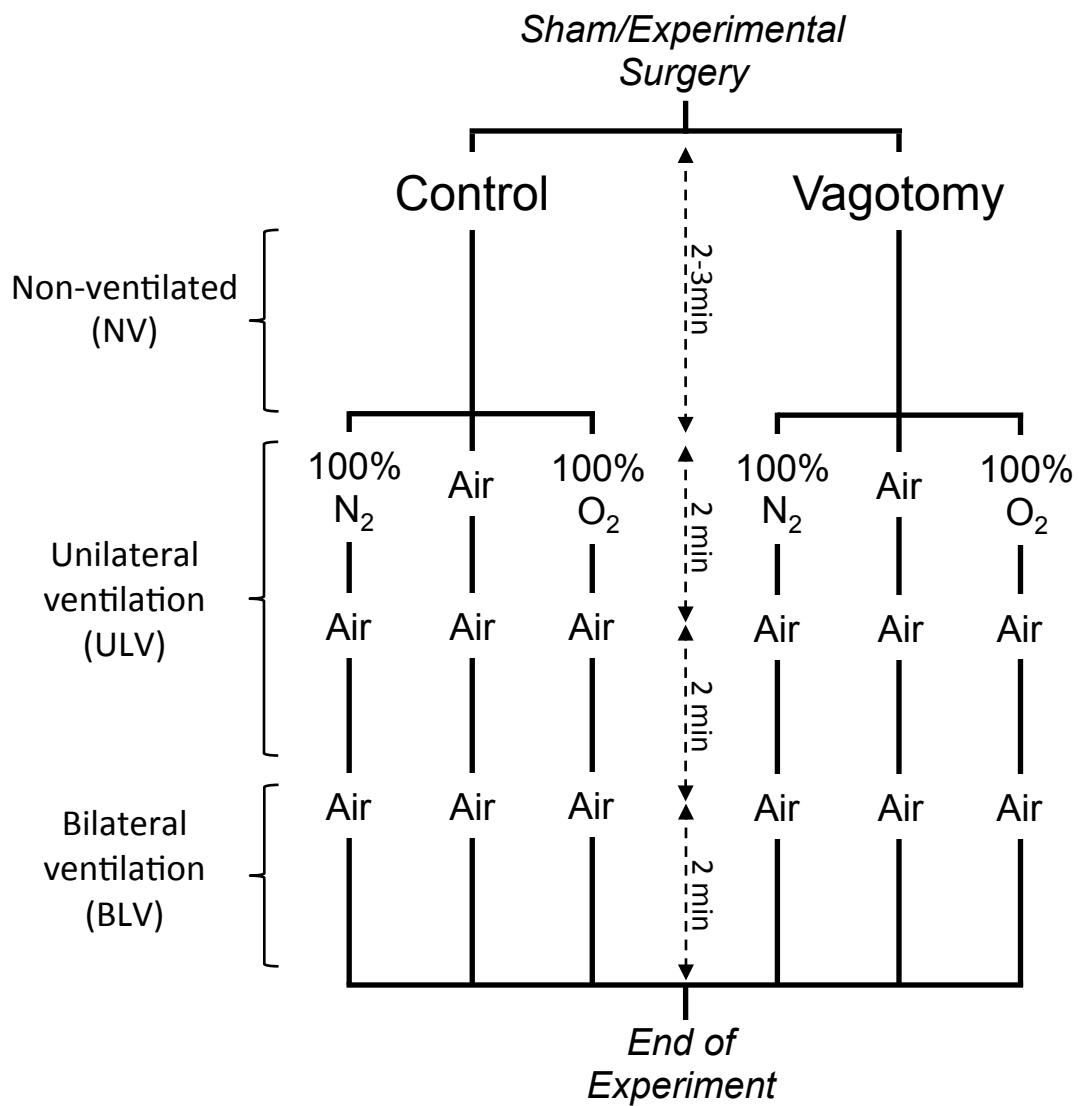


Figure 5.1: Flowchart of experimental procedure

Shown are: experimental groups (control, vagotomy), subgroups (initial gas ventilation of 100% N₂, air or 100% O₂) and timecourse of imaging/ventilation.

All surgical procedures on kittens were performed while the umbilical cord was intact and while the kitten's head remained covered with fetal membranes to prevent lung aeration. The kittens were then delivered, the ET tube obstructed to prevent breathing and the umbilical cord ligated before they were placed upright in a purpose built Perspex frame and positioned within the expected path of the X-ray beam. Electrocardiogram (ECG) leads were attached to the skin of the upper limb and both lower limbs and the ET tube was connected to a purpose-built, time-cycled, pressure-controlled ventilator (Kitchen *et al.*, 2010). Image acquisition began as soon as possible after the kittens were positioned, with ventilation beginning within 2-3 minutes of umbilical cord ligation. Kittens were initially ventilated for 2 minutes in either 100% N₂ (C-N₂, V-N₂), 21% O₂ (C-air, V-air) or 100% O₂ (C-O₂, V-O₂), n = 5 in each treatment group (Figure 5.1), using a peak inflation pressure of 25 cmH₂O and a positive end-expiratory pressure of 5 cmH₂O. Image sequences were obtained: before ventilation onset (not ventilated, NV), during initial ventilation of a single lung (at 30 sec after ventilation start), again during ventilation of a single lung after the inspired gas had switched to air (for an additional 2 minutes, both time points are referred to as unilateral ventilation; ULV) and finally following ventilation of both lungs in air for 2 minutes (bilateral ventilation: BLV), which was achieved by retracting the ET tube. At the conclusion of the ~13 minute experimental period (~10 minutes after ventilation onset for each kitten), animals were humanely killed with an overdose of sodium pentobarbitone (Pentobarbital; >100 mg/kg) administered *I.V.* (doe) or *I.P.* (kittens).

5.3.2 X-ray and angiography imaging

Imaging was achieved using monochromatic X-rays at 33.2 keV with a 1.0 m object-to-detector distance at a frame rate of 10 Hz or 20 Hz during bolus iodine injections (Lang *et al.*, 2014; Lang *et al.*, 2016). The scientific-CMOS (sCMOS) detector (pco.edge; PCO AG, Kehlheim, Germany) was coupled to a 25 μm thick gadolinium oxysulfide ($\text{Gd}_2\text{O}_2\text{S:Tb}^+$) powdered phosphor and a tandem lens system that provided an effective pixel size of 15.3 μm and an active field of view of 29 (W) \times 30 (H) mm^2 . Iodine boluses (Iomeron 350 mg/ml iodine; Bracco-Eisai Pty. Ltd., Tokyo, Japan; 1.5 μL per g of kitten body weight at 11 ml/s) were administered via the jugular vein using a remote-controlled syringe pump (PHD2000, Harvard Apparatus Inc., USA).

5.3.3 Image analysis

Images were analysed using ImageJ (v1.50b; NIH, USA) as described previously (Lang *et al.*, 2016). During the four measurement periods, we analysed the number of visible pulmonary vessels, vessel diameters, heart rate, pulmonary transit time and change in mean grey level profiles over time within the left and right main axial arteries (to give relative PBF) following iodine injection.

5.3.3.1 Vessel quantification

Visible pulmonary vessel branch points, counted during peak opacification during each iodine bolus, were counted as individual vessels and were visible up to the 3rd order of branching.

5.3.3.2 *Main axial artery vessel diameter*

Changes in pixel grey level (intensity) along virtual lines transecting vessels perpendicular to a vessel wall were used to measure vessel internal diameter. Line profiles were drawn over the left and right main axial arteries (taken mid-lung at the 7th intercostal space), to measure changes in internal diameter from the baseline pre-ventilation period (Lang *et al.*, 2014; Lang *et al.*, 2016). To correct for background intensity variations during iodine perfusion, line profiles were divided by the average background intensity averaged over the 10 frames (1 s) immediately prior to the first appearance of iodine within the vessel. Internal vessel edges were determined as the first pixel to drop below 1 standard deviation of the mean intensity of the background at either end of the line profile (~5 pixels past the vessel edge). Vessel diameters measured in pixels from each frame were averaged over 5 frames (0.5 s) then multiplied by the known pixel size (15.3 μm) to estimate a mean vessel internal diameter.

5.3.3.3 *Pulmonary arterial transit time*

A virtual box was placed over the distal end of the left and right main axial arteries before 1st order branching (taken at the level of the 8th intercostal space for consistency). The mean intensity of this region was calculated for each frame. Bolus arrival time was designated as the frame in which half of the peak opacity (maximum % change from background) is reached for the first time (half-peak opacity), this corrects for problems due to steady state peak opacity values in cases of poor wash-out (Shpilfoygel *et al.*, 2000). The elapsed time between the half-peak opacity value in the main pulmonary artery compared to the left and right axial arteries (at the 8th intercostal space) was calculated to give an approximation of bolus transit time through the pulmonary artery.

5.3.3.4 Relative measures of pulmonary blood flow

A virtual box was placed over the left and right main axial arteries at the level of the 7th intercostal space, which provided a centrally-located, clear and unobstructed view of the large conduit arteries during both the pre-ventilation and ventilation imaging time periods. The changes in mean intensity within each box were plotted against time as a percentage change from background levels (mean background intensity averaged over 10 frames before iodine injection) throughout each iodine injection sequence. The maximum of this time-opacity curve was then divided by the pulmonary arterial transit time to provide an indicator of changes in pulmonary arterial flow in both lungs; this value was termed the relative PBF index.

5.3.4 Statistical analysis

Kitten weights were compared between groups using a one-way ANOVA (Prism 6.0, GraphPad Software, Inc., La Jolla, USA). Changes in visible vessel number, blood vessel internal diameter, heart rate, pulmonary arterial transit time and opacity of blood vessels were compared over time and between groups using a two-way ANOVA with repeated measures. Post-hoc analysis used the Holm-Sidak method. A $p < 0.05$ was considered statistically significant.

5.4 Results

5.4.1 Animal data

The mean kitten weight was 42.1 ± 2.5 g, although the kittens in the vagotomised group ventilated with air (V-air) were significantly lighter (33.8 ± 3.2 g) than the other groups (44.8 ± 2.2 g), which were all similar. The majority of kittens were ventilated with the right lung first ($n = 28$), although 2 were ventilated with the left lung first, both in the V-air group.

5.4.2 Observations from PC X-ray videos

Overall, vagotomised kittens appeared to have a less profound increase in PBF following partial lung aeration compared to control kittens (Lang *et al.*, 2014; Lang *et al.*, 2016). This was most evident in the V-N₂ and V-air group (Figure 5.2, Supplemental Videos 5.1 and 5.2 respectively), with the V-O₂ group still displaying an increase in iodine flow in the axial arteries of both the ventilated first (A₁) and unaerated (UA₂) lungs compared to the pre-ventilation period (NV) (Supplemental Video 5.3).

5.4.3 Pulmonary blood vessel recruitment

In control kittens, unilateral ventilation (ULV) significantly increased the total number of visible vessels in both the A₁ and UA₂ lungs of all kittens, irrespective of the oxygen content of the gas used (Figure 5.3). Similarly, ULV of vagotomised kittens increased the total number of visible vessels in both the A₁ and UA₂ lungs of the V-air and V-O₂ groups (Figure 5.3), increasing from 13 ± 5 and 13 ± 4 visible vessels to 32 ± 4 and 35 ± 8 vessels in the A₁ and UA₂ lungs, respectively, in the V-air group and from 19 ± 7 and 22 ± 7 vessels to 50 ± 7 and 50 ± 9 vessels in the A₁ and UA₂ lungs, respectively, in the V-O₂ group; the increase in

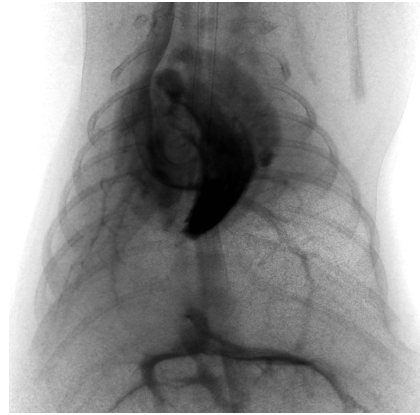
Control

Vagotomy

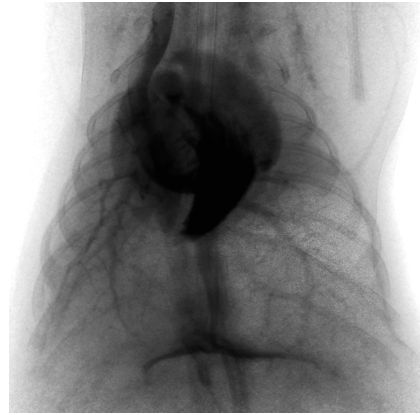
NV



ULV_{N₂}



ULV_{air}



BLV_{air}

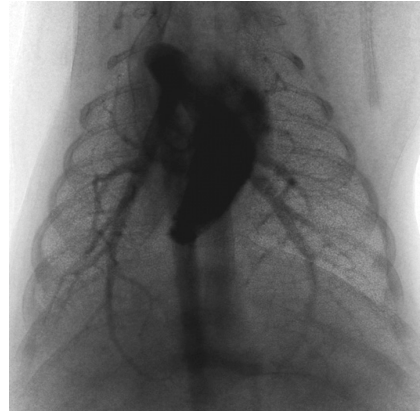


Figure 5.2

Representative PC X-ray angiography image sequences of vagotomised and control newborn rabbits imaged prior to ventilation (NV), following unilateral ventilation (ULV) of the right lung with 100% N₂ (ULV_{N₂}) followed by ULV of the right lung with air (ULV_{air}), followed by bilateral ventilation of the lungs in air (BLV_{air}). Images were obtained 1-3 seconds following iodine bolus injection.

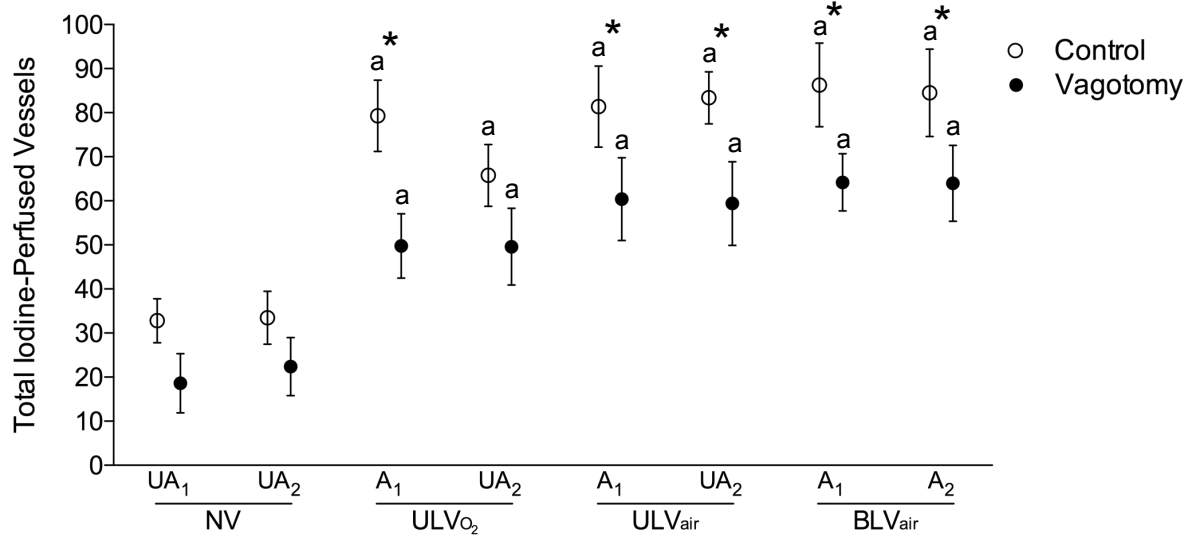
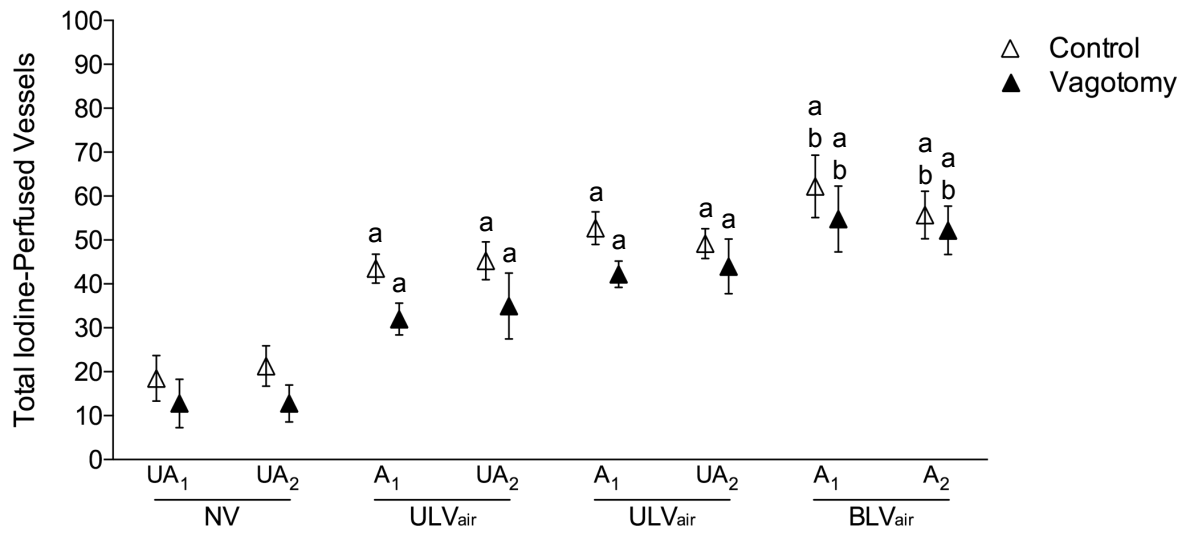
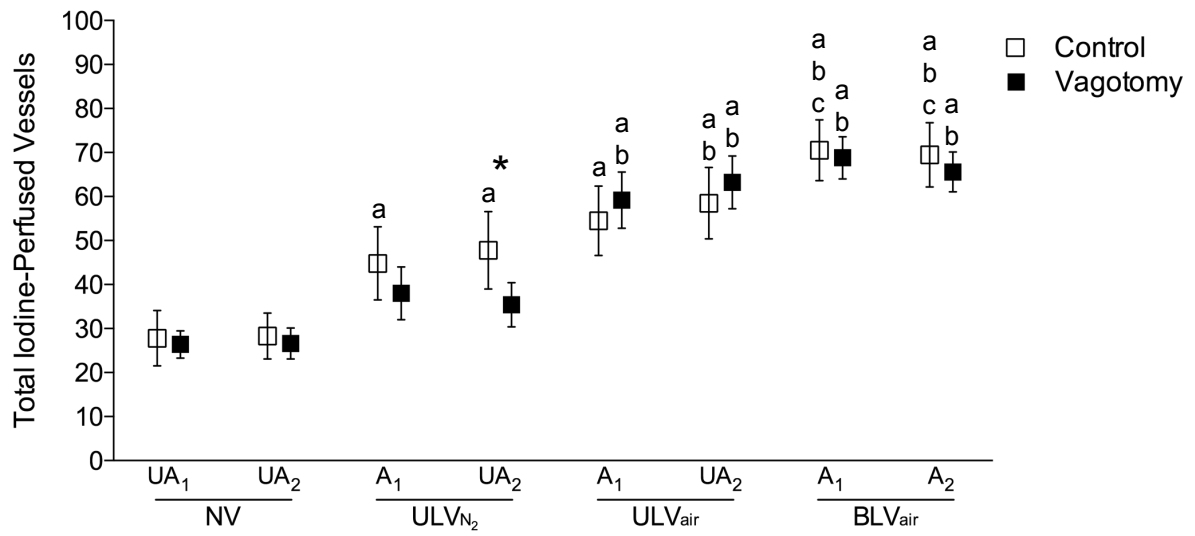


Figure 5.3

Mean iodine-perfused vessel branches (\pm SEM) in control (open symbols) and vagotomised (closed symbols) animals ventilated first with 100% N₂ (squares; upper panel), air (triangles; middle panel) or 100% O₂ (circles; lower panel). Ventilation periods shown are prior to ventilation onset (NV), during the initial unilateral ventilation (ULV_{N₂/air/O₂}) period, during the subsequent unilateral ventilation period with air (ULV_{air}) and during bilateral ventilation with air (BLV_{air}). Lungs are either unaerated (UA) or aerated (A) and ventilated first (1) or second (2). a: $p < 0.05$ compared to the same lung at NV. b: $p < 0.05$ compared to the same lung at ULV_{gas}. c: $p < 0.05$ compared to the same lung at ULV_{air}. *: $p < 0.05$ control compared to vagotomy within the same lung during the same ventilation period.

the V-O₂ group was higher than both other vagotomised groups, but not significantly so. However, in the V-N₂ group, while the number of visible vessels tended to increase in response to ULV with 100% nitrogen (ULV_{N₂}), the increase only reached statistical significance once ULV commenced with air (ULV_{air}); at that time it was significant for both the A₁ and UA₂ lungs compared to the NV time point (Figure 5.3). Compared to control kittens, vagotomy significantly reduced the number of visible vessels (Figure 5.3) in both lungs of kittens initially ventilated with 100% oxygen throughout the experimental period ($p < 0.05$, denoted by asterisks in Figure 5.3 lower panel), except in the UA₂ lung, during initial ventilation with 100% oxygen. This difference between control and vagotomised kittens persisted in both the A₁ (C: 86 ± 10 vessels; V: 64 ± 7 vessels) and A₂ (C: 85 ± 10 vessels; V: 64 ± 9 vessels) lungs during bilateral ventilation in air (BLV_{air}).

5.4.4 Heart rate

In control kittens, the initial ULV period significantly increased heart rates, irrespective of the oxygen content of the gas used (Figure 5.4), increasing from 56 ± 5 , 69 ± 5 and 47 ± 3 to 90 ± 13 , 93 ± 15 and 73 ± 10 in the C-N₂, C-air and C-O₂ groups respectively. However, in vagotomised animals, only ULV with air and 100% oxygen significantly increased heart rates during the initial ULV period; heart rates increased from 60 ± 6 and 67.5 ± 5 bpm to 79 ± 10 and 109 ± 9 bpm in V-air and V-O₂ groups, respectively. In V-N₂ kittens, ULV with 100% N₂ did not significantly increase heart rate; heart rates were 55 ± 6 bpm before and 53 ± 9 bpm after ULV with 100% N₂. In V-N₂ kittens, heart rate did not increase significantly until after ULV had commenced with air, increasing from 53 ± 9 bpm (ULV_{N₂}) to 75 ± 9 bpm (ULV_{air}) and then to 125.2 ± 18.0 bpm following bilateral ventilation with air (BLV_{air}; Figure 5.4). In V-air kittens, the heart rate increased from 62.8 ± 5.3 bpm to 93.2 ± 15.6 bpm during ULV

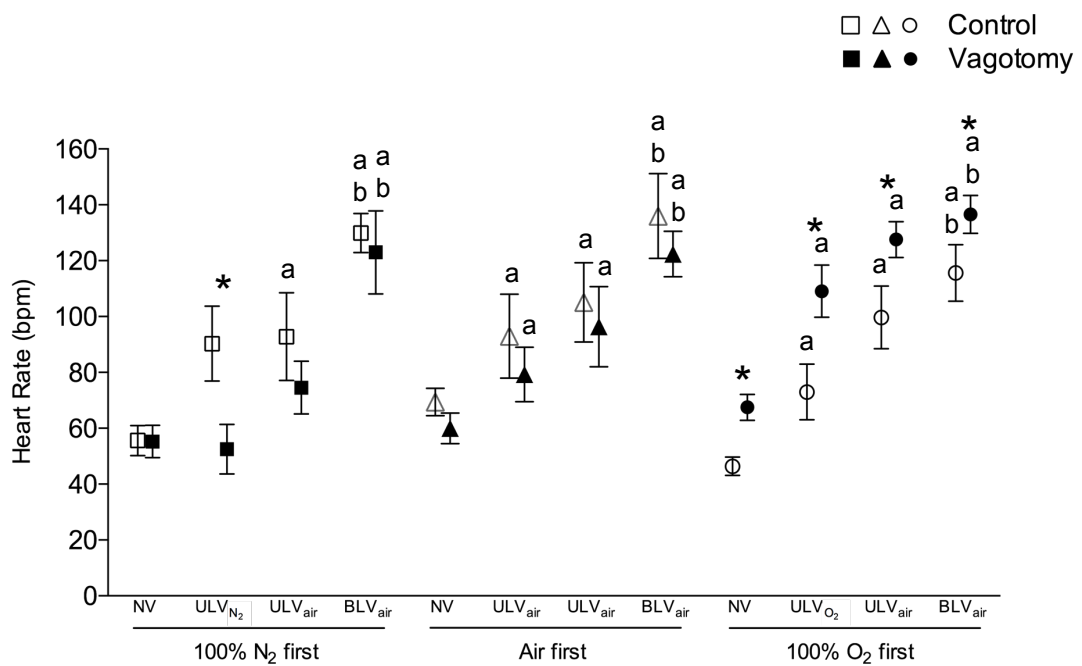


Figure 5.4

Mean heart rate (bpm \pm SEM) in control (open symbols) and vagotomised (closed symbols) kittens ventilated first with 100% N₂, air or 100% O₂. Ventilation periods shown are prior to ventilation onset (NV), during the initial unilateral ventilation (ULV_{N₂/air/O₂}) period, during the subsequent unilateral ventilation period with air (ULV_{air}) and during bilateral ventilation with air (BLV_{air}). a: p<0.05 compared to the same lung at NV. b: p<0.05 compared to the same lung at ULV_{gas}. *: p<0.05 control compared to vagotomy within the same lung during the same ventilation period.

and then increased further to 121.2 ± 9.0 bpm during BLV_{air}. Surprisingly, in kittens initially ventilated with 100% O₂, vagotomy significantly increased heart rate compared with control (C-O₂) kittens and the difference continued throughout all ventilation periods, remaining higher even after BLV with air (BLV_{air}; V-O₂, 137 ± 7 bpm vs. C-O₂ 116 ± 10).

5.4.5 Arterial vessel internal diameter

Compared with control kittens, vagotomy had a marked effect on vessel internal diameter in the axial arteries, resulting in a reduction in vessel internal diameter at all measurement times, even before lung aeration (Figure 5.5). In control kittens, the initial ULV increased vessel internal diameter in the axial arteries of both the aerated (A₁) and unaerated (UA₂) lungs irrespective of the oxygen content of the ventilation gas. In control C-N₂ kittens, vessel internal diameters increased from 505 ± 39 and 505 ± 49 μm to 581 ± 40 and 585 ± 58 μm in response to ULV_{N₂} in the A₁ and the UA₂ lungs, respectively. In vagotomised kittens, ULV significantly increased vessel internal diameter in the axial arteries of both the A₁ and UA₂ lungs of the V-air and V-O₂ groups only. The vessel internal diameters increased from 437 ± 14 and 414 ± 14 μm to 485 ± 17 and 452 ± 24 μm in the A₁ and UA₂ lungs, respectively, of the V-air group and from 400 ± 18 μm and 404 ± 13 μm to 468 ± 19 and 439 ± 23 μm in the A₁ and UA₂ lungs, respectively, of the V-O₂ group (Figure 5.5). In contrast, ULV in the V-N₂ group failed to increase vessel internal diameters, which were similar in both axial arteries before (441 ± 11 and 412 ± 12 μm) and after (464 ± 12 and 437 ± 14 μm) ULV onset with 100% N₂. In both control and vagotomised kittens, there were only minor increases in internal diameter in all groups following ULV in air and bilateral ventilation in air, although internal diameters remained lower in vagotomised kittens than in control kittens at all time points in all ventilation groups (Figure 5.5).

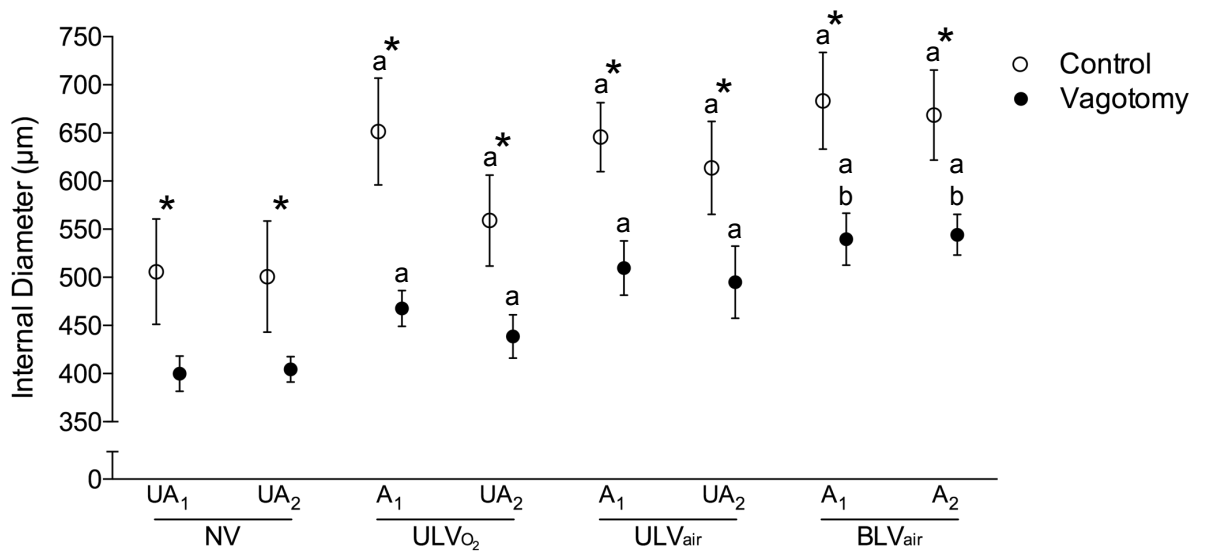
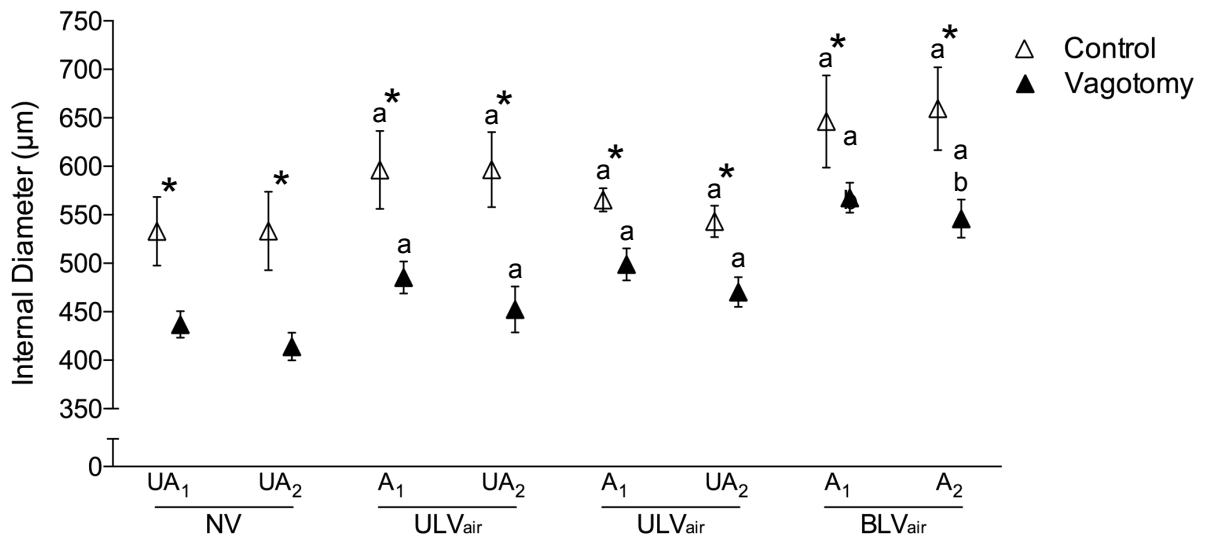
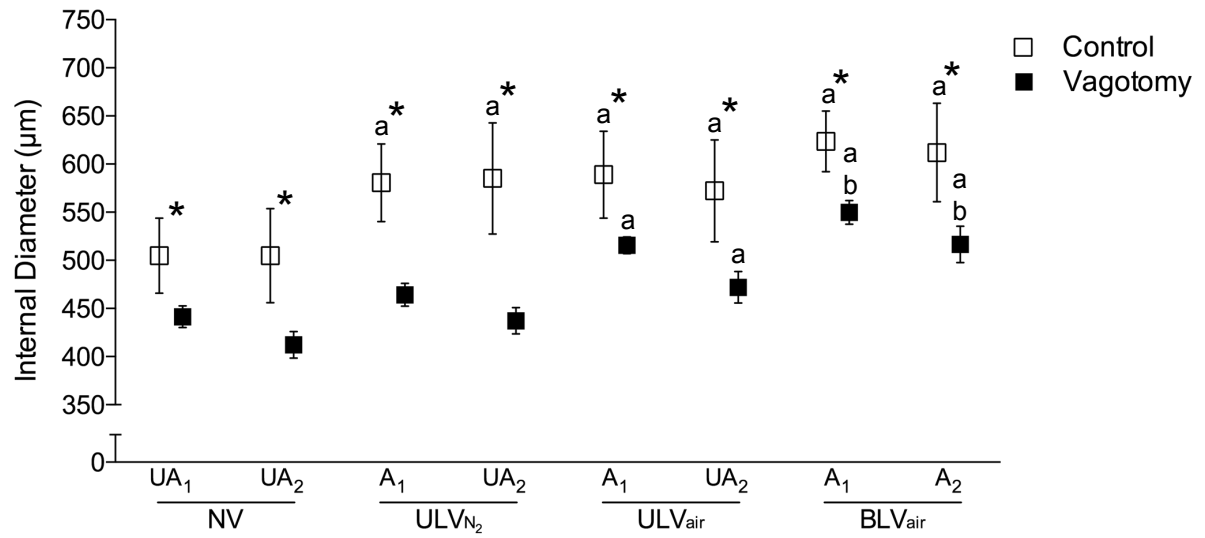


Figure 5.5

Mean internal diameter ($\mu\text{m} \pm \text{SEM}$) of axial arteries in control (open symbols) and vagotomised (closed symbols) kittens ventilated first with 100% N_2 (squares; upper panel), air (triangles; middle panel) or 100% O_2 (circles; lower panel). Ventilation periods shown are prior to ventilation onset (NV), during the initial unilateral ventilation ($\text{ULV}_{\text{N}_2/\text{air}/\text{O}_2}$) period, during the subsequent unilateral ventilation period with air (ULV_{air}) and during bilateral ventilation with air (BLV_{air}). Lungs are either unaerated (UA) or aerated (A) and ventilated first (1) or second (2). a: $p < 0.05$ compared to the same lung at NV. b: $p < 0.05$ compared to the same lung at ULV_{gas} . *: $p < 0.05$ control compared to vagotomy within the same lung during the same ventilation period.

5.4.6 Iodine bolus transit time

Pulmonary arterial transit times (defined as the time for an iodine bolus to progress from the main pulmonary artery to the end of the axial arteries) decreased following ULV in both control and vagotomised kittens initially ventilated in either 100% N₂ or 100% O₂ (Figure 5.6). No difference was observed between control and vagotomised kittens, except in the kittens ventilated in air. Transit times were significantly longer prior to ventilation in vagotomised kittens initially ventilated in air (3.4 ± 0.8 and 4.0 ± 1.7 s in UA₁ and UA₂, respectively) compared to control kittens (1.8 ± 0.4 and 1.3 ± 0.4 s in UA₁ and UA₂, respectively). This difference persisted after the first period of ULV with air, but was not significant during the second ULV period with air and during the BLV period.

5.4.7 Relative PBF index

Vagotomy significantly reduced the increase in relative PBF in the aerated lung of kittens ventilated with 100% N₂, and both aerated and non-aerated lungs in kittens ventilated with air during the initial ULV period (Figure 5.7). For example, in V-air kittens, relative PBF was similar in the A₁ and UA₂ lungs before (3.6 ± 1.1 and 5.2 ± 2.2 % change/sec, respectively) and after (11.8 ± 3.7 and 15.8 ± 7.1 % change/sec, respectively) ULV. In contrast, in C-air kittens relative PBF increased in the A₁ and UA₂ lungs from 6.9 ± 2.5 and 13.8 ± 6.2 % change/sec before ULV onset to 61.1 ± 22.1 and 78.0 ± 32.0 % change/sec, respectively, after ULV onset.

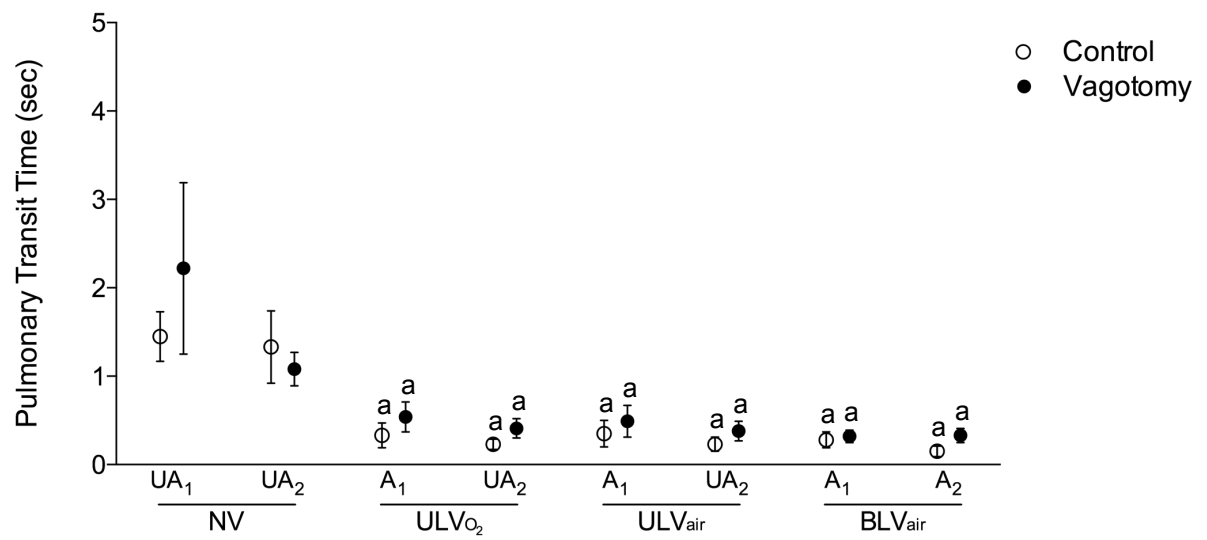
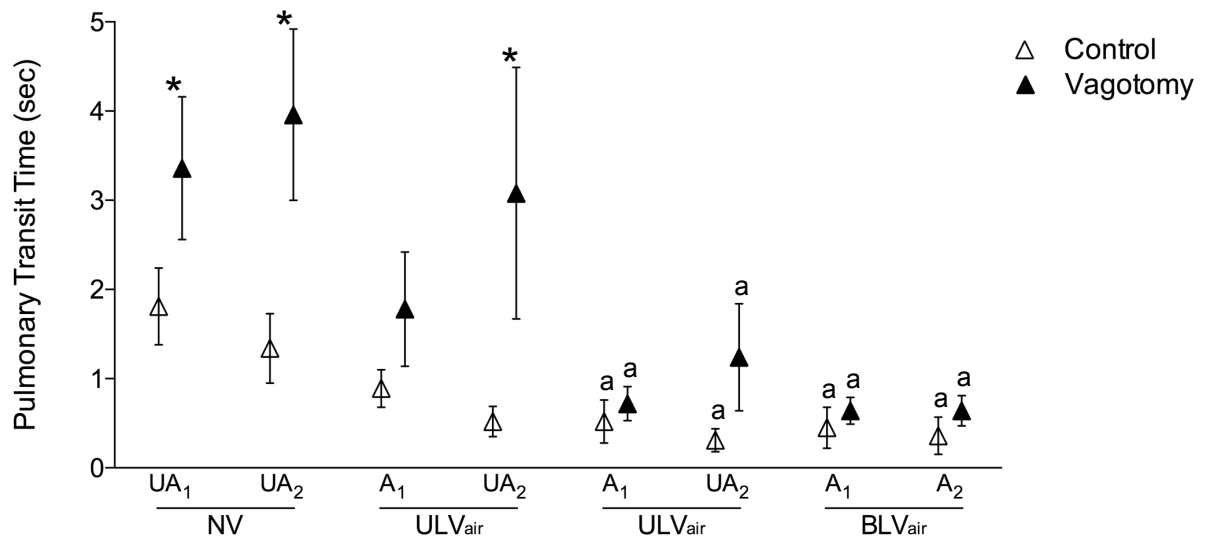
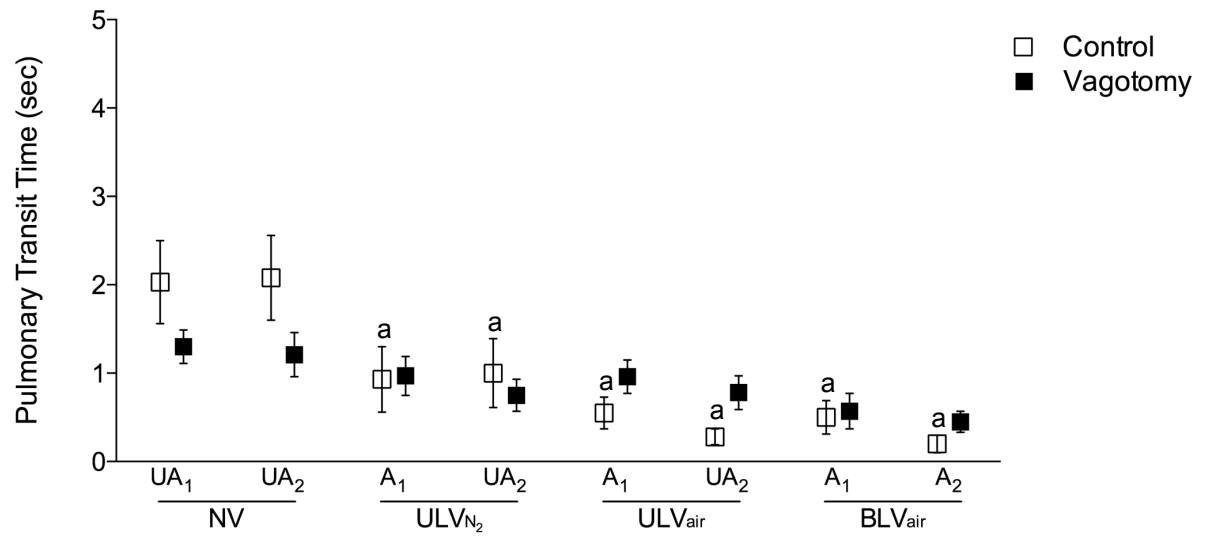


Figure 5.6

Mean arterial transit time ($s \pm SEM$) in control (open symbols) and vagotomised (closed symbols) kittens ventilated first with 100% N₂ (squares; upper panel), air (triangles; middle panel) or 100% O₂ (circles; lower panel). Ventilation periods shown are prior to ventilation onset (NV), during the initial unilateral ventilation (ULV_{N₂/air/O₂}) period, during the subsequent unilateral ventilation period with air (ULV_{air}) and during bilateral ventilation with air (BLV_{air}). Lungs are either unaerated (UA) or aerated (A) and ventilated first (1) or second (2). a: $p < 0.05$ compared to the same lung at NV. *: $p < 0.05$ control compared to vagotomy within the same lung during the same ventilation period.

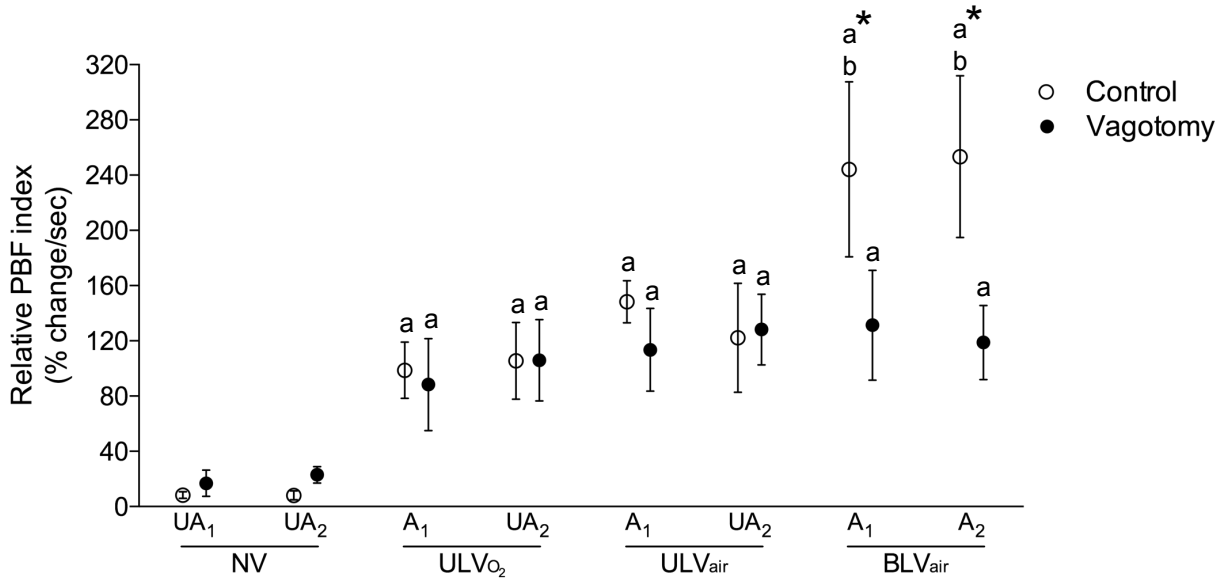
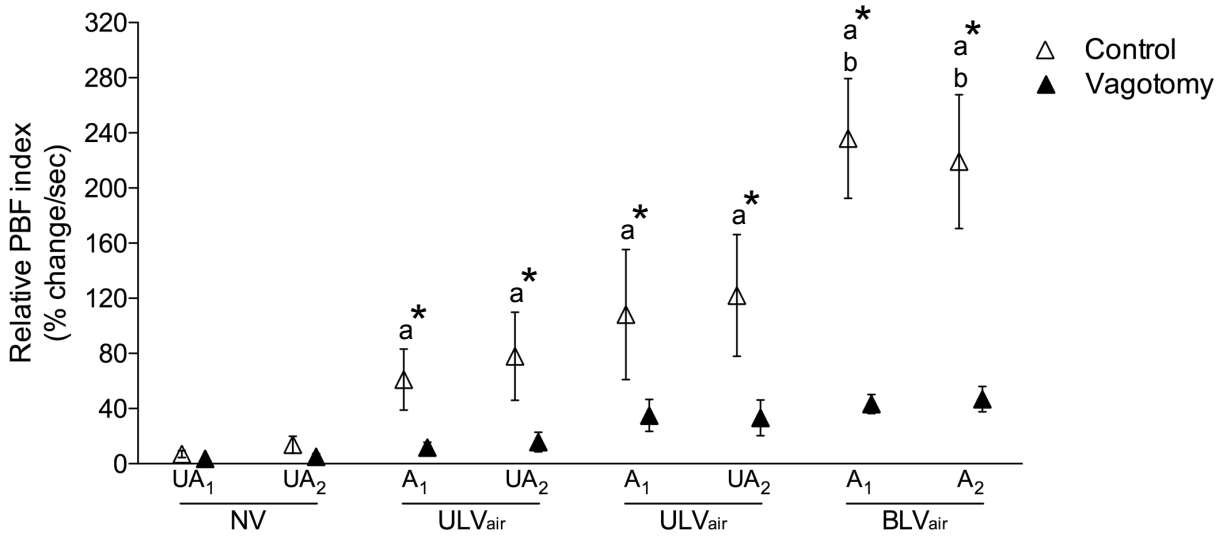
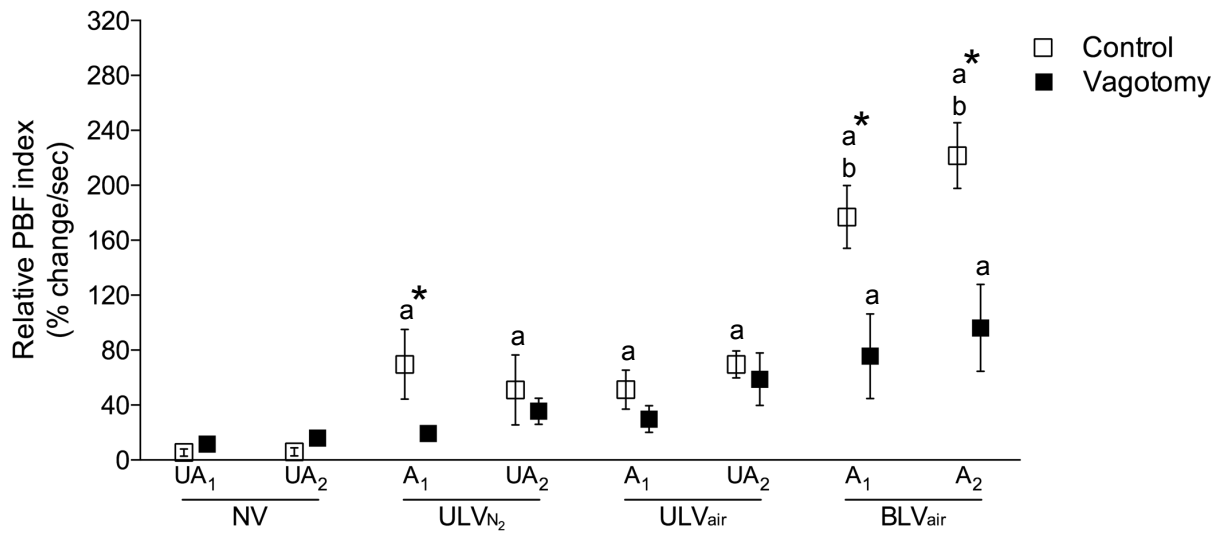


Figure 5.7

Mean relative PBF (% change/s \pm SEM), given by maximum % change grey value in the main axial arteries divided by the arterial transit time, in control (open symbols) and vagotomised (closed symbols) kittens ventilated first with 100% N₂ (squares; upper panel), air (triangles; middle panel) or 100% O₂ (circles; lower panel). Ventilation periods shown are prior to ventilation onset (NV), during the initial unilateral ventilation (ULV_{N₂/air/O₂}) period, during the subsequent unilateral ventilation period with air (ULV_{air}) and during bilateral ventilation with air (BLV_{air}). Lungs are either unaerated (UA) or aerated (A) and ventilated first (1) or second (2). a: p<0.05 compared to the same lung at NV. *: p<0.05 control compared to vagotomy within the same lung during the same ventilation period.

Furthermore, kittens initially ventilated with air also had lower relative PBF in both the A₁ and UA₂ lungs during the second ULV period. The increase in relative PBF following initial ULV was similar between groups in kittens ventilated with 100% O₂ except at BLV_{air}, in which all control groups were significantly higher than their respective vagotomy groups. For instance, in A₁ lungs, relative PBF was markedly greater in control versus vagotomised kittens initially ventilated with 100% N₂ (177.0 ± 22.8 vs. 75.6 ± 30.8 % change/sec), with air (236.0 ± 43.4 vs. 43.3 ± 6.9 % change/sec) and with 100% O₂ (244.2 ± 63.4 vs. 131.3 ± 39.7 % change/sec) (Figure 5.7).

5.5 Discussion

The increase in PBF at birth plays a critical role in the adaptation to newborn life and is thought to be mediated by numerous mechanical and vasoactive factors, particularly an increase in oxygenation (Gao & Raj, 2010). However, recent studies have demonstrated that the increase in PBF is not spatially related to lung aeration, as partial lung aeration leads to a global increase in PBF and is not dependent on increased oxygenation (Sobotka *et al.*, 2011; Lang *et al.*, 2016). Previous studies have indicated that vagal stimulation may induce pulmonary vasodilation at birth (Colebatch *et al.*, 1965) and is required for the establishment of neonatal respiratory function (Wong *et al.*, 1998; Lalani *et al.*, 2002). The results of this study support the suggestion that signaling via the vagus plays a key role in stimulating the global increase in PBF at birth induced by lung aeration. We found that vagotomy inhibits the increase in PBF induced by lung aeration (Figure 5.2, Figure 5.7), although ventilation with high oxygen levels can partially mitigate this inhibitory effect of vagotomy. While the mechanism by which the vagus mediates pulmonary vasodilation in response to lung aeration is unclear, it is possible that the clearance of airway liquid into peri-alveolar interstitial tissue (Bland *et al.*, 1980; Miserocchi *et al.*, 1994) activates receptors, which signal via the vagus nerve. Nevertheless, the finding that ventilation with 100% O₂ can partially mitigate the effect of vagotomy, indicates that O₂ may act separately through an independent mechanism to increase PBF.

Recent studies have clearly demonstrated that partial lung aeration leads to a global increase in PBF, increasing equally in both aerated and unaerated lung regions (Lang *et al.*, 2014; Lang *et al.*, 2016). These findings are consistent with previous studies showing that ventilation of one lung increases vascular conductance in the other, unventilated lung (Cassin

et al., 1964b). While oxygen can enhance the increase in PBF in aerated lung regions, the increase in PBF in unaerated regions is independent of oxygen levels and even occurs in response to ventilation with 100% N₂ (Lang *et al.*, 2016). We have now confirmed and extended these findings, showing that ventilation with 100% N₂ increases blood flow in the aerated and unaerated lungs, of control kittens, whereas vagotomy greatly reduces the ability of both air and 100% N₂ to vasodilate the pulmonary arteries and stimulate a global increase in PBF. This finding is consistent with our hypothesis that a neural reflex, which is activated by lung aeration and incorporates afferent signalling via the vagus nerve, is largely responsible for the global increase in PBF at birth. The finding that ventilation with 100% oxygen was able to reverse the inhibitory effect of vagotomy, is consistent with our previous suggestion that oxygen acts through a separate, independent mechanism to stimulate PBF and enhance the effect of lung aeration (Lang *et al.*, 2016).

Airway liquid clearance at birth leads to liquid accumulation in the pulmonary interstitial tissue, forming perivascular fluid cuffs that are similar to those that occur in the adult lung during pulmonary edema (Bland *et al.*, 1980). J receptors, located along pulmonary blood vessels, are known to be activated in response to pulmonary congestion, and they signal via afferent C-fibres located within the vagus nerve to stimulate tachypnoea (Paintal, 1969). We have previously proposed that the movement of airway liquid into the interstitial tissue following ventilation onset essentially causes pulmonary edema (Lang *et al.*, 2014; Lang *et al.*, 2016), which activates juxtacapillary (J) receptors and stimulates a global increase in PBF irrespective of the oxygen content of the gas. As such, we hypothesised in this study that sectioning the vagus nerve would prevent afferent signalling from the J receptors (Paintal, 1969) and inhibit the increase in PBF induced by partial lung aeration. Recent studies have shown that pulmonary C-fibre activation can dilate arterioles in skeletal muscle (Roberts *et*

al., 2015). As such, it is possible that reflex C-fibre mediated arteriolar dilation may not be limited to skeletal muscle and may extend to other vascular beds, such as the lung. While our findings are largely consistent with this hypothesis, we discerned several disparities. One was the observation that bradycardia was not evoked with initiation of ventilation (Figure 5.4), which may be related to the fact that heart rate is already reduced during the birth transition. Additionally, vagotomy significantly reduced arterial vessel internal diameters in the lung even before ventilation commenced (Figure 5.5). Indeed, the reduction in vessel diameter caused by vagotomy was 50-100 μm (10-20% lower than controls), which must markedly increase PVR as resistance is inversely proportional to the fourth power of the vessel radius. The mechanism by which vagotomy reduces vessel diameter is unknown, although it is possible that low level afferent signaling helps to modulate PVR in the fetus.

Single lung ventilation was confirmed using our established technique of PC X-ray imaging, showing a distinctive speckle pattern that is limited to aerated regions of the lungs (Kitchen *et al.*, 2004). We have now confirmed these findings in three separate studies (Lang *et al.*, 2014; Lang *et al.*, 2016) and shown that the effect of partial lung aeration is greatly diminished by vagotomy except when ventilation occurs with 100% O₂. Although the kittens experienced a delay between umbilical cord ligation and the onset of imaging (2-3 min), due to radiation safety procedures, all kittens experienced the same delay and so any differences were unlikely to be due to the resulting asphyxia. The finding that PBF increases and pulmonary artery vessel dilation occurs in both aerated and unaerated regions clearly indicates that the vessel dilation and increase in PBF is not spatially related to lung aeration. However, it is not clear whether the volume of airway liquid accumulated in the interstitial space determines the degree of PBF increase due to differential neural activation. Indeed, an experimental approach

that examines this possible relationship, and more directly implicates pulmonary C-fibre afferents is required.

The increase in heart rate in response to ULV with 100% N₂ (Figure 5.4) is a phenomenon that we have reported previously and is likely due to the lung aeration-induced increase in PBF, which increases ventricular preload (Lang *et al.*, 2016). In the fetus, as PBF is low, umbilical venous return, which passes via the ductus venosus and foramen ovale to enter the left atrium, provides the vast majority of the preload for the left ventricle. Thus, if the umbilical cord is clamped before the lungs have had an opportunity to aerate, preload for the left ventricle is greatly diminished and cardiac output is greatly reduced (Crossley *et al.*, 2009; Bhatt *et al.*, 2013). This would contribute to the low PBF as observed in the NV period (Figure 5.2), with cardiac output remaining reduced until the lungs aerate and PBF increases to restore preload and replace the venous return lost upon cord clamping. As such, by increasing PBF, ULV with 100% N₂ is thought to increase cardiac output, which is reflected by an increase in heart rate, restoring left ventricular preload lost by umbilical cord clamping.

We expected vagotomy to increase heart rate due to removal of the suppressive effects of parasympathetic tone on pacemaker activity in the sino-atrial node. However, we found that before ventilation onset, heart rate was not increased in vagotomised compared to control kittens except in those destined to be ventilated with 100% O₂. It is unclear why an increase in heart rate was detected in this group, but not in the other two, although it cannot be an oxygen mediated effect as this difference was detected before ventilation commenced. In any event, the finding that vagotomy blocked the increase in heart rate induced by ULV with 100% N₂ supports our contention that this increase in heart rate is due to an increase in PBF, as the latter was also inhibited. While previous studies indicate that direct stimulation of C-fibre

(with capsaicin) induces a bradycardia (Coleridge *et al.*, 1992; Deep *et al.*, 2001), we did not observe a similar response during the birth transition, which is possibly due to competing factors. For instance, heart rate was already depressed during the NV period (Figure 5.4), which may mask changes due to initiation of ventilation. On the other hand, an increase in venous return and left ventricular preload likely contributes to an increase in heart rate and cardiac output, which would oppose induced bradycardia. It is also interesting that this effect of vagotomy on the ULV induced increase in heart rate was not apparent in V-air and V-O₂ kittens, and that the induced increase was greatest in V-O₂ kittens suggesting that the increase in heart rate results from an increase in both oxygenation and PBF.

Although vagal C-fibre stimulation may form the afferent pathway for the ULV-induced global increase in PBF, the efferent side of the pathway remains unknown. It is possible that the efferent side of the pathway involves an increase in sympathetic or parasympathetic activation, or a combination of the two. Sympathetic activation could partly explain our observations due to its mediation of adult pulmonary vasodilation (Sylvester *et al.*, 2012). While the sympathetic nerves contribute to the high vascular tone in the fetus (Nuwayhid *et al.*, 1975), it has been previously shown that noradrenaline can act as a vasoconstrictor during low pulmonary vascular tone, but a vasodilator when vascular tone is enhanced (Silove *et al.*, 1968). Although the influence of autonomic stimulation on the pulmonary vasculature has been investigated previously, the effect on the perinatal circulation remains largely unknown.

The cardiopulmonary transition at birth is a complex process that is triggered by birth related events such as occlusion of the umbilical cord and the entry of air into the lungs, which is known to trigger both mechanical (Hooper, 1998) and vasoactive stimuli to decrease PVR (Teitel *et al.*, 1990; Bhatt *et al.*, 2013). However, we show that a global decrease in PVR in

5: Contributions of the Vagus Nerve and O₂ to the PBF Increase at Birth

response to partial lung aeration can be inhibited with ligation of the vagus nerve, suggesting that an underlying neural reflex triggered by lung aeration may exist. This response is independent of the O₂ content of the inspired gas and while it leads to a high risk of ventilation/perfusion mismatching in the lung at birth, we have previously argued that this response is likely to be highly advantageous and not adverse for the individual (Lang *et al.*, 2014; Lang *et al.*, 2016). Indeed, as PBF takes over the role of providing preload for the left ventricle when the cord is clamped at birth, having a high PBF, irrespective of how much of the lung has aerated, is much more important. This is because an increase and redistribution of cardiac output to increase blood flow and maintain oxygen delivery to vital organs, is the primary defense mechanism against hypoxia in the fetus and newborn. With incomplete aeration of the lungs being inevitable at birth, these findings indicate that a vagal reflex exists to stimulate PBF at birth regardless of aeration and facilitates the transition into newborn life.

Chapter Six

General Discussion

Adaptation of the newborn to life after birth involves the lungs undergoing a remarkable transition, leading them to rapidly take over the role of gas-exchange from the placenta. To achieve this, the airways must be cleared of liquid and the lungs must transform from the high resistance, low perfusion state that persisted in fetal life into a low resistance, highly perfused state after birth. This is an intricate process, with many interconnected factors contributing to the final result of an independently breathing infant. The entry of air into the lungs, which replaces the liquid present in the airways during fetal life, is the primary trigger for this process (te Pas *et al.*, 2008), with the stimulus being mediated by a range of vasoactive and mechanical stimuli (Gao & Raj, 2010). Although much research has focused on the factors controlling the increase in PBF at birth, the suggested mechanisms are based on the assumption that, at birth, air entry stimulates a local increase in PBF to promote ventilation/perfusion matching. This assumption was based on the well-established relationship between ventilation and perfusion in the adult lung, largely because until recently we have not had the technology to investigate this relationship at birth. However, with the development of synchrotron-based X-ray imaging this has now become possible, and my PhD commenced with a study to address this unexplored area.

The combination of phase contrast X-ray imaging and angiography has allowed me to examine the spatial relationship between the increase in pulmonary perfusion and lung aeration immediately after birth with high temporal and spatial resolution. Using this technology I have been able to demonstrate that ventilation/perfusion matching does not occur in the newborn rabbit lung and that previously unrecognised mechanisms enable a global increase in PBF to occur even if only part of the lung is aerated. The primary aim of my PhD was to investigate this phenomenon and explore the spatial relationships between ventilation and perfusion in the lungs at birth.

6.1 Mechanisms Regulating the Increase in Blood Flow at Birth

The rapid and sustained increase in pulmonary perfusion with lung aeration at birth is a crucial part of the intricate adaptation to air breathing at birth. Given that regionalised aeration is a common event when initiating ventilation in very preterm infants, the potential outcomes of this technique are of great interest to caregivers seeking to minimise harm in their approach. Chapter 3 investigated the basic interactions between air entry into only part of the lungs at birth and the resultant changes in perfusion. The results demonstrated that the increase in PBF at birth does not appear to be regionally dependent on lung aeration, and increased oxygenation resulting from aeration was not required for pulmonary vasodilation in unaerated lung regions. This indicates a large ventilation/perfusion mismatch and inefficient gas-exchange can occur with only partial lung aeration and that a previously unrecognised mechanism may contribute to stimulating the increase in PBF at birth. This observation alone, as confirmed by synchrotron X-ray imaging, indicates that our current understanding for how lung aeration stimulates an increase in PBF requires re-evaluation.

In Chapter 4, I expanded my initial observations to investigate the role of oxygen in regulating the increase in PBF in aerated and unaerated lung regions. This study demonstrated that the entry of gas, independent of oxygen levels, is sufficient to induce an increase in PBF in both aerated and unaerated lung regions at birth. X-ray speckle pattern was used to indicate the degree of lung aeration (Kitchen *et al.*, 2004), while the contrast agent in the vasculature was able to indicate downstream vasodilatation, vessel recruitment and an associated fall in PVR. As oxygen was found to have an additive effect on pulmonary vasodilatation, this

suggests that the underlying mechanisms can act independently of oxygenation but are enhanced by increased oxygen levels. These observations were consistent with previous findings that ventilation with a hypoxic gas mixture can increase PBF in sheep without an increase in oxygenation (Teitel *et al.*, 1990). Chapters 3 and 4 were consistent in the unexpected finding that there appears to be an unknown underlying mechanism initiating a global increase in pulmonary blood flow at birth, which is unrelated to oxygen or local lung aeration.

The findings of Chapters 3 and 4 present intriguing insights into the possibility that an additional, unrecognised factor contributes to the birth-related increase in PBF. The significant increase in perfusion to non-aerated regions of the lung cannot be explained by factors normally associated with lung aeration at birth, such as oxygenation and the mechanical effects of lung inflation or aeration. Thus other, not previously considered stimuli must be considered. This stimuli must be rapid and act globally, as these observations occurred within ~30-40 seconds of ventilation onset, which led us to the possibility of a neural reflex, triggered by gas entry into the lungs.

Various studies have suggested that sensory nerves running within the vagal trunk may mediate some PBF responses, which is consistent with the data observed in our first two studies. Building upon Chapters 3 and 4, in Chapter 5 we combined the partial aeration with gases that contain different oxygen levels at birth with vagal denervation in order to examine the potential of role of vagal sensory nerves in the global increase in PBF at birth. Our rationale focused on the possibility that the rapid lung liquid clearance at birth and liquid accumulation in interstitial tissue (Bland *et al.*, 1980; Siew *et al.*, 2009b) could stimulate pulmonary sensory receptors that are sensitive to pulmonary edema. Pulmonary juxtacapillary

receptors, which signal via afferent C-fibres that run within the vagus, are stimulated by interstitial liquid accumulation in lung tissue during edema (Paintal, 1969). This is known to induce tachpnoea and pulmonary C-fibre activation has been shown to trigger vasodilation in other vascular beds (Roberts *et al.*, 2015). As such, we hypothesised that activation of these juxtacapillary receptors may contribute to the global increase in PBF in response to partial lung aeration. Furthermore, as the primary stimulus is interstitial tissue liquid accumulation, it is likely that this mechanism is independent of stimulation by increased oxygenation.

Chapter 5 demonstrated that vagal denervation and subsequent removal of neural transmission via the vagus nerve significantly reduced PBF following partial lung aeration at birth. The disruption of the phenomena observed in Chapters 3 and 4 thus suggests that there is a reflex pathway triggering vasodilation in the whole lung even when only partial aeration occurs at birth. Once again, 100% O₂ induced a significant increase in PBF that was independent of vagal denervation. It was able to largely counteract the inhibitory effects of vagotomy but only in the aerated region exposed to the high oxygen. These results suggested that both an autonomic reflex and oxygenation are major mechanisms underlying the increase in PBF at birth, although the precise contribution of each pathway is unclear and is likely to vary depending upon multiple factors. The hypothesis that juxtacapillary receptor activation caused by increases in interstitial pressures at birth, leading to reflex C-fibre mediated pulmonary arteriolar dilation, remains the most compelling explanation for the findings presented in this thesis. The recent study by Roberts *et al.* (2015) that C-fibre activation can dilate arterioles in skeletal muscle may also relate to changes within the pulmonary vascular bed via a similar pathway. Overall, my findings indicate that the pulmonary vasodilation triggered by lung aeration likely involves a much higher contribution from neural reflexes than previously

considered. The implications of this phenomenon, as well as the possible underlying mechanisms are of great interest in furthering the understanding of this complex process.

6.2 Implications of Ventilation/Perfusion Mismatch at Birth

The observation of a significant ventilation/perfusion mismatch in the lungs was unexpected, because at first this seemed highly detrimental to a newborn infant when oxygen delivery is paramount. However, upon further deliberation, it is possible that this mechanism of increasing PBF irrespective of the degree of lung aeration has major adaptive advantages that outweigh the disadvantages. Indeed, as the increase in PBF is essential for restoring left ventricular preload and cardiac output following cord occlusion, it is essential to protect the infant against periods of hypoxia (Bhatt *et al.*, 2013). For instance, an increase and redistribution of CO plays a vital role in protecting vital organs such as the heart and brain from hypoxia by helping to sustain oxygen delivery in the face of lowered oxygen levels. However, if cardiac output is severely limited during a hypoxic episode, then the combined effect of ischemia and hypoxia is catastrophic. The studies presented in this thesis suggest that increasing PBF and maintaining CO without relying on complete lung aeration, means that CO can be maintained irrespective of how much of the lung aerates. This represents a trade-off between inefficient gas-exchange and supporting left ventricular preload in the newborn.

The complex role of the heart in these changes at birth was consistent over all of my studies, with changes in the function of the heart and lungs at birth being intimately linked. The effect of birth and cord clamping on newborn heart rates is well established, having been documented extensively in studies such as those done by Dawson *et al.* (2010). Nomograms of the heart rate and oxygen saturation levels immediately after birth demonstrate low heart

rates can be considered part of the normal transition (Dawson *et al.*, 2010). This has also been demonstrated in sheep (Bhatt *et al.*, 2013) and now with the studies presented in this thesis, newborn rabbits. With umbilical cord clamping, the loss of preload and simultaneous increase in afterload reduces cardiac output unless PBF is elevated, which underpins the rationale for initiating ventilation before cord clamping (Dawson *et al.*, 2010; Bhatt *et al.*, 2013). Chapter 3, 4 and 5 all show that with unilateral ventilation, there is an increase in heart rate and right ventricle output, as well as an increase in left ventricle function. The restoration of venous return with an increase in PBF likely contributes to the increase in cardiac function, although this represents another interesting facet of the birth-related changes in the body that remain not fully understood. These observations are likely a multifactorial response to both stretch-related stimuli and sympathetic activation, contributing to complex reflex changes during the transition. The cardiopulmonary changes at birth are complex and much remains to be investigated, even on the level of basic physiological concepts.

6.3 Limitations

There are some limitations to the protocols used in these studies, as well as the scope of the topics examined. While synchrotron X-ray imaging is able to confirm partial aeration with the generation of “speckle pattern”, as well as being able to observe processes in an intact animal (Kitchen *et al.*, 2004), the procedures involved have several disadvantages. As discussed particularly in Chapter 5, partial asphyxiation of the animals prior to imaging onset could have detrimentally impacted on the PBF changes at birth. Although all of the animals were subjected to similar conditions, and the modest asphyxia caused by a delay between birth and ventilation onset was unavoidable, this is a confounding factor in these studies. Additionally, the use of live animals generally requires the use of anaesthetic for ethical pain management,

contributing to possible unintentional side-effects on the physiological processes observed (Hildebrandt *et al.*, 2008). For example barbiturates can lead to respiratory depression and affect blood pressure and stroke volume, which is of particular importance when examining pulmonary haemodynamics. With the experiments in this thesis: respiratory effects are unaffected due to the use of mechanical ventilation and cardiovascular effects are most likely dampening the observations made, implying unimpeded physiological processes may be even more pronounced. The experimental procedures of surgery, anaesthesia and mechanical ventilation do, however, have a confounding effect in the physiological observations made.

The reliance on data obtained via image analysis also limits the physiological evidence that can be presented, but is an unfortunate consequence of the synchrotron X-ray imaging setup. The lack of access to the animal during the imaging procedure, as well as the small size of the newborn rabbits meant that taking regular blood samples was unfeasible. Additionally, blood flow information given by ultrasonic flow probes would have been useful, although were completely impractical due to the small size of the kittens. While alternative probes could be used, this would require opening of the chest wall and possible interference with the intact physiological processes as well as the path of the X-ray beam. The parameters that could be derived from additional measurement devices may have given further strength to the conclusions put forward in these studies.

6.4 Future Directions

While Chapter 5 proposed the role for an autonomic reflex influencing PBF at birth, much remains to be fully understood about this possible mechanism. For instance, studies that provide more direct evidence to implicate pulmonary C-fibre afferents and juxtacapillary

receptors are required. Additionally, while vagotomy examines the effect of removal of both afferent and efferent pathways to the lungs, it seems most likely that the afferent pathway is mediated via the vagus itself but the efferent pathway involved remains unknown. This would need to be more selectively examined, for example by using specific blockade of postganglionic sympathetic fibres (e.g. with pentolinium) and comparing with nonspecific ganglionic blockade (e.g. with hexamethonium). Another potential follow-up to the vagotomy studies is the logical next step after examining the removal of stimulation, that is exogenous stimulation of the vagus directly e.g. by chemical or electrical means. Finally, another open question from these results is whether the volume of airway liquid accumulated in the interstitial space determines the degree of PBF increase through differential neural activation. Since this would relate to the postulated role for juxtacapillary receptors operating through a vagal pathway, an experimental approach examining this question would be useful, although may not be possible with imaging. Once more precise mechanisms have been uncovered, this then presents the potential for selective targets in delivery room management. In disease states such as PPHN, a dysfunctional myogenic response might be targeted through the use of drugs that enhance the pulmonary autonomic activity to trigger a global pulmonary vasodilation as a treatment. This could be a consideration for follow-up studies once the efferent pathway of the pulmonary neural reflex at birth is better understood.

As the transitional period of the lungs at birth is highly dynamic, future studies may consider expanding these observations over a more prolonged period. Events occurring in the early minutes of birth differ over the course of hours, with the contribution of flow across the patent ductus arteriosus to PBF one such example (Crossley *et al.*, 2009). While the observation of a significant ventilation/perfusion mismatch was a key observation in these studies, it is possible that the ventilation/perfusion matching process was delayed, potentially due to

immaturity at birth, and may establish itself after an extended period of time. This was not examined due to the limited time-course of these experiments, which an extended observation period can address. Time-dependent responses to dilator stimuli also vary significantly, for example the potent vasodilator effects of oxygen are not sustained in the normal fetus and pulmonary blood flow falls over 1-2 hours in utero. To expand the methods employed in this thesis to cover a wider range of timing would be a worthwhile point to examine in the future. Concurrent to variations in the timing of observations is the consideration of using spontaneously breathing neonates, as the normal response may be influenced by force of mechanical ventilation and the changes in lung liquid clearance (Hooper *et al.*, 2007). Previous imaging has shown that lung liquid clearance is affected by factors such as PEEP, and as our hypothesis relates to lung liquid clearance and accumulation in the tissue, a study examining spontaneously breathing neonates is also a consideration for future exploration of this process.

6.5 Overall Summary

The studies reported in this thesis investigated the factors involved in the increase in PBF in response to lung aeration at birth using simultaneous PC X-ray imaging and angiography. My findings suggest that factors unrelated to oxygen or local aeration are able to induce a rapid and sustained global increase in pulmonary perfusion despite only partial aeration. Moreover, this increase in PBF to non-aerated regions appears to be mediated by the autonomic nervous system, stimulated by gas entry into the lungs at birth and independent of oxygenation. Although the details of this pathway remain incomplete, such as whether these changes can be stimulated directly via nerve stimulation or differential lung liquid absorption, this represents further directions that can be explored in the future.

These findings are a fascinating novel discovery, and have the potential to influence delivery room management. Regionalised aeration is a common occurrence during ventilation of very preterm infants, with a significant ventilation/perfusion mismatch possibly occurring in non-aerated lung regions. Given that monitoring of the newborn is focused on oxygen delivery, earlier management of uniform aeration may be of higher importance to minimise this ventilation/perfusion mismatch we have observed. Additionally, with the proposal of significant autonomic involvement in this process, future clinical practice may be influenced through potential drug targets to stimulate autonomic activity. Although this would require future studies to confirm the more detailed mechanisms and efferent pathways, this would potentially assist cases such as very preterm infants in which heterogeneous lung expansion occurs due to surfactant deficiency and nerve reflexes may be underdeveloped. Overall, my studies provide compelling data that the current paradigm for PBF control at birth requires re-evaluation, and it appears a major regulatory factor is missing.

Chapter Seven

References

- Abman SH. (2007). Recent advances in the pathogenesis and treatment of persistent pulmonary hypertension of the newborn. *Neonatology* **91**, 283-290.
- Abman SH & Accurso FJ. (1989). Acute effects of partial compression of ductus arteriosus on fetal pulmonary circulation. *American Journal of Physiology: Heart and Circulatory Physiology* **257**, H626-H634.
- Abman SH, Chatfield BA, Hall S & McMurtry I. (1990). Role of endothelium-derived relaxing factor during transition of pulmonary circulation at birth. *American Journal of Physiology: Heart and Circulatory Physiology* **259**, H1921-H1927.
- Adams FH, Yanagisawa M, Kuzela D & Martinek H. (1971). The disappearance of fetal lung fluid following birth. *Journal of Pediatrics* **78**, 837-843.
- Adzick NS, Harrison MR, Glick PL, Villa RL & Finkbeiner W. (1984). Experimental pulmonary hypoplasia and oligohydramnios: relative contributions of lung fluid and fetal breathing movements. *Journal of Pediatric Surgery* **19**, 658-665.
- Alcorn D, Adamson TM, Lambert TF, Maloney JE, Ritchie BC & Robinson PM. (1977). Morphological effects of chronic tracheal ligation and drainage in the fetal lamb lung. *Journal of Anatomy* **123**, 649-660.
- Alcorn DG, Adamson TM, Maloney JE & Robinson PM. (1981). A morphologic and morphometric analysis of fetal lung development in the sheep. *The Anatomical Record* **201**, 655-667.
- Allison BJ, Crossley KJ, Flecknoe SJ, Morley CJ, Polglase GR & Hooper SB. (2010). Pulmonary hemodynamic responses to in utero ventilation in very immature fetal sheep. *Respiratory Research* **11**, 111-121.
- Anderson RH, Webb S, Brown NA, Lamers W & Moorman A. (2003). Development of the heart:(2) Septation of the atriums and ventricles. *Heart* **89**, 949-958.
- Andersson O, Hellström-Westas L, Andersson D & Domellöf M. (2011). Effect of delayed versus early umbilical cord clamping on neonatal outcomes and iron status at 4 months: a randomised controlled trial. *BMJ* **343**, d7157-d7168.
- Armstead W. (1995). Role of nitric oxide and cAMP in prostaglandin-induced pial arterial vasodilation. *American Journal of Physiology: Heart and Circulatory Physiology* **268**, H1436-H1440.

- Arrigoni F, Hislop A, Pollock J, Haworth S & Mitchell J. (2002). Birth upregulates nitric oxide synthase activity in the porcine lung. *Life Sciences* **70**, 1609-1620.
- Avery ME & Cook CD. (1961). Volume-pressure relationships of lungs and thorax in fetal, newborn, and adult goats. *Journal of Applied Physiology* **16**, 1034-1038.
- Ballard PL, Merrill JD, Godinez RI, Godinez MH, Truog WE & Ballard RA. (2003). Surfactant protein profile of pulmonary surfactant in premature infants. *American Journal of Respiratory and Critical Care Medicine* **168**, 1123-1128.
- Bartle D, Patole S & Rao S. (2010). Current and future therapeutic options for persistent pulmonary hypertension in the newborn. *Expert Review of Cardiovascular Therapy* **8**, 845-862.
- Bellotti M, Pennati G, De Gasperi C, Battaglia FC & Ferrazzi E. (2000). Role of ductus venosus in distribution of umbilical blood flow in human fetuses during second half of pregnancy. *American Journal of Physiology: Heart and Circulatory Physiology* **279**, H1256-H1263.
- Berhrsins J & Gibson A. (2011). Cardiovascular system adaptation at birth. *Paediatrics & Child Health* **21**, 1-6.
- Bhatt S, Alison BJ, Wallace EM, Crossley KJ, Gill AW, Kluckow M, te Pas AB, Morley CJ, Polglase GR & Hooper SB. (2013). Delaying cord clamping until ventilation onset improves cardiovascular function at birth in preterm lambs. *Journal of Physiology* **591**, 2113-2126.
- Black SM, Johengen MJ, Ma Z-D, Bristow J & Soifer SJ. (1997). Ventilation and oxygenation induce endothelial nitric oxide synthase gene expression in the lungs of fetal lambs. *Journal of Clinical Investigation* **100**, 1448-1458.
- Blanco C, Martin C, Rankin J, Landauer M & Phernetton T. (1988). Changes in fetal organ flow during intrauterine mechanical ventilation with or without oxygen. *Journal of Developmental Physiology* **10**, 53-62.
- Bland R, McMillan D, Bressack M & Dong L. (1980). Clearance of liquid from lungs of newborn rabbits. *Journal of Applied Physiology* **49**, 171-177.
- Bland RD, Hansen TN, Haberkern CM, Bressack M, Hazinski T, Raj JU & Goldberg R. (1982). Lung fluid balance in lambs before and after birth. *Journal of Applied Physiology* **53**, 992-1004.

- Brimioulle S, Vachiéry J-L, Brichant J-F, Delcroix M, Lejeune P & Naeije R. (1997). Sympathetic modulation of hypoxic pulmonary vasoconstriction in intact dogs. *Cardiovascular Research* **34**, 384-392.
- Brown M, Olver R, Ramsden C, Strang L & Walters D. (1983). Effects of adrenaline and of spontaneous labour on the secretion and absorption of lung liquid in the fetal lamb. *Journal of Physiology* **344**, 137-152.
- Burri PH. (1984). Fetal and postnatal development of the lung. *Annual Review of Physiology* **46**, 617-628.
- Butler MG, Isogai S & Weinstein BM. (2009). Lymphatic development. *Birth Defects Research Part C: Embryo Today: Reviews* **87**, 222-231.
- Caduff J, Fischer L & Burri P. (1986). Scanning electron microscope study of the developing microvasculature in the postnatal rat lung. *The Anatomical Record* **216**, 154-164.
- Cargill RI & Lipworth BJ. (1996). Atrial natriuretic peptide and brain natriuretic peptide in cor pulmonale: hemodynamic and endocrine effects. *CHEST Journal* **110**, 1220-1225.
- Cassin S, Dawes G & Ross B. (1964a). Pulmonary blood flow and vascular resistance in immature foetal lambs. *Journal of Physiology* **171**, 80-89.
- Cassin S, Dawes GS, Mott JC, Ross BB & Strang LB. (1964b). The vascular resistance of the foetal and newly ventilated lung of the lamb. *Journal of Physiology* **171**, 61-79.
- Challis JRG, Dilley SR, Robinson JS & Thorburn GD. (1976). Prostaglandins in the circulation of the fetal lamb. *Prostaglandins* **11**, 1041-1052.
- Clyman RI, Mauray F, Roman C & Rudolph AM. (1978). PGE₂ is a more potent vasodilator of the lamb ductus arteriosus than is either PGI₂ or 6 keto PGF α . *Prostaglandins* **16**, 259-264.
- Coceani F, Kelsey L & Seidlitz E. (1992). Evidence for an effector role of endothelin in closure of the ductus arteriosus at birth. *Canadian Journal of Physiology and Pharmacology* **70**, 1061-1064.

- Coceani F & Olley P. (1988). The control of cardiovascular shunts in the fetal and perinatal period. *Canadian Journal of Physiology and Pharmacology* **66**, 1129-1134.
- Coggins MP & Bloch KD. (2007). Nitric oxide in the pulmonary vasculature. *Arteriosclerosis, Thrombosis, and Vascular Biology* **27**, 1877-1885.
- Cohn H, Sacks E, Heymann M & Rudolph A. (1974). Cardiovascular responses to hypoxemia and acidemia in fetal lambs. *American Journal of Obstetrics and Gynecology* **120**, 817-824.
- Colebatch H, Dawes G, Goodwin J & Nadeau R. (1965). The nervous control of the circulation in the foetal and newly expanded lungs of the lamb. *Journal of Physiology* **178**, 544-562.
- Coleridge H, Coleridge J, Green J & Parsons G. (1992). Pulmonary C-fiber stimulation by capsaicin evokes reflex cholinergic bronchial vasodilation in sheep. *Journal of Applied Physiology* **72**, 770-778.
- Crapo JD, Young SL, Fram EK, Pinkerton KE, Barry BE & Crapo RO. (1983). Morphometric Characteristics of Cells in the Alveolar Region of Mammalian Lungs 1–3. *American Review of Respiratory Disease* **128**, S42-S46.
- Crossley KJ, Allison BJ, Polglase GR, Morley CJ, Davis PG & Hooper SB. (2009). Dynamic changes in the direction of blood flow through the ductus arteriosus at birth. *Journal of Physiology* **587**, 4695-4704.
- Crouch E & Wright JR. (2001). Surfactant proteins A and D and pulmonary host defense. *Annual Review of Physiology* **63**, 521-554.
- Davis RP & Mychaliska GB. (2013). Neonatal pulmonary physiology. In *Seminars in Pediatric Surgery*, pp. 179-184. Elsevier.
- Dawes G, Fox H, Leduc B, Liggins G & Richards R. (1972). Respiratory movements and rapid eye movement sleep in the foetal lamb. *Journal of Physiology* **220**, 119-143.
- Dawes G & Mott JC. (1959). Reflex respiratory activity in the new - born rabbit. *Journal of Physiology* **145**, 85-97.
- Dawes G, Mott JC & Widdicombe J. (1955). Closure of the foramen ovale in newborn lambs. *Journal of Physiology* **128**, 384-395.

- Dawes G, Mott JC, Widdicombe J & Wyatt D. (1953). Changes in the lungs of the new - born lamb. *Journal of Physiology* **121**, 141-162.
- Dawes GS. (1961). Changes in the circulation at birth. *British Medical Bulletin* **17**, 148-153.
- Dawes GS, Lewis BV, Milligan JE, Roach MR & Talner NS. (1968). Vasomotor responses in the hind limbs of foetal and new-born lambs to asphyxia and aortic chemoreceptor stimulation. *Journal of Physiology* **195**, 55-81.
- Dawson J, Kamlin C, Wong C, Te Pas A, Vento M, Cole T, Donath S, Hooper S, Davis P & Morley C. (2010). Changes in heart rate in the first minutes after birth. *Archives of Disease in Childhood: Fetal and Neonatal Edition* **95**, F177-F181.
- de Mello DE, Sawyer D, Galvin N & Reid LM. (1997). Early fetal development of lung vasculature. *American Journal of Respiratory Cell and Molecular Biology* **16**, 568-581.
- Deep V, Singh M & Ravi K. (2001). Role of vagal afferents in the reflex effects of capsaicin and lobeline in monkeys. *Respiration Physiology* **125**, 155-168.
- Di Maio M, Gil J, Ciurea D & Kattan M. (1989). Structural maturation of the human fetal lung: a morphometric study of the development of air-blood barriers. *Pediatric Research* **26**, 88-93.
- DiFiore JW, Fauza DO, Slavin R, Peters CA, Fackler JC & Wilson JM. (1994). Experimental fetal tracheal ligation reverses the structural and physiological effects of pulmonary hypoplasia in congenital diaphragmatic hernia. *Journal of Pediatric Surgery* **29**, 248-257.
- Downing SE & Lee JC. (1980). Nervous control of the pulmonary circulation. *Annual Review of Physiology* **42**, 199-210.
- Dusting GJ, Mullins EM & Nolan RD. (1981). Prostacyclin (PGI₂) release accompanying angiotensin conversion in rat mesenteric vasculature. *European Journal of Pharmacology* **70**, 129-137.
- Edelstone DI, Rudolph AM & Heymann MA. (1978). Liver and ductus venosus blood flows in fetal lambs in utero. *Circulation Research* **42**, 426-433.

- El-Bermani A-W, Bloomquist E & Montvilo J. (1982). Distribution of pulmonary cholinergic nerves in the rabbit. *Thorax* **37**, 703-710.
- Eldridge D, Johnson D & Sedgwick K. (2015). Australia's mothers and babies 2013—in brief. Perinatal statistics series no. 31. Cat no. PER 72. Canberra: AIHW.
- Fineman JR, Soifer SJ & Heymann MA. (1995). Regulation of Pulmonary Vascular Tone in the Perinatal Period. *Annual Review of Physiology* **57**, 115-134.
- Flecknoe SJ, Wallace MJ, Cock ML, Harding R & Hooper SB. (2003). Changes in alveolar epithelial cell proportions during fetal and postnatal development in sheep. *American Journal of Physiology: Lung Cellular and Molecular Physiology* **285**, L664-L670.
- Fouras A, Kitchen MJ, Dubsky S, Lewis RA, Hooper SB & Hourigan K. (2009). The past, present, and future of x-ray technology for in vivo imaging of function and form. *Journal of Applied Physics* **105**, 102009.
- Frantz E, Soifer SJ, Clyman RI & Heymann MA. (1989). Bradykinin produces pulmonary vasodilation in fetal lambs: role of prostaglandin production. *Journal of Applied Physiology* **67**, 1512-1517.
- Fuhrman BP, Smith-Wright DL, Kulik TJ & Lock JE. (1986). Effects of static and fluctuating airway pressure on intact pulmonary circulation. *Journal of Applied Physiology* **60**, 114-122.
- Gale GE, Torrebuena JR, Moon RE, Saltzman HA & Wagner PD. (1985). Ventilation-perfusion inequality in normal humans during exercise at sea level and simulated altitude. *Journal of Applied Physiology* **58**, 978-988.
- Gao Y & Raj JU. (2010). Regulation of the pulmonary circulation in the fetus and newborn. *Physiological Reviews* **90**, 1291-1335.
- Gao Y, Tolsa J-F, Shen H & Raj JU. (1998). A single dose of antenatal betamethasone enhances isoprenaline and prostaglandin E2-induced relaxation of preterm ovine pulmonary arteries. *Neonatology* **73**, 182-189.
- Ghanayem NS & Gordon JB. (2001). Modulation of pulmonary vasomotor tone in the fetus and neonate. *Respiratory Research* **2**, 139-144.

- Gluckman P & Johnston B. (1987). Lesions in the upper lateral pons abolish the hypoxic depression of breathing in unanaesthetized fetal lambs in utero. *Journal of Physiology* **382**, 373-383.
- Grant DA, Hollander E, Skuza EM & Fauchère J-C. (1999). Interactions between the right ventricle and pulmonary vasculature in the fetus. *Journal of Applied Physiology* **87**, 1637-1643.
- Haies DM, Gil J & Weibel ER. (1981). Morphometric Study of Rat Lung Cells: I. Numerical and Dimensional Characteristics of Parenchymal Cell Population 1, 2. *American Review of Respiratory Disease* **123**, 533-541.
- Hall SM, Hislop AA, Pierce CM & Haworth SG. (2000). Prenatal origins of human intrapulmonary arteries: formation and smooth muscle maturation. *American Journal of Respiratory Cell and Molecular Biology* **23**, 194-203.
- Hamasaki Y, Mojarad M, Saga T, Tai H-H & Said SI. (1984). Platelet-Activating Factor Raises Airway and Vascular Pressures and Induces Edema in Lungs Perfused with Platelet-Free Solution 1–3. *American Review of Respiratory Disease* **129**, 742-746.
- Hanson KA, Burns F, Rybalkin SD, Miller JW, Beavo J & Clarke WR. (1998a). Developmental changes in lung cGMP phosphodiesterase-5 activity, protein, and message. *American Journal of Respiratory and Critical Care Medicine* **158**, 279-288.
- Hanson KA, Ziegler JW, Rybalkin SD, Miller JW, Abman SH & Clarke WR. (1998b). Chronic pulmonary hypertension increases fetal lung cGMP phosphodiesterase activity. *American Journal of Physiology: Lung Cellular and Molecular Physiology* **275**, L931-L941.
- Harding R & Hooper S. (1996). Regulation of lung expansion and lung growth before birth. *Journal of Applied Physiology* **81**, 209-224.
- Harding R, Hooper SB & Dickson KA. (1990). A mechanism leading to reduced lung expansion and lung hypoplasia in fetal sheep during oligohydramnios. *American Journal of Obstetrics and Gynecology* **163**, 1904-1913.
- Hasan SU, Lalani S & Remmers JE. (2000). Significance of vagal innervation in perinatal breathing and gas exchange. *Respiration Physiology* **119**, 133-141.

- Hew KW & Keller KA. (2003). Postnatal anatomical and functional development of the heart: a species comparison. *Birth Defects Research Part B: Developmental and Reproductive Toxicology* **68**, 309-320.
- Heymann MA. (1999). Control of the pulmonary circulation in the fetus and during the transitional period to air breathing. *European Journal of Obstetrics Gynecology and Reproductive Biology* **84**, 127-132.
- Heymann MA, Rudolph AM, Nies AS & Melmon KL. (1969). Bradykinin production associated with oxygenation of the fetal lamb. *Circulation Research* **25**, 521-534.
- Heymann MA, Rudolph AM & Silverman NH. (1976). Closure of the ductus arteriosus in premature infants by inhibition of prostaglandin synthesis. *New England Journal of Medicine* **295**, 530-533.
- Hiedl S, Schwepcke A, Weber F & Genzel-Boroviczeny O. (2010). Microcirculation in preterm infants: profound effects of patent ductus arteriosus. *The Journal of pediatrics* **156**, 191-196.
- Hildebrandt IJ, Su H & Weber WA. (2008). Anesthesia and other considerations for in vivo imaging of small animals. *ILAR journal* **49**, 17-26.
- Hirschi KK, Rohovsky SA, Beck LH, Smith SR & D'Amore PA. (1999). Endothelial cells modulate the proliferation of mural cell precursors via platelet-derived growth factor-BB and heterotypic cell contact. *Circulation Research* **84**, 298-305.
- Hislop A. (2005). Developmental biology of the pulmonary circulation. *Paediatric Respiratory Reviews* **6**, 35-43.
- Hislop A & Reid LM. (1972). Intra-pulmonary arterial development during fetal life-branching pattern and structure. *Journal of Anatomy* **113**, 35-48.
- Hislop AA. (2002). Airway and blood vessel interaction during lung development. *Journal of Anatomy* **201**, 325-334.
- Hooper SB. (1998). Role of luminal volume changes in the increase in pulmonary blood flow at birth in sheep. *Experimental Physiology* **83**, 833-842.

- Hooper SB & Harding R. (1995). Fetal lung liquid: a major determinant of the growth and functional development of the fetal lung. *Clinical and Experimental Pharmacology and Physiology* **22**, 235-241.
- Hooper SB & Harding R. (2005). Role of Aeration in the Physiological Adaptation of the Lung to Air- Breathing at Birth. *Current Respiratory Medicine Reviews* **1**, 185-195.
- Hooper SB, Kitchen MJ, Wallace MJ, Yagi N, Uesugi K, Morgan MJ, Hall C, Siu KKW, Williams IM, Siew M, Irvine SC, Pavlov K & Lewis RA. (2007). Imaging lung aeration and lung liquid clearance at birth. *FASEB Journal* **21**, 3329-3337.
- Hooper SB, te Pas AB, Lang J, van Vonderen JJ, Roehr CC, Kluckow M, Gill AW, Wallace EM & Polglase GR. (2015). Cardiovascular transition at birth: a physiological sequence. *Pediatric Research* **77**, 608-614.
- Hunter LE & Simpson JM. (2014). Prenatal screening for structural congenital heart disease. *Nature Reviews Cardiology* **11**, 323-334.
- Ibe BO, Hibler S & Raj JU. (1998). Platelet-activating factor modulates pulmonary vasomotor tone in the perinatal lamb. *Journal of Applied Physiology* **85**, 1079-1085.
- Ibe BO, Sander FC & Raj JU. (2000). Platelet activating factor acetylhydrolase activity in lamb lungs is up-regulated in the immediate newborn period. *Molecular Genetics and Metabolism* **69**, 46-55.
- Ivy D, Kinsella J & Abman S. (1994). Physiologic characterization of endothelin A and B receptor activity in the ovine fetal pulmonary circulation. *Journal of Clinical Investigation* **93**, 2141-2148.
- Ivy D, Lee D, Rairigh RL, Parker TA & Abman SH. (2004). Endothelin B receptor blockade attenuates pulmonary vasodilation in oxygen-ventilated fetal lambs. *Neonatology* **86**, 155-159.
- Ivy DD, Parker TA, Ziegler JW, Galan HL, Kinsella JP, Tuder RM & Abman SH. (1997). Prolonged endothelin A receptor blockade attenuates chronic pulmonary hypertension in the ovine fetus. *Journal of Clinical Investigation* **99**, 1179-1186.
- Ivy DD, Timothy D, Parker TA, Zenge JP, Jakkula M, Markham NE, Kinsella JP & Abman SH. (2000). Developmental changes in endothelin expression and activity in the ovine fetal lung. *American Journal of Physiology: Lung Cellular and Molecular Physiology* **278**, L785-L793.

- Iwamoto HS, Teitel D & Rudolph AM. (1987). Effects of birth-related events on blood flow distribution. *Pediatric Research* **22**, 634-640.
- Jaillard S, Houfflin-Debarge V, Riou Y, Rakza T, Klosowski S, Lequien P & Storme L. (2001). Effects of catecholamines on the pulmonary circulation in the ovine fetus. *American Journal of Physiology: Regulatory, Integrative and Comparative Physiology* **281**, R607-R614.
- Jain L & Eaton DC. (2006). Physiology of fetal lung fluid clearance and the effect of labor. In *Seminars in Perinatology*, pp. 34-43. Elsevier.
- Jain RK. (2003). Molecular regulation of vessel maturation. *Nature Medicine* **9**, 685-693.
- Jakus Z, Gleghorn JP, Enis DR, Sen A, Chia S, Liu X, Rawnsley DR, Yang Y, Hess PR & Zou Z. (2014). Lymphatic function is required prenatally for lung inflation at birth. *The Journal of experimental medicine* **211**, 815-826.
- Jeffery PK. (1998). The development of large and small airways. *American Journal of Respiratory and Critical Care Medicine* **157**, S174-S180.
- Jobe A & Ikegami M. (1987). Surfactant for the treatment of respiratory distress syndrome. *American Review of Respiratory Disease* **136**, 1256-1275.
- Kikkawa Y, Yoneda K, Smith F, Packard B & Suzuki K. (1975). The type II epithelial cells of the lung. II. Chemical composition and phospholipid synthesis. *Laboratory Investigation* **32**, 295-302.
- Kiserud T & Acharya G. (2004). The fetal circulation. *Prenatal Diagnosis* **24**, 1049-1059.
- Kiserud T, Rasmussen S & Skulstad S. (2000). Blood flow and the degree of shunting through the ductus venosus in the human fetus. *American Journal of Obstetrics and Gynecology* **182**, 147-153.
- Kitchen MJ, Habib A, Fouras A, Dubsky S, Lewis RA, Wallace MJ & Hooper SB. (2010). A new design for high stability pressure-controlled ventilation for small animal lung imaging. *Journal of Instrumentation* **5**, T02002-T02013.

- Kitchen MJ, Lewis RA, Morgan MJ, Wallace MJ, Siew ML, Siu KKW, Habib A, Fouras A, Yagi N, Uesugi K & Hooper SB. (2008). Dynamic measures of regional lung air volume using phase contrast x-ray imaging. *Physics in Medicine and Biology* **53**, 6065-6077.
- Kitchen MJ, Lewis RA, Yagi N, Uesugi K, Paganin D, Hooper SB, Adams G, Jureczek S, Singh J, Christensen CR, Hufton AP, Hall CJ, Cheung KC & Pavlov KM. (2005). Phase contrast X-ray imaging of mice and rabbit lungs: a comparative study. *British Journal of Radiology* **78**, 1018-1027.
- Kitchen MJ, Paganin D, Lewis RA, Yagi N, Uesugi K & Mudie ST. (2004). On the origin of speckle in x-ray phase contrast images of lung tissue. *Physics in Medicine and Biology* **49**, 4335-4348.
- Kluckow M & Hooper SB. (2015). Using physiology to guide time to cord clamping. In *Seminars in Fetal and Neonatal Medicine*. Elsevier.
- Konduri GG, Gervasio CT & Theodorou AA. (1993). Role of adenosine triphosphate and adenosine in oxygen-induced pulmonary vasodilation in fetal lambs. *Pediatric Research* **33**, 533-538.
- Kosch PC & Stark A. (1984). Dynamic maintenance of end-expiratory lung volume in full-term infants. *Journal of Applied Physiology* **57**, 1126-1133.
- Kotecha S. (2000). Lung growth: implications for the newborn infant. *Archives of Disease in Childhood: Fetal and Neonatal Edition* **82**, F69-F74.
- Lahm T, Crisostomo PR, Markel TA, Wang M, Weil BR, Novotny NM & Meldrum DR. (2008). The effects of estrogen on pulmonary artery vasoreactivity and hypoxic pulmonary vasoconstriction: potential new clinical implications for an old hormone. *Critical Care Medicine* **36**, 2174-2183.
- Lakshminrusimha S & Steinhorn RH. (1999). Pulmonary vascular biology during neonatal transition. *Clinics in Perinatology* **26**, 601-619.
- Lalani S, Remmers JE, MacKinnon Y, Ford GT & Hasan SU. (2002). Hypoxemia and low Crs in vagally denervated lambs result from reduced lung volume and not pulmonary edema. *Journal of Applied Physiology* **93**, 601-610.

- Lang JA, Pearson JT, Binder-Heschl C, Wallace MJ, Siew ML, Kitchen MJ, te Pas AB, Fouras A, Lewis RA, Polglase GR, Shirai M & Hooper SB. (2016). Increase in pulmonary blood flow at birth: role of oxygen and lung aeration. *Journal of Physiology* **594**, 1389-1398.
- Lang JA, Pearson JT, te Pas AB, Wallace MJ, Siew ML, Kitchen MJ, Fouras A, Lewis RA, Wheeler K, Polglase GR, Shirai M, Sonobe T & Hooper SB. (2014). Ventilation/perfusion mismatch during lung aeration at birth. *Journal of Applied Physiology* **117**, 535-543.
- Leffler CW, Hessler JR & Green RS. (1984). The onset of breathing at birth stimulates pulmonary vascular prostacyclin synthesis. *Pediatric Research* **18**, 938-942.
- Leong AF, Fouras A, Islam MS, Wallace MJ, Hooper SB & Kitchen MJ. (2013). High spatiotemporal resolution measurement of regional lung air volumes from 2D phase contrast x-ray images. *Medical Physics* **40**, 041909.
- Levin DL, Rudolph AM, Heymann MA & Phibbs RH. (1976). Morphological development of the pulmonary vascular bed in fetal lambs. *Circulation* **53**, 144-151.
- Levy M, Maurey C, Chailley-Heu B, Martinovic J, Jaubert F & Israël-Biet D. (2005). Developmental changes in endothelial vasoactive and angiogenic growth factors in the human perinatal lung. *Pediatric Research* **57**, 248-253.
- Lévy M, Maurey C, Dinh-Xuan AT, Vouhé P & Israël-Biet D. (2005). Developmental expression of vasoactive and growth factors in human lung. Role in pulmonary vascular resistance adaptation at birth. *Pediatric Research* **57**, 21R-25R.
- Lewis AB, Heymann MA & Rudolph AM. (1976). Gestational changes in pulmonary vascular responses in fetal lambs in utero. *Circulation Research* **39**, 536-541.
- Lewis RA, Yagi N, Kitchen MJ, Morgan MJ, Paganin D, Siu KKW, Pavlov K, Williams I, Uesugi K, Wallace MJ, Hall CJ, Whitley J & Hooper SB. (2005). Dynamic imaging of the lungs using x-ray phase contrast. *Physics in Medicine and Biology* **50**, 5031-5040.
- Li F, Wang X, Capasso JM & Gerdes AM. (1996). Rapid transition of cardiac myocytes from hyperplasia to hypertrophy during postnatal development. *Journal of Molecular and Cellular Cardiology* **28**, 1737-1746.

- Lister G, Walter TK, Versmold HT, Dallman PR & Rudolph AM. (1979). Oxygen delivery in lambs: cardiovascular and hematologic development. *American Journal of Physiology: Heart and Circulatory Physiology* **237**, H668-H675.
- Liu Q, Sham J, Shimoda L & Sylvester J. (2001). Hypoxic constriction of porcine distal pulmonary arteries: endothelium and endothelin dependence. *American Journal of Physiology: Lung Cellular and Molecular Physiology* **280**, L856-L865.
- Lu D & Kassab GS. (2011). Role of shear stress and stretch in vascular mechanobiology. *Journal of The Royal Society Interface*, 1379–1385.
- Luscher TF. (1990). Endothelium-derived vasoactive factors and regulation of vascular tone in human blood vessels. *Lung* **168**, 27-34.
- Maloney J, Adamson T, Brodecky V, Dowling M & Ritchie B. (1975). Modification of respiratory center output in the unanesthetized fetal sheep "in utero". *Journal of Applied Physiology* **39**, 552-558.
- McCray P, Bettencourt J & Bastacky J. (1992). Developing bronchopulmonary epithelium of the human fetus secretes fluid. *American Journal of Physiology: Lung Cellular and Molecular Physiology* **262**, L270-L279.
- Mcintyre TM, Zimmerman GA, Satoh K & Prescott SM. (1985). Cultured endothelial cells synthesize both platelet-activating factor and prostacyclin in response to histamine, bradykinin, and adenosine triphosphate. *Journal of Clinical Investigation* **76**, 271-280.
- Mielke G & Benda N. (2001). Cardiac output and central distribution of blood flow in the human fetus. *Circulation* **103**, 1662-1668.
- Miserocchi G, Poskurica BH & Del Fabbro M. (1994). Pulmonary interstitial pressure in anesthetized paralyzed newborn rabbits. *Journal of Applied Physiology* **77**, 2260-2268.
- Moessinger A, Harding R, Adamson T, Singh M & Kiu G. (1990). Role of lung fluid volume in growth and maturation of the fetal sheep lung. *Journal of Clinical Investigation* **86**, 1270-1277.
- Momma K, Ito T, Mori Y & Yamamura Y. (1992). Perinatal adaptation of the cardiovascular system. *Early Human Development* **29**, 167-170.

- Morin F & Egan E. (1992). Pulmonary hemodynamics in fetal lambs during development at normal and increased oxygen tension. *Journal of Applied Physiology* **73**, 213-218.
- Moro MA, Russel R, Cellek S, Lizasoain I, Su Y, Darley-USmar VM, Radomski MW & Moncada S. (1996). cGMP mediates the vascular and platelet actions of nitric oxide: confirmation using an inhibitor of the soluble guanylyl cyclase. *Proceedings of the National Academy of Sciences* **93**, 1480-1485.
- Moss AJ, Emmanouilides G & Duffie ER. (1963). Closure of the ductus arteriosus in the newborn infant. *Pediatrics* **32**, 25-30.
- Moss TJ. (2006). Respiratory consequences of preterm birth. *Clinical and Experimental Pharmacology and Physiology* **33**, 280-284.
- Murray TR, Chen L, Marshall BE & Macarak EJ. (1990). Hypoxic contraction of cultured pulmonary vascular smooth muscle cells. *American Journal of Respiratory Cell and Molecular Biology* **3**, 457-465.
- Nardo L, Hooper SB & Harding R. (1998). Stimulation of lung growth by tracheal obstruction in fetal sheep: relation to luminal pressure and lung liquid volume. *Pediatric Research* **43**, 184-190.
- Nuwayhid B, Brinkman C, Su C, Bevan J & Assali N. (1975). Development of autonomic control of fetal circulation. *American Journal of Physiology* **228**, 337-344.
- Olver R, Ramsden C, Strang L & Walters D. (1986). The role of amiloride - blockable sodium transport in adrenaline - induced lung liquid reabsorption in the fetal lamb. *Journal of Physiology* **376**, 321-340.
- Olver R & Strang L. (1974). Ion fluxes across the pulmonary epithelium and the secretion of lung liquid in the foetal lamb. *Journal of Physiology* **241**, 327-357.
- Olver RE, Walters DV & Wilson SM. (2004). Developmental regulation of lung liquid transport. *Annual Review of Physiology* **66**, 77-101.
- Ostrea EM, Villanueva-Uy ET, Natarajan G & Uy HG. (2006). Persistent Pulmonary Hypertension of the Newborn: Pathogenesis, Etiology, and Management. *Paediatric Drugs* **8**, 179-188.

- Paintal A. (1969). Mechanism of stimulation of type J pulmonary receptors. *Journal of Physiology* **203**, 511-532.
- Papastamelos C, Panitch HB, England SE & Allen JL. (1995). Developmental changes in chest wall compliance in infancy and early childhood. *Journal of Applied Physiology* **78**, 179-184.
- Parera MC, Van Dooren M, Van Kempen M, De Krijger R, Grosveld F, Tibboel D & Rottier R. (2005). Distal angiogenesis: a new concept for lung vascular morphogenesis. *American Journal of Physiology: Lung Cellular and Molecular Physiology* **288**, L141-L149.
- Parker TA, Afshar S, Kinsella JP, Grover TR, Gebb S, Geraci M, Shaul PW, Cryer CM & Abman SH. (2001). Effects of chronic estrogen-receptor blockade on ovine perinatal pulmonary circulation. *American Journal of Physiology: Heart and Circulatory Physiology* **281**, H1005-H1014.
- Peng T, Tian Y, Boogerd CJ, Lu MM, Kadzik RS, Stewart KM, Evans SM & Morrissey EE. (2013). Coordination of heart and lung co-development by a multipotent cardiopulmonary progenitor. *Nature* **500**, 589-592.
- Polglase GR, Dawson JA, Kluckow M, Gill AW, Davis PG, te Pas AB, Crossley KJ, McDougall A, Wallace EM & Hooper SB. (2015). Ventilation onset prior to umbilical cord clamping (physiological-based cord clamping) Improves systemic and cerebral oxygenation in preterm lambs. *PloS One* **10**, e0117504.
- Polglase GR & Hooper SB. (2006). Role of intra-luminal pressure in regulating PBF in the fetus and after birth. *Current Pediatric Reviews* **2**, 287-299.
- Polglase GR, Wallace MJ, Grant DA & Hooper SB. (2004). Influence of fetal breathing movements on pulmonary hemodynamics in fetal sheep. *Pediatric Research* **56**, 932-938.
- Post JM, Hume JR, Archer SL & Weir EK. (1992). Direct role for potassium channel inhibition in hypoxic pulmonary vasoconstriction. *American Journal of Physiology: Cell Physiology* **262**, C882-C890.
- Rairigh RL, Parker TA, Ivy DD, Kinsella JP & Fan I. (2001). Role of inducible nitric oxide synthase in the pulmonary vascular response to birth-related stimuli in the ovine fetus. *Circulation Research* **88**, 721-726.

- Rasanen J, Wood DC, Debbs RH, Cohen J, Weiner S & Huhta JC. (1998). Reactivity of the human fetal pulmonary circulation to maternal hyperoxygenation increases during the second half of pregnancy a randomized study. *Circulation* **97**, 257-262.
- Reid DL & Thornburg KL. (1990). Pulmonary pressure-flow relationships in the fetal lamb during in utero ventilation. *Journal of Applied Physiology* **69**, 1630-1636.
- Reynolds S. (1956). The fetal and neonatal pulmonary vasculature in the guinea pig in relation to hemodynamic changes at birth. *American Journal of Anatomy* **98**, 97-127.
- Roberts AM, Yu J & Joshua IG. (2015). Microvascular dilation evoked by chemical stimulation of C-fibers in rats. *Journal of Applied Physiology* **118**, 55-60.
- Robertson TP, Aaronson PI & Ward JP. (2003). Ca²⁺ sensitization during sustained hypoxic pulmonary vasoconstriction is endothelium dependent. *American Journal of Physiology: Lung Cellular and Molecular Physiology* **284**, L1121-L1126.
- Robin ED, Theodore J, Burke CM, Oesterle SN, Fowler MB, Jamieson SW, Baldwin JC, Morris AJ, Hunt SA & Vankessel A. (1987). Hypoxic pulmonary vasoconstriction persists in the human transplanted lung. *Clinical Science (London, England: 1979)* **72**, 283-287.
- Rudolph A & Yuan S. (1966). Response of the pulmonary vasculature to hypoxia and H⁺ ion concentration changes. *Journal of Clinical Investigation* **45**, 399-411.
- Rudolph AM. (1979). Fetal and neonatal pulmonary circulation. *Annual Review of Physiology* **41**, 383-395.
- Rudolph AM. (1985). Distribution and regulation of blood flow in the fetal and neonatal lamb. *Circulation Research* **57**, 811-821.
- Rudolph AM & Heyman M. (1974). Fetal and neonatal circulation and respiration. *Annual Review of Physiology* **36**, 187-207.
- Rudolph AM & Heymann MA. (1970). Circulatory changes during growth in the fetal lamb. *Circulation Research* **26**, 289-299.
- Schellenberg JC. (2006). Preterm Birth: A Review. *Current Women's Health Reviews* **2**, 257-318.

- Schwenke DO, Pearson JT, Kangawa K, Umetani K & Shirai M. (2008). Changes in macrovessel pulmonary blood flow distribution following chronic hypoxia: assessed using synchrotron radiation microangiography. *Journal of Applied Physiology* **104**, 88-96.
- Schwenke DO, Pearson JT, Umetani K, Kangawa K & Shirai M. (2007). Imaging of the pulmonary circulation in the closed-chest rat using synchrotron radiation microangiography. *Journal of Applied Physiology* **102**, 787-793.
- Shaddy RE, Tyndall MR, Teitel DF, Li C & Rudolph AM. (1988). Regulation of cardiac output with controlled heart rate in newborn lambs. *Pediatric Research* **24**, 577-582.
- Shannon JM, Nielsen LD, Gebb SA & Randell SH. (1998). Mesenchyme specifies epithelial differentiation in reciprocal recombinants of embryonic lung and trachea. *Developmental Dynamics* **212**, 482-494.
- Shimizu T & Wolfe LS. (1990). Arachidonic acid cascade and signal transduction. *Journal of Neurochemistry* **55**, 1-15.
- Shirai M, Schwenke DO, Eppel GA, Evans RG, Edgley AJ, Tsuchimochi H, Umetani K & Pearson JT. (2009). Synchrotron-based angiography for investigation of the regulation of vasomotor function in the microcirculation in vivo. *Clinical and Experimental Pharmacology & Physiology* **36**, 107-116.
- Shpilfoygel SD, Close RA, Valentino DJ & Duckwiler GR. (2000). X-ray videodensitometric methods for blood flow and velocity measurement: A critical review of literature. *Medical Physics* **27**, 2008-2023.
- Siew ML, Te Pas AB, Wallace MJ, Kitchen MJ, Lewis RA, Fouras A, Morley CJ, Davis PG, Yagi N, Uesugi K & Hooper SB. (2009a). Positive end-expiratory pressure enhances development of a functional residual capacity in preterm rabbits ventilated from birth. *Journal of Applied Physiology* **106**, 1487-1493.
- Siew ML, Wallace MJ, Kitchen MJ, Lewis RA, Fouras A, Te Pas AB, Yagi N, Uesugi K, Siu KKW & Hooper SB. (2009b). Inspiration regulates the rate and temporal pattern of lung liquid clearance and lung aeration at birth. *Journal of Applied Physiology* **106**, 1888-1895.
- Silove ED, Inoue T & Grover RF. (1968). Comparison of hypoxia, pH, and sympathomimetic drugs on bovine pulmonary vasculature. *Journal of Applied Physiology* **24**, 355-365.

- Sinha SK & Donn SM. (2006). Fetal-to-neonatal maladaptation. In *Seminars in Fetal and Neonatal Medicine*, pp. 166-173. Elsevier.
- Smith LJ, McKay KO, van Asperen PP, Selvadurai H & Fitzgerald DA. (2010). Normal development of the lung and premature birth. *Paediatric Respiratory Reviews* **11**, 135-142.
- Smolich JJ, Cox HS, Eisenhofer G & Esler MD. (1997). Pulmonary clearance and release of norepinephrine and epinephrine in newborn lambs. *American Journal of Physiology: Lung Cellular and Molecular Physiology* **273**, L264-L274.
- Smolich JJ, Walker AM, Campbell GR & Adamson TM. (1989). Left and right ventricular myocardial morphometry in fetal, neonatal, and adult sheep. *American Journal of Physiology: Heart and Circulatory Physiology* **257**, H1-H9.
- Snigirev A, Snigireva I, Kohn V, Kuznetsov S & Schelokov I. (1995). On the possibilities of x ray phase contrast microimaging by coherent high energy synchrotron radiation. *Review of Scientific Instruments* **66**, 5486-5492.
- Sobotka KS, Hooper SB, Allison BJ, te Pas AB, Davis PG, Morley CJ & Moss TJ. (2011). An initial sustained inflation improves the respiratory and cardiovascular transition at birth in preterm lambs. *Pediatric Research* **70**, 56-60.
- Soifer S, Morin 3rd F, Kaslow D & Heymann M. (1983). The developmental effects of prostaglandin D2 on the pulmonary and systemic circulations in the newborn lamb. *Journal of Developmental Physiology* **5**, 237-250.
- Soifer SJ, Loitz RD, Roman C & Heymann MA. (1985). Leukotriene end organ antagonists increase pulmonary blood flow in fetal lambs. *American Journal of Physiology: Heart and Circulatory Physiology* **249**, H570-H576.
- Soll R. (2000). Prophylactic natural surfactant extract for preventing morbidity and mortality in preterm infants. *Cochrane Database of Systematic Reviews* **2**.
- Spooner BS & Wessells NK. (1970). Mammalian lung development: interactions in primordium formation and bronchial morphogenesis. *Journal of Experimental Zoology* **175**, 445-454.

- Storme L, Rairigh RL, Parker TA, Cornfield DN, Kinsella JP & Abman SH. (1999). K⁺-channel blockade inhibits shear stress-induced pulmonary vasodilation in the ovine fetus. *American Journal of Physiology: Lung Cellular and Molecular Physiology* **276**, L220-L228.
- Stroud RC & Rahn H. (1953). Effect of O₂ and CO₂ tensions upon the resistance of pulmonary blood vessels. *American Journal of Physiology* **172**, 211-220.
- Stuart B, Drumm J, Fitzgerald D & Duignan N. (1980). Fetal blood velocity waveforms in normal pregnancy. *BJOG: An International Journal of Obstetrics and Gynaecology* **87**, 780-785.
- Sylvester J, Shimoda LA, Aaronson PI & Ward JP. (2012). Hypoxic pulmonary vasoconstriction. *Physiological Reviews* **92**, 367-520.
- Takahashi Y, De Vroomen M, Gournay V, Roman C, Rudolph AM & Heymann MA. (1999). Mechanisms of adrenomedullin-induced increase of pulmonary blood flow in fetal sheep. *Pediatric Research* **45**, 276-281.
- te Pas A, Siew M, Wallace MJ, Kitchen MJ, Fouras A, Lewis RA, Yagi N, Uesugi K, Donath S, Davis PG, Morley CJ & Hooper SB. (2009). Effect of sustained inflation length on establishing functional residual capacity at birth in ventilated premature rabbits. *Pediatric Research* **66**, 295-300.
- te Pas AB, Davis PG, Hooper SB & Morley CJ. (2008). From liquid to air: breathing after birth. *Journal of Pediatrics* **152**, 607-611.
- Teitel D & Rudolph A. (1985). Perinatal oxygen delivery and cardiac function. *Advances in Pediatrics* **32**, 321-347.
- Teitel DF, Iwamoto HS & Rudolph AM. (1990). Changes in the pulmonary circulation during birth-related events. *Pediatric Research* **27**, 372-378.
- Tiktinsky M & Morin F. (1993). Increasing oxygen tension dilates fetal pulmonary circulation via endothelium-derived relaxing factor. *American Journal of Physiology: Heart and Circulatory Physiology* **265**, H376-H380.
- Tod ML & Cassin S. (1985). Thromboxane synthase inhibition and perinatal pulmonary response to arachidonic acid. *Journal of Applied Physiology* **58**, 710-716.

- Tod ML & Cassin S. (1992). Endothelin-1-induced pulmonary arterial dilation is reduced by N omega-nitro-L-arginine in fetal lambs. *Journal of Applied Physiology* **72**, 1730-1734.
- Uhlig S, Goggel R & Engel S. (2005). Mechanisms of platelet-activating factor (PAF)-mediated responses in the lung. *Pharmacological Reports* **57**, 206-221.
- van Grondelle A, Worthen GS, Ellis DE, Mathias MM, Murphy RC, Strife RJ, Reeves JT & Voelkel NF. (1984). Altering hydrodynamic variables influences PGI₂ production by isolated lungs and endothelial cells. *Journal of Applied Physiology* **57**, 388-395.
- Velvis H, Moore P & Heymann MA. (1991). Prostaglandin inhibition prevents the fall in pulmonary vascular resistance as a result of rhythmic distension of the lungs in fetal lambs. *Pediatric Research* **30**, 62-68.
- Walker A, Ritchie B, Adamson T & Maloney J. (1988). Effect of changing lung liquid volume on the pulmonary circulation of fetal lambs. *Journal of Applied Physiology* **64**, 61-67.
- Walther FJ, Benders MJ & Leighton JO. (1993). Early changes in the neonatal circulatory transition. *The Journal of pediatrics* **123**, 625-632.
- Wardrop CA & Holland BM. (1995). The roles and vital importance of placental blood to the newborn infant. *Journal of Perinatal Medicine* **23**, 139-143.
- Waypa GB, Chandel NS & Schumacker PT. (2001). Model for hypoxic pulmonary vasoconstriction involving mitochondrial oxygen sensing. *Circulation Research* **88**, 1259-1266.
- Wedgwood S, Bekker JM & Black SM. (2001). Shear stress regulation of endothelial NOS in fetal pulmonary arterial endothelial cells involves PKC. *American Journal of Physiology: Lung Cellular and Molecular Physiology* **281**, L490-L498.
- Weissmann N, Sommer N, Schermuly RT, Ghofrani HA, Seeger W & Grimminger F. (2006). Oxygen sensors in hypoxic pulmonary vasoconstriction. *Cardiovascular Research* **71**, 620-629.
- Winters JW, Wong J, Van Dyke D, Johengen M, Heymann MA & Fineman JR. (1996). Endothelin receptor blockade does not alter the increase in pulmonary blood flow due to oxygen ventilation in fetal lambs. *Pediatric Research* **40**, 152-157.

- Wong KA, Bano A, Rigaux A, Wang B, Bharadwaj B, Schürch S, Green F, Remmers JE & Hasan SU. (1998). Pulmonary vagal innervation is required to establish adequate alveolar ventilation in the newborn lamb. *Journal of Applied Physiology* **85**, 849-859.
- Zenge JP, Rairigh RL, Grover TR, Storme L, Parker TA, Kinsella JP & Abman SH. (2001). NO and prostaglandin interactions during hemodynamic stress in the fetal ovine pulmonary circulation. *American Journal of Physiology: Lung Cellular and Molecular Physiology* **281**, L1157-L1163.
- Zhou H, Gao Y & Raj JU. (1996). Antenatal betamethasone therapy augments nitric oxide-mediated relaxation of preterm ovine pulmonary veins. *Journal of Applied Physiology* **80**, 390-396.
- Ziegler JW, Ivy DD, Kinsella JP & Abman SH. (1995). The role of nitric oxide, endothelin, and prostaglandins in the transition of the pulmonary circulation. *Clinics in Perinatology* **22**, 387-403.

Appendices

*Published Works &
Supplemental Videos*

Appendix A

Lang JA, Pearson JT, te Pas AB, Wallace MJ, Siew ML, Kitchen MJ, Fouras A, Lewis RA, Wheeler K, Polglase GR, Shirai M, Sonobe T & Hooper SB (2014) Ventilation/perfusion mismatch during lung aeration at birth. *Journal of Applied Physiology* 117(5): 535-543.

Ventilation/perfusion mismatch during lung aeration at birth

Justin A. R. Lang,^{1,2} James T. Pearson,^{3,4} Arjan B. te Pas,⁵ Megan J. Wallace,^{1,2} Melissa L. Siew,^{1,2} Marcus J. Kitchen,⁶ Andreas Fouras,⁷ Robert A. Lewis,^{8,9} Kevin I. Wheeler,^{1,10} Graeme R. Polglase,^{1,2} Mikiyasu Shirai,¹¹ Takashi Sonobe,¹¹ and Stuart B. Hooper^{1,2}

¹The Ritchie Centre, MIMR-PHI Institute of Medical Research, Melbourne, Australia; ²Department of Obstetrics and Gynaecology, Monash University, Melbourne, Australia; ³Monash Biomedical Imaging, Melbourne, Australia; ⁴Australian Synchrotron, Melbourne, Australia; ⁵Department of Pediatrics, Leiden University Medical Centre, Leiden, Netherlands; ⁶School of Physics, Monash University, Melbourne, Australia; ⁷Department of Mechanical and Aerospace Engineering, Monash University, Melbourne, Australia; ⁸Medical Imaging and Radiation Sciences, Monash University, Melbourne, Australia; ⁹Department of Medical Imaging, University of Saskatchewan, Saskatoon, Canada; ¹⁰Royal Hobart Hospital, Hobart, Australia; and ¹¹Department of Cardiac Physiology, National Cerebral and Cardiovascular Center Research Institute, Osaka, Japan

Submitted 17 December 2013; accepted in final form 24 June 2014

Lang JAR, Pearson JT, te Pas AB, Wallace MJ, Siew ML, Kitchen MJ, Fouras A, Lewis RA, Wheeler KI, Polglase GR, Shirai M, Sonobe T, Hooper SB. Ventilation/perfusion mismatch during lung aeration at birth. *J Appl Physiol* 117: 535–543, 2014. First published July 18, 2014; doi:10.1152/jappphysiol.01358.2013.—At birth, the transition to newborn life is triggered by lung aeration, which stimulates a large increase in pulmonary blood flow (PBF). Current theories predict that the increase in PBF is spatially related to ventilated lung regions as they aerate after birth. Using simultaneous phase-contrast X-ray imaging and angiography we investigated the spatial relationships between lung aeration and the increase in PBF after birth. Six near-term (30-day gestation) rabbits were delivered by caesarean section, intubated and an intravenous catheter inserted, before they were positioned for X-ray imaging. During imaging, iodine was injected before ventilation onset, after ventilation of the right lung only, and after ventilation of both lungs. Unilateral ventilation increased iodine levels entering both left and right pulmonary arteries (PAs) and significantly increased heart rate, iodine ejection per beat, diameters of both left and right PAs, and number of visible vessels in both lungs. Within the 6th intercostal space, the mean gray level (relative measure of iodine level) increased from 68.3 ± 11.6 and $70.3 \pm 7.5\%$ s to 136.3 ± 22.6 and $136.3 \pm 23.7\%$ s in the left and right PAs, respectively. No differences were observed between vessels in the left and right lungs, despite the left lung not initially being ventilated. The increase in PBF at birth is not spatially related to lung aeration allowing a large ventilation/perfusion mismatch, or pulmonary shunting, to occur in the partially aerated lung at birth.

pulmonary blood flow; newborn; ventilation; perfusion; angiography

DURING FETAL LIFE, pulmonary vascular resistance (PVR) is high and ~90% of right ventricular output bypasses the lungs and enters the systemic circulation via the ductus arteriosus. As pulmonary blood flow (PBF) is low, preload for the left ventricle depends on umbilical venous return, which flows via the ductus venosus, inferior vena cava, and foramen ovale before entering the left ventricle (27). Thus, clamping the umbilical cord at birth causes umbilical venous return to cease and preload for the left and right ventricles to suddenly decrease (3, 27, 35). As a result, the increase in PBF after birth is not only critical for facilitating pulmonary gas exchange, but also provides preload for the left ventricle (3, 6). As such, the decrease in PVR and increase in PBF at birth are central to the

transition to newborn life and although lung aeration is known to be the primary trigger, the major underlying mechanisms remain unclear (2, 10).

The decrease in PVR at birth is thought to be an integrated response to a number of vasoactive stimuli (10–12). Increased oxygenation and mechanical shear stress, caused by ventilation onset, are thought to increase nitric oxide (NO) and prostaglandin synthesis causing vasodilation of pulmonary vessels (5, 12, 36). In addition, the development of surface tension at the air-liquid interface following lung aeration increases transmural pressures across the fused capillary/alveolar wall, causing an increase in capillary recruitment and reduction in capillary resistance (7, 13, 25). However, the underlying assumption with these mechanisms is that vasodilation is spatially related to aerated or ventilated regions of the lung. Although the temporal association is well established (4, 25, 35), the spatial relationship between lung aeration and the increase in PBF at birth is unknown.

Ventilation/perfusion ratios normally vary in a spatially dependent manner across the adult lung and are thought to be largely oxygen and gravity dependent. The effect of oxygen is driven by increased NO synthesis, whereas the effect of gravity is mediated by altering capillary/alveolar wall transmural pressures. Higher transmural pressures (capillary > alveolar) cause capillary distension and recruitment leading to a decrease in PVR. Ideally, regional perfusion should spatially match regional ventilation for efficient gas exchange as a large mismatch reduces gas exchange efficiency (9). Despite the existence of this relationship in adult lung, the possibility that partial lung aeration may cause global vasodilation of the lung at birth has previously been raised, albeit in an animal model that involved major surgical alterations to the pulmonary arterial supply (4).

Phase-contrast (PC) X-ray imaging studies have provided new insights into the process of lung aeration after birth in both spontaneously breathing and ventilated neonates (8, 14, 17, 20, 31, 34). PC X-ray imaging exploits the refractive index differences between air and water to provide contrast of the air/liquid interfaces within the lung (18, 32). This technique is ideal for studying and measuring the temporal and spatial pattern of lung aeration (22) and can be combined with the use of contrast agents to simultaneously highlight pulmonary blood vessels (28–30). Our aim was to combine PC X-ray imaging with angiography to examine regional ventilation/perfusion relationships during lung aeration at birth. We hypothesized that the increase in PBF

Address for reprint requests and other correspondence: S. Hooper, The Ritchie Centre, Monash Institute of Medical Research, Monash Univ., PO Box 5418, Clayton 3168, Victoria, Australia (e-mail: Stuart.Hooper@monash.edu).

would be spatially related to regional lung aeration, with the greatest increase in PBF occurring in aerated regions. The relationship between PBF and lung aeration was examined by imaging pulmonary vessels using an iodine-based contrast agent before lung aeration, during aeration of the right lung, and following aeration of both lungs in ventilated newborn rabbits.

METHODS

Experimental Procedure

All animal procedures were approved by the SPring-8 Animal Care and Monash University's School of Biomedical Science's Animal Ethics Committees. All studies were conducted in experimental hutch 3 of beamline 20B2, in the Biomedical Imaging Centre at the SPring-8 synchrotron, Japan.

Pregnant New Zealand White rabbits at 30 days gestation (term \approx 32 days) were anesthetized using Rapinivet (12 mg/kg bolus iv; propofol, Schering-Plough Animal Health), and intubated, and anesthesia was maintained by isoflurane inhalation (1.5–4%; Isoflurane, Delvet, Australia). Fetal rabbits ($n = 6$) were partially delivered by caesarean section, sedated with sodium pentobarbitone (pentobarbital; 0.1 mg ip), and a jugular vein catheter (24G intracath, Becton-Dickson) and an endotracheal (ET) tube (18G; via tracheostomy) were inserted; the tip of the ET tube was directed into the right bronchus so that with ventilation onset only the right lung was ventilated (unilateral ventilation). During the surgical procedure, the kitten's head remained covered with fetal membranes to prevent lung aeration and the umbilical cord remained intact. The kittens were then delivered, the umbilical cord ligated and placed upright in a perspex frame before the ET tube was connected to a purpose-built, time-cycled, pressure-controlled ventilator (16); image acquisition began as soon as possible after the kittens were positioned. Kittens were ventilated in air using a peak inflation pressure of 25 cmH₂O and a positive end-expiratory pressure of 5 cmH₂O. At the conclusion of the experiment (\sim 10 min after ventilation onset for kittens), all animals were humanely killed with an overdose of sodium pentobarbitone (pentobarbital; 100 mg/kg) administered intravenously (doe) or intraperitoneally (kittens).

X-ray and Angiography Imaging

The energy was 33.2 keV, just above the iodine k-edge, and kittens were positioned 1.0 m upstream of the detector. The detectors used (either: EM-CCD C9100–02 or C9300–124F, Hamamatsu Photonics Hamamatsu, Japan or pco.edge, PCO AG, Germany) had a maximum effective pixel size of 31.8 μ m (range 15.3–31.8 μ m) and an active field of view of 21–29 (W) \times 21–30 (H) mm²; images were acquired at frame rates of 5–10 Hz. During imaging, iodine boluses (Iopromide, 370 mg/ml iodine; Schering, Germany; 1.5 μ l/g of kitten weight) were infused into the kitten via the jugular vein using a remote-controlled syringe pump (PHD2000, Harvard Apparatus). Iodine boluses were injected and images acquired for \sim 2 min before ventilation onset, during ventilation of the right lung (for \sim 3 min), and then during ventilation of both lungs (for \sim 2 min); the latter was achieved by retracting the tip of the ET tube. Subsequent iodine infusions allowed comparative analysis of pulmonary vasculature at each stage of ventilation.

Image Analysis

Images were analyzed using ImageJ (v1.47; NIH) to compare the heart rate, iodine ejection per beat, number of visible pulmonary vessels, vessel diameters and change in mean grey level profiles within the left and right pulmonary arteries (PAs), the aorta and inferior vena cava (IVC) following iodine injection.

Vessel quantification. Visible blood vessels were counted using a composite image constructed from all X-ray images beginning from

the first heartbeat immediately after iodine administration until after the iodine had left the pulmonary arteries. Images acquired during lung inflation were excluded due to motion blur and to ensure maximum possible overlap of vessels. Branches of each PA were classified according to branching generation; vessels distal to branching points were counted as individual vessels and were visible up to the 3rd order of branching.

Pulmonary artery vessel diameter. Changes in pixel gray level (intensity) along virtual lines transecting vessels perpendicular to the vessel wall were used to measure vessel diameter. For each line profile, the average background pixel gray level was calculated by measuring the average gray level along the line over 2–10 frames immediately prior to the first appearance of contrast within the vessel. This background gray level was subtracted from the pixel gray level along the transecting line following contrast injection and the resulting gray level plotted as a function of distance (pixels) along each line (Fig. 1). Vessel edges were identified when the pixel gray level decreased below 1 standard deviation (SD) of the background average on each side (Fig. 1, bottom panel). Nonuniform line profile plots, typically caused by iodine streaming towards the end of a heartbeat, were excluded from analysis. Vessel diameters from each frame were averaged over 10 frames to calculate a mean vessel diameter.

Changes in relative iodine levels within vessels. A virtual box was placed over the aorta, the IVC, the main PA immediately distal to the right ventricular outlet as well as over the left and right PAs at specific points along the main axial arteries. The latter were located within clear sections of the 6th, 7th, and 8th intercostal spaces, which provided the clearest, unobstructed view of the vessel during both the preventilation and ventilation imaging stages. The changes in mean pixel gray level within each box were measured throughout an iodine injection sequence and expressed as a percentage of the background mean pixel gray level averaged over 2–10 frames before iodine injection. The temporal changes in relative iodine levels within the 3 virtual boxes along the left and right pulmonary arteries following iodine injection were integrated to provide a relative measure of iodine flow over time within these vessels. Heart rates were determined from the mean pixel gray level changes within the main pulmonary artery collected over several heart beats during an iodine injection sequence.

Statistical Analysis

Data are presented as means \pm SE. Changes in vessel quantity, vessel diameter, and integrated relative iodine levels within vessels were analyzed using a two-way repeated-measures ANOVA. Post hoc analysis used the Holm-Sidak method. A $P < 0.05$ was considered statistically significant.

RESULTS

Animal Data

Six near-term rabbit kittens (from 5 does) underwent imaging before ventilation, during ventilation of the right lung (unilateral ventilation), and then during ventilation of both lungs (bilateral ventilation). Nonaerated regions of the lung are clearly evident by the absence of speckle pattern in the X-ray images. The gestational age of kittens at delivery was 30 days.

Observations from PC X-ray Videos

Compared with preventilation, the flow of iodine (contrast agent) into both main PAs markedly increased ($P < 0.05$) in response to unilateral ventilation (Fig. 2; Supplemental Video 1, available with the online version of this article). As such, the number and amount of iodine flowing into the pulmonary vessels were markedly increased (Fig. 2; Supplemental Video

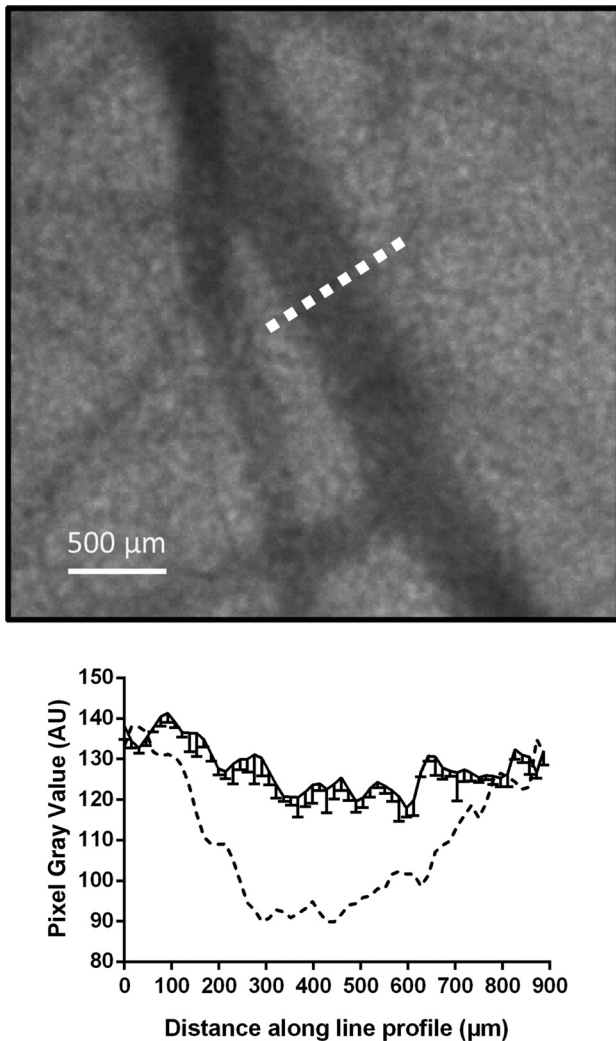


Fig. 1. Simultaneous phase contrast X-ray image and angiogram (top panel), using iodine as a contrast agent, of a small segment of the right pulmonary artery acquired following lung aeration. The background speckle pattern surrounding the vessel is caused by the small airways, particularly alveoli, acting as aberrant focusing lenses causing X-ray diffraction at each air/liquid interface (19). The pixel gray level along a virtual line (white dotted line) placed perpendicular to the vessel wall and transecting the vessel was measured to provide a profile of the pixel gray level change across the vessel. The bottom panel shows the change in pixel gray level plotted against distance along the line both before (background; unbroken line; mean \pm SD) and after (broken line; mean) iodine injection to define the vessel edges and determine vessel diameter.

1). The increase in iodine flow through vessels of the nonaerated left lung was very similar to the aerated right lung, displaying a uniform global increase in iodine visibility and, therefore, in PBF. This effect was consistently observed in all animals ($n = 6$) and was sustained following bilateral ventilation (Fig. 2).

Numbers of Visible Vessels

Compared with preventilation, unilateral ventilation of the right lung markedly increased the number of vessels visible in both lungs using angiography (Fig. 3). The number of vessels increased significantly from 15 ± 1 and 12 ± 2 vessels to 44 ± 4 and 42 ± 4 vessels in the left and right lungs, respectively,

in response to unilateral ventilation of the right lung. Bilateral ventilation further increased the number of visible vessels (compared with unilateral ventilation) to 49 ± 8 and 59 ± 11 in the left and right lungs, respectively ($P < 0.05$); at this time the number of vessels in the right lung was significantly greater than the left lung. This difference in vessel visibility between left and right lungs during bilateral ventilation was due to the number of third-order branching generation vessels (10 ± 4 in left vs. 14 ± 4 in right).

Internal Vessel Diameter

The axial PAs (both left and right) gradually narrow as they branch and penetrate into the more caudal lung lobes, penetrating at least into the 8th intercostal space (see Figs. 2 and 3). Internal vessel diameters of both the left and right axial PAs were measured in each intercostal space between ribs 6 to 8. Prior to ventilation, mean vessel diameters were $\sim 550 \mu\text{m}$ (intercostal space 6), $\sim 430 \mu\text{m}$ (intercostal space 7), and $\sim 315 \mu\text{m}$ (intercostal space 8), which reflects the decreasing vessel diameter as it branches and penetrates into the distal lung regions (Fig. 4). Compared with preventilation values, the PA diameters in both lungs were significantly increased by unilateral ventilation in all intercostal spaces measured. In the 7th intercostal space, unilateral ventilation increased the vessel diameter from 432 ± 46 and $428 \pm 31 \mu\text{m}$ to 490 ± 45 and $498 \pm 31 \mu\text{m}$ in the left and right lungs, respectively; in the 8th intercostal spaces, vessel diameters increased from 299 ± 21 and $332 \pm 13 \mu\text{m}$ to 352 ± 18 and $379 \pm 18 \mu\text{m}$ in the left and right lungs, respectively. Compared with unilateral ventilation, bilateral ventilation significantly increased vessel diameter further to $555 \pm 36 \mu\text{m}$ (left lung) and $559 \pm 34 \mu\text{m}$ (right lung) in the 7th intercostal space and to $401 \pm 23 \mu\text{m}$ (left lung) and $434 \pm 23 \mu\text{m}$ (right lung) in the 8th intercostal space (Fig. 4).

Heart Rate and Beat-to-Beat Changes in Iodine Ejection

Compared with the preventilation period, unilateral ventilation increased the heart rate from 69 ± 7 to 98 ± 17 beats/min, which was increased further to 140 ± 14 beats/min following bilateral ventilation ($P < 0.05$; Fig. 5). The relative amount of iodine ejected per heart beat, as determined by the % change in gray level (below background) measured within the main pulmonary trunk, was increased by unilateral ventilation ($P < 0.05$; Fig. 5). The amount of iodine ejected during the first and second heart beats was significantly increased from $23.2 \pm 6.3\%$ and $31.0 \pm 5.1\%$ to $54.8 \pm 7.1\%$ and $64.4 \pm 5.0\%$, respectively, following ventilation onset (Fig. 5).

Temporal Changes in Iodine Levels Within the IVC and Aorta

The temporal increase in relative iodine levels (% change in pixel gray level below background) within the IVC following iodine injection was significantly reduced in response to both unilateral and bilateral ventilation (Fig. 6). At 0.8 s after iodine injection, the relative iodine level was $29.6 \pm 6.2\%$ (% change in pixel gray level below background) before ventilation onset and was reduced to $17.4 \pm 7.1\%$ in response to unilateral ventilation and to $5.7 \pm 2.2\%$ following bilateral ventilation of the lung (Fig. 6); this indicates less iodine flowing into the IVC following injection in response to ventilation. Within the de-

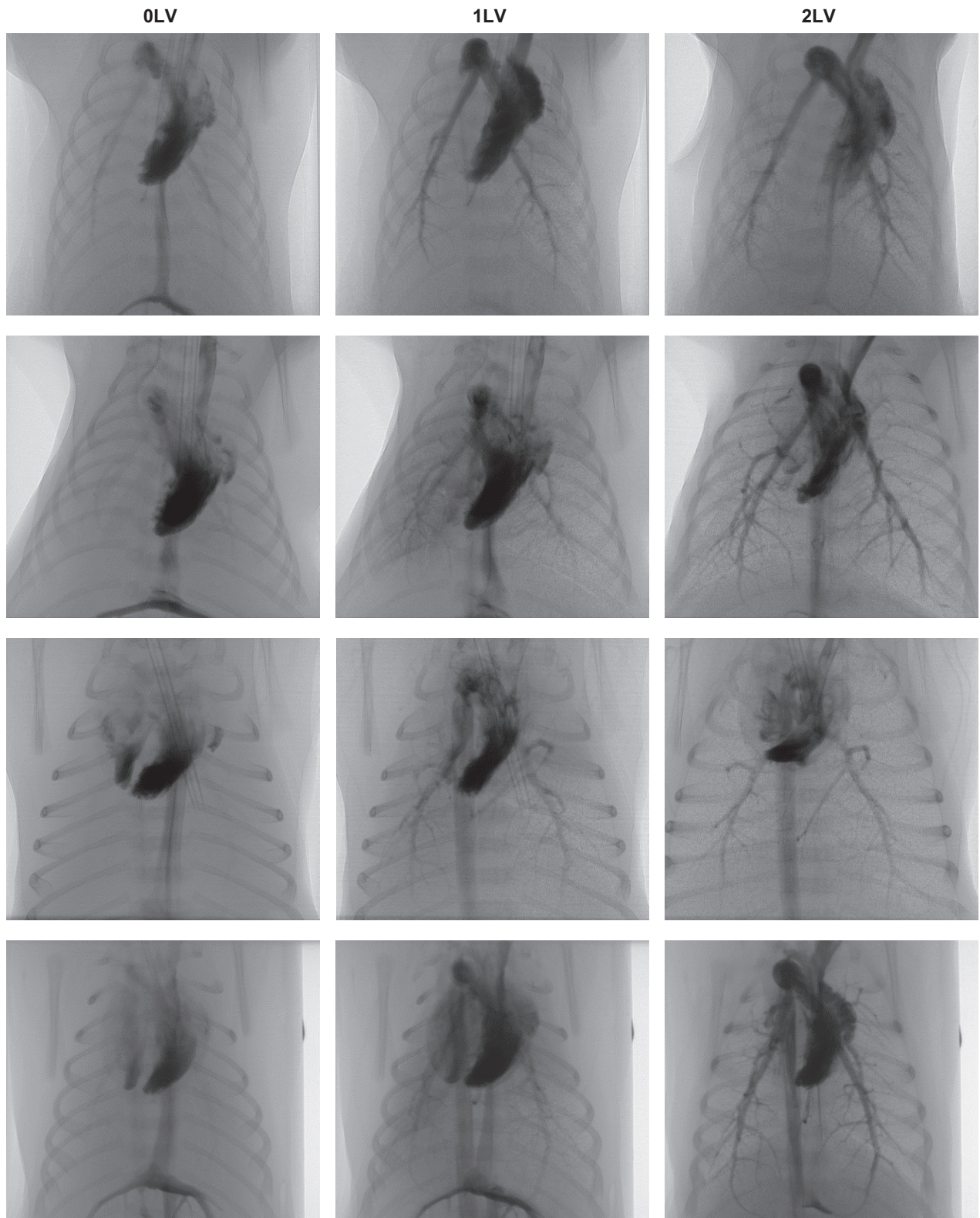


Fig. 2. Simultaneous PC X-ray images and angiograms of 4 newborn rabbits prior to ventilation (0LV), following unilateral ventilation of the right lung (1LV) and following ventilation of both lungs (2LV). Images were acquired 2–6 s after iodine injection.

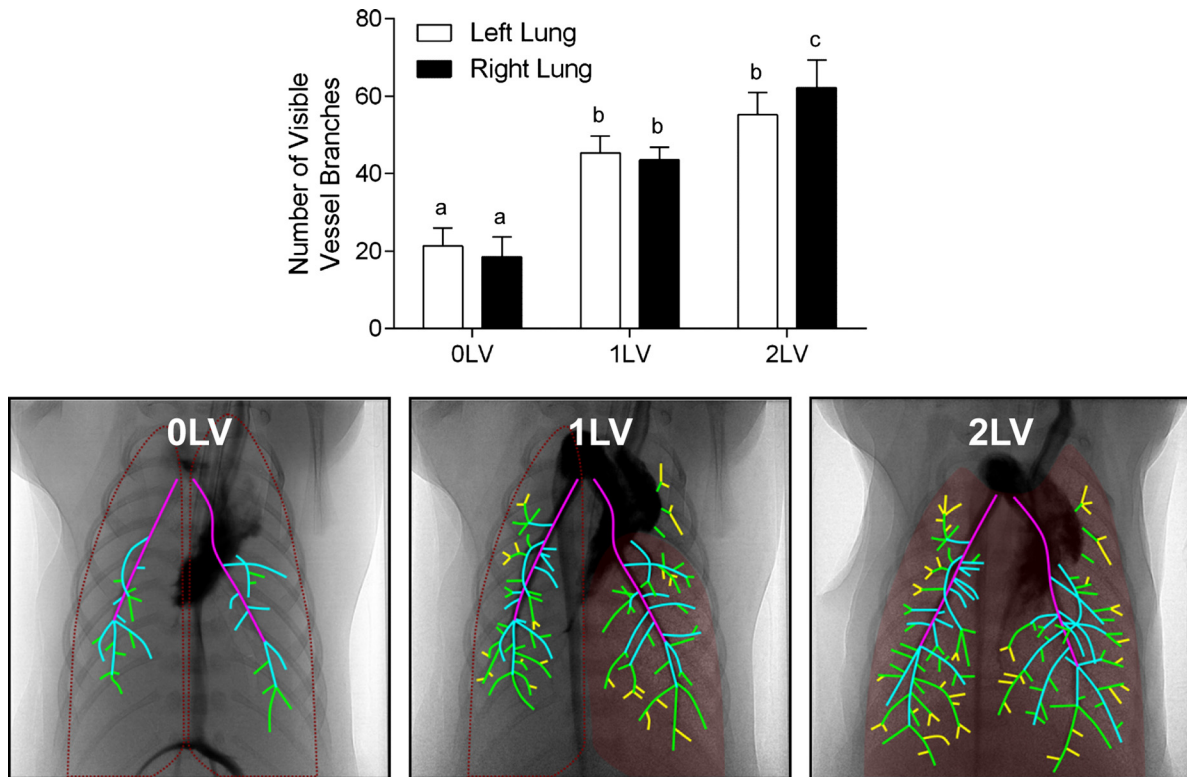


Fig. 3. *Top*: no. of visible vessels measured in the right and left lungs before ventilation (0LV), during unilateral ventilation of the right lung (1LV), and during ventilation of both lungs (2LV). *Bottom*: traced overlay of all visible blood vessels (filled with iodine) superimposed over the X-ray images of the lung acquired before ventilation onset (0LV), during unilateral ventilation of the right lung (1LV), and during ventilation of both lungs (2LV) in the same kitten. Outlined are the approximate boundaries of nonaerated regions of the lungs (red dotted line) and aerated regions of the lungs (solid red background). Shown are the left and right pulmonary arteries (purple), 1st generation branches (blue), 2nd generation branches (green), and 3rd generation branches (yellow). Within each graph, bars that do not share a letter are significantly different from each other ($P < 0.05$).

scending thoracic aorta, the temporal increase in relative iodine levels was significantly increased in response to unilateral ventilation and was increased further following bilateral ventilation (Fig. 6).

Change in Mean Pixel Gray Level Over Time Within the Pulmonary Artery

In response to unilateral ventilation, the integrated (over time) changes in relative iodine levels (% change in pixel gray level below background) within the left and right PAs following iodine injection were significantly and equally increased (Fig. 7). At the level of the 6th intercostal space, the integrated relative iodine level (%·s) increased from 68.3 ± 11.6 and 70.3 ± 7.5 %·s to 136.3 ± 22.6 and 136.3 ± 23.7 %·s in the left and right PAs, respectively. In the 7th intercostal space, the integrated relative iodine level increased from 59.2 ± 10.0 and 64.7 ± 8.6 %·s to 138.6 ± 34.8 and 139.1 ± 22.5 %·s in the left and right PAs, respectively. Bilateral ventilation tended to increase the integrated relative iodine level further, but these changes were not significant except for the region of PA within the 6th intercostal space (Fig. 7).

DISCUSSION

Our results confirm previous studies demonstrating that lung aeration at birth triggers a major hemodynamic response in the newborn, particularly an increase in PBF. However, contrary to what was hypothesized, we found that the relationship between

lung aeration and the increase in PBF at birth was not spatially related. Specifically, we found that partial lung aeration triggered a marked increase in PBF in both aerated and unaerated lung regions, resulting in a major ventilation/perfusion mismatch in unaerated regions (Figs. 2 and 7; Supplemental Video 1). These findings were unexpected as, based on the mechanisms thought to be responsible for the increase in PBF at birth (e.g., increased oxygen and NO release), we hypothesized that the stimulus would be greatest in aerated compared with unaerated lung regions. However, in every parameter examined, we found that the response to unilateral ventilation was similar in pulmonary vessels supplying aerated and nonaerated lung regions. Although some differences were observed between unilateral and bilateral ventilation periods, as the observed changes were mostly similar between lungs, irrespective of whether they were previously aerated (right) or unaerated (left), these changes more likely reflect an “increasing time after birth” related response, for example, due to a gradual increase in oxygenation.

The images clearly show major differences in iodine flow into the PAs before and after lung aeration, which greatly alters their visibility, with only the primary branches (Figs. 2 and 3) being visible before lung aeration. As it is well established that PVR is high and PBF is low before lung aeration (1), the primary reason for this reduced flow of iodine is due to the low PBF, although other factors may have contributed. For instance, a reduced venous return likely contributed via a sub-

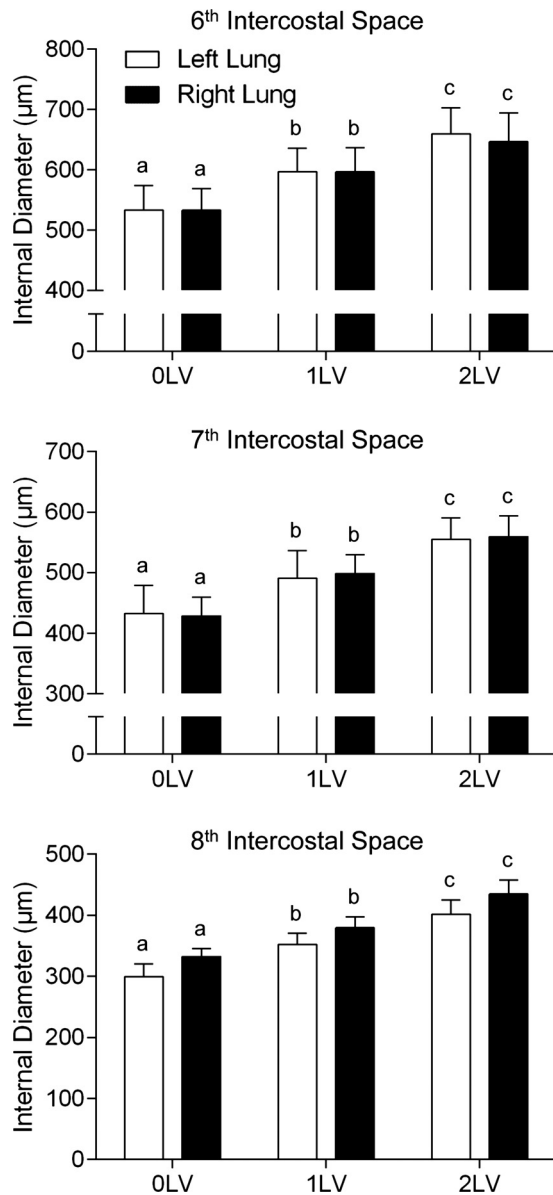


Fig. 4. Changes in internal vessel diameter along the main axial branches of the left and right pulmonary arteries at the level of the 6th (top panel), 7th (middle panel), and 8th (bottom panel) intercostal spaces, measured before ventilation onset (0LV), during unilateral ventilation of the right lung (1LV), and during ventilation of both lungs (2LV). Within each graph, bars that do not share a letter are significantly different from each other ($P < 0.05$).

stantial reduction in IVC flow caused by umbilical cord clamping, which causes umbilical venous return to cease. As umbilical venous return is an important contributor to IVC flow and preload for the fetal heart, these factors are dramatically reduced upon cord clamping and are only restored following the increase in PBF. This explanation is consistent with the finding that retrograde iodine flow along the IVC was substantially reduced following lung aeration, indicating that venous return and forward flow in the IVC was rapidly restored following ventilation onset and the associated increase in cardiac output (CO) (3). This is also consistent with previous studies showing that RV output is reduced by ~50% following umbilical cord clamping and the loss of umbilical venous return (3, 6). Our

finding that the amount of iodine ejected per beat from the RV and the heart rate were significantly lower prior to lung aeration and markedly increased with ventilation onset are entirely consistent with these previous observations.

The integrated changes (over time) in relative iodine levels measured at different positions along the main left and right axial PAs were used to assess the relative amounts of iodine passing through the PAs following iodine injection (Fig. 7). Although this analysis does not provide a quantitative measure of PBF, the changes measured must reflect increases in PBF resulting from decreases in PVR, which are known to occur following ventilation onset (3, 6). These findings are consistent with the increases in vessel diameters measured at specific points along these vessels. Although the vessel diameter changes are relatively modest (~10% and 20%), as the resistance to blood flow is inversely proportional to the vessel radius to the 4th power, these increases in diameter reflect substantial decreases in resistance; a 10% increase in diameter equates to a 40% reduction, whereas a 20% increase equates to a 60% reduction in resistance. These reductions in resistance are similar in magnitude to the reductions in PVR that have been reported previously with ventilation onset at birth (26, 27, 35).

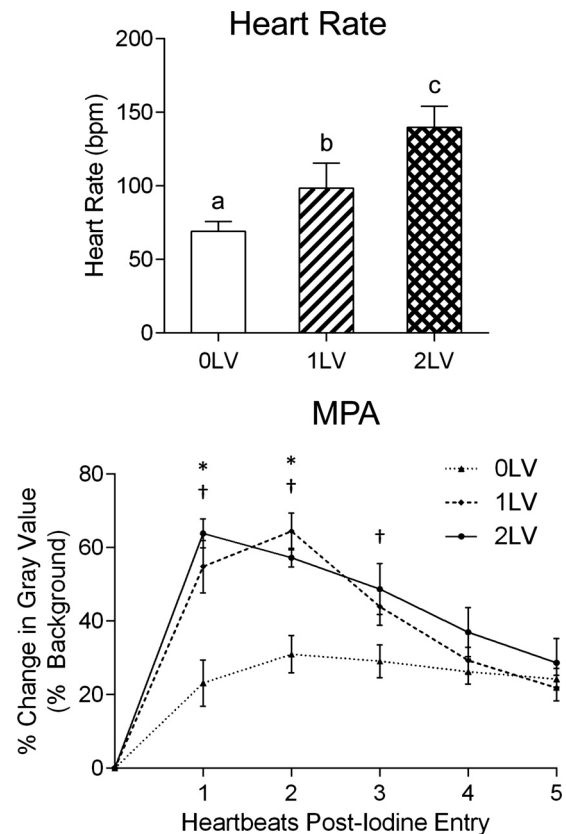


Fig. 5. Changes in heart rate (top panel) and the change in relative iodine levels (% change in pixel gray level below background) measured within the main pulmonary artery (MPA) immediately distal to the right ventricular outlet during peak systole over consecutive heartbeats following iodine injection (bottom panel). The latter provides a relative measure of the amount of iodine ejected per ventricular contraction. Measurements were made before ventilation onset (0LV), during unilateral ventilation of the right lung (1LV), and during ventilation of both lungs (2LV). * $P < 0.05$, 0LV vs. 1LV; † $P < 0.05$, 0LV vs. 2LV. Within each graph, bars that do not share a letter are significantly different from each other ($P < 0.05$).

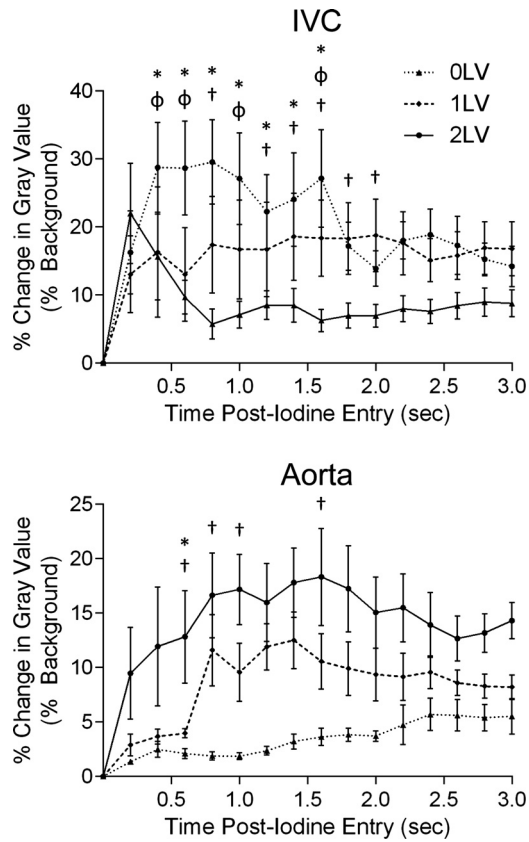


Fig. 6. Changes in relative iodine levels (% change in pixel gray level below background) measured in the midthoracic inferior vena cava (top panel) and aorta (bottom panel) at fixed time intervals after iodine injection. Measurements were made before ventilation onset (OLV), during unilateral ventilation of the right lung (1LV), and during ventilation of both lungs (2LV). **P* < 0.05, 0LV vs. 1LV; †*P* < 0.05, 0LV vs. 2LV; Φ*P* < 0.05, 1LV vs. 2LV.

Our finding that unilateral ventilation dilated pulmonary vessels and increased PBF in both aerated and unaerated regions of the lung indicates that the initial ventilation-induced increase in PBF is not spatially related to aerated lung regions. This was a surprising finding as the primary mechanisms thought to mediate the ventilation-induced increase in PBF should act locally to dilate adjacent blood vessels (1). For instance, the increase in tissue P_{O_2} associated with aerating distal gas exchange regions was thought to stimulate endothelial NO release, which acts on vascular smooth muscle to dilate resistance vessels within the lung (15). Similarly, the entry of air and the formation of surface tension within the lungs is thought to decrease PVR by increasing alveolar wall recoil, which increases pulmonary capillary recruitment and expansion. Based on this mechanism, one would also assume that the decrease in PVR would be limited to aerated lung regions (13). Thus it is possible that an additional, currently unknown, mechanism is responsible for initiating the increase in PBF at birth, which is largely independent of oxygen and the localized effects of surface tension and increased lung recoil. One possible explanation is the activation of “J” receptors (24) in response to liquid accumulation within the tissue, which triggers a parasympathetic mediated decrease in PVR via vagal reflex. Whatever the mechanism, its activation only requires aeration of a small region of the lung and includes global

vasodilation of the pulmonary vascular bed. Theoretically, this should benefit the infant, because lung aeration is often not uniform at birth and if the increase in PBF was dependent on complete lung aeration, then both CO and gas exchange will be compromised until this is achieved. As increasing PBF and restoring CO is arguably more important than simply achieving complete lung aeration immediately after birth, it is of greater benefit to the transitioning infant if the increase in PBF is not quantitatively linked to the degree of lung aeration.

The contention that the initial ventilation-induced increase in PBF is not oxygen dependent is also supported by previous studies (15, 33). For example, in fetal sheep ventilated in utero, the majority (~70%) of the increase in PBF was achieved by ventilating fetuses with a hypoxic gas mixture (35). Switching

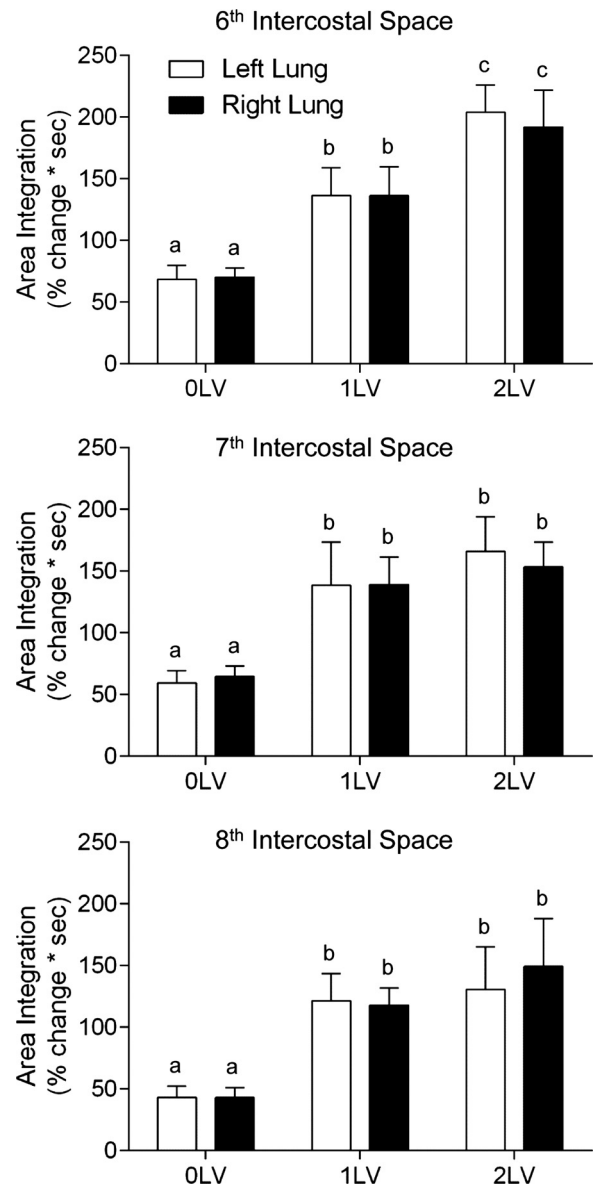


Fig. 7. Integrated (over time) change in relative iodine levels (% change in pixel gray level below background) measured in the left and right axial pulmonary arteries within the 6th (top panel), 7th (middle panel), and 8th (bottom panel) intercostal spaces. Within each graph, bars that do not share a letter are significantly different from each other (*P* < 0.05).

ventilation to 100% O₂ increased PBF further, indicating that increasing oxygen can contribute, but they concluded that oxygen is not the dominant factor and an unknown “effect of ventilation” was primarily responsible. Similarly, in lambs delivered and ventilated at birth, using strategies that either increased or decreased oxygenation levels resulted in a similar increase in PBF (33). In our study, we found that some of the factors measured increased, or tended to increase, between the periods of unilateral and bilateral ventilation, which may reflect increased oxygenation of the kitten. Indeed, it is well established that the pulmonary vasculature is sensitive to changes in oxygen tension from early in gestation, with both fetal hypoxia and hyperoxia causing vasoconstriction and vasodilation of the pulmonary vasculature bed, respectively (21). However, the fact that the increase was similar in both lungs, irrespective of whether the lung had previously been aerated (right) or unaerated (left), indicates that this mechanism is time-related and may be independent of the mechanism that was initially triggered by lung aeration.

Increased cardiac function, resulting from both an increase in HR and contractility, may have also contributed to the time-related increases of our indirect measures of PBF. With the onset of lung aeration, the infused iodine primarily entered the right ventricle and was immediately ejected, within one or two heartbeats, into either the pulmonary vasculature or the descending aorta via the ductus arteriosus. As a result, both the proportion of iodine entering the RV and the amount of iodine that was ejected per beat increased (Fig. 5), indicating that RV output had increased. This finding is consistent with the finding of an increase in HR (Fig. 5) and is also consistent with numerous previous studies (2, 6, 23). However, recent studies have also indicated that the increase in PBF is a critical determinant of the increase in cardiac function (HR and contractility) after birth, which increases before an increase in oxygenation can be detected (3). As preload for both ventricles is greatly diminished following umbilical cord clamping, causing large reductions in both stroke volumes and HR, it is not until PBF increases that preload for the LV is restored (3, 6). The important role of PBF in CO at birth was recently demonstrated by a study that delayed umbilical cord clamping until after ventilation had commenced and PBF had increased. This procedure completely abolished the reduction in CO associated with umbilical cord clamping, indicating that the source of preload can immediately switch from the umbilical circulation to PBF, without disrupting CO (3). As such, the increase in RV output and increase in HR we observed in response to unilateral ventilation is more likely to be a consequence of the increase in PBF than a cause.

We have used simultaneous angiography and PC X-ray imaging to investigate the spatial relationship between lung aeration and the increase in PBF at birth. Although we hypothesized that lung aeration and the increase in PBF would be spatially related, our finding that they are unrelated demonstrates that our current understanding of the mechanisms driving the initial increase in PBF requires reevaluation. Indeed, we found that partial lung aeration can lead to large ventilation/perfusion mismatches in nonaerated lung regions. This suggests that factors such as Po₂ and mechanical expansion, which are well-established factors thought to reduce PVR at birth, may have nonlocal effects in the lungs. However, it is not known how these factors could lead to reductions in resistance

simultaneously across the entire lung, particularly in unaerated regions, when perfusion is initially so low. It is possible that other physiological factors, such as vasodilators, simultaneously reduce resistance across the aerated and nonaerated regions, but these are generally thought not to be dominant factors (2, 10). Again, while these factors may potentiate any response, it is hard to envisage how they could initiate such an effect when pulmonary perfusion is initially so low.

Our observations of a global increase in PBF within the lungs were observed to occur within ~40 s of ventilation onset, which indicates the presence of a rapidly acting highly potent vasoactive process. This may be the result of a previously unsuspected mechanism that provides the initial stimulus for the increase in PBF at birth. In any event, it highlights our lack of understanding of the mechanisms that regulate this crucial process, despite the fact that it underpins the transition to newborn life.

ACKNOWLEDGMENTS

The authors gratefully acknowledge the support provided by the SPring-8 synchrotron facility (Japan), which was granted by the SPring-8 Program Review Committee, for providing access to the X-ray beamline and associated facilities.

GRANTS

This research was supported by the Australian Research Council, the Australian National Health and Medical Research Council and the Victorian Government's Operational Infrastructure Support Program. We acknowledge travel funding provided by the International Synchrotron Access Program (ISAP) managed by the Australian Synchrotron and funded by the Australian Government. M. J. Kitchen and A. Fouras are the recipients of ARC Australian Research Fellowship (DP110101941) and NHMRC Career Development Fellowships respectively. A. B. te Pas is recipient of a Veni-grant, The Netherlands Organisation for Health Research and Development (ZonMw), part of the Innovational Research Incentives Scheme Veni-Vidi-Vici.

DISCLOSURES

No conflicts of interest, financial or otherwise, are declared by the author(s).

AUTHOR CONTRIBUTIONS

Author contributions: J.A.R.L., J.T.P., R.A.L., and S.B.H. conception and design of research; J.A.R.L., J.T.P., A.B.t.P., M.J.W., M.L.-L.S., M.J.K., A.F., R.A.L., K.W., G.R.P., M.S., T.S., and S.B.H. performed experiments; J.A.R.L. analyzed data; J.A.R.L., J.T.P., A.B.t.P., M.J.W., M.L.-L.S., M.J.K., A.F., R.A.L., K.W., G.R.P., M.S., T.S., and S.B.H. interpreted results of experiments; J.A.R.L. and S.B.H. prepared figures; J.A.R.L. and S.B.H. drafted manuscript; J.A.R.L., J.T.P., A.B.t.P., M.J.W., M.L.-L.S., M.J.K., A.F., R.A.L., K.W., G.R.P., M.S., T.S., and S.B.H. edited and revised manuscript; J.A.R.L., J.T.P., A.B.t.P., M.J.W., M.L.-L.S., M.J.K., A.F., R.A.L., K.W., G.R.P., M.S., T.S., and S.B.H. approved final version of manuscript.

REFERENCES

1. **Abman SH.** Recent advances in the pathogenesis and treatment of persistent pulmonary hypertension of the newborn. *Neonatology* 91: 283–290, 2007.
2. **Berhrsin J, Gibson AT.** Cardiovascular system adaptation at birth. *Paediatr Child Health* 21: 1–6, 2011.
3. **Bhatt S, Alison BJ, Wallace EM, Crossley KJ, Gill AW, Kluckow M, te Pas AB, Morley CJ, Polglase GR, Hooper SB.** Delaying cord clamping until ventilation onset improves cardiovascular function at birth in preterm lambs. *J Physiol* 591: 2113–2126, 2013.
4. **Cassin S, Dawes GS, Mott JC, Ross BB, Strang LB.** The vascular resistance of the foetal and newly ventilated lung of the lamb. *J Physiol* 171: 61–79, 1964.
5. **Coggins MP, Bloch KD.** Nitric oxide in the pulmonary vasculature. *Arterioscler Thromb Vasc Biol* 27: 1877–1885, 2007.

6. Crossley KJ, Allison BJ, Polglase GR, Morley CJ, Davis PG, Hooper SB. Dynamic changes in the direction of blood flow through the ductus arteriosus at birth. *J Physiol* 587: 4695–4704, 2009.
7. Dawes GS, Lewis BV, Milligan JE, Roach MR, Talner NS. Vasomotor responses in the hind limbs of foetal and new-born lambs to asphyxia and aortic chemoreceptor stimulation. *J Physiol* 195: 55–81, 1968.
8. Fouras A, Kitchen MJ, Dubsky S, Lewis RA, Hooper SB, Hourigan K. The past, present, and future of x-ray technology for in vivo imaging of function and form. *J Appl Phys* 105: 102009, 2009.
9. Gale GE, Torrebueno JR, Moon RE, Saltzman HA, Wagner PD. Ventilation-perfusion inequality in normal humans during exercise at sea level and simulated altitude. *J Appl Physiol* 58: 978–988, 1985.
10. Gao Y, Raj JU. Regulation of the pulmonary circulation in the fetus and newborn. *Physiol Rev* 90: 1291–1335, 2010.
11. Ghanayem NS, Gordon JB. Modulation of pulmonary vasomotor tone in the fetus and neonate. *Respir Res* 2: 139–144, 2001.
12. Heymann MA. Control of the pulmonary circulation in the fetus and during the transitional period to air breathing. *Eur J Obstet Gynecol Reprod Biol* 84: 127–132, 1999.
13. Hooper SB. Role of luminal volume changes in the increase in pulmonary blood flow at birth in sheep. *Exp Physiol* 83: 833–842, 1998.
14. Hooper SB, Kitchen MJ, Wallace MJ, Yagi N, Uesugi K, Morgan MJ, Hall C, Siu KKW, Williams IM, Siew M, Irvine SC, Pavlov K, Lewis RA. Imaging lung aeration and lung liquid clearance at birth. *FASEB J* 21: 3329–3337, 2007.
15. Iwamoto HS, Teitel D, Rudolph AM. Effects of birth-related events on blood flow distribution. *Pediatr Res* 22: 634–640, 1987.
16. Kitchen MJ, Habib A, Fouras A, Dubsky S, Lewis RA, Wallace MJ, Hooper SB. A new design for high stability pressure-controlled ventilation for small animal lung imaging. *J Instrum* 5: T02002, 2010.
17. Kitchen MJ, Lewis RA, Morgan MJ, Wallace MJ, Siew ML, Siu KKW, Habib A, Fouras A, Yagi N, Uesugi K, Hooper SB. Dynamic measures of regional lung air volume using phase contrast x-ray imaging. *Phys Med Biol* 53: 6065–6077, 2008.
18. Kitchen MJ, Lewis RA, Yagi N, Uesugi K, Paganin D, Hooper SB, Adams G, Jureczek S, Singh J, Christensen CR, Hufton AP, Hall CJ, Cheung KC, Pavlov KM. Phase contrast X-ray imaging of mice and rabbit lungs: a comparative study. *Br J Radiol* 78: 1018–1027, 2005.
19. Kitchen MJ, Paganin D, Lewis RA, Yagi N, Uesugi K, Mudie ST. On the origin of speckle in x-ray phase contrast images of lung tissue. *Phys Med Biol* 49: 4335–4348, 2004.
20. Leong AF, Fouras A, Islam MS, Wallace MJ, Hooper SB, Kitchen MJ. High spatiotemporal resolution measurement of regional lung air volumes from 2D phase contrast x-ray images. *Med Phys* 40: 041909, 2013.
21. Lewis AB, Heymann MA, Rudolph AM. Gestational changes in pulmonary vascular responses in fetal lambs in utero. *Circ Res* 39: 536–541, 1976.
22. Lewis RA, Yagi N, Kitchen MJ, Morgan MJ, Paganin D, Siu KKW, Pavlov K, Williams I, Uesugi K, Wallace MJ, Hall CJ, Whitley J, Hooper SB. Dynamic imaging of the lungs using x-ray phase contrast. *Phys Med Biol* 50: 5031–5040, 2005.
23. Momma K, Ito T, Mori Y, Yamamura Y. Perinatal adaptation of the cardiovascular system. *Early Hum Dev* 29: 167–170, 1992.
24. Paintal A. Mechanism of stimulation of type J pulmonary receptors. *J Physiol* 203: 511–532, 1969.
25. Polglase GR, Hooper SB. Role of intra-luminal pressure in regulating PBF in the fetus and after birth. *Curr Pediatr Rev* 2: 287–299, 2006.
26. Rudolph AM. Distribution and regulation of blood flow in the fetal and neonatal lamb. *Circ Res* 57: 811–821, 1985.
27. Rudolph AM. Fetal and neonatal pulmonary circulation. *Annu Rev Physiol* 41: 383–395, 1979.
28. Schwenke DO, Pearson JT, Kangawa K, Umetani K, Shirai M. Changes in macrovessel pulmonary blood flow distribution following chronic hypoxia: assessed using synchrotron radiation microangiography. *J Appl Physiol* 104: 88–96, 2008.
29. Schwenke DO, Pearson JT, Umetani K, Kangawa K, Shirai M. Imaging of the pulmonary circulation in the closed-chest rat using synchrotron radiation microangiography. *J Appl Physiol* 102: 787–793, 2007.
30. Shirai M, Schwenke DO, Eppel GA, Evans RG, Edgley AJ, Tsuchimochi H, Umetani K, Pearson JT. Synchrotron-based angiography for investigation of the regulation of vasomotor function in the microcirculation in vivo. *Clin Exper Pharmacol Physiol* 36: 107–116, 2009.
31. Siew ML, Te Pas AB, Wallace MJ, Kitchen MJ, Lewis RA, Fouras A, Morley CJ, Davis PG, Yagi N, Uesugi K, Hooper SB. Positive end-expiratory pressure enhances development of a functional residual capacity in preterm rabbits ventilated from birth. *J Appl Physiol* 106: 1487–1493, 2009.
32. Snigireva A, Snigireva I, Kohn V, Kuznetsov S, Schelokov I. On the possibilities of x ray phase contrast microimaging by coherent high energy synchrotron radiation. *Rev Sci Instrum* 66: 5486–5492, 1995.
33. Sobotka KS, Hooper SB, Allison BJ, te Pas AB, Davis PG, Morley CJ, Moss TJ. An initial sustained inflation improves the respiratory and cardiovascular transition at birth in preterm lambs. *Pediatr Res* 70: 56–60, 2011.
34. te Pas A, Siew M, Wallace MJ, Kitchen MJ, Fouras A, Lewis RA, Yagi N, Uesugi K, Donath S, Davis PG, Morley CJ, Hooper SB. Effect of sustained inflation length on establishing functional residual capacity at birth in ventilated premature rabbits. *Pediatr Res* 66: 295–300, 2009.
35. Teitel DF, Iwamoto HS, Rudolph AM. Changes in the pulmonary circulation during birth-related events. *Pediatr Res* 27: 372–378, 1990.
36. Velvis H, Moore P, Heymann MA. Prostaglandin inhibition prevents the fall in pulmonary vascular resistance as a result of rhythmic distension of the lungs in fetal lambs. *Pediatr Res* 30: 62–68, 1991.

Appendix B

Lang JA, Pearson JT, Binder-Heschl C, Wallace MJ, Siew ML, Kitchen MJ, te Pas AB, Fouras A, Lewis RA, Polglase GR, Shirai M & Hooper SB (2016) Increase in pulmonary blood flow at birth: role of oxygen and lung aeration. *The Journal of Physiology* 594(5): 1389-1398

Increase in pulmonary blood flow at birth: role of oxygen and lung aeration

Justin A.R. Lang^{1,2}, James T. Pearson^{3,4}, Corinna Binder-Heschl^{1,2,5}, Megan J. Wallace^{1,2}, Melissa L. Siew^{1,2}, Marcus J. Kitchen⁶, Arjan B. te Pas⁷, Andreas Fouras⁸, Robert A. Lewis^{9,10}, Graeme R. Polglase^{1,2}, Mikiyasu Shirai¹¹ and Stuart B. Hooper^{1,2}

¹The Ritchie Centre, Hudson Institute of Medical Research, Melbourne, Australia

²Department of Obstetrics and Gynaecology, Monash University, Melbourne, Australia

³Monash Biomedical Imaging Facility and Department of Physiology, Monash University, Melbourne, Australia

⁴Australian Synchrotron, Melbourne, Australia

⁵Medical University of Graz, Austria

⁶School of Physics and Astronomy, Monash University, Melbourne, Australia

⁷Department of Pediatrics, Leiden University Medical Centre, Leiden, Netherlands

⁸Department of Mechanical and Aerospace Engineering, Monash University, Melbourne, Australia

⁹Medical Imaging and Radiation Sciences, Monash University, Melbourne, Australia

¹⁰Department of Medical Imaging, University of Saskatchewan, Saskatoon, Canada

¹¹Department of Cardiac Physiology, National Cerebral and Cardiovascular Center Research Institute, Osaka, Japan

Key points

- There is no well-established, direct correlation between local aeration and perfusion in the lungs immediately following birth.
- In a new study of simultaneous X-ray imaging and angiography in near-term rabbits, we investigated the relative contributions of lung aeration and increased oxygenation in the increase in pulmonary perfusion at birth.
- We demonstrated that partial lung aeration induces a global increase in pulmonary blood flow that is independent of changes in inspired oxygen.
- These results show that mechanisms unrelated to oxygenation or the spatial relationships that match ventilation to perfusion initiate the large increase in pulmonary blood flow at birth.

Abstract Lung aeration stimulates the increase in pulmonary blood flow (PBF) at birth, but the spatial relationships between PBF and lung aeration and the role of increased oxygenation remain unclear. Using simultaneous phase-contrast X-ray imaging and angiography, we have investigated the separate roles of lung aeration and increased oxygenation in PBF changes at birth using near-term (30 days of gestation) rabbit kits ($n = 18$). Rabbits were imaged before ventilation, then the right lung was ventilated with 100% nitrogen (N_2), air or 100% O_2 (oxygen), before all kits were switched to ventilation in air, followed by ventilation of both lungs using air. Unilateral ventilation of the right lung with 100% N_2 significantly increased heart rate (from 69.4 ± 4.9 to 93.0 ± 15.0 bpm), the diameters of both left and right pulmonary axial arteries, number of visible vessels in both left and right lungs, relative PBF index in both pulmonary arteries, and reduced bolus transit time for both left and right axial arteries (from 1.34 ± 0.39 and 1.81 ± 0.43 s to 0.52 ± 0.17 and 0.89 ± 0.21 s in the left and right axial arteries, respectively). Similar changes were observed with 100% oxygen, but increases in visible vessel number and vessel diameter of the axial arteries were greater in the ventilated right lung during unilateral ventilation. These findings confirm that PBF increase at birth is not spatially related to lung aeration and that the increase in PBF to unventilated regions is unrelated to oxygenation, although oxygen can potentiate this increase.

(Received 13 May 2015; accepted after revision 4 August 2015; first published online 17 August 2015)

Corresponding author Prof. S. Hooper: The Ritchie Centre, Hudson Institute of Medical Research, 27–31 Wright Street, Clayton, 3168, Victoria, Australia. Email: Stuart.Hooper@monash.edu

Abbreviations ET, endotracheal tube; ID, internal diameter; MPA, main pulmonary artery; PC, phase contrast; PBF, pulmonary blood flow; PVR, pulmonary vascular resistance.

Introduction

The increase in pulmonary blood flow (PBF) at birth underpins the circulatory transition that is critical for postnatal survival (Iwamoto *et al.* 1987). Shifting the site of gas exchange from the placenta to the lungs requires aeration of the lung and a reduction in pulmonary vascular resistance (PVR) to increase pulmonary perfusion (Rudolph, 1979; Berhrnsin & Gibson, 2011). This is not only necessary for efficient pulmonary gas exchange but also restores venous return to the heart, which is markedly reduced following umbilical cord clamping (Rudolph, 1979; Crossley *et al.* 2009; Bhatt *et al.* 2013). The increase in PBF at birth is thought to result from an integration of multiple mechanical and vasoactive factors acting in concert and, until recently, was assumed to occur in a spatially dependent manner as lung regions aerated (Morin & Egan, 1992; Gao & Raj, 2010). Although the temporal relationship between lung aeration and the rapid increase in PBF at birth is well established (Teitel *et al.* 1990; Polglase & Hooper, 2006), recent findings suggest there is no simple, direct correlation between local aeration and perfusion (Lang *et al.* 2014).

The factors contributing to the high PVR *in utero* are thought to include high intraluminal pressures induced by airway liquid accumulation and relatively low fetal oxygen tensions, resulting in sustained vasoconstriction of the pulmonary vasculature (Morin & Egan, 1992; Polglase & Hooper, 2006). As the developing pulmonary vasculature becomes sensitive to small changes in oxygen tension from about mid-gestation (Lewis *et al.* 1976; Blanco *et al.* 1988; Morin & Egan, 1992), increased oxygenation at birth is widely regarded as a major driver of pulmonary vasodilatation at birth. Indeed, alteration in oxygen tension is a well-known mediator of ventilation/perfusion relationships in the adult lung (Weissmann *et al.* 2006; Sylvester *et al.* 2012). Oxygen (O_2) stimulates vasodilatation directly via mitochondria, as well as through vasodilator intermediates including nitric oxide (NO) (Tiktinsky & Morin, 1993), the vasodilatory prostaglandins PGI_2 (prostacyclin) and PGE_2 , bradykinin and purine nucleotides (Gao & Raj, 2010). However, despite the well-known role for O_2 , ventilation with a hypoxic gas mixture is able to elicit the majority (60%) of the breathing-related increase in PBF at birth (Teitel *et al.* 1990). Similarly, both increases and decreases in oxygenation status are associated with ventilation-induced increases in PBF that are identical in magnitude at birth

(Sobotka *et al.* 2011). While the precise mechanisms are unclear, it is clear that the initial entry of gas into the lungs is the most significant factor responsible for the increase in PBF at birth.

Our recent study has demonstrated that the increase in PBF at birth is not spatially related to lung aeration as partial lung aeration caused a global increase in PBF (Lang *et al.* 2014). It was expected that regional lung aeration would cause localized reductions in PVR through (i) an increase in oxygenation and (ii) capillary expansion and recruitment due to an increase in alveolar/capillary wall transmural pressures resulting from a surface tension-mediated increase in lung recoil (Hooper, 1998). As neither mechanism was expected to be active in non-ventilated lung regions, the finding that the increase in PBF is not spatially related to lung aeration (Lang *et al.* 2014) indicates that the mechanisms responsible for the increase in PBF at birth require re-evaluation. It is possible that regional lung aeration increased levels of circulating partial pressure of oxygen in arterial blood (P_{aO_2}), causing vasodilatation in non-aerated lung regions. Our aim was to examine this hypothesis by partially aerating the lung in the absence of O_2 , and determine the effect on PBF in unaerated lung regions. We hypothesized that partial lung aeration with 100% nitrogen (N_2) (0% oxygen) would trigger a global increase in PBF and increasing O_2 levels in the inspired gas would enhance the increase in PBF in aerated regions. To assess the regional changes in PBF and the spatial relationships between PBF and lung aeration, we used our previously established imaging technique that combines phase-contrast (PC) X-ray imaging with angiography in near-term rabbit neonates.

Methods

Experimental procedure

All animal procedures were approved by the SPring-8 Animal Care and Monash University's School of Biomedical Science's Animal Ethics Committees and the Japan Synchrotron Radiation Research Institute, SPring-8 Animal Experiment Committee (proposals 2012A0047, 2012A1314). All studies were conducted in experimental hutch 3 of beamline 20B2, in the Biomedical Imaging Centre at the SPring-8 synchrotron, Japan.

Pregnant New Zealand white rabbits at 30 days of gestation (term \approx 32 days) were anaesthetized

using propofol (i.v.; 12 mg kg⁻¹ bolus; Rapinovel, Schering-Plough Animal Health, Tokyo, Japan) and intubated. Anaesthesia was maintained by isoflurane inhalation (1.5–4%; Isoflu, Dainippon Sumitomo Pharma Co., Osaka, Japan). Fetal rabbits ($n = 18$) were partially delivered by caesarean section, sedated with sodium pentobarbitone (13 mg kg⁻¹ i.p.; Somnopentyl, Kyoritsu Seiyaku Co., Ltd, Tokyo, Japan) and a jugular vein catheter (24 G Intracath, Becton Dickinson, Franklin Lakes, NJ, USA) and an endotracheal (ET) tube (18 G Intracath; via tracheostomy) were inserted. The tip of the ET tube was directed into the right bronchus so that with ventilation onset only the right lung was ventilated (unilateral ventilation). During the surgical procedure, the kit's head remained covered with fetal membranes to prevent lung aeration, the umbilical cord remained intact and the ET tube was obstructed to prevent breathing. The kits were then delivered and the umbilical cord was ligated before they were placed upright in an acrylic frame. ECG leads were attached to the skin of the upper limb and both lower limbs. The ET tube was then connected to a purpose-built, time-cycled, pressure-controlled ventilator (Kitchen *et al.* 2010) and image acquisition began as soon as possible after the kits were positioned. Kits were initially ventilated in either 100% N₂, 21% O₂ (air) or 100% O₂ using a peak inflation pressure of 25 cmH₂O and a positive end-expiratory pressure of 5 cmH₂O. At the conclusion of the experiment (~10 min after ventilation onset for kits), all animals were humanely killed with an overdose of sodium pentobarbitone (Pentobarbital; > 100 mg kg⁻¹) administered i.v. (doe) or i.p. (kits).

X-ray and angiography imaging

Monochromatic X-rays at 33.2 keV and a photon flux of ~10⁸ photons mm⁻² s⁻¹ was used for imaging with the kits positioned 1.0 m upstream of the detector. The scientific-CMOS (sCMOS) detector (pco.edge; PCO AG, Kehlheim, Germany) was coupled to a 25 μm thick gadolinium oxysulfide (Gd₂O₂S:Tb+) powdered phosphor and a tandem lens system that provided an effective pixel size of 15.3 μm and an active field of view of 29 (W) × 30 (H) mm². Images were acquired at a frame rate of 10 Hz. During imaging, iodine boluses (Iomeron 350 mg ml⁻¹ iodine; Bracco-Eisai Pty. Ltd, Tokyo, Japan; 1.5 μl per gram kit body weight at 11 ml s⁻¹) were administered via the jugular vein using a remote-controlled syringe pump (PHD2000, Harvard Apparatus Inc., Holliston, MA, USA). Iodine boluses were injected and images were acquired for an average of 44 ± 9 s before ventilation onset and for a further 97 ± 14 s during unilateral ventilation of the right lung with either 100% N₂ ($n = 6$), 21% O₂ ($n = 6$) or 100% O₂ ($n = 6$). Following this period, unilateral ventilation continued in air in all groups for 184 ± 14 s, after which the ET tube was

retracted to ventilate both lungs in air, which continued for 118 ± 12 s. The elapsed time between ventilation periods was consistent between groups.

Image analysis

Images were analysed using ImageJ (v1.49; NIH, Bethesda, MD, USA) as described previously (Lang *et al.* 2014). Comparisons were made between the number of visible pulmonary vessels, vessel diameters, heart rate, iodine ejection per beat, pulmonary transit time and change in mean grey level profiles within the left and right main axial arteries and the aorta following iodine injection. When ECG recordings were unsuccessful, heart rate was calculated from the inter-beat interval derived from the imaging sequence.

Vessel quantification

Visible blood vessels were counted using a composite image constructed from 10 X-ray image frames (1 s) of peak opacification during an iodine bolus (Lang *et al.* 2014). Images acquired during lung movement were excluded due to motion blur. Iodine-perfused arterial vessels distal to branching points were counted as individual vessels and were visible up to the third order of branching.

Main axial artery vessel diameter

Changes in pixel grey level (intensity) along virtual lines transecting vessels perpendicular to a vessel wall were used to measure vessel internal diameter (ID). Line profiles were drawn over the left and right main axial arteries (taken mid-lung at the seventh intercostal space), tracking ID changes from the baseline pre-ventilation period (Lang *et al.* 2014). To correct for background variation, during iodine perfusion line profiles were divided by the average background intensity, over the 10 frames (1 s) immediately prior to the first appearance of contrast within the vessel. Internal vessel edges were determined as the first pixel to drop below one standard deviation of the mean intensity of the background tissue at either end of the line profile (~5 pixels past the vessel edge). Vessel diameters measured in pixels from each frame were averaged over five frames (0.5 s) then multiplied by the known pixel size (15.3 μm) to estimate a mean vessel ID.

Pulmonary arterial transit time

A virtual box was placed over the distal end of the left and right main axial arteries before first-order branching (taken at the level of the eighth intercostal

space for consistency). The mean intensity of this region was calculated for each frame. Bolus arrival time was designated as the frame in which half of the peak opacity (maximum % change from background) is reached for the first time (half-peak opacity), which corrects for problems due to steady state peak opacity values in cases of poor wash-out (Shpilfoygel *et al.* 2000). The elapsed time between the half-peak opacity value in the main pulmonary artery (MPA) compared to the left and right axial arteries (at the eighth intercostal space) was calculated to give an approximation of bolus pulmonary artery transit time.

Changes in opacity over time within the MPAs and aorta

A virtual box was placed over the MPA immediately distal to the right ventricular outlet, the descending aorta, and the left and right main axial arteries at the level of the seventh intercostal space, the last providing a centrally located, clear and unobstructed view of the large conduit arteries during both the pre-ventilation and the ventilation imaging time periods. The changes in mean intensity within each box were plotted against time as a percentage change from background levels (mean background intensity averaged over 10 frames before iodine injection) throughout each iodine injection sequence. The maximum of this time–opacity curve was then divided by the pulmonary arterial transit time to provide an indicator of changes in pulmonary arterial flow in both lungs, right ventricular output and the relative contribution of right ventricular output to flow in the aorta during all ventilation periods.

Statistical analysis

Changes in visible vessel number, blood vessel ID, heart rate, pulmonary arterial transit time and opacity of blood vessels were analysed using a two-way repeated measures ANOVA. Post-hoc analysis used the Holm–Sidak method. A *P* value of < 0.05 was considered statistically significant.

Results

Animal data

PC X-ray images were obtained from 18 kits (30 days gestational age) from eight pregnant rabbits. Mean kit weight was 42.3 ± 1.3 g, which was similar between groups.

Observations from PC X-ray videos

Consistent with our previous findings (Lang *et al.* 2014), unilateral ventilation of the right lung (1LV₁) markedly

increased iodine flow into both left (un-aerated) and right (aerated) axial arteries compared to the pre-ventilation period (0LV). The increase in flow in the un-aerated lung was similar irrespective of whether the initial gas used to ventilate the right lung was 100% N₂ (Fig. 1; Supplementary Video S1), air (Lang *et al.* 2014) or 100% O₂ (Fig. 1; Supplementary Video S2). As such, iodine distribution increased to the non-aerated left lung despite ventilation with a gas mixture that had no oxygen. Continued unilateral ventilation in air (1LV₂) and subsequent ventilation of both lungs with air (2LV) sustained this increase in PBF and appeared to cause only modest (potentially time-related) increases compared to the initial increase in PBF in all groups (Fig. 1).

Indices of vessel recruitment

Following unilateral ventilation of the right lung with 100% N₂ (1LV₁ in Fig. 2), the total number of visible vessels increased in the left and right lungs respectively from 21 ± 5 and 19 ± 5 to 45 ± 4 and 44 ± 4 following ventilation onset. Similarly, unilateral ventilation of the right lung with air increased the number of visible vessels from 28 ± 5 and 28 ± 6 to 48 ± 9 and 45 ± 8 in the left and right lungs, respectively; the percentage increase was similar to ventilation with 100% N₂. Unilateral ventilation with 100% O₂ (1LV₁) increased vessel numbers from 34 ± 6 and 33 ± 5 to 65 ± 7 and 79 ± 8 in left and right lungs, respectively. While unilateral ventilation of the right lung with 100% N₂ and air increased visible vessel numbers similarly in both left and right lungs, ventilation with 100% O₂ resulted in a greater increase in the ventilated right lung (79 ± 8 vessels in the right lung compared to 66 ± 7 vessels in the unventilated left lung). Following the period of unilateral ventilation with 100% N₂, unilateral ventilation of the right lung (1LV₂) and then bilateral ventilation (2LV) with air increased the number of visible vessels further to 56 ± 5 and 62 ± 7 in the left and right lungs, respectively. Similarly, following the period of unilateral ventilation with air and 100% O₂, the subsequent ventilation periods of unilateral ventilation with air and bilateral ventilation with air tended to increase the number of visible vessels further, but this increase was not significant.

Heart rate and opacity changes in the MPA and aorta over time

Heart rate increased from 69.4 ± 4.9 to 93.0 ± 15.0 bpm following unilateral ventilation of the right lung with 100% N₂. Similarly, unilateral ventilation of the right lung with air or 100% O₂ increased heart rates from 55 ± 5 and 46.4 ± 3.3 bpm to 90.3 ± 13.4 and 73.0 ± 10.0 bpm, respectively (Fig. 3A). Heart rates were

not significantly changed during the subsequent period of unilateral lung ventilation with air in all groups (1LV₂), but increased further to 136.0 ± 15.2 , 129.9 ± 7.0 and 115.6 ± 10 bpm during bilateral ventilation (2LV) in pups initially ventilated with 100% N₂, air and 100% O₂, respectively. No differences in heart rate were detected between groups.

Peak opacity within the MPA (Fig. 3B), which provides an indicator of right ventricle output, increased significantly following unilateral ventilation of the right lung with either air or 100% O₂. Unilateral ventilation of the right lung with air increased peak opacity from 39.9 ± 7.3 to $72.8 \pm 4.4\%$ above background, whereas unilateral ventilation of the right lung with 100% O₂ increased peak opacity from 35.5 ± 6.1 to $64.2 \pm 5.6\%$ above background; these values did not increase further after continued ventilation (1LV₂ or 2LV). Unilateral ventilation of the right lung with 100% N₂ also tended to increase MPA peak opacity, from 31.3 ± 5.6 to $45.8 \pm 7.0\%$ above background, but this increase only became statistically significant after the switch to air (1LV₂), when it increased to $57.3 \pm 2.8\%$ above background; this did not significantly increase further with continued ventilation (2LV). Peak opacification in the descending aorta (Fig. 3C), representing the contrast agent diverted through the ductus arteriosus, increased significantly in response to unilateral ventilation when

ventilated with either air or 100% O₂ but did not significantly increase further with continued ventilation.

Arterial vessel internal diameter

Compared to pre-ventilation values, unilateral ventilation (1LV₁) of the right lung significantly increased ID of the left and right main axial arteries at the level of the seventh intercostal space in both lungs in all three groups (Fig. 4). The diameters increased from 533 ± 40 and 533 ± 35 μm in the left and right main axial arteries to 597 ± 39 and 596 ± 40 μm , respectively, in response to unilateral ventilation of the right lung with 100% N₂. These increases were similar to those observed following unilateral ventilation with air (increased from 505 ± 49 and 505 ± 39 μm to 585 ± 58 and 581 ± 40 μm , in left and right vessels, respectively) and 100% O₂ (increased from 500 ± 58 and 506 ± 55 μm to 559 ± 47 and 651 ± 56 μm in left and right vessels, respectively), except that the increase in the right axial artery ventilated with 100% O₂ tended to be greater. While ID tended to increase during the subsequent ventilation periods, this increase was not significant. IDs between the groups were not significantly different at any point although IDs in the right lung following initial ventilation with O₂ tended to be greater.

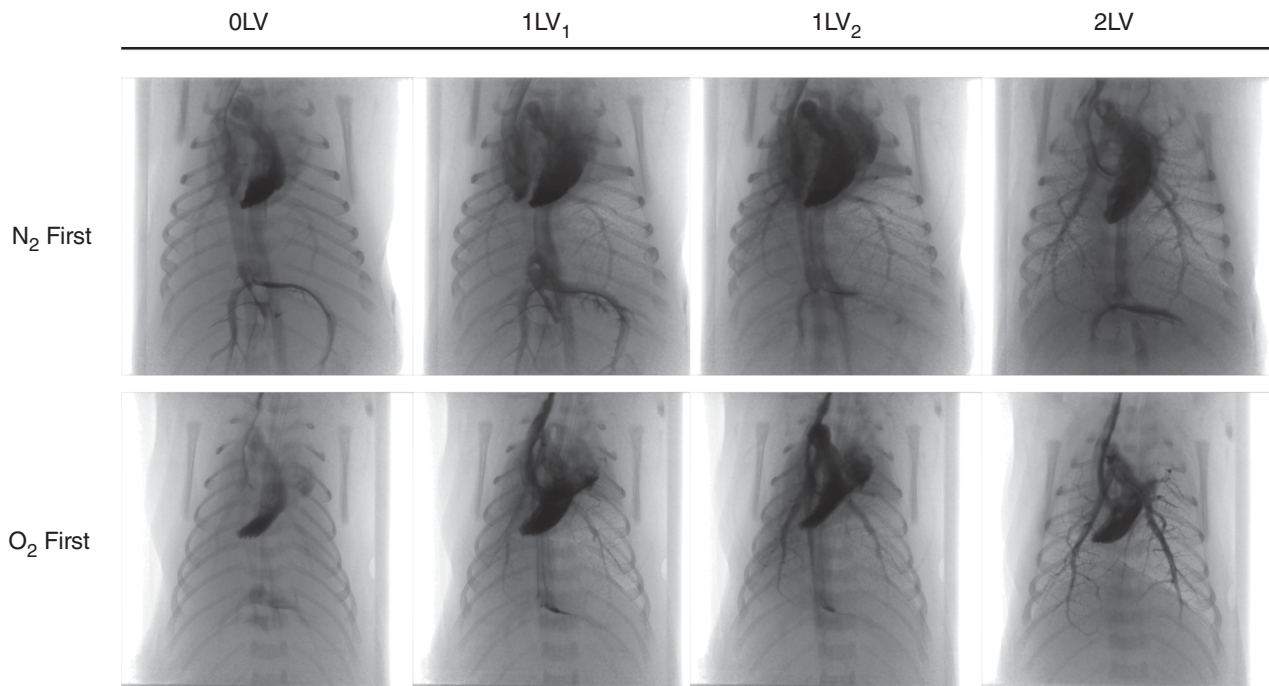


Figure 1. PC X-ray and angiography images

Representative X-ray image sequences of newborn rabbits imaged prior to ventilation (OLV), following unilateral ventilation of the right lung (1LV₁) with either 100% N₂ or 100% O₂, subsequent ventilation with air (21% O₂) in all kits (1LV₂), and later ventilation of both lungs in air (2LV). Images were obtained 1–3 s following iodine bolus injection.

Iodine bolus transit time

Pulmonary arterial transit time, given by the elapsed time between iodine bolus passage from the MPA to arrival at the distal end of the left and right axial arteries, decreased significantly in response to unilateral ventilation (1LV₁) in all groups irrespective of the gas used (100% N₂, air or 100% O₂) (Fig. 5A). Unilateral ventilation of the right lung with 100% N₂ decreased the transit time from 1.34 ± 0.39 and 1.81 ± 0.43 s to 0.52 ± 0.17 and 0.89 ± 0.21 s in the left and right pulmonary arteries, respectively. Similarly, unilateral ventilation with 100% O₂ decreased the transit times from 1.33 ± 0.41 and 1.45 ± 0.28 s to 0.23 ± 0.06 and 0.33 ± 0.14 s in the left and right axial arteries, respectively. Subsequent ventilation periods (1LV₂, 2LV) did not significantly alter the transit time from the initial decrease and no difference was detected between lungs or between groups.

Changes in relative PBF indices

Relative PBF indices, given by the maximum change in relative iodine levels (% decrease in intensity below background) divided by the arterial transit time, increased significantly in response to unilateral ventilation in all groups irrespective of the gas used (100% N₂, air or 100% O₂) (Fig. 5B). Unilateral ventilation of the right lung with 100% N₂ increased the relative PBF index from 6.0 ± 2.9 and 5.5 ± 2.6% s⁻¹ to 51.0 ± 25.1 and 69.7 ± 25.4% s⁻¹ in the left and right pulmonary arteries, respectively. Unilateral ventilation of the right lung with air increased

relative PBF index from 13.8 ± 6.2 and 6.9 ± 2.3% s⁻¹ to 78.0 ± 32.0 and 61.1 ± 22.1% s⁻¹ in the left and right pulmonary arteries, respectively. Unilateral ventilation of the right lung with 100% O₂ increased relative PBF index from 8.1 ± 3.2 and 8.3 ± 2.4% s⁻¹ to 105.5 ± 27.8 and 98.7 ± 20.4% s⁻¹ in the left and right pulmonary arteries, respectively. The subsequent ventilation period (1LV₂) did not significantly alter the relative PBF values in any group but relative PBF increased significantly after changing to bilateral ventilation (2LV). No difference was detected between lungs or between groups.

Discussion

The recent finding that partial lung aeration causes a global increase in lung perfusion indicates that pulmonary vasodilatation at birth is not spatially related to lung aeration and that an additional, previously unsuspected mechanism may be involved (Lang *et al.* 2014). However, the possibility of re-circulation of oxygenated blood-causing increased oxygenation and vasodilatation in these unventilated lung regions could not be completely dismissed. The data presented in this study now confirm that the global increase in PBF that is initiated by partial lung aeration immediately following birth is independent of changes in oxygenation. However, inhalation of 100% oxygen was found to have an additive effect on pulmonary vasodilatation and PBF, which was localized to aerated lung regions. This indicates that there are a number of factors that work independently to increase PBF at birth.

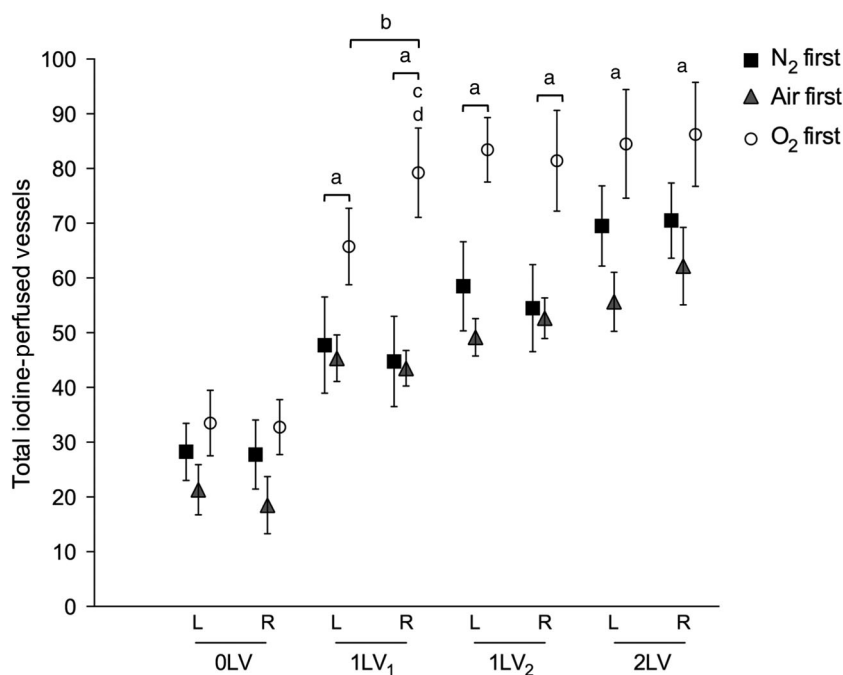


Figure 2. Changes in visualized blood vessel number

Mean iodine-perfused vessel number (±SEM) in the left and right lungs at each ventilation period (OLV, 1LV₁, 1LV₂ and 2LV) in the N₂ first (black solid squares), air first (grey solid triangles) and O₂ first (open circles) groups. ^a*P* < 0.05 compared to baseline (OLV) in the same lung in all groups; ^b*P* < 0.05 left lung vs. right lung in O₂ first; ^c*P* < 0.05 air first vs. O₂ first; ^d*P* < 0.05 N₂ first vs. O₂ first.

In this study, partial aeration of the right lung was confirmed by PC X-ray imaging, which gives rise to a distinctive speckle pattern caused by multiple phase shifts at the air/liquid boundaries in the distal airways (Kitchen *et al.* 2004). As such, we are able to confirm from the

images the lack of aeration in lung regions not being ventilated. Findings were consistent with previous studies, showing that a significant ventilation/perfusion mismatch occurs after birth when the lung is partially aerated (Fig. 1; Supplementary Videos S1 and S2) (Lang *et al.* 2014). This observation has been extended to show that unilateral ventilation of near-term newborn rabbit kits with an oxygen-free inspired gas also causes a global increase in PBF. We consistently found that, in all parameters measured, the greatest change occurs between the pre-ventilation and the initial unilateral ventilation periods, with relatively minor changes occurring thereafter. This indicates that partial lung aeration induces a large global increase in PBF, which is mediated by a potent mechanism that is unrelated to oxygenation levels.

As pulmonary perfusion is low prior to lung aeration (Rudolph, 1979; Crossley *et al.* 2009), the number of visible vessels and the penetration of contrast agent into distal vessels is low and the transit time for the flow of contrast through the pulmonary vessels is long. Following partial lung aeration, irrespective of the inspired gas content, the number of visible vessels, the diameter of the pulmonary vessels and the penetration of contrast agent into the distal pulmonary vasculature tree increased, and transit time for the flow of contrast agent markedly decreased (Fig. 1; Supplementary Videos S1 and S2). These changes are all indicative of downstream vasodilatation, vessel recruitment and an associated fall in PVR. This confirms the role of initial lung aeration as the primary stimulus for the increase in PBF at birth, although the precise mechanism involved remains intriguing. Indeed,

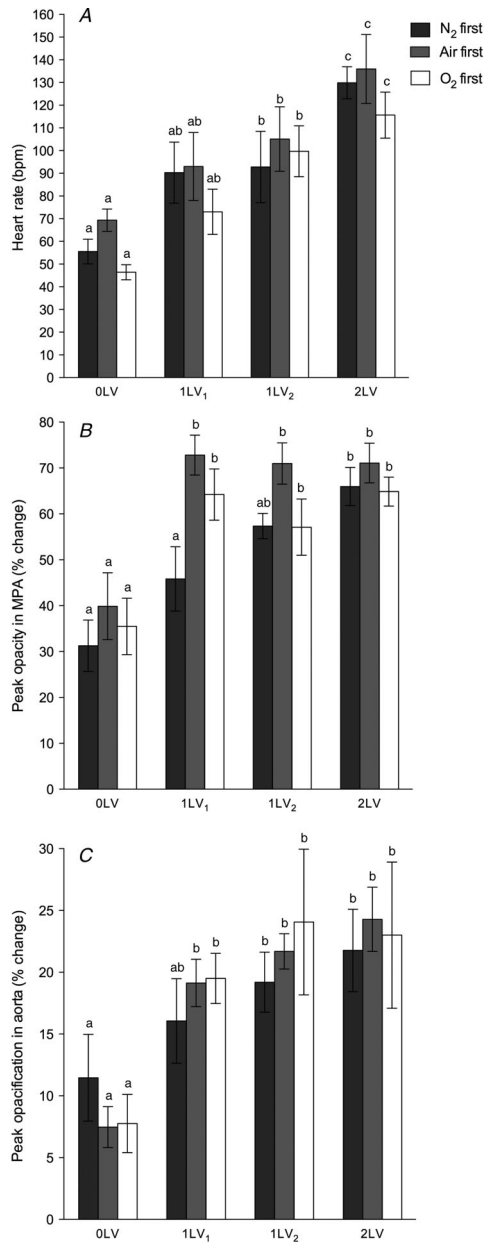


Figure 3. Heart rate and iodine distribution changes during ventilation

A, heart rate (bpm). B, an index of right ventricle output given by peak opacification (% intensity change from background) in the MPA (immediately distal to the right ventricle). C, peak opacification (% intensity change from background) in the descending aorta. In all panels data shown are mean \pm SEM at each ventilation period (0LV, 1LV₁, 1LV₂ and 2LV) in the N₂ first (dark bars), air first (grey bars) and O₂ first (white bars) groups. Within each graph, bars that do not share a letter are significantly different from each other ($P < 0.05$).

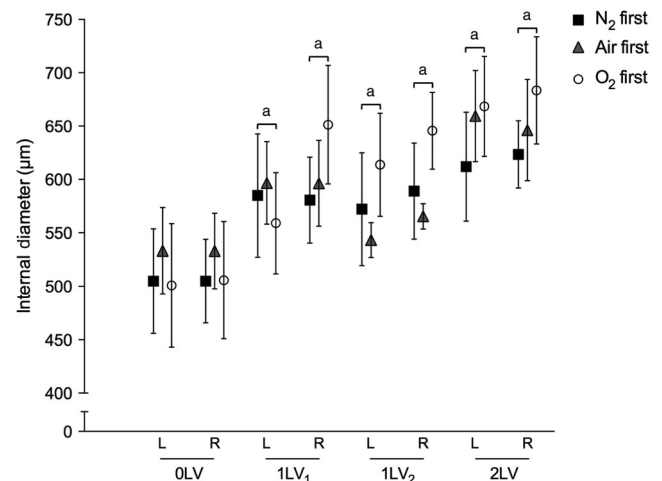


Figure 4. Blood vessel internal diameter changes during ventilation

Mean internal diameter (μm , \pm SEM) of the left and right axial arteries at the seventh intercostal space at each ventilation period (0LV, 1LV₁, 1LV₂ and 2LV) in the N₂ first (black solid squares), air first (grey solid triangles) and O₂ first (open circles) groups. $^aP < 0.05$ compared to baseline (0LV) in the same lung in the same group.

this mechanism is independent of oxygenation, but may be enhanced by oxygen, and while it can be activated by aeration of localized regions, it is translated into a global vasodilatory response. We speculate that, with gas entry into the lungs, the rapid lung liquid accumulation in the interstitial tissue (Bland *et al.* 1980; Siew *et al.* 2009) may be the stimulus for these changes, possibly via activation of J-receptors. These receptors, located within the alveolar walls, are known to respond to fluid accumulation, particularly pulmonary oedema, and signal via vagal C-fibres to cause global pulmonary vasodilatation (Paintal, 1969).

Unilateral ventilation of the right lung with 100% O₂ caused a greater increase in the number of visible vessels and vessel ID in the ventilated right lung compared to the unventilated left lung. As these differences between the left and right lungs were not evident in kits ventilated with 100% N₂ or air, this difference probably reflects an oxygen-dependent effect. However, the vasodilatory effect of oxygen appeared to be localized to aerated lung regions and was additive to the effect of lung aeration with any gas. This provides further evidence to suggest that the initial effect of lung aeration on the global increase in PBF is mediated by factors that are independent of oxygen. This suggestion is consistent with previous findings that ventilation with a hypoxic gas mixture can increase PBF in sheep without an increase in oxygenation (Teitel *et al.* 1990). Similarly, the increase in PBF with ventilation onset was shown to be similar between two groups of neonatal lambs, despite the fact that oxygenation increased in one group, but decreased in the other compared to fetal levels (Sobotka *et al.* 2011). In this study, an effect of local oxygen concentration is seen; however, the majority of the differences we observed derive from the initial entry of gas into the lungs after birth, irrespective of the gas content.

The increase in cardiac function in response to unilateral ventilation, as shown by the increase in heart rate and right ventricle output, probably also contributes to the increase in PBF observed (Fig. 3). This is possible directly via the pulmonary arteries, or indirectly via an increase in aortic pressure from the increased left ventricle function, thereby supporting the increase in PBF via the patent ductus arteriosus. However, this increase in cardiac output is also dependent upon an increase in PBF. As the umbilical circulation provides a large component of the venous return and preload for both left and right ventricles, when the umbilical cord is clamped at birth, cardiac output can decrease by up to 50% (Crossley *et al.* 2009; Bhatt *et al.* 2013). Venous return is only restored after birth following lung aeration and the increase in PBF, which takes over the role of supplying preload for the left ventricle (Crossley *et al.* 2009; Bhatt *et al.* 2013). As such, the increase in PBF at birth is vital for sustaining cardiac output after birth. Interestingly, an increase in cardiac output was observed (Fig. 3A) in response to unilateral ventilation of the right lung with 100% N₂ (Fig. 3). As the increase in cardiac output could not be due to increased oxygenation, it can only have resulted from an increase in PBF leading to an increase in ventricular preload (Sylvester *et al.* 2012). As such, we postulate that the increase in cardiac function at birth in humans is mostly a consequence of the increase in PBF, which may be a result of an increase in oxygenation. This underpins the importance of lung aeration as the defining event that initiates the cascade of changes that characterize the transition from fetal to newborn life at birth. It not only allows gas exchange to commence and stimulates an increase in

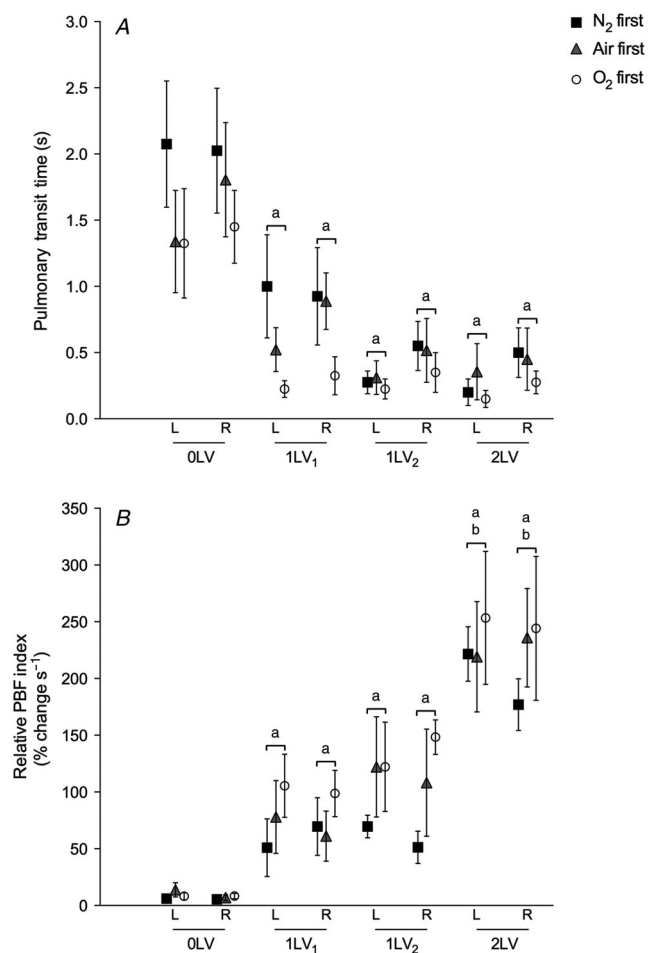


Figure 5. Indices of pulmonary blood flow changes during ventilation

A, mean arterial transit time (s, \pm SEM) in the left and right lungs. **B**, maximum percentage change grey value in the left and right main axial arteries at the seventh intercostal space divided by the arterial transit time (% change s⁻¹ \pm SEM). Data shown are at each ventilation period (0LV, 1LV₁, 1LV₂ and 2LV) in N₂ first (solid squares), air first (crosses) and O₂ first (open circles) groups. ^a*P* < 0.05 compared to baseline (0LV) in the same lung in the same group; ^b*P* < 0.05 compared to single-lung ventilation (both 1LV₁ and 1LV₂) in the same lung in the same group.

PBF, but it also increases cardiac output by restoring the venous return lost by cord clamping.

Although the increases in main axial artery IDs induced by lung aeration were modest (increase by $\sim 10\%$; Fig. 4), because the resistance decreases exponentially with increasing vessel radius (resistance $\approx 1/\text{radius}^4$), such increases in diameter reflect large decreases in resistance (Fig. 5). This is consistent with the finding of markedly reduced pulmonary transit times, which is an index of flow velocity, resulting from the decrease in PVR, although an increase in cardiac output may also have contributed. Nevertheless, unilateral ventilation with 100% N₂ both increased vessel diameter and reduced pulmonary transit times. While the decrease in transit times were not different at any point between groups, kits ventilated with 100% O₂ rapidly hit the maximum detection velocity as determined by the 10 Hz frame rate. As such, the reduction in transit times in this group may have been underestimated and may explain why a left/right difference was not observed in this parameter. Nonetheless, the rapid increase in flow velocity to both lungs and the large increase in relative PBF index (Fig 5B) provide a robust indication of the increase in PBF associated with lung aeration.

In fetal life, the maintenance of a high PVR restricts perfusion of non-aerated lungs, whereas at birth, lung aeration rapidly decreases PVR resulting in a large increase in PBF so that gas exchange can commence (Fineman *et al.* 1995). This study confirms that lung aeration and the increase in PBF are not spatially related and that limited aeration of the lungs leads to global PBF changes (Lang *et al.* 2014). Furthermore, we have now shown that partial aeration of the lung with a gas that has no oxygen can activate a global decrease in PVR. This indicates that a highly potent stimulus that is unrelated to oxygen can initiate the aeration-induced changes in PBF; however, the underlying mechanisms are currently unknown and require further investigation.

References

- Berhrsins J & Gibson A (2011). Cardiovascular system adaptation at birth. *Paediatr Child Health* **21**, 1–6.
- Bhatt S, Allison BJ, Wallace EM, Crossley KJ, Gill AW, Kluckow M, te Pas AB, Morley CJ, Polglase GR & Hooper SB (2013). Delaying cord clamping until ventilation onset improves cardiovascular function at birth in preterm lambs. *J Physiol* **591**, 2113–2126.
- Blanco C, Martin C, Rankin J, Landauer M & Phernetton T (1988). Changes in fetal organ flow during intrauterine mechanical ventilation with or without oxygen. *J Dev Physiol* **10**, 53–62.
- Bland R, McMillan D, Bressack M & Dong L (1980). Clearance of liquid from lungs of newborn rabbits. *J Appl Physiol* **49**, 171–177.
- Crossley KJ, Allison BJ, Polglase GR, Morley CJ, Davis PG & Hooper SB (2009). Dynamic changes in the direction of blood flow through the ductus arteriosus at birth. *J Physiol* **587**, 4695–4704.
- Fineman JR, Soifer SJ & Heymann MA (1995). Regulation of pulmonary vascular tone in the perinatal period. *Annu Rev Physiol* **57**, 115–134.
- Gao Y & Raj JU (2010). Regulation of the pulmonary circulation in the fetus and newborn. *Physiol Rev* **90**, 1291–1335.
- Hooper SB (1998). Role of luminal volume changes in the increase in pulmonary blood flow at birth in sheep. *Exp Physiol* **83**, 833–842.
- Iwamoto HS, Teitel D & Rudolph AM (1987). Effects of birth-related events on blood flow distribution. *Pediatr Res* **22**, 634–640.
- Kitchen MJ, Habib A, Fouras A, Dubsy S, Lewis RA, Wallace MJ & Hooper SB (2010). A new design for high stability pressure-controlled ventilation for small animal lung imaging. *J Instrum* **5**, T02002.
- Kitchen MJ, Paganin D, Lewis RA, Yagi N, Uesugi K & Mudie ST (2004). On the origin of speckle in x-ray phase contrast images of lung tissue. *Phys Med Biol* **49**, 4335–4348.
- Lang JA, Pearson JT, te Pas AB, Wallace MJ, Siew ML, Kitchen MJ, Fouras A, Lewis RA, Wheeler K, Polglase GR, Shirai M, Sonobe T & Hooper SB (2014). Ventilation/perfusion mismatch during lung aeration at birth. *J Appl Physiol* **117**, 535–543.
- Lewis AB, Heymann MA & Rudolph AM (1976). Gestational changes in pulmonary vascular responses in fetal lambs in utero. *Circ Res* **39**, 536–541.
- Morin F & Egan E (1992). Pulmonary hemodynamics in fetal lambs during development at normal and increased oxygen tension. *J Appl Physiol* **73**, 213–218.
- Paintal A (1969). Mechanism of stimulation of type J pulmonary receptors. *J Physiol* **203**, 511–532.
- Polglase GR & Hooper SB (2006). Role of intra-luminal pressure in regulating PBF in the fetus and after birth. *Curr Pediatr Rev* **2**, 287–299.
- Rudolph AM (1979). Fetal and neonatal pulmonary circulation. *Annu Rev Physiol* **41**, 383–395.
- Shpilfoylgel SD, Close RA, Valentino DJ & Duckwiler GR (2000). X-ray videodensitometric methods for blood flow and velocity measurement: a critical review of literature. *Med Phys* **27**, 2008–2023.
- Siew ML, Wallace MJ, Kitchen MJ, Lewis RA, Fouras A, te Pas AB, Yagi N, Uesugi K, Siu KKW & Hooper SB (2009). Inspiration regulates the rate and temporal pattern of lung liquid clearance and lung aeration at birth. *J Appl Physiol* **106**, 1888–1895.
- Sobotka KS, Hooper SB, Allison BJ, te Pas AB, Davis PG, Morley CJ & Moss TJ (2011). An initial sustained inflation improves the respiratory and cardiovascular transition at birth in preterm lambs. *Pediatr Res* **70**, 56–60.
- Sylvester J, Shimoda LA, Aaronson PI & Ward JP (2012). Hypoxic pulmonary vasoconstriction. *Physiol Rev* **92**, 367–520.

- Teitel DF, Iwamoto HS & Rudolph AM (1990). Changes in the pulmonary circulation during birth-related events. *Pediatr Res* **27**, 372–378.
- Tiktinsky M & Morin F (1993). Increasing oxygen tension dilates fetal pulmonary circulation via endothelium-derived relaxing factor. *Am J Physiol* **265**, H376–H380.
- Weissmann N, Sommer N, Schermuly RT, Ghofrani HA, Seeger W & Grimminger F (2006). Oxygen sensors in hypoxic pulmonary vasoconstriction. *Cardiovasc Res* **71**, 620–629.

Additional information

Competing interests

The authors declare that they have no competing interests.

Author contributions

Conception and design of the experiments: J.A.R.L., J.T.P., R.A.L., S.B.H. Collection, assembly, analysis and interpretation of data: J.A.R.L., J.T.P., C.B., M.J.W., M.L.S., M.J.K., A.B.t.P., A.F., R.A.L., G.R.P., M.S., S.B.H. Drafting the article or revising it critically for important intellectual content: J.A.R.L., J.T.P., C.B., M.J.W., M.L.S., M.J.K., A.B.t.P., A.F., R.A.L., G.R.P., M.S., S.B.H. All authors approved the final version of the manuscript.

Funding

This research was supported by the Australian Research Council, the Australian National Health and Medical Research Council and the Victorian Government's Operational Infrastructure Support Program. We acknowledge travel funding provided by the International Synchrotron Access Program (ISAP) managed by the Australian Synchrotron and funded by the Australian Government. C.B.-H. is supported by the Austrian Science Fund (FWF): J 3595-B19. M.J.K. and A.F. are the recipients of ARC Australian Research Fellowship (DP110101941) and NHMRC Career Development Fellowships, respectively. A.B.t.P. is recipient of a Veni-grant, The Netherlands

Organisation for Health Research and Development (ZonMw), part of the Innovational Research Incentives Scheme Veni-Vidi-Vici.

Acknowledgements

The authors gratefully acknowledge the support provided by the SPring-8 synchrotron facility (Japan), which was granted by the SPring-8 Program Review Committee, for providing access to the X-ray beamline and associated facilities.

Supporting information

The following supporting information is available in the online version of this article.

Video S1. Simultaneous phase contrast X-ray and angiography recordings in a newborn rabbit (30d gestation) imaged with only the right lung ventilated with 100% N₂ (~30 sec post-ventilation) immediately following birth while the left lung was non-aerated and liquid-filled. Blood vessels are visualized via infusion of iodinated contrast agent; non-aerated regions of the lung are clearly evident by the absence of speckle pattern. The data was acquired at 10 frames per second with a pixel size of 15.3 μm.

Video S2. Simultaneous phase contrast X-ray and angiography recordings in a newborn rabbit (30d gestation) imaged with only the right lung ventilated with 100% O₂ (~30 sec post-ventilation) immediately following birth while the left lung was non-aerated and liquid-filled. Blood vessels are visualized via infusion of iodinated contrast agent; non-aerated regions of the lung are clearly evident by the absence of speckle pattern. The data was acquired at 10 frames per second with a pixel size of 15.3 μm.

Appendix C

Lang, JAR, Pearson JT, Binder-Heschl C, Wallace MJ, Siew ML, Kitchen MJ, te Pas AB, Fouras A, Lewis RA, Polglase GR, Shirai M & Hooper SB (2017) Vagal denervation inhibits the increase in pulmonary blood flow during partial lung aeration at birth. *The Journal of Physiology* 595(5): 1593-1606

Vagal denervation inhibits the increase in pulmonary blood flow during partial lung aeration at birth

Justin A. R. Lang^{1,2}, James T. Pearson^{3,4,5}, Corinna Binder-Heschl^{1,2,6}, Megan J. Wallace^{1,2}, Melissa L. Siew^{1,2}, Marcus J. Kitchen⁷, Arjan B. te Pas⁸, Robert A. Lewis^{9,10}, Graeme R. Polglase^{1,2}, Mikiyasu Shirai⁵ and Stuart B. Hooper^{1,2}

¹The Ritchie Centre, Hudson Institute of Medical Research, Melbourne, Australia

²Department of Obstetrics and Gynaecology, Monash University, Melbourne, Australia

³Monash Biomedical Imaging Facility and Department of Physiology, Monash University, Melbourne, Australia

⁴Australian Synchrotron, Melbourne, Australia

⁵Department of Cardiac Physiology, National Cerebral and Cardiovascular Centre Research Institute, Osaka, Japan

⁶Medical University of Graz, Austria

⁷School of Physics and Astronomy, Monash University, Melbourne, Australia

⁸Department of Pediatrics, Leiden University Medical Centre, Leiden, Netherlands

⁹Medical Imaging and Radiation Sciences, Monash University, Melbourne, Australia

¹⁰Department of Medical Imaging, University of Saskatchewan, Saskatoon, Canada

Key points

- Lung aeration at birth significantly increases pulmonary blood flow, which is unrelated to increased oxygenation or other spatial relationships that match ventilation to perfusion.
- Using simultaneous X-ray imaging and angiography in near-term rabbits, we investigated the relative contributions of the vagus nerve and oxygenation to the increase in pulmonary blood flow at birth.
- Vagal denervation inhibited the global increase in pulmonary blood flow induced by partial lung aeration, although high inspired oxygen concentrations can partially mitigate this effect.
- The results of the present study indicate that a vagal reflex may mediate a rapid global increase in pulmonary blood flow in response to partial lung aeration.

Abstract Air entry into the lungs at birth triggers major cardiovascular changes, including a large increase in pulmonary blood flow (PBF) that is not spatially related to regional lung aeration. To investigate the possible underlying role of a vagally-mediated stimulus, we used simultaneous phase-contrast X-ray imaging and angiography in near-term (30 days of gestation) vagotomized ($n = 15$) or sham-operated ($n = 15$) rabbit kittens. Rabbits were imaged before ventilation, when one lung was ventilated (unilateral) with 100% nitrogen (N_2), air or 100% oxygen (O_2), and after all kittens were switched to unilateral ventilation in air and then ventilation of both lungs using air. Compared to control kittens, vagotomized kittens had little or no increase in PBF in both lungs following unilateral ventilation when ventilation occurred with 100% N_2 or with air. However, relative PBF did increase in vagotomized animals ventilated with 100% O_2 , indicating the independent stimulatory effects of local oxygen concentration and autonomic innervation on the changes in PBF at birth. These findings demonstrate that vagal denervation inhibits the previously observed increase in PBF with partial lung aeration, although high inspired oxygen concentrations can partially mitigate this effect.

(Resubmitted 23 October 2016; accepted after revision 15 November 2016; first published online 30 November 2016)

Corresponding author S. Hooper: The Ritchie Centre, Hudson Institute of Medical Research, 27–31 Wright Street, Clayton 3168, Victoria, Australia. Email: stuart.hooper@monash.edu

Abbreviations A, aerated; BLV, bilateral ventilation; ET, endotracheal; J, juxtacapillary; NV, not ventilated; PBF, pulmonary blood flow; PVR, pulmonary vascular resistance; UA, unaerated; ULV, unilateral ventilation.

Introduction

Lung aeration and the displacement of airway liquid into the pulmonary interstitium at birth not only allows pulmonary gas exchange to commence, but also stimulates a large increase in pulmonary blood flow (PBF) (Rudolph, 1985; Hooper *et al.* 2007; Hooper *et al.* 2015). During fetal life, gas exchange occurs across the placenta and PBF is low as a result of high pulmonary vascular resistance (PVR). As such, in the fetus, PBF contributes little to preload for the left ventricle, which is primarily derived from umbilical venous return, via the ductus venosus and foramen ovale (Rudolph, 1985; Crossley *et al.* 2009; Bhatt *et al.* 2013). Following birth, umbilical venous return is lost with clamping of the umbilical cord and so PBF must rapidly increase to facilitate pulmonary gas exchange and supply preload for the left ventricle (Bhatt *et al.* 2013). Although the increase in PBF underpins the transition to newborn life at birth, the precise mechanisms by which lung aeration triggers this process remain poorly understood.

Numerous factors, which include increased oxygenation and the release of vasodilators (e.g. nitric oxide), as well as mechanical factors, are considered to contribute to the increase in PBF at birth (Gao & Raj, 2010). Increased oxygenation dilates pulmonary vessels through mediators such as nitric oxide, prostaglandin I₂ (prostacyclin), prostaglandin E₂, bradykinin and purine nucleotides (Abman *et al.* 1990). Similarly, an increase in lung recoil caused by air entry and the formation of surface tension at the air/liquid interface increases recruitment and expansion of peri-alveolar capillaries, leading to a decrease in PVR (Hooper, 1998). Recent findings have identified an additional, previously unrecognized factor that contributes to the increase in PBF at birth (Lang *et al.* 2014; Lang *et al.* 2016). Those studies showed that partial lung aeration without O₂ increased PBF equally in both aerated and non-aerated lung regions (Lang *et al.* 2016). Although these findings are consistent with previous studies showing that ventilation can increase PBF in the absence of increased oxygenation (Teitel *et al.* 1990; Sobotka *et al.* 2011), the large increase in PBF in unventilated regions was unexpected and could not be readily explained (Lang *et al.* 2014).

The global increase in PBF following partial lung aeration indicates the possible role of a neural reflex at birth that is triggered by the entry of gas into the lungs. Intrathoracic vagal denervation, which selectively denervates the lungs, reduces respiratory function at birth and the increase in arterial oxygenation in newborn lambs (Wong *et al.* 1998; Lalani *et al.* 2002). Although this was primarily assumed to result from respiratory failure (Wong *et al.* 1998; Lalani *et al.* 2002), an impaired increase in PBF was raised as a possibility (Wong *et al.* 1998), which is consistent with previous studies showing that

vagal stimulation causes pulmonary vasodilatation in fetal sheep (Colebatch *et al.* 1965). Although a reduction in PBF was later discounted (Hasan *et al.* 2000), the effects of vagotomy on regional changes in pulmonary blood flow or ventilation/perfusion relationships have not been examined previously.

In the present study, we investigated the role of the vagus nerve in mediating the increase in PBF at birth using our unique technique of simultaneous phase contrast X-ray imaging and angiography in newborn rabbits. We hypothesized that vagotomy would disrupt vasodilatation in non-aerated lung regions following partial lung aeration, regardless of the O₂ content of the inspired gas.

Methods

Experimental procedures

All animal procedures were approved by a Monash University Animal Ethics Committee and the Japan Synchrotron Radiation Research Institute, SPring-8 Animal Experiment Committee. All studies were conducted in experimental hutch 3 of beamline 20B2, in the Biomedical Imaging Centre at the SPring-8 synchrotron, Japan.

Pregnant New Zealand white rabbits at 30 days of gestation (term ~32 days) were initially anaesthetized using propofol (i.v.; 12 mg kg⁻¹ bolus; Rapinovel, Schering-Plough Animal Health, Tokyo, Japan) and intubated. Anaesthesia was then maintained by isoflurane inhalation (1.5–4%; Isoflu, Dainippon Sumitomo Pharma Co., Osaka, Japan). Doe wellbeing was monitored via an absence of withdrawal reflexes (corneal reflex and toe pinch reflex) measuring oxygenation and heart rate (using a pulse oximeter) and pupil diameter, with the isoflurane concentration adjusted accordingly. Fetal rabbits ($n = 30$) were partially delivered by Caesarean section, and sedated with sodium pentobarbitone (13 mg kg⁻¹ i.p.; Somnopentyl, Kyoritsu Seiyaku Co., Ltd, Tokyo, Japan). Kitten wellbeing was monitored via an absence of withdrawal reflex (toe pinch), with additional sodium pentobarbitone given accordingly. Prior to delivery, kittens were randomly divided into either a sham operated, control group (C: $n = 15$) (Fig. 1) or into a group that underwent bilateral sectioning of the mid-cervical branches of the vagus nerve, above the cardiac and pulmonary vagus branches (V: $n = 15$) (Fig. 1). A jugular vein catheter (24 G Intracath; Becton Dickinson, Franklin Lakes, NJ, USA) and an endotracheal (ET) tube (18 G Intracath; via tracheostomy) were also inserted. The tip of the ET tube was directed into one main bronchus under visual control, to ensure unilateral ventilation.

All surgical procedures on kittens were performed with the umbilical cord intact and while the head of the kitten remained covered with fetal membranes to prevent lung

aeration. The kittens were then delivered, the ET tube obstructed to prevent breathing and the umbilical cord ligated before they were placed upright in a purpose built Perspex frame and positioned within the expected path of the X-ray beam. ECG leads were attached to the skin of the upper limb and both lower limbs and the ET tube was connected to a purpose-built, time-cycled, pressure-controlled ventilator (Kitchen *et al.* 2010). Image acquisition began as soon as possible after the kittens were positioned, with ventilation beginning within 2–3 min of umbilical cord ligation. Kittens were initially ventilated for 2 min in either 100% N₂ (C-N₂, V-N₂), 21% O₂ (C-air, V-air) or 100% O₂ (C-O₂, V-O₂) (*n* = 5 in each treatment group) (Fig. 1), using a peak inflation pressure of 25 cmH₂O and a positive end-expiratory pressure of 5 cmH₂O. Image sequences were obtained: before ventilation onset [not ventilated (NV)], during initial ventilation of a single lung (at 30 s after ventilation start), again during ventilation of a single lung after the inspired gas had switched to air [for an additional 2 min; both time points are referred to as unilateral ventilation (ULV)] and, finally, following ventilation of both lungs in air for 2 min [bilateral ventilation (BLV)], which was achieved by retracting the ET tube. At the conclusion of the ~13 min experimental period (~10 min after ventilation onset for each kitten), animals were humanely killed with an overdose of sodium pentobarbitone (Pentobarbital; > 100 mg kg⁻¹) administered I.V. (doe) or I.P. (kittens).

X-ray and angiography imaging

Imaging was achieved using monochromatic X-rays at 33.2 keV with a 1.0 m object-to-detector distance at a frame rate of 10 or 20 Hz during bolus iodine injections (Lang *et al.* 2014; Lang *et al.* 2016). The scientific-CMOS detector (pco.edge; PCO AG, Kehlheim, Germany) was coupled to a 25 μm thick gadolinium oxysulphide (Gd₂O₂S:Tb³⁺) powdered phosphor and a tandem lens system that provided an effective pixel size of 15.3 μm and an active field of view of 29 × 30 mm² (width × height). Iodine boluses (Iomeron 350 mg/ml iodine; Bracco-Eisai Pty Ltd, Tokyo, Japan; 1.5 μL g⁻¹ body weight at 11 ml s⁻¹) were administered via the jugular vein using a remote-controlled syringe pump (PHD2000; Harvard Apparatus Inc., Cambridge, MA, USA).

Image analysis

Images were analysed using ImageJ, version 1.50b (NIH, Bethesda, MD, USA) as described previously (Lang *et al.* 2016). During the four measurement periods, we analysed the number of visible pulmonary vessels, vessel diameters, heart rate, pulmonary transit time and change in mean grey level profiles over time within the left and right main axial arteries (to give relative PBF) following iodine injection.

Vessel quantification. Visible pulmonary vessel branch points at peak opacification during each iodine bolus were counted as individual vessels and were visible up to the third order of branching.

Main axial artery vessel diameter. Changes in pixel grey level (intensity) along virtual lines transecting vessels perpendicular to a vessel wall were used to measure vessel internal diameter. Line profiles were drawn over the left and right main axial arteries (taken mid-lung at the seventh intercostal space) to measure changes in internal diameter from the baseline pre-ventilation period (Lang *et al.* 2014; Lang *et al.* 2016). To correct for background intensity variations during iodine perfusion, line profiles were divided by the average background intensity averaged over the 10 frames (1 s) immediately prior to the first appearance of iodine within the vessel. Internal vessel edges were determined as the first pixel to drop below 1 SD of the mean intensity of the background at either end of the line profile (~5 pixels past the vessel edge). Vessel diameters measured in pixels from each frame were averaged over five frames (0.5 s) and then multiplied by the known pixel size (15.3 μm) to estimate a mean vessel internal diameter.

Pulmonary arterial transit time. A virtual box was placed over the distal end of the left and right main axial arteries before first-order branching (taken at the level of the eighth intercostal space for consistency). The mean intensity of

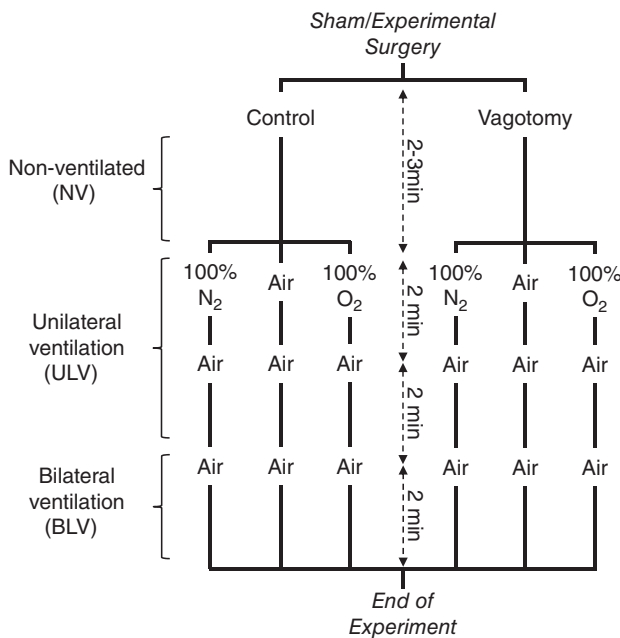


Figure 1. Flowchart of experimental procedure
Experimental groups (control, vagotomy), subgroups (initial gas ventilation of 100% N₂, air or 100% O₂) and timecourse of imaging/ventilation are shown.

this region was calculated for each frame. Bolus arrival time was designated as the frame in which half of the peak opacity (maximum percentage change from background) is reached for the first time (half-peak opacity); this corrects for problems as a result of steady-state peak opacity values in cases of poor washout (Shpilfoygel *et al.* 2000). The elapsed time between the half-peak opacity value in the main pulmonary artery compared to the left and right axial arteries (at the eighth intercostal space) was calculated to give an approximation of bolus transit time through the pulmonary artery.

Relative measures of pulmonary blood flow. A virtual box was placed over the left and right main axial arteries at the level of the seventh intercostal space, which provided a centrally-located, clear and unobstructed view of the large conduit arteries during both the pre-ventilation and ventilation imaging time periods. The changes in mean intensity within each box were plotted against time as a percentage change from background levels (mean background intensity averaged over 10 frames before iodine injection) throughout each iodine injection sequence. The maximum of this time-opacity curve was then divided by the pulmonary arterial transit time to provide an indicator of changes in pulmonary arterial flow in both lungs; this value was termed the relative PBF index.

Statistical analysis

Kitten weights were compared between groups using one-way ANOVA (Prism, version 6.0; GraphPad Software, Inc., La Jolla, CA, USA). Changes in visible vessel number, blood vessel internal diameter, heart rate, pulmonary arterial transit time and opacity of blood vessels were compared over time and between groups using a two-way ANOVA with repeated measures. *Post hoc* analysis used the Holm–Sidak method. $P < 0.05$ was considered statistically significant.

Results

Animal data

The mean \pm SEM kitten weight was 42.1 ± 2.5 g, although the kittens in the vagotomized group ventilated with air (V-air) were significantly lighter (33.8 ± 3.2 g) than the other groups (44.8 ± 2.2 g), which were all similar. The majority of kittens were ventilated with the right lung first ($n = 28$), although two were ventilated with the left lung first, both in the V-air group.

Observations from phase contrast X-ray videos

Overall, vagotomized kittens appeared to have a less profound increase in PBF following partial lung aeration compared to control kittens (Lang *et al.* 2014; Lang

et al. 2016). This was most evident in the V-N₂ and V-air group (see Supporting information, Supplementary Videos 1 and 2, respectively), with the V-O₂ group still displaying an increase in iodine flow in the axial arteries of both the ventilated first (A₁) and un-aerated (UA₂) lungs compared to the pre-ventilation period (NV) (see Supporting information, Supplementary Video 3) (Fig. 2).

Pulmonary blood vessel recruitment

In control kittens, ULV significantly increased the total number of visible vessels in both the A₁ and UA₂ lungs of all kittens, irrespective of the oxygen content of the gas used (Fig. 3). Similarly, ULV of vagotomized kittens increased the total number of visible vessels in both the A₁ and UA₂ lungs of the V-air and V-O₂ groups (Fig. 3), increasing from 13 ± 5 and 13 ± 4 visible vessels to 32 ± 4 and 35 ± 8 vessels in the A₁ and UA₂ lungs, respectively, in the V-air group and from 19 ± 7 and 22 ± 7 vessels to 50 ± 7 and 50 ± 9 vessels in the A₁ and UA₂ lungs, respectively, in the V-O₂ group; the increase in the V-O₂ group was higher than both other vagotomized groups, although not significantly so. However, in the V-N₂ group, although the number of visible vessels tended to increase in response to ULV with 100% nitrogen (ULV_{N₂}), the increase was only reached statistical significance once ULV commenced with air (ULV_{air}); at that time, it was significant for both the A₁ and UA₂ lungs compared to the NV time point (Fig. 3). Compared to control kittens, vagotomy significantly reduced the number of visible vessels (Fig. 3) in both lungs of kittens initially ventilated with 100% oxygen throughout the experimental period ($P < 0.05$; asterisks in Fig. 3, lower), except in the UA₂ lung, during initial ventilation with 100% oxygen. This difference between control and vagotomized kittens persisted in both the A₁ (C: 86 ± 10 vessels; V: 64 ± 7 vessels) and A₂ (C: 85 ± 10 vessels; V: 64 ± 9 vessels) lungs during bilateral ventilation in air (BLV_{air}).

Heart rate

In control kittens, the initial ULV period significantly increased heart rates, irrespective of the oxygen content of the gas used (Fig. 4), increasing from 56 ± 5 , 69 ± 5 and 47 ± 3 to 90 ± 13 , 93 ± 15 and 73 ± 10 beats min⁻¹ in the C-N₂, C-air and C-O₂ groups, respectively. However, in vagotomized animals, only ULV with air and 100% oxygen significantly increased heart rates during the initial ULV period; heart rates increased from 60 ± 6 and 67.5 ± 5 beats min⁻¹ to 79 ± 10 and 109 ± 9 beats min⁻¹ in V-air and V-O₂ groups, respectively. In V-N₂ kittens, ULV with 100% N₂ did not significantly increase heart rate; heart rates were 55 ± 6 beats min⁻¹ before and 53 ± 9 beats min⁻¹ after ULV with 100% N₂. In V-N₂ kittens, heart rate did not increase significantly until

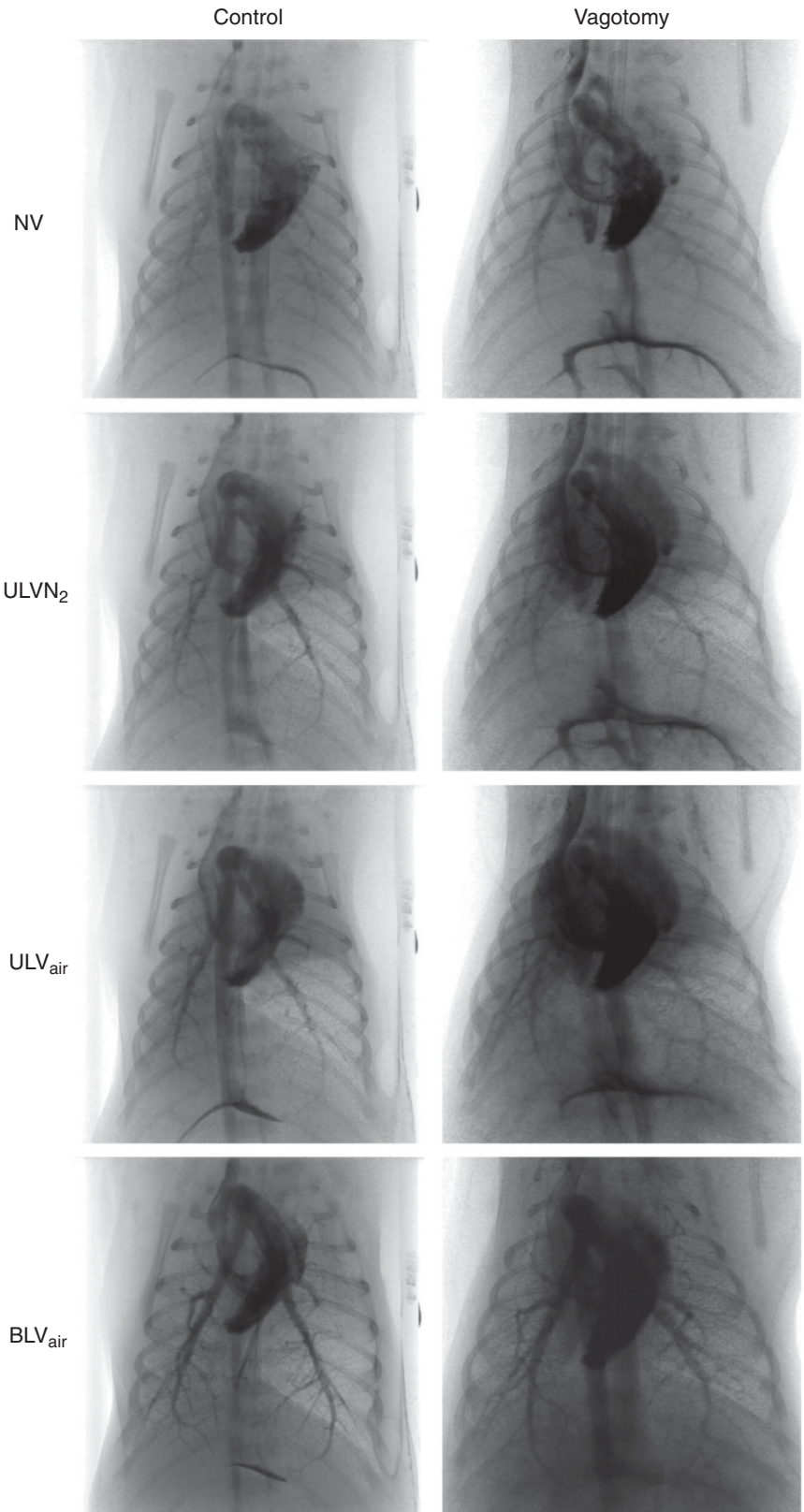


Figure 2. Representative phase contrast X-ray angiography image sequences of vagotomized and control newborn rabbits

Imaged prior to ventilation (NV), following unilateral ventilation (ULV) of the right lung with 100% N₂ (ULV_{N₂}), followed by ULV of the right lung with air (ULV_{air}), followed by bilateral ventilation of the lungs in air (BLV_{air}). Images were obtained 1–3 s following iodine bolus injection.

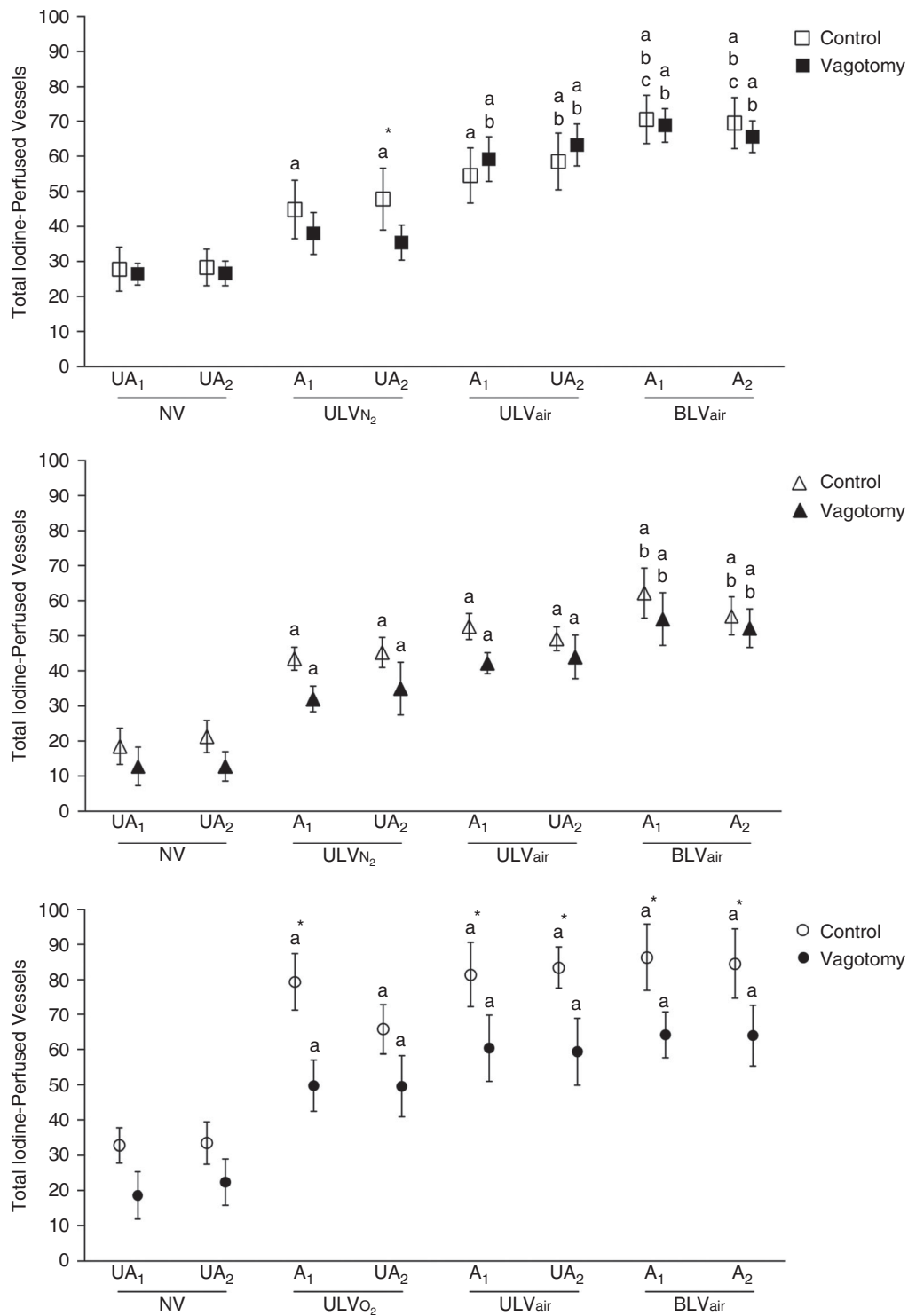


Figure 3. Mean ± SEM iodine-perfused vessel branches in control (open symbols) and vagotomized (closed symbols) animals ventilated first with 100% N₂ (squares; upper), air (triangles; middle) or 100% O₂ (circles; lower)

Ventilation periods shown are prior to ventilation onset (NV), during the initial unilateral ventilation (ULV_{N₂/air/O₂}) period, during the subsequent unilateral ventilation period with air (ULV_{air}) and during bilateral ventilation with air (BLV_{air}). Lungs are either un-aerated (UA) or aerated (A) and ventilated first (UA₁ and A₁) or second (UA₂ and A₂). a, P < 0.05 compared to the same lung at NV. b, P < 0.05 compared to the same lung at ULV_{gas}. c, P < 0.05 compared to the same lung at ULV_{air}. *P < 0.05 control compared to vagotomy within the same lung during the same ventilation period.

after ULV had commenced with air, increasing from 53 ± 9 beats min⁻¹ (ULV_{N₂}) to 75 ± 9 beats min⁻¹ (ULV_{air}) and then to 125.2 ± 18.0 beats min⁻¹ following bilateral ventilation with air (BLV_{air}) (Fig. 4). In V-air kittens, the heart rate increased from 63 ± 5 beats min⁻¹ to 93 ± 16 beats min⁻¹ during ULV and then increased further to 121 ± 9 beats min⁻¹ during BLV_{air}. Unexpectedly, in kittens initially ventilated with 100% O₂, vagotomy significantly increased heart rate compared to control (C-O₂) kittens and the difference continued throughout all ventilation periods, remaining higher even after BLV with air (BLV_{air}; V-O₂, 137 ± 7 beats min⁻¹ vs. C-O₂ 116 ± 10 beats min⁻¹).

Arterial vessel internal diameter

Compared with control kittens, vagotomy had a marked effect on vessel internal diameter in the axial arteries, resulting in a reduction in vessel internal diameter at all measurement times, even before lung aeration (Fig. 5). In control kittens, the initial ULV increased vessel internal diameter in the axial arteries of both the aerated (A₁) and unaerated (UA₂) lungs irrespective of the oxygen content of the ventilation gas. In control C-N₂ kittens, vessel internal diameters increased from 505 ± 39 and 505 ± 49 μm to 581 ± 40 and 585 ± 58 μm in response to ULV_{N₂} in the A₁ and the UA₂ lungs, respectively. In vagotomized kittens, ULV significantly increased vessel internal diameter in the axial arteries of both the A₁ and UA₂ lungs of the V-air and V-O₂ groups only. The vessel internal diameters increased from 437 ± 14 and 414 ± 14 μm to 485 ± 17 and 452 ± 24 μm in the A₁ and UA₂ lungs, respectively, of the V-air group and from 400 ± 18 and 404 ± 13 μm

to 468 ± 19 and 439 ± 23 μm in the A₁ and UA₂ lungs, respectively, of the V-O₂ group (Fig. 5). In contrast, ULV in the V-N₂ group failed to increase vessel internal diameters, which were similar in both axial arteries before (441 ± 11 and 412 ± 12 μm) and after (464 ± 12 and 437 ± 14 μm) ULV onset with 100% N₂. In both control and vagotomized kittens, there were only minor increases in internal diameter in all groups following ULV in air and bilateral ventilation in air, although internal diameters remained lower in vagotomized kittens than in control kittens at all timepoints in all ventilation groups (Fig. 5).

Iodine bolus transit time

Pulmonary arterial transit times (defined as the time for an iodine bolus to progress from the main pulmonary artery to the end of the axial arteries) decreased following ULV in both control and vagotomized kittens initially ventilated in either 100% N₂ or 100% O₂ (Fig. 6). No difference was observed between control and vagotomized kittens, except in the kittens ventilated in air. Transit times were significantly longer prior to ventilation in vagotomized kittens initially ventilated in air (3.4 ± 0.8 and 4.0 ± 1.7 s in UA₁ and UA₂, respectively) compared to control kittens (1.8 ± 0.4 and 1.3 ± 0.4 s in UA₁ and UA₂, respectively). This difference persisted after the first period of ULV with air, although it was not significant during the second ULV period with air and during the BLV period.

Relative PBF index

Vagotomy significantly reduced the increase in relative PBF in the aerated lung of kittens ventilated with 100% N₂, and

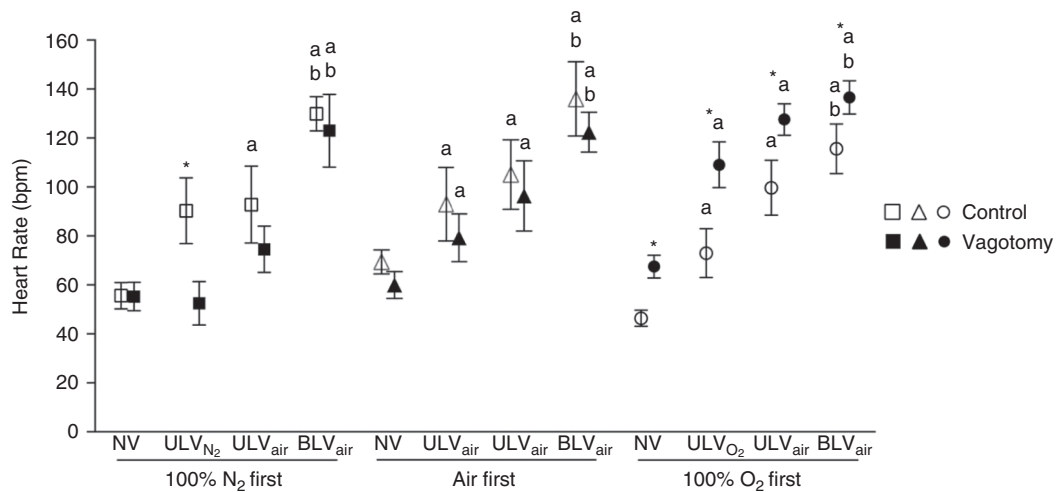


Figure 4. Mean ± SEM heart rate (beats min⁻¹) in control (open symbols) and vagotomized (closed symbols) kittens ventilated first with 100% N₂, air or 100% O₂. Ventilation periods shown are prior to ventilation onset (NV), during the initial unilateral ventilation (ULV_{N₂/air/O₂}) period, during the subsequent unilateral ventilation period with air (ULV_{air}) and during bilateral ventilation with air (BLV_{air}). a, P < 0.05 compared to the same lung at NV. b, P < 0.05 compared to the same lung at ULV_{gas}. *P < 0.05 control compared to vagotomy within the same lung during the same ventilation period.

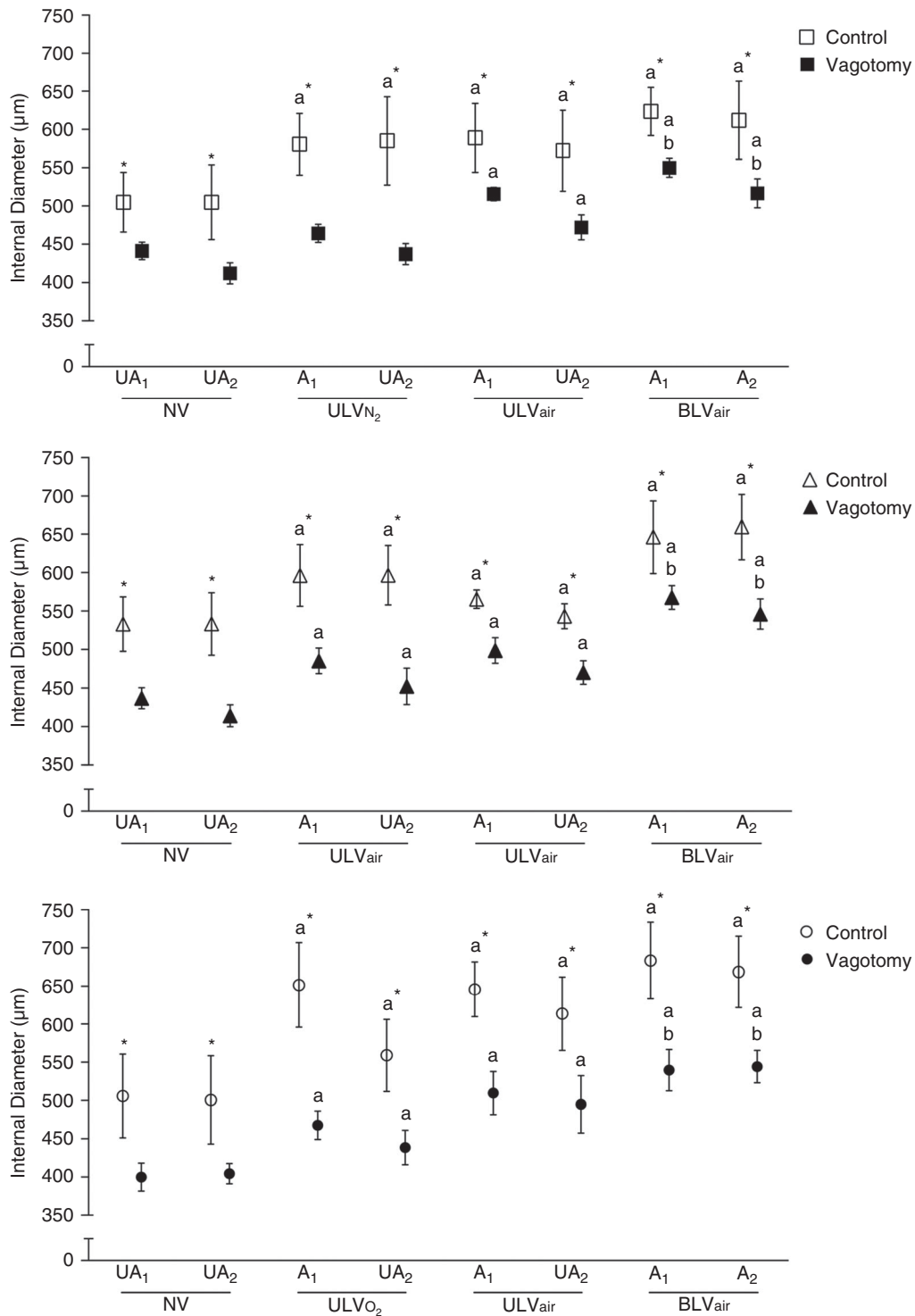


Figure 5. Mean \pm SEM internal diameter (μm) of axial arteries in control (open symbols) and vagotomized (closed symbols) kittens ventilated first with 100% N₂ (squares; upper panel), air (triangles; middle panel) or 100% O₂ (circles; lower panel)

Ventilation periods shown are prior to ventilation onset (NV), during the initial unilateral ventilation (ULV_{N₂/air/O₂}) period, during the subsequent unilateral ventilation period with air (ULV_{air}) and during bilateral ventilation with air (BLV_{air}). Lungs are either unaterated (UA) or aerated (A) and ventilated first (UA₁ and A₁) or second (UA₂ and A₂). a, $P < 0.05$ compared to the same lung at NV. b, $P < 0.05$ compared to the same lung at ULV_{gas}. * $P < 0.05$ control compared to vagotomy within the same lung during the same ventilation period.

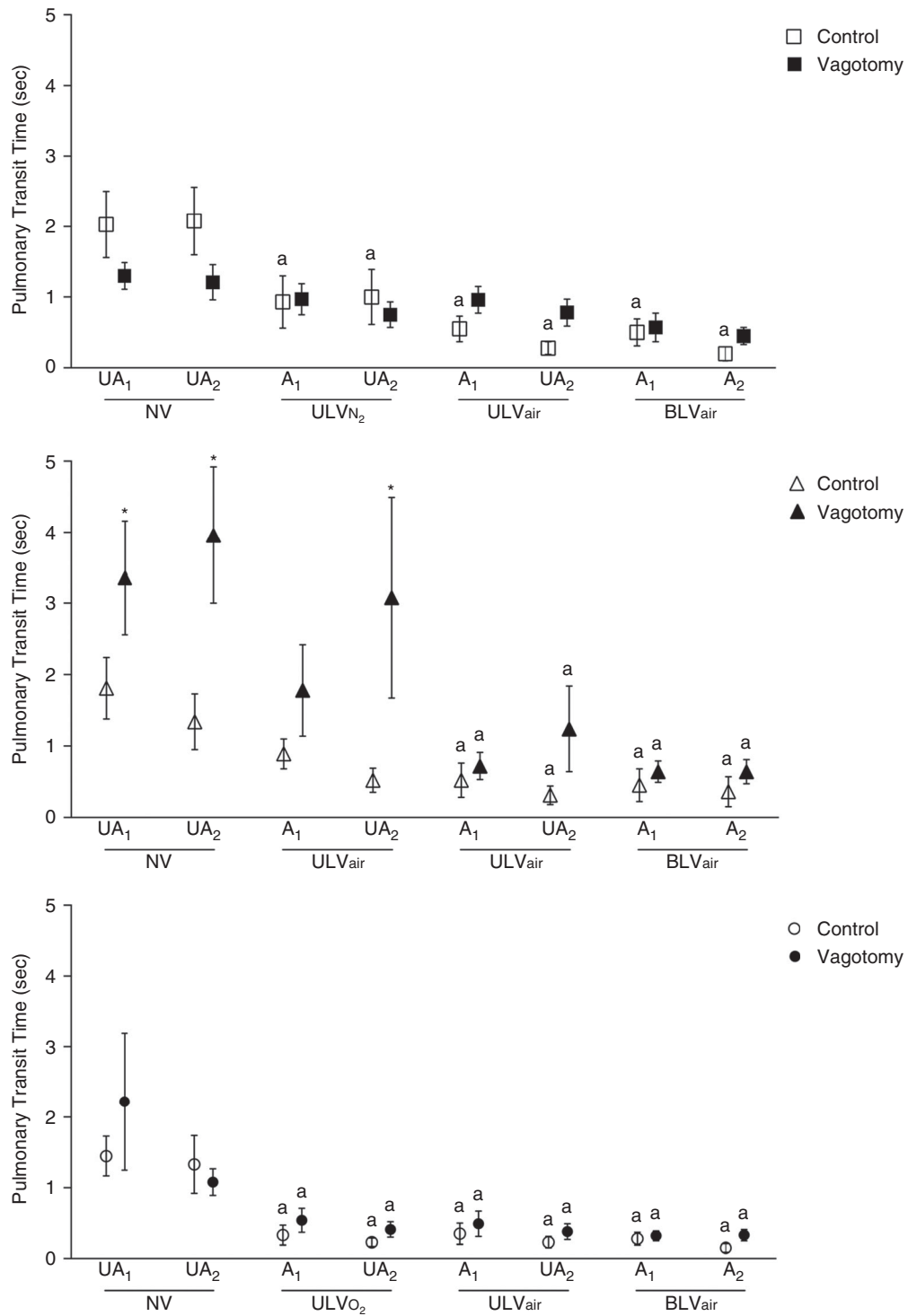


Figure 6. Mean ± SEM arterial transit time (s) in control (open symbols) and vagotomized (closed symbols) kittens ventilated first with 100% N₂ (squares; upper panel), air (triangles; middle panel) or 100% O₂ (circles; lower panel)

Ventilation periods shown are prior to ventilation onset (NV), during the initial unilateral ventilation (ULV_{N₂/air/O₂}) period, during the subsequent unilateral ventilation period with air (ULV_{air}) and during bilateral ventilation with air (BLV_{air}). Lungs are either unaerated (UA) or aerated (A) and ventilated first (UA₁ and A₁) or second (UA₂ and A₂). a, P < 0.05 compared to the same lung at NV. *P < 0.05 control compared to vagotomy within the same lung during the same ventilation period.

both aerated and non-aerated lungs in kittens ventilated with air during the initial ULV period (Fig. 7). For example, in V-air kittens, relative PBF was similar in the A₁ and UA₂ lungs before (3.6 ± 1.1 and $5.2 \pm 2.2\%$ change s⁻¹, respectively) and after (11.8 ± 3.7 and $15.8 \pm 7.1\%$ change s⁻¹, respectively) ULV. By contrast, in C-air kittens relative PBF increased in the A₁ and UA₂ lungs from 6.9 ± 2.5 and $13.8 \pm 6.2\%$ change s⁻¹ before ULV onset to 61.1 ± 22.1 and $78.0 \pm 32.0\%$ change s⁻¹, respectively, after ULV onset.

Furthermore, kittens initially ventilated with air also had lower relative PBF in both the A₁ and UA₂ lungs during the second ULV period. The increase in relative PBF following initial ULV was similar between groups in kittens ventilated with 100% O₂ except at BLV_{air}, in which all control groups were significantly higher than their respective vagotomy groups. For example, in A₁ lungs, relative PBF was markedly greater in control vs. vagotomized kittens initially ventilated with 100% N₂ (177.0 ± 22.8 vs. $75.6 \pm 30.8\%$ change s⁻¹), with air (236.0 ± 43.4 vs. $43.3 \pm 6.9\%$ change s⁻¹) and with 100% O₂ ($244.2\% \pm 63.4$ vs. $131.3 \pm 39.7\%$ change s⁻¹) (Fig. 7).

Discussion

The increase in PBF at birth plays a critical role in the adaptation to newborn life and is considered to be mediated by numerous mechanical and vasoactive factors, particularly an increase in oxygenation (Gao & Raj, 2010). However, recent studies have demonstrated that the increase in PBF is not spatially related to lung aeration because partial lung aeration leads to a global increase in PBF and is not dependent on increased oxygenation (Sobotka *et al.* 2011; Lang *et al.* 2016). Previous studies have indicated that vagal stimulation may induce pulmonary vasodilatation at birth (Colebatch *et al.* 1965) and is required for the establishment of neonatal respiratory function (Wong *et al.* 1998; Lalani *et al.* 2002). The results of the present study support the suggestion that signalling via the vagus plays a key role in stimulating the global increase in PBF at birth induced by lung aeration. We found that vagotomy inhibits the increase in PBF induced by lung aeration (Figs 2 and 7), although ventilation with high oxygen levels can partially mitigate this inhibitory effect of vagotomy. Although the mechanism by which the vagus mediates pulmonary vasodilatation in response to lung aeration is unclear, it is possible that the clearance of airway liquid into peri-alveolar interstitial tissue (Bland *et al.* 1980; Miserocchi *et al.* 1994) activates receptors, which signal via the vagus nerve. Nevertheless, the finding that ventilation with 100% O₂ can partially mitigate the effect of vagotomy indicates that O₂ may act separately through an independent mechanism to increase PBF.

Recent studies have clearly demonstrated that partial lung aeration leads to a global increase in PBF, increasing equally in both aerated and unaerated lung regions (Lang *et al.* 2014; Lang *et al.* 2016). These findings are consistent with previous studies showing that ventilation of one lung increases vascular conductance in the other unventilated lung (Cassin *et al.* 1964). Although oxygen can enhance the increase in PBF in aerated lung regions, the increase in PBF in unaerated regions is independent of oxygen levels and even occurs in response to ventilation with 100% N₂ (Lang *et al.* 2016). We have now confirmed and extended these findings, showing that ventilation with 100% N₂ increases blood flow in the aerated and unaerated lungs, of control kittens, whereas vagotomy greatly reduces the ability of both air and 100% N₂ to vasodilate the pulmonary arteries and stimulate a global increase in PBF. This finding is consistent with our hypothesis that a neural reflex, which is activated by lung aeration and incorporates afferent signalling via the vagus nerve, is largely responsible for the global increase in PBF at birth. The finding that ventilation with 100% oxygen was able to reverse the inhibitory effect of vagotomy is consistent with our previous suggestion that oxygen acts through an independent mechanism to stimulate PBF and enhance the effect of lung aeration (Lang *et al.* 2016).

Airway liquid clearance at birth leads to liquid accumulation in the pulmonary interstitial tissue, forming perivascular fluid cuffs that are similar to those that occur in the adult lung during pulmonary edema (Bland *et al.* 1980). Juxtacapillary (J) receptors located along pulmonary blood vessels are known to be activated in response to pulmonary congestion and they signal via afferent C-fibres located within the vagus nerve to stimulate tachypnoea (Paintal, 1969). We have previously proposed that the movement of airway liquid into the interstitial tissue following ventilation onset essentially causes pulmonary oedema (Lang *et al.* 2014; Lang *et al.* 2016), which activates J receptors and stimulates a global increase in PBF irrespective of the oxygen content of the gas. As such, in the present study, we hypothesized that sectioning the vagus nerve would prevent afferent signalling from the J receptors (Paintal, 1969) and inhibit the increase in PBF induced by partial lung aeration. Recent studies have shown that pulmonary C-fibre activation can dilate arterioles in skeletal muscle (Roberts *et al.* 2015). As such, it is possible that reflex C-fibre mediated arteriolar dilatation may not be limited to skeletal muscle and may extend to other vascular beds, such as the lung. Although our findings are largely consistent with this hypothesis, we discerned several disparities. One was the observation that bradycardia was not evoked with initiation of ventilation (Fig. 4), which may be related to the fact that heart rate is already reduced during the birth transition. Additionally, vagotomy significantly reduced arterial vessel internal

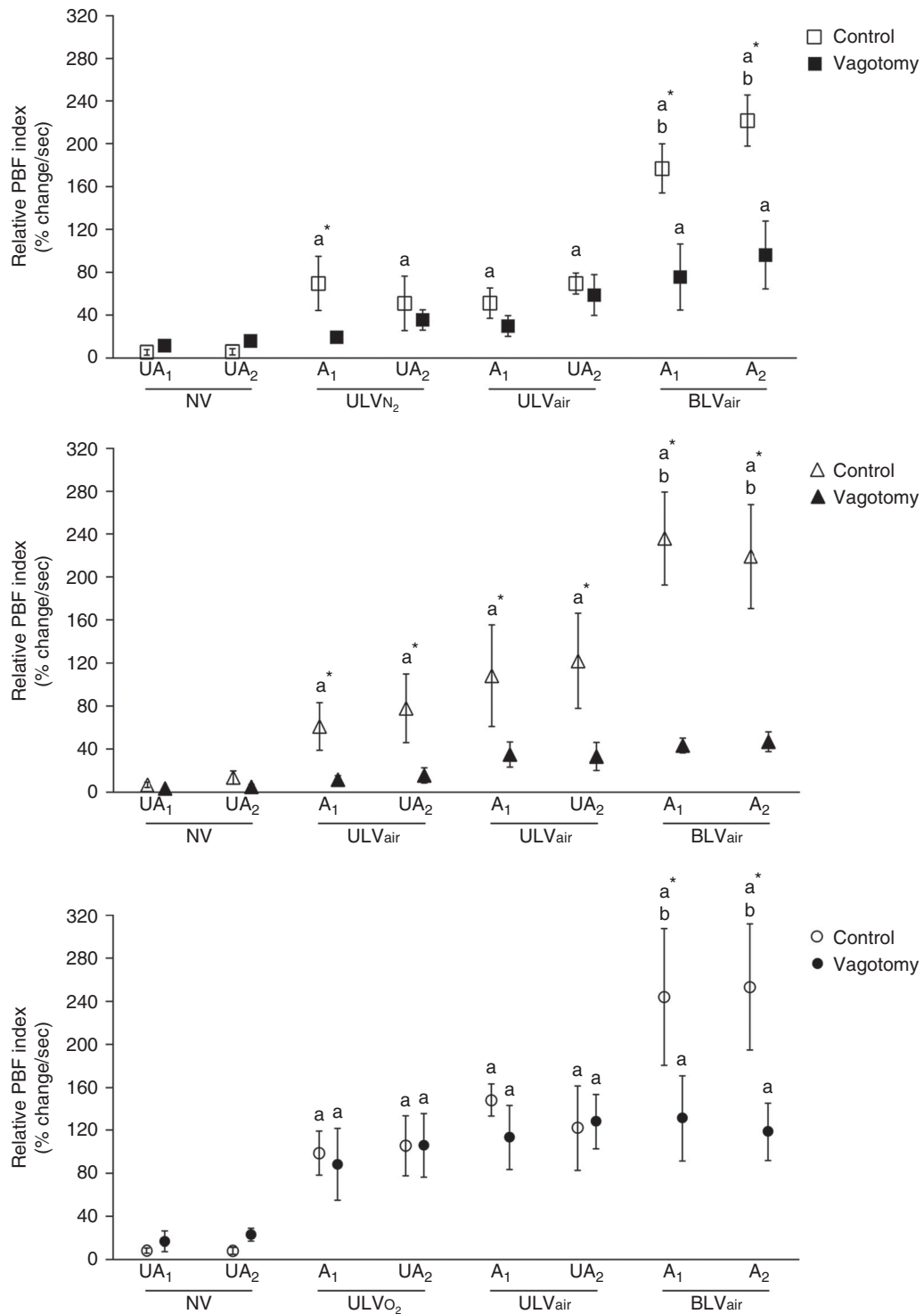


Figure 7. Mean \pm SEM relative PBF (% change s^{-1}), given by maximum % change grey value in the main axial arteries divided by the arterial transit time, in control (open symbols) and vagotomized (closed symbols) kittens ventilated first with 100% N₂ (squares; upper panel), air (triangles; middle panel) or 100% O₂ (circles; lower panel). Ventilation periods shown are prior to ventilation onset (NV), during the initial unilateral ventilation (ULV_{N₂/air/O₂}) period, during the subsequent unilateral ventilation period with air (ULV_{air}) and during bilateral ventilation with air (BLV_{air}). Lungs are either un-aerated (UA) or aerated (A) and ventilated first (UA₁ and A₁) or second (UA₂ and A₂). a, $P < 0.05$ compared to the same lung at NV. * $P < 0.05$ control compared to vagotomy within the same lung during the same ventilation period.

diameters in the lung even before ventilation commenced (Fig. 5). Indeed, the reduction in vessel diameter caused by vagotomy was 50–100 μm (10–20% lower than controls), which must markedly increase PVR because resistance is inversely proportional to the fourth power of the vessel radius. The mechanism by which vagotomy reduces vessel diameter is unknown, although it is possible that low level afferent signalling helps to modulate PVR in the fetus.

Single lung ventilation was confirmed using our established technique of phase contrast X-ray imaging, showing a distinctive speckle pattern that is limited to aerated regions of the lungs (Kitchen *et al.* 2004). We have now confirmed these findings in three separate studies (Lang *et al.* 2014; Lang *et al.* 2016) and shown that the effect of partial lung aeration is greatly diminished by vagotomy except when ventilation occurs with 100% O_2 . Although the kittens experienced a delay between umbilical cord ligation and the onset of imaging (2–3 min), as a result of radiation safety procedures, all kittens experienced the same delay and so any differences were unlikely to be caused by the resulting partial asphyxia. The finding that PBF increases and pulmonary artery vessel dilatation occurs in both aerated and unaerated regions clearly indicates that the vessel dilatation and increase in PBF is not spatially related to lung aeration. However, it is not clear whether the volume of airway liquid accumulated in the interstitial space determines the degree of PBF increase as a result of differential neural activation. Indeed, an experimental approach that examines this possible relationship and more directly implicates pulmonary C-fibre afferents is required.

The increase in heart rate in response to ULV with 100% N_2 (Fig. 4) is a phenomenon that we have reported previously and is probably a result of the lung aeration-induced increase in PBF, which increases ventricular preload (Lang *et al.* 2016). In the fetus, because PBF is low, umbilical venous return, which passes via the ductus venosus and foramen ovale to enter the left atrium, provides the vast majority of the preload for the left ventricle. Thus, if the umbilical cord is clamped before the lungs have had an opportunity to aerate, preload for the left ventricle is greatly diminished and cardiac output is greatly reduced (Crossley *et al.* 2009; Bhatt *et al.* 2013). This would contribute to the low PBF as observed in the NV period (Fig. 2), with cardiac output remaining reduced until the lungs aerate and PBF increases to restore preload and replace the venous return lost upon cord clamping. As such, by increasing PBF, ULV with 100% N_2 is considered to increase cardiac output, which is reflected by an increase in heart rate, restoring left ventricular preload lost by umbilical cord clamping.

We expected vagotomy to increase heart rate due to removal of the suppressive effects of parasympathetic tone on pacemaker activity in the sino-atrial node. However,

we found that, before ventilation onset, heart rate was not increased in vagotomized compared to control kittens except in those destined to be ventilated with 100% O_2 . It is unclear why an increase in heart rate was detected in this group but not in the other two, although it is probably not an oxygen-mediated effect because this difference was detected before ventilation commenced. In any event, the finding that vagotomy blocked the increase in heart rate induced by ULV with 100% N_2 supports our contention that this increase in heart rate is the result of an increase in PBF because the latter was also inhibited. Although previous studies indicate that direct stimulation of C-fibres (with capsaicin) induces a bradycardia (Coleridge *et al.* 1992; Deep *et al.* 2001), we did not observe a similar response during the birth transition, which is possibly a result of competing factors. For example, heart rate was already depressed during the NV period (Fig. 4), which may mask changes resulting from the initiation of ventilation. On the other hand, an increase in venous return and left ventricular preload likely contributes to an increase in heart rate and cardiac output, which would oppose induced bradycardia. Interestingly, this effect of vagotomy on the ULV-induced increase in heart rate was not apparent in V-air and V- O_2 kittens and, in addition, the induced increase was greatest in V- O_2 kittens, suggesting that the increase in heart rate results from an increase in both oxygenation and PBF.

Although vagal C-fibre stimulation may form the afferent pathway for the ULV-induced global increase in PBF, the efferent side of the pathway remains unknown. It is possible that the efferent side of the pathway involves an increase in sympathetic or parasympathetic activation, or a combination of the two. Sympathetic activation could partly explain our observations due to its mediation of adult pulmonary vasodilatation (Sylvester *et al.* 2012). Although the sympathetic nerves contribute to the high vascular tone in the fetus (Nuwayhid *et al.* 1975), it was reported previously that noradrenaline can act as a vasoconstrictor during low pulmonary vascular tone but as a vasodilator when vascular tone is enhanced (Silove *et al.* 1968). Although the influence of autonomic stimulation on the pulmonary vasculature has been investigated previously, the effect on the perinatal circulation remains largely unknown.

The cardiopulmonary transition at birth is a complex process that is triggered by birth related events such as occlusion of the umbilical cord and the entry of air into the lungs, which is known to trigger both mechanical (Hooper, 1998) and vasoactive stimuli to decrease PVR (Teitel *et al.* 1990; Bhatt *et al.* 2013). However, we show that a global decrease in PVR in response to partial lung aeration can be inhibited with ligation of the vagus nerve, suggesting that an underlying neural reflex triggered by lung aeration may exist. This response is independent of the O_2 content of the inspired gas and, although it

leads to a high risk of ventilation/perfusion mismatching in the lung at birth, we have previously argued that this response is probably highly advantageous and not adverse for the individual (Lang *et al.* 2014; Lang *et al.* 2016). Indeed, as PBF takes over the role of providing preload for the left ventricle when the cord is clamped at birth, having a high PBF, irrespective of how much of the lung has aerated, is much more important. This is because an increase and redistribution of cardiac output to increase blood flow and maintain oxygen delivery to vital organs is the primary defence mechanism against hypoxia in the fetus and newborn. With incomplete aeration of the lungs being inevitable at birth, these findings indicate that a vagal reflex exists to stimulate PBF at birth regardless of aeration, facilitating the transition into newborn life.

References

- Abman SH, Chatfield BA, Hall S & McMurtry I (1990). Role of endothelium-derived relaxing factor during transition of pulmonary circulation at birth. *Am J Physiol Heart Circ Physiol* **259**, H1921.
- Bhatt S, Alison BJ, Wallace EM, Crossley KJ, Gill AW, Kluckow M, te Pas AB, Morley CJ, Polglase GR & Hooper SB (2013). Delaying cord clamping until ventilation onset improves cardiovascular function at birth in preterm lambs. *J Physiol* **591**, 2113–2126.
- Bland R, McMillan D, Bressack M & Dong L (1980). Clearance of liquid from lungs of newborn rabbits. *J Appl Physiol* **49**, 171–177.
- Cassin S, Dawes GS, Mott JC, Ross BB & Strang LB (1964). The vascular resistance of the foetal and newly ventilated lung of the lamb. *J Physiol* **171**, 61–79.
- Colebatch H, Dawes G, Goodwin J & Nadeau R (1965). The nervous control of the circulation in the foetal and newly expanded lungs of the lamb. *J Physiol* **178**, 544.
- Coleridge H, Coleridge J, Green J & Parsons G (1992). Pulmonary C-fibre stimulation by capsaicin evokes reflex cholinergic bronchial vasodilation in sheep. *J Appl Physiol* **72**, 770–778.
- Crossley KJ, Allison BJ, Polglase GR, Morley CJ, Davis PG & Hooper SB (2009). Dynamic changes in the direction of blood flow through the ductus arteriosus at birth. *J Physiol* **587**, 4695–4704.
- Deep V, Singh M & Ravi K (2001). Role of vagal afferents in the reflex effects of capsaicin and lobeline in monkeys. *Respir Physiol* **125**, 155–168.
- Gao Y & Raj JU (2010). Regulation of the pulmonary circulation in the fetus and newborn. *Physiol Rev* **90**, 1291–1335.
- Hasan SU, Lalani S & Remmers JE (2000). Significance of vagal innervation in perinatal breathing and gas exchange. *Respir Physiol* **119**, 133–141.
- Hooper SB (1998). Role of luminal volume changes in the increase in pulmonary blood flow at birth in sheep. *Exp Physiol* **83**, 833–842.
- Hooper SB, Kitchen MJ, Wallace MJ, Yagi N, Uesugi K, Morgan MJ, Hall C, Siu KKW, Williams IM, Siew M, Irvine SC, Pavlov K & Lewis RA (2007). Imaging lung aeration and lung liquid clearance at birth. *FASEB J* **21**, 3329–3337.
- Hooper SB, te Pas AB, Lang J, van Vonderen JJ, Roehr CC, Kluckow M, Gill AW, Wallace EM & Polglase GR (2015). Cardiovascular transition at birth: a physiological sequence. *Pediatr Res* **77**, 608–614.
- Kitchen MJ, Habib A, Fouras A, Dubsy S, Lewis RA, Wallace MJ & Hooper SB (2010). A new design for high stability pressure-controlled ventilation for small animal lung imaging. *J Instrum* **5**, T02002.
- Kitchen MJ, Paganin D, Lewis RA, Yagi N, Uesugi K & Mudie ST (2004). On the origin of speckle in x-ray phase contrast images of lung tissue. *Phys Med Biol* **49**, 4335–4348.
- Lalani S, Remmers JE, MacKinnon Y, Ford GT & Hasan SU (2002). Hypoxemia and low Crs in vagally denervated lambs result from reduced lung volume and not pulmonary edema. *J Appl Physiol* **93**, 601–610.
- Lang JA, Pearson JT, Binder-Heschl C, Wallace MJ, Siew ML, Kitchen MJ, te Pas AB, Fouras A, Lewis RA, Polglase GR, Shirai M & Hooper SB (2016). Increase in pulmonary blood flow at birth: role of oxygen and lung aeration. *J Physiol* **594**, 1389–1398.
- Lang JA, Pearson JT, te Pas AB, Wallace MJ, Siew ML, Kitchen MJ, Fouras A, Lewis RA, Wheeler K, Polglase GR, Shirai M, Sonobe T & Hooper SB (2014). Ventilation/perfusion mismatch during lung aeration at birth. *J Appl Physiol* **117**, 535–543.
- Miserocchi G, Poskurica BH & Del Fabbro M (1994). Pulmonary interstitial pressure in anaesthetized paralyzed newborn rabbits. *J Appl Physiol* **77**, 2260–2268.
- Nuwayhid B, Brinkman C, Su C, Bevan J & Assali N (1975). Development of autonomic control of fetal circulation. *Am J Physiol* **228**, 337–344.
- Paintal A (1969). Mechanism of stimulation of type J pulmonary receptors. *J Physiol* **203**, 511–532.
- Roberts AM, Yu J & Joshua IG (2015). Microvascular dilation evoked by chemical stimulation of C-fibres in rats. *J Appl Physiol* **118**, 55–60.
- Rudolph AM (1985). Distribution and regulation of blood flow in the fetal and neonatal lamb. *Circ Res* **57**, 811–821.
- Shpilfoyl SD, Close RA, Valentino DJ & Duckwiler GR (2000). X-ray videodensitometric methods for blood flow and velocity measurement: a critical review of literature. *Med Phys* **27**, 2008–2023.
- Silove ED, Inoue T & Grover RF (1968). Comparison of hypoxia, pH, and sympathomimetic drugs on bovine pulmonary vasculature. *J Appl Physiol* **24**, 355–365.
- Sobotka KS, Hooper SB, Allison BJ, te Pas AB, Davis PG, Morley CJ & Moss TJ (2011). An initial sustained inflation improves the respiratory and cardiovascular transition at birth in preterm lambs. *Pediatr Res* **70**, 56–60.
- Sylvester J, Shimoda LA, Aaronson PI & Ward JP (2012). Hypoxic pulmonary vasoconstriction. *Physiol Rev* **92**, 367–520.
- Teitel DF, Iwamoto HS & Rudolph AM (1990). Changes in the pulmonary circulation during birth-related events. *Pediatr Res* **27**, 372–378.

Wong KA, Bano A, Rigaux A, Wang B, Bharadwaj B, Schürch S, Green F, Remmers JE & Hasan SU (1998). Pulmonary vagal innervation is required to establish adequate alveolar ventilation in the newborn lamb. *J Appl Physiol* **85**, 849–859.

Additional information

Competing interests

The authors declare that they have no competing interests.

Author contributions

JARL, JTP, RAL and SBH conceived and designed the experiments. JARL, JTP, CB, MJW, MLS, MJK, ABtP, RAL, GRP, MS and SBH collected, assembled, analysed and interpreted data. JARL, JTP, CB, MJW, MLS, MJK, ABtP, RAL, GRP, MS and SBH drafted the article or revised it critically for important intellectual content. All authors approved the final version of the manuscript. All persons designated as authors qualify for authorship, and all those who qualify for authorship are listed.

Translational perspective

Regionalized inhomogeneous aeration of the lung is common in newborn infants, particularly very preterm infants during the onset of air breathing. Our studies demonstrate that partial lung aeration leads to a global increase in pulmonary blood flow (PBF), leading to a potential mismatch between pulmonary ventilation and perfusion (Lang *et al.* 2014; Lang *et al.* 2016). The underlying mechanisms that initiate a global increase in PBF with only partial aeration are largely independent of oxygenation (Lang *et al.* 2016) and involve neural signalling via the vagus nerve. Although an increase in perfusion to poorly aerated lung regions at birth may appear to be a disadvantage, we suggest that this offers a major adaptive advantage. Indeed, maintaining or increasing cardiac output is vital for avoiding ischaemia contributing to any hypoxic event that may occur at birth; therefore, increasing PBF is critically important to provide preload for the left ventricle and maintain cardiac output that is lost following umbilical cord occlusion. As such, restricting the increase in PBF as a consequence of partial lung aeration would restrict cardiac output after birth.

Supporting information

The following supporting information is available in the online version of this article.

Supplementary Video 1 Simultaneous phase contrast X-ray and angiography recordings in a newborn rabbit (30 days of gestation) imaged with the lungs liquid-filled and non-aerated, and then with only the right lung ventilated with 100% N₂ (~30 s post-ventilation) immediately following birth. Blood vessels are visualized via infusion of iodinated contrast agent; non-aerated regions of the lung are clearly evident as indicated by the absence of speckle pattern. The data were acquired at 20 frames s⁻¹ with a pixel size of 14.28 μm.

Supplementary Video 2 Simultaneous phase contrast X-ray and angiography recordings in a newborn rabbit (30 days of gestation) imaged with the lungs liquid-filled and non-aerated, and then with only the left lung

Funding

This research was supported by the Australian Research Council, the Australian National Health and Medical Research Council and the Victorian Government's Operational Infrastructure Support Program. We acknowledge travel funding provided by the International Synchrotron Access Program (ISAP) managed by the Australian Synchrotron and funded by the Australian Government. C. Binder is supported by the Austrian Science Fund (FWF): J 3595-B19. M. J. Kitchen is the recipient of an ARC Australian Research Fellowship (DP110101941). A. B. te Pas is the recipient of a Veni-grant from The Netherlands Organisation for Health Research and Development (ZonMw), part of the Innovational Research Incentives Scheme Veni-Vidi-Vici.

Acknowledgements

The authors gratefully acknowledge the support provided by the SPring-8 synchrotron facility (Japan), which was granted by the SPring-8 Program Review Committee, for providing access to the X-ray beamline and associated facilities.

ventilated with air (21% O₂) (~30 s post-ventilation) immediately following birth when the right lung was non-aerated and liquid-filled. Blood vessels are visualized via infusion of iodinated contrast agent; non-aerated regions of the lung are clearly evident as indicated by the absence of speckle pattern. The data were acquired at 10 frames s⁻¹ with a pixel size of 15.3 μm.

Supplementary Video 3 Simultaneous phase contrast X-ray and angiography recordings in a newborn rabbit (30 days of gestation) imaged with the lungs liquid-filled and non-aerated, then with only the right lung ventilated with 100% O₂ (~30 s post-ventilation) immediately following birth when the left lung was non-aerated and liquid-filled. Blood vessels are visualized via infusion of iodinated contrast agent; non-aerated regions of the lung are clearly evident as indicated by the absence of speckle pattern. The data were acquired at 20 frames s⁻¹ with a pixel size of 14.28 μm.

Appendix D

Supplementary Video Online Links (Also Available on Physical Media)

Supplementary Video 3.1

<http://jap.physiology.org/content/117/5/535>

http://jap.physiology.org/highwire/filestream/110323/field_highwire_adjunct_files/0/videoS1.avi

Supplementary Video 4.1-4.2

<http://onlinelibrary.wiley.com/doi/10.1113/JP270926/full>

<http://onlinelibrary.wiley.com/store/10.1113/JP270926/asset/supinfo/tjp6813-sup-0001-SupMat.zip?v=1&s=cbdadcdebef8ec997b24f84eaa1dbb63f71bbd23>

Supplementary Video 5.1-5.3

<http://onlinelibrary.wiley.com/doi/10.1113/JP273682/full>

<http://onlinelibrary.wiley.com/store/10.1113/JP273682/asset/supinfo/tjp12134-sup-0001-SupMat.zip?v=1&s=29ba80a1ddcbaed4a114ebc4c4a819164173b33b>

Supplementary Video Legends

Supplementary Video 3.1

Simultaneous phase contrast X-ray and angiography recordings in a newborn rabbit (30d gestation) imaged with only the right lung ventilated (~30 sec post-ventilation) immediately following birth while the left lung was non-aerated and liquid-filled. Blood vessels are visualized via infusion of iodinated contrast agent; non-aerated regions of the lung are clearly evident by the absence of speckle pattern. The data was acquired at 30 frames per second with a pixel size of 31.8 μm .

Supplementary Video 4.1

Simultaneous phase contrast X-ray and angiography recordings in a newborn rabbit (30d gestation) imaged with only the right lung ventilated with 100% N₂ (~30 sec post-ventilation) immediately following birth while the left lung was non-aerated and liquid-filled. Blood vessels are visualized via infusion of iodinated contrast agent; non-aerated regions of the lung are clearly evident by the absence of speckle pattern. The data was acquired at 10 frames per second with a pixel size of 15.3 μm .

Supplementary Video 4.2

Simultaneous phase contrast X-ray and angiography recordings in a newborn rabbit (30d gestation) imaged with only the right lung ventilated with 100% O₂ (~30 sec post-ventilation) immediately following birth while the left lung was non-aerated and liquid-filled. Blood vessels are visualized via infusion of iodinated contrast agent; non-aerated regions of the lung are clearly evident by the absence of speckle pattern. The data was acquired at 10 frames per second with a pixel size of 15.3 μm .

Supplementary Video 5.1

Simultaneous phase contrast X-ray and angiography recordings in a newborn rabbit (30d gestation) imaged with the lungs liquid-filled and non-aerated, then with only the right lung ventilated with 100% N₂ (~30 sec post-ventilation) immediately following birth. Blood vessels are visualized via infusion of iodinated contrast agent; non-aerated regions of the lung are clearly evident by the absence of speckle pattern. The data was acquired at 20 frames per second with a pixel size of 14.28 μm.

Supplementary Video 5.2

Simultaneous phase contrast X-ray and angiography recordings in a newborn rabbit (30d gestation) imaged with the lungs liquid-filled and non-aerated, then with only the left lung ventilated with air (21% O₂) (~30 sec post-ventilation) immediately following birth while the right lung was non-aerated and liquid-filled. Blood vessels are visualized via infusion of iodinated contrast agent; non-aerated regions of the lung are clearly evident by the absence of speckle pattern. The data was acquired at 10 frames per second with a pixel size of 15.3 μm.

Supplementary Video 5.3

Simultaneous phase contrast X-ray and angiography recordings in a newborn rabbit (30d gestation) imaged with the lungs liquid-filled and non-aerated, then with only the right lung ventilated with 100% O₂ (~30 sec post-ventilation) immediately following birth while the left lung was non-aerated and liquid-filled. Blood vessels are visualized via infusion of iodinated contrast agent; non-aerated regions of the lung are clearly evident by the absence of speckle pattern. The data was acquired at 20 frames per second with a pixel size of 14.28 μm.